# MOLECULAR MECHANISMS OF PRE- AND POSTSYNAPTIC EPHB/EPHRIN-B SIGNALING IN SYNAPSE FORMATION AND FUNCTION

Sean Isaac Sheffler-Collins

A DISSERTATION

in

Neuroscience

Presented to the Faculties of the University of Pennsylvania

in Partial Fulfillment of the Requirements for the Degree of Doctor of Philosophy

2012

SUPERVISOR OF DISSERTATION

_____

Matthew B. Dalva, Ph.D.

Associate Professor of Neuroscience

GRADUATE GROUP CHAIRPERSON

_____

Joshua I. Gold, Ph.D.

Associate Professor of Neuroscience

DISSERTATION COMMITTEE

Michael B. Robinson Ph.D., Professor of Pediatrics and Pharmacology

David R. Lynch, M.D., Ph.D., Professor of Neurology and Pediatrics

Greg J. Bashaw, Ph.D., Associate Professor of Neuroscience

Kelly L. Jordan-Sciutto, Ph.D., Associate Professor of Pathology

# ACKNOWLEDGMENT

First and foremost, I would like to thank my advisor Dr. Matthew B. Dalva for his mentorship and support, for challenging me intellectually, and for his infectious enthusiasm about science. I would like to thank the members of my thesis committee: Greg Bashaw, Kelly Jordan-Sciutto, David Lynch, and Michael Robinson for their incredible help, advice, support, and for always opening their offices and laboratories to me. Great thanks are also owed to my colleagues in the Dalva laboratory, especially Kenji Hanamura, Martin Hruska, Sylvain Le Marchand, James Munoz, Mark Nolt, and Wei Zhou for their friendship, humor, and contributions to my project. These studies were supported, in part, by the National Eye Institute Vision Training grant EY007035. I am extremely grateful to my friends and family especially my parents Kathie and Craig Sheffler-Collins, my brother Seth, my parents-in-law, Karen and Mark Reber, and my sister-in-law Rebecca for their unconditional love and support. Lastly, to my amazing wife Kate Reber who has always brought out the best in me; and whose support, encouragement, and love have made this possible.

# ABSTRACT

## Molecular mechanisms of pre- and postsynaptic EphB/ephrin-B signaling in synapse formation and function

Sean Isaac Sheffler-Collins

Matthew B. Dalva

Proper function of the central nervous system relies on precise and coordinated cell-cell interactions and communication via synaptic transmission to assemble neuronal networks. Aberrant synaptic transmission is a hallmark of neuronal disease. The EphB family of receptor tyrosine kinases and their ephrin-B ligands play critical roles in the central nervous system in axon guidance, formation of pre- and post-synaptic specializations, localization of glutamate receptors, synaptic plasticity, and disease. EphB/ephrin-B signaling has been reported to modulate these processes, but the molecular mechanisms remain poorly understood. Our laboratory has previously shown that EphBs organize the formation of both pre- and postsynaptic specializations, and interact directly with NMDA-type glutamate receptors. Therefore, I sought to investigate the molecular mechanisms for formation of presynaptic specializations and the interaction domain between EphBs and NMDA receptors. I found that EphBs can induce the formation of presynaptic specializations by trans-synaptic

interactions with both ephrin-B1 and ephrin-B2. These ephrin-Bs can then recruit the machinery for neurotransmitter release through the multiple PDZ-domain containing adaptor protein syntenin-1. Furthermore, ephrin-B1 and ephrin-B2 act independently for formation of presynaptic specializations, but together to recruit syntenin-1 to synaptic sites. Based on this work and that of other laboratories, I was able to define the molecular pathway from postsynaptic EphBs to presynaptic glutamatergic vesicles. Furthermore, on the postsynaptic side of the synapse, I define a single amino acid that is necessary and sufficient to mediate the EphB-NMDAR interaction. In a novel molecular mechanism, I show that extracellular phosphorylation of this residue after ephrin-B binding is sufficient to induce the EphB-NMDAR interaction. Furthermore, I show that in the mature brain, the EphB-NMDAR interaction preferentially regulates NR2B-subunit containing NMDA receptor localization, function, and downstream gene transcription. Together, these findings impact our understanding of synapse formation and function, and highlight the EphB-NMDAR interaction as a potential target to treat neurological disease.

TABLE OF CONTENTS

# LIST OF ILLUSTRATIONS

**Chapter 1**



**Chapter 2**

**Chapter 3**

**Chapter 4**



**Appendix 1**

CHAPTER 1

# EphBs: an integral link between synaptic function and synaptopathies

Sean I. Sheffler-Collins[1, 2] and Matthew B. Dalva[1*]

[1]Department of Neuroscience and Farber Institute for Neurosciences, Thomas Jefferson University, 900 Walnut Street, Suite 462, Philadelphia, PA, 19107.

[2]Neuroscience Graduate Group, University of Pennsylvania School of Medicine, Philadelphia, PA 19104

* Corresponding Author:

Matthew B. Dalva

Thomas Jefferson University

Department of Neuroscience

The Farber Institute for Neurosciences

900 Walnut Street, Suite 462

Philadelphia, PA 19107

Matthew.Dalva@jefferson.edu

Contributions: All sections and figures were drafted by S.I.S-C. All sections and figured were revised and edited by M.B.D. and S.I.S-C.

**Abstract**

Assembly and function of neuronal circuits rely on selective cell-cell interactions to control axon targeting, generate pre- and postsynaptic specialization, and recruit neurotransmitter receptors. In neurons, EphB receptor tyrosine kinases mediate excitatory synaptogenesis early in development, and then later coordinate synaptic function by controlling NMDAR synaptic localization and function. EphBs direct synapse formation and function to regulate cellular morphology through downstream signaling mechanisms and by interacting with glutamate receptors. In humans, defective EphB-dependent regulation of NMDAR localization and function is associated with synaptopathies such as neuropathic pain, anxiety disorders, and Alzheimer's disease. Here, we propose that EphBs act as a central organizer of excitatory synapse formation and function, and as a key regulator of diseases linked to NMDAR dysfunction.

## Introduction

Synapses are the fundamental unit of information flow within the central nervous system. Early in development there is a period of new synapse addition followed by synapse maturation (Fu et al., 2011; Shen and Cowan, 2010; Shen and Scheiffele, 2010; Tallafuss et al., 2010). Formation of excitatory synapses requires precise coordination between two contacting neurons to organize a presynaptic terminal capable of neurotransmitter release, and a postsynaptic specialization equipped with the proper neurotransmitter receptors (Fu et al., 2011; Jin and Garner, 2008; McMahon and Diaz, 2011; Shen and Scheiffele, 2010; Siddiqui and Craig, 2010; Tallafuss et al., 2010). Maturation of synapses involves the pruning of inappropriate connections, stabilization of pre- and postsynaptic components, and formation of appropriate morphological specializations. Finally, maintenance and plasticity are required at sites of contact for proper function (Fu et al., 2011; Shen and Scheiffele, 2010). The improper formation and function of synapses can have devastating consequences for the adult brain. Malformations in synaptic formation and maturation are implicated in a wide variety of disease including Angelman syndrome, autism spectrum disorders, neuropathic pain, anxiety disorders, and Alzheimer's disease (Mabb et al., 2011; Penzes et al., 2011; Sloniowski and Ethell, 2011; Sudhof, 2008; van Spronsen and Hoogenraad, 2010) (see Glossary for definitions).

Excitatory synaptic transmission is mediated by α-amino-3-hydroxy-5-methyl-4-isoxazolepropionic acid (AMPA)-type (Bredt and Nicoll, 2003; Kessels

and Malinow, 2009) and *N*-Methyl-d-aspartate (NMDA)-type (Lau and Zukin, 2007; Perez-Otano and Ehlers, 2005) glutamate receptors. AMPARs and NMDARs are directed to the cell surface and synaptic sites by both neuronal activity and intermolecular interactions. At synaptic sites, glutamate receptors are dynamically regulated and changes in the size and number of AMPARs and NMDARs at synaptic sites are thought to underlie the expression of synaptic plasticity (Groc et al., 2009; Henley et al., 2011; Kerchner and Nicoll, 2008; Lu and Roche, 2011; Yashiro and Philpot, 2008). Many of the molecular mechanisms governing glutamate receptor trafficking, retention, and maintenance at synaptic sites are well characterized. Especially important are associations of glutamate receptors with scaffolding proteins such as PSD-95 and GRIP, and with synaptic adhesion molecules such as EphBs, neuroligins, and ErbBs (McMahon and Diaz, 2011; Siddiqui and Craig, 2010; Tallafuss et al., 2010). Dynamic glutamate receptor trafficking is not only important for normal brain function, but deficits in trafficking are associated with diseases including Alzheimer's disease, addiction and schizophrenia (Lau and Zukin, 2007; Opazo and Choquet, 2010).

Numerous cell signaling and adhesion molecules coordinate the differentiation, morphological changes, and precise organization of proteins required to generate a functional synapse (Dalva et al., 2007; McMahon and Diaz, 2011; Shen and Scheiffele, 2010; Siddiqui and Craig, 2010; Tallafuss et al., 2010). An important member of these multifunctional synaptogenic molecules are the EphBs (Chen et al., 2011; Klein, 2009; Lai and Ip, 2009; Sloniowski and

Ethell, 2011). The EphBs are part of the larger Eph (erythropoietin-producing hepatocellular carcinoma) family of receptor tyrosine kinases (RTKs), which is the largest family of RTKs in the human genome. The Eph receptors are divided into two classes (A and B) by their ability to bind their membrane-attached ephrin ligands. In mammals there are nine members of the EphA class (A1-A8, A10) and five members of the EphB class (B1-B4, B6) (Klein, 2009). Ephrin-As (A1-A5) are attached by a Glycophosphatidylinositol (GPI) anchor, whereas ephrin-Bs (B1-B3) contains a short intracellular signaling domain (Egea and Klein, 2007). For the most part, EphAs specifically bind ephrin-A ligands, and EphBs bind ephrin-B ligands. However, EphA4 has a high binding affinity for ephrin-B ligands, and EphB2 binds ephrin-A5 (Flanagan and Vanderhaeghen, 1998; Himanen et al., 2004). Generally, Ephs act to coordinate signaling events that occur between cells including: axon guidance, synaptogenesis, dendritic filopodia motility, neural crest cell and stem cell migration, angiogenesis, cell sorting at compartmental boundaries, bone formation, and synaptic plasticity (Genander and Frisen, 2010; Klein, 2009; Lai and Ip, 2009; Pasquale, 2008; Suetterlin et al., 2011).

This review will focus on the role of EphB/ephrin-B signaling mechanisms that control NMDAR function and localization. We will highlight how EphB-dependent misregulation of NMDARs contributes to synaptic diseases such as neuropathic pain, anxiety disorders, and Alzheimer's disease.

**EphBs and Synapse Formation**

*In vivo* and *in vitro* evidence suggest that there is a rapid phase of synapse addition early in neuronal development followed by a plateau phase, and later synaptic loss as contacts begin to mature (Kayser et al., 2008; Papa et al., 1995; Ziv and Smith, 1996). During the phase of rapid synaptogenesis, dendrites and axons have motile filopodia that appear to search for contacts. Different molecules control specific aspects of new synapse accumulation: SynCAM1 restricts the number of filopodia at axonal growth cones (Stagi et al., 2010), neuroligin stabilizes dendritic filopodia (Chen et al., 2010), and EphBs controls dendritic filopodia motility enabling synapse formation (Kayser et al., 2008). EphB-dependent synapse formation driven by filopodia motility requires ephrin-B binding, EphB kinase activity, and p21 activated kinase (PAK) (Kayser et al., 2008). These data are consistent with a model (Figure 1) in which filopodia find appropriate target axons, and motility subsequently decreases leading to stabilized synaptic contacts. Next, through transynaptic interactions with ephrin-Bs, EphBs initiate a program of pre- and postsynaptic maturation through both extracellular protein-protein interactions and intracellular signaling.

EphBs organize functional presynaptic specializations by binding specific ephrin-B ligands at sites of contact between dendrites and axons (Kayser et al., 2006; McClelland et al., 2009). The number of presynaptic specializations is decreased by knockdown of postsynaptic EphB2 or presynaptic ephrin-B1 or ephrin-B2 (Ethell et al., 2001; Kayser et al., 2006; McClelland et al., 2009). Ephrin-B1 and ephrin-B2 organize presynaptic terminals through interactions with

presynaptic scaffolding molecules containing PDZ-binding domains. Specifically, ephrin-Bs recruit the adaptor protein syntenin-1 to new presynaptic sites (McClelland et al., 2009). Mixed culture assays indicate that the syntenin-1 is required in contacting axons for EphB-dependent presynaptic specializations (McClelland et al., 2009). Syntenin-1 could then recruit synaptic vesicles by interacting with ERC2/CAST1/RM1 (Ko et al., 2006). Together, these results provide a direct link (**Figure 1.1**) from postsynaptic EphB through presynaptic ephrin-B1/2 and syntenin-1 to formation of functional presynaptic specializations.

EphBs regulate maturation of postsynaptic sites by inducing spine morphogenesis and recruiting neurotransmitter receptors. Consistent with their importance in these functions, in *EphB1*$^{-/-}$*, 2*$^{-/-}$*, 3*$^{-/-}$ triple knockout (TKO) mice there is a significant reduction in excitatory synapse density (~40% cortex, ~25% hippocampus) (Henkemeyer et al., 2003; Kayser et al., 2006). The effects of EphBs on spine development appear similar in cortex and hippocampus. Spine density and postsynaptic density size are reduced in the hippocampus of EphB TKO animals (Henkemeyer et al., 2003). Similarly, synapse and spine density are decreased in the cortex of EphB TKO, but not DKO animals (Kayser et al., 2006). In the cerebellum it appears that EphBs may act differently because EphB TKO mice have increased numbers of spines (Cesa et al., 2011). However, these may be so called “naked” spines that lack presynaptic specializations and are associated with defective synaptogenesis in the cerebellum (Hendelman and Aggerwal, 1980). More work will be need to resolve the mechanisms mediating these differences in EphB function.

Changes in spine and synapse density in the cerebral cortex are likely due to the decreases in dendritic filopodia motility (Kayser et al., 2008). Filopodia motility is impaired in cortical slices from EphB TKO, but not DKO animals (Kayser et al., 2008). Interestingly in cultured hippocampal neurons, expression of any EphB is sufficient to rescue defects in synapse development (Henkemeyer et al., 2003). This finding suggests that any EphB is sufficient to initiate EphB-dependent synaptogenesis. Similarly, re-expression of EphB2 in EphB TKO slices rescues deficits in synapse density and spine formation (Kayser et al., 2006). Although EphBs may play redundant functions, individual EphBs appear to exert their effects on specific circuits or domains of neurons. The pattern of EphB expression in the hippocampus reflects the possibility of localized function: EphB2 and EphB3 are expressed in CA1, and EphB2 and EphB1 are expressed in CA3 (Henderson et al., 2001; Henkemeyer et al., 2003; Liebl et al., 2003). In the cortex, EphBs appear to preferentially affect dendritic protrusions in basal dendrites of pyramidal neurons (Kayser et al., 2011). Together, these finding suggest that in addition to regulating synapse formation, specific EphB family members may have selective functions in different brain regions.

EphBs control neuronal morphology and motility by modulation of the actin cytoskeleton. EphBs exert these effects through GTPases such as Rho, Rac1, and Cdc-42 (Klein, 2009; Sloniowski and Ethell, 2011), by activation of the actin-severing protein cofilin (Shi et al., 2009; Simon et al., 2009), and by the phosphorylation of the cell surface proteoglycan syndecan-2 (Ethell et al., 2001). A principle mechanism enabling EphBs to signal to the actin cytoskeleton is by

interacting with guanine exchange factors (GEFs), which accelerate the exchange of GDP for GTP (Klein, 2009; Sloniowski and Ethell, 2011). EphBs interact directly with GEFs such as Rho/Rac1-GEF Kalirin-7(Penzes et al., 2003), Rac1-GEF Tiam1 (Tolias et al., 2005; Tolias et al., 2007), and with Rho-GEF intersectin-1 through the adaptor protein Numb (Irie and Yamaguchi, 2002; Nishimura et al., 2006) recruiting these proteins to synapses and spines. In addition to their interaction with EphBs, intersectin-1 and Tiam1 can associate directly with NMDARs at synaptic sites to modulate receptor function (Irie and Yamaguchi, 2002; Nishimura et al., 2006; Tolias et al., 2005; Tolias et al., 2007). By linking to both Rac1 and Rho/Cdc-42 signaling pathways, EphBs can prevent depolymerization of the actin cytoskeleton. Preventing depolymerization drives synapses to mature and form mushroom shaped spines.

In addition to coupling with positive regulators of synapse development, the synaptogenic activities of EphBs are subjected to a specific negative regulatory pathway. EphB activity is inhibited by binding the RhoA-GEF called Ephexin5 (Margolis et al., 2010). Ephexin5's inhibition of EphB is released by ephrin-B activation of EphBs (Margolis et al., 2010). EphB activation causes phosphorylation of Ephexin5 on tyrosine-361 that enables the E3 ligase Ube3A to bind and ubiquitinate Ephexin5 (Margolis et al., 2010). Then ubiquitinated Ephexin5 undergoes proteasomal degradation, which allows EphBs to initiate synapse formation (Margolis et al., 2010). Notably, Ephexin5 knockout mice have increased synapse number (Margolis et al., 2010). Consistent with a negative regulatory function, overexpression of Ephexin5 reduces the number of excitatory

synapses (Margolis et al., 2010). Intriguingly, these findings link EphBs to human cognitive disorders: Angelman syndrome (AS) and Autism Spectrum Disorders (ASDs). Mutations or deletions of Ube3A are a cause of AS and duplications in the 5q11–q13 locus, which includes Ube3A, are found in genetic forms of ASDs (Mabb et al., 2011). Whether these diseases result from a misregulation of Ube3a function during synapse maturation (Yashiro et al., 2009), or regulation of AMPAR trafficking (Greer et al., 2010) remains to be elucidated. However, these findings place EphB signaling pathways in a key position to regulate diseases of cognitive dysfunction.

As neurons mature, synapse addition slows while synaptic function becomes more stable and reliable (Papa et al., 1995; Ziv and Smith, 1996). EphBs also act as central organizers to coordinate these events. In the mature cerebral cortex and hippocampus, both immuno-electron microscopy and biochemical fractionation experiments indicate that EphBs are localized to the pre- and postsynaptic terminal suggesting that EphBs continue to play a role at mature synapses (Bouvier et al., 2008; Buchert et al., 1999; Nolt et al., 2011). However, EphBs are not critical to maintain synapse density once synapses have formed (Kayser et al., 2008). Thus, if EphB2 expression is reduced with shRNA knockdown at mature synapses (DIV14-21), there is no effect on synapse density (Kayser et al., 2008). Moreover, overexpression of EphB2 in neurons from TKO mice rescues synapse density early in development (DIV3) but fails to rescue synapse formation when expressed later (DIV10) (Kayser et al., 2008). These findings suggest that EphBs control synaptogenesis selectively during the rapid

phase of synapse addition (DIV0-14) (Kayser et al., 2008). Interestingly, Ephexin5 expression is down regulated as EphBs begin to function to control synaptogensis (DIV7-8) (Margolis et al., 2010; Sahin et al., 2005) suggesting a possible restrictive mechanism. After synapses begin to mature (>DIV14), EphBs are not required for synapse maintenance and function of EphBs appears to shift to the regulation of synaptic function. While it remains to be determined what causes this change in EphB function, the role of EphBs in the mature brain is the focus of the next two sections of this review.

**EphB Trafficking and Regulation of AMPARs**

Receptors undergo regulated delivery to the plasma membrane and removal from the cell surface (Andersson, 2011; Conner and Schmid, 2003). For EphBs, receptor trafficking is critical to coordinate pre- and postsynaptic formation, and to regulate glutamate receptor function, while EphB receptor cleavage and internalization may mediate detachment of contacts and repulsion (Cowan et al., 2005; Egea and Klein, 2007; Lin et al., 2008; Litterst et al., 2007; Marston et al., 2003; Pitulescu and Adams, 2010; Zimmer et al., 2003). Although the mechanisms controlling EphB delivery to the membrane are poorly understood, work from non-neuronal and neuronal systems demonstrate that EphB membrane localization is tightly regulated (Egea and Klein, 2007; Fasen et al., 2008; Pitulescu and Adams, 2010). The key points of regulation are EphB receptor cleavage, internalization, and degradation (Pitulescu and Adams, 2010). Activated EphBs undergo proteolytic processing by ADAM10 and matrix

metalloproteinases (MMPs) (Lin et al., 2008; Litterst et al., 2007). To enable events such as growth cone collapse, the EphB2 receptor can be endocytosed via clathrin-mediated mechanisms, ubiquitinated, and targeted for degradation in the proteasome (Andersson, 2011; Fasen et al., 2008; Margolis et al., 2010; Pitulescu and Adams, 2010). Interestingly, the entire EphB-ephrin-B receptor-ligand complex can be trans-endocytosed bidirectionally into the EphB or ephrin-B expressing cell (Marston et al., 2003; Zimmer et al., 2003). Although what differentiates amoung these various modes of receptor trafficking is poorly understood, receptor trafficking is clearly important for regulation of synaptic proteins.

EphBs can regulate both surface localization and function of AMPA-type glutamate receptors (**Figure 1.2**). In cultured neurons, EphB2 and AMPARs associate by each binding to the PDZ-adaptor proteins PICK1 and GRIP1 (Contractor et al., 2002; Torres et al., 1998). Both PICK1 and GRIP1 bind directly to AMPARs and are thought to act in opposition: GRIP1 promotes AMPAR surface retention, while PICK1 acts to remove AMPARs from the cell surface (Lu and Roche, 2011). However, a link between PICK1, EphB2 and AMPAR trafficking has not been shown (Calo et al., 2006). Instead, PICK1 appears to cluster EphB/ephrin-Bs at synaptic sites (Torres et al., 1998). In neurons, GRIP1 appears to help localize both EphB2 and GluA2-containing AMPARs to the dendritic plasma membrane (Hoogenraad et al., 2005). Consistent with a role for EphBs in control of AMPAR trafficking, EphBs are important for retention of AMPARs in the receptor recycling pool (Kayser et al., 2006). This control of

AMPAR trafficking requires ephrin-B activation, the PDZ-binding domain, and kinase activation of EphB2 receptors (Kayser et al., 2006). EphB-dependent internalization of AMPARs likely relies on synaptojanin-1, which is phosphorylated by EphB2, promoting its activation (Irie et al., 2005). Since GRIP1 and PICK1 preferentially interact with the GluA2 subunits, which regulate calcium influx through AMPARs (Bredt and Nicoll, 2003; Kessels and Malinow, 2009; Lu and Roche, 2011), these findings suggest that EphB receptors may be an important regulator of AMPAR subunit composition at synaptic sites.

Physiological evidence demonstrates that EphBs modulate AMPAR function at synapses. The AMPAR-dependent component of mEPSC in mature (DIV21-23) neurons can be increased by EphB2 overexpression, and reduced by knockdown of EphB2 (Nolt et al., 2011). However, consistent with the different developmental functions of EphB2, knockdown of EphB2 in younger neurons has no effect on mEPSC amplitude (Kayser et al., 2006). The changes in AMPAR currents may be explained by the observation that levels of GluA2 in EphB TKO mice are unchanged at cortical synapses compared to wild-type mice (Nolt et al., 2011). These observations suggest that EphBs may act to regulate synaptic AMPAR subunit composition rather than overall number. However, additional work is required to demonstrate the overall impact of EphB-dependent regulation of AMPARs.

## EphBs and NMDA Receptors

EphB receptors regulate multiple facets of NMDAR surface localization, function, and downstream signaling. EphBs and NMDARs colocalize at synaptic sites, and mice lacking EphB2 have reduced levels of NMDARs at synapses in the hippocampus and cortex (Dalva et al., 2000; Henkemeyer et al., 2003; Kayser et al., 2006). Upon ephrin-B binding, EphBs interact directly with NMDARs through their extracellular domains (Attwood et al., 2011; Dalva et al., 2000; Grunwald et al., 2001; Slack et al., 2008). However, the specific region of the extracellular domains involved in this interaction for both EphB2 and the NMDAR remains to be identified. Ephrin-B activation of EphBs not only induces the EphB-NMDAR interaction, but also potentiates NMDAR function (Dalva et al., 2000; Takasu et al., 2002). Ephrin-B activation of the EphB-NMDAR interaction causes src kinase-dependent phosphorylation of the NR2B subunit of the NMDAR at tyrosines 1226, 1336 and 1472 (Takasu et al., 2002). Phosphorylation at tyrosine 1472 of NR2B-containing NMDARs blocks binding of the AP-2 complex preventing clathrin-mediated endocytosis (Chen and Roche, 2007). Thus, the EphB-NMDAR interaction can increase the surface retention of NR2B-containing NMDARs. Additionally, EphB2 can increase calcium influx through NR2B-containing NMDARs by decreasing calcium-dependent inactivation rates (Nolt et al., 2011; Takasu et al., 2002). Notably, EphB2 does not appear to act similarly on calcium inactivation of NR2A-containing NMDARs (Nolt et al., 2011). The enhanced calcium influx through the NMDAR also results in enhanced downstream gene transcription (Takasu et al., 2002). In EphB TKO mice there is

a reduction in NR2B at synaptic sites in cerebral cortex and cultured hippocampal neurons (Henkemeyer et al., 2003; Kayser et al., 2006). At the mature synapse, knockdown of EphB2 causes a reduction in mEPSC amplitude and NMDAR-dependent decay time (Nolt et al., 2011). Similarly, overexpression of EphB2 causes an increase in mEPSC amplitude and NMDAR-dependent decay time (Nolt et al., 2011). This study specifically implicated NR2B-containing NMDAR being trafficked onto the surface at synaptic sites after ephrin-B activation in the mature brain (Nolt et al., 2011). Interestingly, a recent report suggests that EphBs may also interact with and regulate the function of nAChRs (Liu et al., 2008), suggesting the possibility that EphBs play a larger role in the regulation of neurotransmitter function than previously appreciated. Regardless, these data support a model (**Figure 1.2**) where EphBs are not required for synapse maintenance, but are instead critical regulators of NMDAR localization, function, and signaling in the mature brain.

The extracellular domain mediated EphB-NMDAR interaction has also been implicated in NMDAR-dependent forms of hippocampal synaptic plasticity, particularly for EphB2. *EphB2*$^{-/-}$ null mice have reduced synaptic NMDAR, but not AMPAR currents, reduced long-term potentiation (LTP), and long-term depression (LTD) (Grunwald et al., 2001; Henderson et al., 2001). Importantly, these effects are rescued by transgenic expression of a truncated EphB2 receptor lacking its kinase domain (Grunwald et al., 2001). These data suggest that EphB-dependent regulation of synaptic plasticity requires the extracellular domain-mediated interaction between EphB and the NMDAR. Consistent with

these deficits in synaptic plasticity, *EphB2*$^{-/-}$ mice perform poorly in behavioral learning tasks such as the Morris water maze (Grunwald et al., 2001). Taken together, these data imply that the EphB-NMDAR interaction is required for proper synaptic function, synaptic plasticity, and behavior.

## EphB-NMDAR Interaction in Disease

There is a growing body of evidence that suggests a synaptic origin for diseases of neuronal development and in the aging brain. Proper NMDAR synaptic localization and function has long been placed at the epicenter of these synaptopathies. By direct interaction and functional modulation of the NMDAR, EphBs and ephrin-Bs appear to be key synaptic regulators implicated in many of these diseases. Specifically, we will discuss three examples of EphB/ephrin-B signaling in disease: neuropathic pain, anxiety disorders and Alzheimer's disease (AD).

### *Neuropathic pain and hyperalgesia*

Control of NMDAR function by EphBs plays a critical role in the enhancement of pain. In the spinal cord and periphery, neuropathic pain (chronic pain caused by injury) and hyperalgesia (increased sensitivity to painful stimuli) are linked to EphB1/ephrin-B signaling through modulation of NMDAR function. Remarkably, in four different models of pain - thermal hyperalgesia, spontaneous, crush, and mechanical allodynia - EphB1 functions similarly (**Figure 1.3**). Despite differences in models, neurons, and brain regions

mediating pain, downstream signaling mechanisms are well conserved. Therefore, EphB-dependent modulation of NMDAR function may be an important target for the control of pain.

Induction of neuropathic pain in the spinal cord is mediated by dysregulation of excitatory glutamatergic synapses between the axons from sensory neurons in the dorsal root ganglia (DRG) and second-order neurons in the dorsal horn (DH) (Kuner, 2010). At the DRG-DH synapses, induction of neuropathic pain depends on NMDAR function (Kuner, 2010). Specifically, NMDAR dependent LTP-like changes in synaptic strength are suggested as the cellular mechanism for pain amplification and hyperexcitability of the DRG-DH circuit (Kuner, 2010).

The levels of ephrin-B1, ephrin-B2, and EphB1 expression are upregulated after injury in the DRG and spinal cord suggesting that these proteins are involved in the response to pain (Kobayashi et al., 2007; Song et al., 2008a; Song et al., 2008b). Indeed, intrathecal injection of EphB1/B2-Fc or shRNA against ephrin-B2 prevents EphB/ephrin-B signaling, and decreases hyperalgesia and mechanical allodynia suggesting a role for EphB signaling in regulation of pain after injury (Kobayashi et al., 2007; Song et al., 2008b). Moreover, injection of ephrin-B2-Fc to activate EphBs induces pain (Battaglia et al., 2003; Conover et al., 2000; Slack et al., 2008; Song et al., 2008b).

EphB-dependent modulation of NMDAR function appears to drive EphBs' function in pain responses (**Figure 1.3**). Similar to the cerebral cortex, injury induced upregulation of EphB1 and ephrin-B expression appear to directly

modulate the function of NR2B-containing NMDARs. EphB-dependent hyperalgesia depends upon tyrosine phosphorylation of NR2B in the spinal cord (Guo et al., 2002), while blocking NMDARs and src kinase activity is sufficient to prevent hyperalgesia (Battaglia et al., 2003; Slack et al., 2008; Song et al., 2008b). As expected from work on the EphB-NMDAR interaction, src kinase exerts its effects by phosphorylating NR2B at Y1472 (Dalva et al., 2000; Slack et al., 2008; Takasu et al., 2002). EphB-dependent regulation of NMDAR function also appears to regulate the changes in synaptic strength thought to underlie induction and maintenance of hyperalgesia. In the spinal cord, EphB activation lowers the threshold for LTP induction and increases phosphorylation of NR2B-containing NMDARs (Battaglia et al., 2003; Song et al., 2008b). Moreover, inhibition of EphB signaling blocks pain-induced activity-dependent gene transcription of the immediate early gene *c-Fos* (Battaglia et al., 2003; Song et al., 2008b). These findings suggest that EphB/ephrin-B signaling is critical for suppressing the injury-induced hyperexcitability of the DRG-DH circuit.

EphB-dependent neuropathic hyperalgesia appears to be mediated specifically by EphB1. EphB1 is expressed at high levels in the spinal cord, and *EphB1*$^{-/-}$ and *EphB1*$^{+/-}$ mice have significantly reduced thermal hyperalgesia and pain-induced hyperexcitablity of DH neurons (Han et al., 2008; Liu et al., 2009). Consistent with the importance of EphB1 in control of pain sensitivity, *EphB1*$^{-/-}$ mice show defects in enhancement of pain after morphine-induced withdraw (Han et al., 2008). EphB1 appears to be the only EphB receptor required for ephrin-B1 induced hyperalgesia because treatment with ephrin-B1-Fc has no

effect on pain sensitivity in *EphB1*$^{-/-}$ or *EphB1*$^{+/-}$ mice (Han et al., 2008). These changes in hyperalgesia in *EphB1*$^{-/-}$ mice are linked to NMDAR-dependent increases in p-CaMKII, p-ERK and p-CREB and the induction of *c-fos* expression (Han et al., 2008; Liu et al., 2009). Interestingly, EphB1 upregulation after injury appears to be dependent on MMP-2/9, although the specific signaling mechanisms remain to be determined (Liu et al., 2011).

The EphB-dependent modulation of NMDAR function is also critically important in pain sensitivity outside of the spinal cord in the periphery. As in the spinal cord, in the peripheral nervous system injection of ephrin-B1-Fc, which activates EphBs, induces hyperalgesia dependent on NMDARs (Cao et al., 2008; Guan et al., 2010; Ruan et al., 2010). This leads to increased *c-fos* expression and activation of NMDAR-dependent phosphorylation of two pathways: MAPKs (p-p38, pERK and pJNK) (Cao et al., 2008; Ruan et al., 2010) and PI3K, Akt, and ERK (Guan et al., 2010). Taken together, these results suggest that in the periphery a similar mechanism for hyperalgesia occurs with EphB1 upregulation, NMDAR-dependent phosphorylation of targets required for synaptic plasticity, and changes in gene transcription.

Similar to the central and peripheral pain mechanisms, the EphB-dependent modulation of NMDAR function is implicated in cancer-induced pain for both bone and pancreatic cancer. In models of cancer-induced pain, expression of ephrin-B1 and EphB1 are upregulated (Dong et al., 2011; Liu et al., 2011; Orikawa et al., 2010). Here, the EphB-NMDAR interaction is also specifically implicated because blocking EphB1 signaling alleviates mechanical

allodynia (Liu et al., 2011). The mechanism for this alleviation is decreased activation of NR2B-containing NMDARs, which reduces the phosphorylation of downstream targets pSrc (Tyr418), pERK1/2, pCaMKII, and pCREB, and gene transcription of *c-fos* (Liu et al., 2011). The changes in EphB and ephrin-B1 expression in cancer-induced pain are likely to be downstream of the inflammatory cytokines IL-1β, IL-6 and TNF-α (Dong et al., 2011). Consistent with this, inhibiting the CCK2/gastrin receptor with a drug (Z-360) reduces IL-1β levels, prevents upregulation of ephrin-B1 expression, and reduces NR2B phosphorylation in models of cancer pain (Orikawa et al., 2010). The observation that blocking EphB1 with EphB receptor bodies also alleviates morphine tolerance in models of bone cancer pain (Liu et al., 2011) suggests that modulating EphB receptor signaling may be a promising avenue for treating chronic pain. More broadly, there is extensive evidence linking EphB-dependent regulation of NMDAR function to the induction and expression of chronic pain.

*Anxiety*

Emerging evidence links both regulation of EphB receptor cleavage and EphB-dependent regulation of NMDAR function to anxiety (**Figure 1.4**). Severe or sustained stress can result in changes to synaptic architecture and function mirroring those found after induction of synaptic plasticity, and lead to behavioral changes associated with fear and anxiety disorders (Lupien et al., 2009). The pathogenic plasticity involved in these changes requires NMDAR activation and increases neuronal activity in the hippocampus and amygdala (Lupien et al.,

2009). Antagonists of NMDAR receptors can produce anxiolytic effects in animal models of anxiety like the elevated plus maze (Barkus et al., 2010). Several lines of evidence suggest that changes in the extracellular matrix mediated by proteolysis promote an anxiety response (Lohman et al., 2009; Matys et al., 2004; Pawlak et al., 2003; Pawlak et al., 2005). The serine protease neuropsin (also known as kalikrein-related peptidase 8) is highly expressed in the hippocampus and amygdala (Chen et al., 1995). Furthermore, genetic variations in human neuropsin are associated with bipolar disorder and cognitive functions (Izumi et al., 2008). Neuropsin-deficient mice have defects in spatial working memory, impaired ability in the Morris water maze assay, and reduced long-lasting LTP (Chen et al., 1995; Ishikawa et al., 2008b; Matsumoto-Miyai et al., 2003; Tamura et al., 2006). In the amygdala, EphB2 and neuropsin colocalize and neuropsin expression is upregulated after stress (Attwood et al., 2011; Izumi et al., 2008). Furthermore, neuropsin upregulation and colocalization with EphBs in the amygdala result in cleavage of the EphB2 ectodomain (Attwood et al., 2011; Izumi et al., 2008). Neuropsin-dependent cleavage of EphB2 decouples the EphB-NMDAR interaction, likely explaining the changes in NMDAR currents observed in neuropsin null mice (Attwood et al., 2011). Furthermore, injection of function blocking antibodies to EphB2 or neuroposin can prevent behaviorally stress-induced anxiety in the elevated plus maze task (Attwood et al., 2011). Taken together, these data suggest that targeting neuropsin-dependent cleavage of EphB2 is a potential strategy for treating stress-related and anxiety disorders.

In models of stress, EphBs appear to increase the amount of NMDAR currents at the synapse after neuropsin-dependent cleavage (Attwood et al., 2011). One potential explanation for the molecular mechanism of these findings comes from the studies on γ-secretase cleavage of EphB2 (Litterst et al., 2007; Xu et al., 2009). Intriguingly, after MMP-dependent cleavage of the EphB2 extracellular domain, the γ-secretase releases a kinase-active fragment in non-neuronal cells (Xu et al., 2009). Expression of a soluble kinase active intracellular fragment was shown to phosphorylate NR2B subunits of NMDARs, resulting in increased NMDAR surface localization (Xu et al., 2009). Whether a similar mechanism plays a role in neurons remains to be determined. However, these non-neuronal experiments raise the possibility that EphBs may regulate NMDAR function both through direct interactions and by indirectly phosphorylating the NMDAR. It will be important to determine whether direct or indirect interactions between EphBs and the NMDAR are important for anxiety.

*Alzheimer's disease*

EphB-dependent modulation of NMDAR function appears to play a role in the pathogenesis of Alzheimer's disease (AD). AD is a progressive neurodegenerative disorder characterized by declarative memory defects and dementia (Walsh and Selkoe, 2004). Among the many pathological changes seen in patient brains is the loss of excitatory synapses and increased neuronal death (Penzes et al., 2011; Selkoe, 2002). The reduction in synapse density in the cortex and hippocampus is found early during the onset of AD and correlates

with the level cognitive impairment (Penzes et al., 2011; Selkoe, 2002). These observations suggest that elucidating the underlying mechanisms causing deficits in synaptic function will be important to understanding the disease. AD patient data links EphBs and NMDARs with the observation that both EphB and NMDAR subunit expression is reduced early in AD progression (Ikonomovic et al., 1999; Simon et al., 2009; Sze et al., 2001). In addition, there are reduced levels of NR2 subunit phosphorylation in AD patient brains (Sze et al., 2001).

Building on these observations in patients, work has focused on whether these effects on NMDAR expression are linked to prominent disease mechanisms such as amyloid-β (Wilcox et al., 2011). In patients with AD, the level of a 40- or 42-amino acid peptide called amyloid-β (Aβ) in the brain correlates with disease onset and progression (Wilcox et al., 2011). In mouse models and in cell culture, the presence of Aβ can cause NMDAR endocytosis, reduced surface expression of NMDARs, and reduced NMDAR currents (Snyder et al., 2005). Also in mouse models of AD, the Aβ-dependent reduction in EphB2 expression levels occurs prior to detectable behavioral impairments (Simon et al., 2009). Interestingly these effects appear more pronounced on NR2B-containing NMDARs (Snyder et al., 2005).

Recently, a strong link has emerged between EphB2, Aβ, and Alzheimer's disease through NMDAR phosphorylation and regulation at the plasma membrane (**Figure 1.4**). Consistent with experiments demonstrating reduced EphB2 expression levels in AD (Simon et al., 2009), Aβ binds to the extracellular FnIII domains of EphB2, causing receptor internalization and degradation (Cisse

et al., 2011). The functional consequence of the removal of EphB2 from the cell surface by Aβ appears to be reduced NMDAR surface expression (Cisse et al., 2011). Furthermore, EphB2 depletion by knockdown or knockout, can phenocopy the Aβ-dependent reduction in NMDAR surface localization (Cisse et al., 2011; Nolt et al., 2011). Similarly, targeted knockdown of EphB2 in the dentate gyrus causes deficits in LTP and NMDAR (but not AMPAR) currents (Cisse et al., 2011). These findings are consistent with previous observations on the effects on LTP in mice lacking EphB2 and on synaptic function following the knockdown of EphB2 in cortical neurons (Dalva et al., 2000; Grunwald et al., 2001; Henderson et al., 2001; Nolt et al., 2011). The effects of targeted knockdown of EphB2 in the dentate gyrus are mirrored in the hAPP overexpressing mouse (Cisse et al., 2011). Not only does knockdown of EphB2 cause defects in LTP, but viral overexpression of EphB2 in the dentate gyrus of hAPP overexpressing mice rescues LTP and NMDAR current deficits to wild-type levels (Cisse et al., 2011). Remarkably, targeted overexpression of EphB2 in the dentate gyrus rescues hippocampal-dependent cognitive deficits in the Morris water maze in hAPP mice (Cisse et al., 2011). These effects were seen despite infection of a relatively low percentage of neurons in the dentate gyrus, suggesting that functional modulation of synapses for only a subset of neurons in a network can have significant effects on behavior. In summary, increasing neuronal EphB2 levels in hAPP mice reversed cognitive and behavioral defects associated with AD, while EphB2 knockdown appears to mimic many of the defects in NMDAR function in

these mice. Therefore, these findings suggest that Aβ may principally dysregulate synaptic and NMDAR function in AD.

**Conclusions and future directions**

EphBs regulate excitatory synapse development and function at mammalian synapses by controlling dendritic morphology and excitatory neurotransmitter receptor content. Dysfunction of EphB-dependent control of synaptic NMDAR function and surface localization appears to lead to profound synaptopathy including AD and pain. In each of these diseases, the role of EphBs is linked to direct extracellular interaction between EphB and the NMDAR. However, the domain mediating this interaction has yet to be identified (see Outstanding Questions). In anxiety, EphB-dependent regulation of NMDAR function is also important, but may be regulated by a different mechanism governed by the release of the EphB intracellular domain. However, in these three cases, EphB-dependent regulation of NMDAR function and surface localization has profound consequences. Given the potential significance for modulation of the EphB-NMDAR in treating human disease, understanding the mechanisms enabling these proteins to interact will be of significant importance.

It will be especially important for future work to understand the extracellular nature of the EphB-NMDAR interaction. One intriguing idea is that since the EphB-NMDAR interaction occurs in the extracellular space, the interaction may be dependent on an extracellular modification to either protein such as extracellular phosphorylation. Phosphorylation of residues destined to

be extracellular has been shown to be critical to Drosophila limb and wing development *in vivo* (Ishikawa et al., 2008a). Soluble and membrane-attached protein kinases have been found in neurons to regulate synaptic plasticity and aggregation of Aβ in AD patients (Chen et al., 1996; Fujii et al., 2000; Kumar et al., 2011; Redegeld et al., 1999). Furthermore, the extracellular domain of EphB2 receptors is phosphorylated after ligand binding (D.S.S., T.A.N., S.I.S-C, and M.B.D., *unpublished observations*). Thus, extracellular phosphorylation appears to an underappreciated mechanism for disease, and a potential modifier of the EphB-NMDAR interaction.

In addition to EphBs, a number of other regulators of synapse development have developmental shifts in function. Focal adhesion kinase (Moeller et al., 2006; Shi et al., 2009), synCAM (Robbins et al., 2010), SALM1/2 (Ko et al., 2006; Wang et al., 2006), and neuroligin/neurexin (Sara et al., 2005; Varoqueaux et al., 2006) all regulate synaptic function in more mature neurons, while controlling synaptogenesis early in development. These findings suggest that synaptic organizing proteins play dual functions, first to generate synapses and later to control their function. The dual function of these proteins could explain some of their complex linkage to disease. We propose that there may be sufficient redundancy in synaptogenic factors that most synapses are still able to form normally after malfunction of any one of these organizers. Once the circuitry begins to mature, however, each of these proteins is required for proper mature synaptic function and breakdowns in these molecules might then manifest as neuronal or cognitive dysfunction. Thus, a better understanding of these synaptic

organizing proteins is needed in three broad areas: 1) to investigate their functions in organizing synapses, 2) to appreciate how the activity of these molecules changes during development, and 3) to determine their different roles in controlling synaptic function. Exploring these three areas will be critical to discerning brain function and treating synaptopathies.

**Outstanding Questions Box:**

- What are the domains on EphBs and the NMDAR that mediates the EphB-NMDAR interaction?
- How do EphBs differentially regulate downstream GEF signaling pathways?
- Does Ephexin-5 signaling contribute to autism spectrum disorders?
- What is the mechanism for EphBs in regulating the function of NR2B-containing NMDARs?
- Do EphBs regulate AMPARs at mature synapses?
- How is the activity of EphBs switched from synaptogenesis to synaptic maintenance?
- Are there pharmacological agents that can block the EphB-NMDAR interaction for neuropathic pain?
- What is the specific domain for Aβ binding to EphB2?
- Are there pharmacological agents that can potentiate the EphB-NMDAR interaction for human cognitive disorders?

**Glossary Box:**

**Adaptor protein:** A protein with multiple protein-protein interaction domains that recruits other proteins to a signaling complex.

**Allodynia:** Pain caused by an innocuous stimulus.

**Alzheimer's disease (AD):** The most common form of dementia and a fatal neurodegenerative disease characterized by progressive memory loss, deficits in cognitive ability, and aberrant behavior.

**AMPA receptor:** α-amino-3-hydroxy-5-methyl-4-isoxazolepropionic acid-type ionotropic glutamate receptor.

**Amyloid precursor protein (APP):** Neuronal integral membrane protein concentrated at synaptic sites. Proteolysis of APP first extracellular by Beta-secretase 1 (BACE1) then subsequently γ-secretase generates the 40-42 amino acid β-amyloid (Aβ) found in amyloid plaques of AD patients.

**Angelman syndrome (AS):** Neuro-genetic disorder characterized by intellectual and developmental delay, lack of speech, seizures, and disorders in walking and balance.

**Crush pain model:** Under deep anesthesia a spinal nerve distal to the dorsal root ganglions (DRG) is crushed. Thermal hyperalgesia or mechanical allodynia are then tested.

**Dendritic filopodia:** Thin, motile dendritic process seeking axonal contact and thought to be the precursor of dendritic spine synapses.

**Dendritic spine:** Mushroom-shaped extension from the dendrite equipped with neurotransmitter receptors to review local axonal input.

**DH neuron:** Integration of DRG inputs occurs in deep layers of spinal dorsal horn (DH) neurons. Output is carried to projection sites in the brain.

**DRG neuron:** Nocioceptive afferents carrying noxious stimuli (heat, noxious cold, pressure, or chemicals) have glutamatergic synapses onto relay neurons in the dorsal root ganglion (DRG).

**GTPase:** Small momeric G-proteins which binds and hydrolyzes guanosine triphosphate (GTP) to guanosine diphosphate (GDP) to stimulate downstream effectors.

**Guanine Nucleotide Exchange Factor (GEF):** A protein which activates small monomeric GTPase activity by accelerating the exchange of guanosine diphosphate (GDP) for guanosine triphosphate (GTP).

**Hyperalgesia:** Increased sensitivity to pain.

**Hyperexcitability of DRG neurons:** This is characterized by lower current threshold for action potentials, an increase in spontaneous activity, and repetitive discharge.

**Intraplantar injection:** Injection into the plantar surface of the paw.

**Intrathecal injection:** Injection into the arachnoid membrane of the spinal cord.

**Long-term Depression (LTD):** Prolonged weakening of synaptic inputs.

**Long-term Potentiation (LTP):** Prolonged strengthening of synaptic inputs.

**Mechanical Allodynia model:** The plantar surface of each hind paw with a sharp, cylindrical probe. Incidence of foot withdraw is measured.

**Miniature synaptic current:** Postsynaptic current evoked by single vesicle (or quanta) of neurotransmitter.

**Neuropathic pain:** Chronic pain caused by injury to the central or peripheral nervous system.

**NMDA receptor:** *N*-Methyl-d-aspartate-type ionotropic glutamate receptor.

**PDZ-domain:** A carboxy-terminal protein binding domain named after its three indentifying member proteins (PSD-95, Drosophila discs large protein and Zona Occludens-1).

**Receptor Trafficking:** Active process by which receptor proteins are moved between regions of the cell, and on and off of the plasma membrane.

**Receptor tyrosine kinase (RTK):** Cell-surface localized single-subunit transmembrane protein with intracellular catalytic activity to autophosphorylate and phosphorylate tyrosine residues on signaling substrates.

**RNA Interference (RNAi):** A method using small hairpin RNAs (shRNAs) to bind the mRNA encoding a protein of interest to suppress its expression.

**Spontaneous pain model:** Formalin is subcutaneously injected into a hind paw. Amount of time licking, biting, and flinching on the injected paw is assessed.

**Synaptic cell adhesion molecules (SAMs):** Pairs of molecules that interact across adjacent cells to stabilize the initial contacts between axon and dendrite to form a synapse. SAMs also regulate function of existing synapses through protein-protein interactions and intracellular signaling cascades.

**Thermal hyperalgesia pain model:** Animals are placed in a testing box with a temperature-controlled floor. A heat source is then focused on the hind paw flushed to the floor and foot withdraw latency is measured.

**Figure Legends:**

**Figure 1.1. EphBs regulate excitatory synapse development.** (**a**) The domain structure of the EphB receptor: G - Gobular domain (purple). C - Cistine Rich domain (yellow), F – Fibronectin type III domains (light blue), K – Kinase domain (red), S – SAM domain (green), and P – PDZ binding domain (orange). (**b**) Early in neuronal development (DIV0-10), EphB receptors direct formation of excitatory synapses by regulating motility of filopodia via p21 activated kinase (PAK) and receptor tyrosine kinase activity. (**c**) During the rapid phase of synapse addition (DIV7-14), EphBs interact *in trans* with ephrin-B1 or ephrin-B2 expressed on axons of adjacent cells. This EphB/ephrin-B interaction activates EphB kinase activity, which removes inhibition of synapse formation by the specific negative regulator Ephexin-5. EphB activation phosphorylates Ephexin-5, inhibiting RhoA-GTPase activity, and promoting ubuiqitination and proteasomal degradation of Ephexin-5 by the E3 ligase Ube3A. To promote synapse maturation, EphB kinase activation recruits GEFs to hydrolyze GDP into GTP, activating Rho-GTPases that enable synapse formation through PAK. (**d**) Postsynaptically, EphBs directly cluster NMDA-type glutamate receptors (green) through an extracellular interaction, and cluster AMPA-type glutamate receptors (purple) via a PDZ-domain dependent interaction with GRIP1. Furthermore, EphBs modulate the change in morphology of the actin cytoskeleton into mature mushroom-shaped dendritic spines. Presynaptically, EphBs direct presynaptic differentiation by clustering ephrin-B1 and ephrin-B2 at presynaptic terminals.

The EphB/ephrin-B1/2 interaction recruits the adaptor protein syntenin-1 to these signaling complexes through the PDZ-binding domain of ephrin-Bs. Syntenin-1 enables EphBs to recruit the machinery required for neurotransmitter release to presynaptic specializations.

**Figure 1.2. EphBs regulate glutamate receptor trafficking and function.** (**a**) EphBs regulate AMPAR trafficking through a PDZ-dependent interaction with GRIP1 and indirect interactions with synaptojanin-1 (Stj1), a phosphatidylinositol 5'-phosphatase. If an EphB receptor is interacting with GRIP1, kinase activation by ephrin-Bs promotes AMPAR insertion into the membrane from the recycling pool. Alternatively, EphB kinase activation by ephrin-Bs can also promote AMPAR internalization by phosphorylation of synaptojanin-1, which activates clathrin-mediated endocytotic mechanisms. (**b**) After binding ephrin-B ligand, EphBs directly interact with NMDARs to regulate their synaptic surface localization and function. Activation of EphBs promotes insertion of NR2B-containing NMDARs into the synaptic membrane of mature neurons. Furthermore, after activation, EphBs recruit src kinase to phosphorylate NR2B-constaining NMDARs at Y1472 blocking binding of the AP-2 complex and clathrin-mediated endocytosis. Functionally, EphB activation decreases calcium-dependent desensitization, mEPSC amplitude, and decay time of NR2B-containing NMDAR. This increased calcium influx through NMDARs also leads to EphB-dependent increases in gene expression of *c-fos*.

**Figure 1.3. EphBs and neuropathic pain.** (**a**) Under physiological pain conditions, ephrin-B and EphB1 expression remains low and NR2B-containing NMDAR signaling remains normal. (**b**) For pathological central pain, both ephrin-Bs and EphB1 are upregulated. Activation of EphBs leads to recruitment and activation of src, insertion of NMDARs into the membrane, NR2B phosphorylation at Y1472, and increased calcium influx leading to *c-fos* gene transcription. (**c**) Pathological peripheral pain shares common mechanisms with central pain. However, three parallel signaling pathways have been well characterized leading to gene transcription of *c-fos* and CRE. First, src phosphorylates CamKII, which phosphorylates CREB causing nuclear translocation and CRE gene transcription. Second, PI3K is phosphorylated, which phosphorylates Akt, which phosphorylates ERK, which translocates to the nucleus to activate *c-Fos* gene transcription. Finally, JNK gets phosphorylated and activated, which phosphorylates p-38 and converges to activate ERK. (**d**) Pathological cancer-induced pain shares a remarkable number of the same mechanisms as pathological central and peripheral pain. Unique to cancer-induced pain is that src kinase directly phosphorylates ERK to activate gene transcription of *c-fos*. Additionally, inflammatory cytokines TNFα, IL-6, and IL-1β are upregulated leading to hyperalgesia, and hyperexcitability of nerve afferents.

**Figure 1.4. EphBs and Synaptic Disease.** (**a**) Physiological EphB signaling affects both synaptic plasticity and synapse maturation. Ephrin-B activation of EphBs promotes the direct EphB- NMDAR interaction. This interaction modulates

NMDAR function by increasing calcium influx, inserting new NR2B-containing NMDARs into the membrane, and activating calcium-dependent gene transcription required for LTP. In anxiety disorders, there is a stress-induced upregulation of the serine protease neuropsin (also known as kalikrein-related peptidase 8). At the membrane, neuropsin cleaves the EphB receptor ectodomain, releasing the intracellular domain into the cytosol. This intracellular kinase may be active and able to phosphorylate downstream intracellular targets including NMDARs. Cleavage of the EphB ectodomain dissociates the EphB-NMDAR interaction, leading to NMDAR internalization and activation of Fkbp51 gene transcription in the nucleus. (**b**) In Alzheimer's disease, there is an overabundance of soluble Aβ oligomers, which appear to bind directly to EphB2. The EphB2-Aβ interaction inhibits receptor activation and causes internalization and degradation of both EphBs and NMDARs. Degradation of EphB receptors inhibits their ability to retain NMDARs on the membrane potentially though the EphB-NMDAR interaction. Fewer NMDARs on the cell surface leads to decreased calcium influx and none of the changes in gene transcription required for LTP.

**Acknowledgements**

We thank Dr. S. J. Le Marchand and other members of the Dalva lab for helpful comments, discussions, and advice. We acknowledge the generous support of the National Eye Institute Vision Training Grant (EY007035) to S. I. S-C., and the Dana Foundation, National Institute on Drug Abuse (DA022727), National Institute of Mental Health (MH086425) to M.B.D.

# Figure 1.1

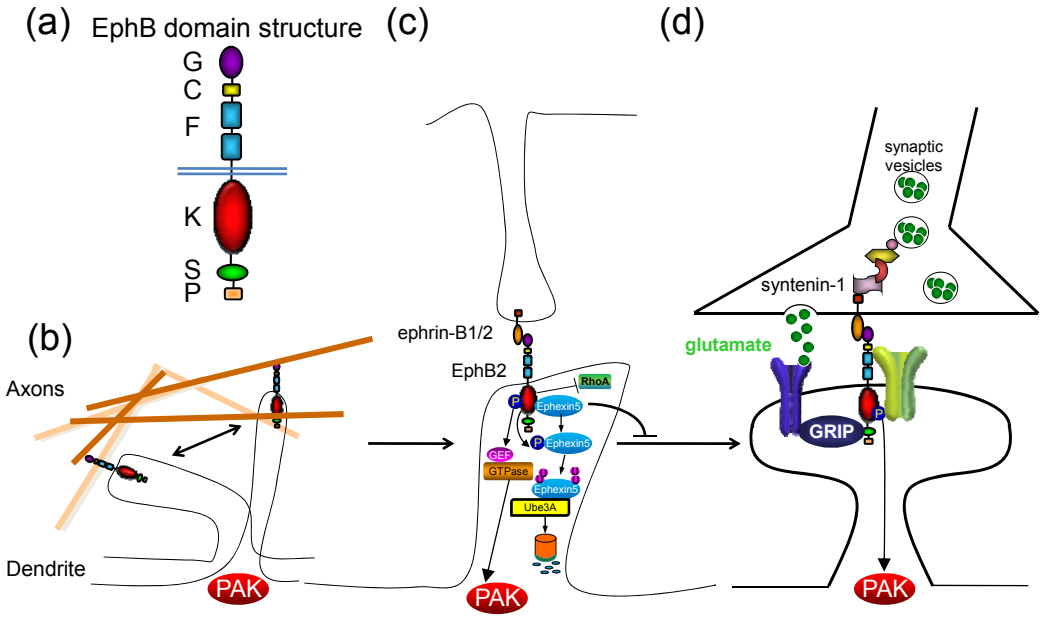
(a) EphB domain structure
G
C
F
K
S
P
(b)
Axons
Dendrite
PAK
(c)
ephrin-B1/2
EphB2
RhoA
Ephexin5
GEF
GTPase
Ube3A
PAK
(d)
synaptic vesicles
syntenin-1
glutamate
GRIP
PAK

# Figure 1.2

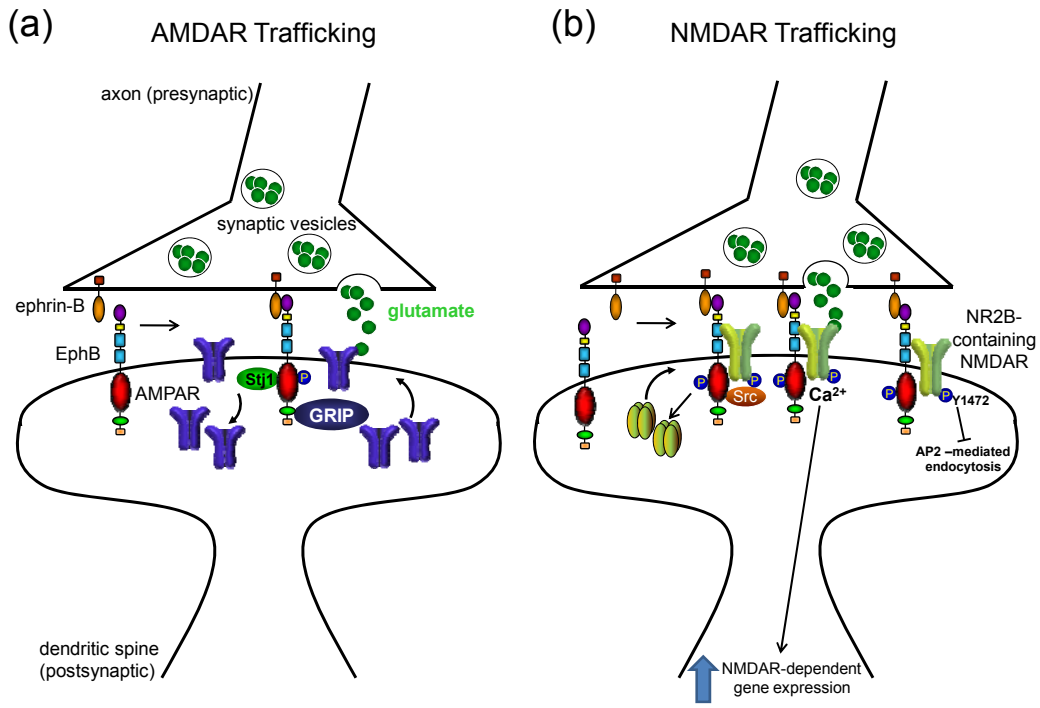
(a)
AMDAR Trafficking
axon (presynaptic)
synaptic vesicles
ephrin-B
EphB
glutamate
AMPAR
Sti1
P
GRIP
dendritic spine
(postsynaptic)
(b)
NMDAR Trafficking
NR2B-
containing
NMDAR
Src
Ca2+
Y1472
AP2 –mediated
endocytosis
NMDAR-dependent
gene expression

# Figure 1.3

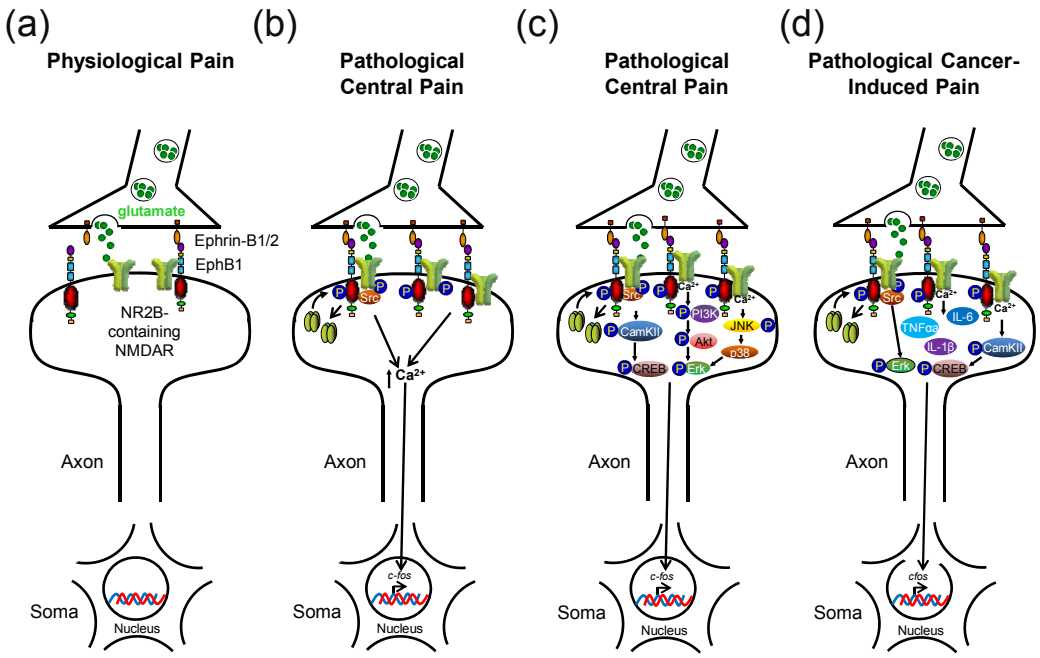
(a)
Physiological Pain
glutamate
Ephrin-B1/2
EphB1
NR2B-containing NMDAR
Axon
Soma
Nucleus
(b)
Pathological Central Pain
Src
Ca2+
Axon
Soma
c-fos
Nucleus
(c)
Pathological Central Pain
Src
Ca2+
PI3K
JNK
CamKII
Akt
p38
CREB
Erk
Axon
Soma
c-fos
Nucleus
(d)
Pathological Cancer-Induced Pain
Src
Ca2+
IL-6
TNFα
IL-1β
CamKII
Erk
CREB
Axon
Soma
cfos
Nucleus

# Figure 1.4

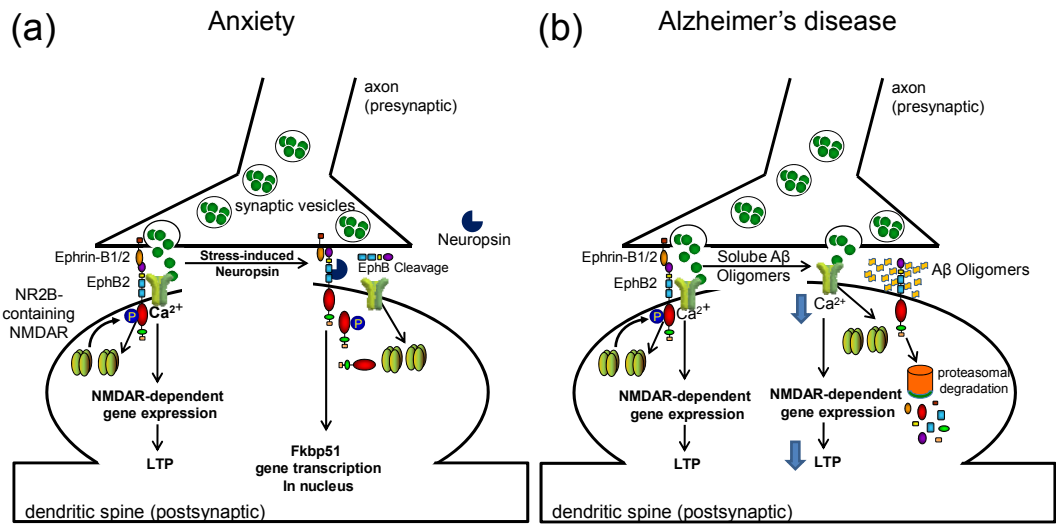
(a)
Anxiety
axon
(presynaptic)
synaptic vesicles
Neuropsin
Ephrin-B1/2
EphB2
Stress-induced
Neuropsin
EphB Cleavage
NR2B-
containing
NMDAR
Ca2+
NMDAR-dependent
gene expression
LTP
Fkbp51
gene transcription
In nucleus
dendritic spine (postsynaptic)
(b)
Alzheimer's disease
axon
(presynaptic)
Ephrin-B1/2
EphB2
Solube Aβ
Oligomers
Aβ Oligomers
Ca2+
Ca2+
proteasomal
degradation
NMDAR-dependent
gene expression
NMDAR-dependent
gene expression
LTP
LTP
dendritic spine (postsynaptic)

CHAPTER 2

# Ephrin-B1 and ephrin-B2 mediate EphB-dependent presynaptic development via syntenin-1

Andrew C. McClelland[1], Sean I. Sheffler-Collins[1], Matthew S. Kayser, and Matthew B. Dalva[2]

Department of Neuroscience, University of Pennsylvania School of Medicine, 1114 BRBII/III, 421 Curie Boulevard, Philadelphia, PA 19104

[1]A.C.M. and S.I.S-C. contributed equally to this work

[2]To whom correspondence should be addressed.

Contributions: A.C.M. generated constructs, wrote ImageJ macros, performed and analyzed experiments, and generated figures (Figure 2.1C,F; Figure 2.3A-C; Figure 2.4A-E; Supplementary Figures 2.1, 2.3, 2.4, 2.6; and part of Supplementary Table 2.1). S.I.S-C. generated constructs, perfomed and analyzed experiments, and generated figures (Figure 2.1A,C,E; Figure 2.2, Figure 2.3D-E, Figure 2.4F-J, Supplementary Figures 2.2, 2.5, and most of Supplementary Table 2.1). M.S.K. performed and analyzed experiments for Figure 2.1A-B. M.B.D. performed immunostaining for Figure 2.3A-C. A.C.M. and M.B.D. designed experiments and drafted all sections of the paper. A.C.M, S.I.S-C., M.S.K., and M.B.D. revised and edited the paper.

**Abstract**

The development of central nervous system synapses requires precise coordination between presynaptic and postsynaptic components. The EphB family controls postsynaptic development by interacting with glutamate receptors and regulating dendritic filopodia motility, but how EphBs induce the formation of presynaptic specializations is less well understood. Here, we show that knockdown of presynaptic ephrin-B1, ephrin-B2, or syntenin-1, but not ephrin-B3, prevents EphB-dependent presynaptic development. Ephrin-B1, ephrin-B2, and syntenin-1 are clustered together with presynaptic markers, suggesting that these molecules function jointly in presynaptic development. Knockdown of ephrin-B1 or ephrin-B2 reduces the number of synaptic specializations and the colocalization of syntenin-1 with synaptic markers. Simultaneous knockdown of ephrin-B1 and ephrin-B2 suggests that they function independently in the formation of synaptic contacts, but act together to recruit syntenin-1 to presynaptic terminals. Taken together, these results demonstrate that ephrin-B1 and ephrin-B2 function with EphB to mediate presynaptic development via syntenin-1.

## Introduction

The EphB family of receptor tyrosine kinases directs postsynaptic development by interacting with NMDA- and AMPA-type glutamate receptors, controlling dendritic filopodia motility, and regulating spine formation (Dalva et al., 2000; Kayser et al., 2006; Kayser et al., 2008). EphBs can also signal trans-synaptically to induce presynaptic development, suggesting that EphB receptors are capable of coordinating the development of both presynaptic and postsynaptic compartments (Kayser et al., 2006). However, the mechanisms by which EphBs induce presynaptic development are not well described. The ligands for EphBs are the ephrin-Bs, a family of three (ephrin-B1–B3) transmembrane molecules that, in addition to "forward" signaling through the activation of EphBs, can also signal in the "reverse" direction through intracellular phosphotyrosines and a C-terminal PDZ-binding domain. Ephrin-Bs have recently been shown to regulate presynaptic development in the Xenopus tectum (Lim et al., 2008) and are expressed in mouse cortex (Lein et al., 2007; Migani et al., 2007, 2009; Tang et al., 1997). Although it is thought that ephrin-Bs might have unique functions at the synapse (Aoto and Chen, 2007; Essmann et al., 2008; Grunwald et al., 2004), whether particular ephrin-Bs interact with postsynaptic EphBs to regulate synapse development in the mammalian CNS, and what the downstream mechanisms are that mediate this process, are not known.

The syntenin family consists of two (syntenin-1 and syntenin-2) tandem PDZ domain-containing proteins implicated in a number of cellular processes

such as trafficking, signaling, and cancer metastasis (Beekman and Coffer, 2008). Initially identified as binding partners for the heparan sulfate proteoglycan syndecan (Grootjans et al., 1997), syntenins are comprised mainly of two PDZ domains that enable self-association and interactions with a number of synaptically localized transmembrane molecules such as glutamate receptors, β-neurexin, SynCAM, and ephrin-Bs (Biederer et al., 2002; Grootjans et al., 2000; Hirbec et al., 2002; Koroll et al., 2001; Lin et al., 1999; Torres et al., 1998). In addition, syntenin-1 may regulate the organization of presynaptic active zones through interactions with the ERC/CAST family of active zone molecules (Ko et al., 2006).

Here, we show that two members of the ephrin-B family (ephrin-B1 and ephrin-B2) function to mediate EphB-dependent presynaptic development via PDZ-binding domain-dependent interaction with syntenin-1. Simultaneous knockdown of ephrin-B1 and ephrin-B2 suggest that these molecules function independently in the formation of synapses, but function together in the localization of syntenin-1 to synaptic specializations.

## Results

### Ephrin-B Family Members Are Required for EphB2-Dependent Presynaptic Development.

A presynaptic role for ephrin-Bs has been suggested by the finding that EphB-expressing non-neuronal cells can induce presynaptic development (Kayser et al., 2006). To determine whether EphB-dependent presynaptic induction is mediated by specific presynaptic ephrin-B family members, we asked whether non-neuronal cells expressing EphB2 could induce presynaptic specializations when ephrin-B expression is reduced in axons by RNAi-mediated knockdown. We generated constructs encoding 19-nt shRNAs targeting individual ephrin-B family members and confirmed that these constructs were capable of reducing the expression of the target molecule (**Figure 2.1F and Supplementary Figure 2.1**). We transfected shRNA constructs into days in vitro (DIV) 3 cortical neurons along with a GFP-tagged version of the presynaptic vesicle marker synaptophysin (syn-GFP) to label transfected axons. At DIV9, transfected neurons were cocultured with HEK293T cells expressing either FLAG epitope-tagged EphB2 (fEphB2) or red fluorescent protein (RFP) and fixed 16–18 h later. Because our transfection efficiency in neurons was low (<1%), expression of syn-GFP revealed easily identifiable stretches of axons with discrete puncta of syn-GFP that colocalized with the excitatory presynaptic marker VGlut1. Labeled HEK293T cells were scattered throughout the culture and occasionally found to be contacting a syn-GFP-expressing axon. To determine the effect of transfected

HEK293T cells on presynaptic development, we compared the linear density of syn-GFP in the stretch of axon contacting the HEK293T cells to the density in the adjacent axon region (see SI Text).

In control neurons coexpressing syn-GFP with the shRNA vector control, the density of syn-GFP in axon regions contacting RFP-expressing HEK293T cells was similar to that in adjacent regions, resulting in a density ratio near 1.0 (**Figure 2.1A and B**). However, consistent with our previous findings (Kayser et al., 2006), syn-GFP puncta density increased by ≈1.5-fold underneath EphB2-expressing HEK293T cells (**Figure 2.1A and B**). These results confirm that EphB2-expressing HEK293T cells can induce presynaptic differentiation in segments of single axons.

To test whether this process is mediated by presynaptic ephrin-Bs, neurons were cotransfected with syn-GFP and shRNA constructs targeting each ephrin-B family member (**Figure 2.1F and Supplementary Figure 2.1**). In axons from neurons transfected with shRNA targeting ephrin-B3, HEK293T cells expressing EphB2 caused a significant increase in syn-GFP density similar to that seen in control neurons (**Figure 2.1A and B**). However, in axons from neurons expressing shRNA targeting ephrin-B1 or ephrin-B2, HEK293T cells expressing EphB2 failed to induce presynaptic vesicle clustering (**Figure 2.1A-C**). To confirm that the effect of these shRNAs are specific, we determined that blockade of EphB2-induced presynaptic differentiation can be rescued by coexpressing ephrin-B1 or ephrin-B2 shRNAs with constructs encoding the appropriate molecule rendered insensitive to knockdown (**Figure 2.1A and E**).

These results suggest that EphB-dependent presynaptic differentiation is controlled by ephrin-B1 and ephrin-B2.

Presynaptic assembly is mediated in part by protein–protein interactions with multidomain scaffolding molecules, many of which contain multiple PDZ domains (Bresler et al., 2004). To test whether the ephrin-B PDZ-binding domain is required for EphB-dependent presynaptic development, we coexpressed syn-GFP with HA-tagged ephrin-B1 lacking the PDZ-binding domain (HAeB1ΔPDZ) in DIV3 neurons. Because the known intracellular signaling domains are highly conserved, overexpression of intracellular mutants such as HAeB1ΔPDZ are thought to act as dominant negatives and block PDZ-binding domain-dependent signaling through all ephrin-B subtypes (Segura et al., 2007; Zimmer et al., 2003). In DIV9 axons coexpressing HAeB1ΔPDZ and syn-GFP, EphB2-expressing HEK293T cells failed to induce an increase in syn-GFP density similar to that seen with knockdown of ephrin-B1 or ephrin-B2 (**Figure 2.1D**). These results indicate that, similar to other molecules that mediate presynaptic development (Dalva et al., 2007; Jin and Garner, 2008), EphB-dependent presynaptic differentiation likely relies on protein–protein interactions with the ephrin-B PDZ-binding domain.

Syntenin-1 Is Required for EphB-Dependent Presynaptic Development. Interactions between the ephrin-B PDZ-binding domain and the tandem PDZ domain-containing protein syntenin-1 have been demonstrated by GST pull-down (Grootjans et al., 2000; Lin et al., 1999), yeast two-hybrid assay (Ko et al., 2006; Terashima et al., 2004; Torres et al., 1998), and X-ray crystallography

(Grembecka et al., 2006). Because a recent report (Ko et al., 2006) demonstrated that syntenin-1 participates in the organization of presynaptic terminals through interactions with ERC/CAST family members, we hypothesized that ephrin-B may recruit presynaptic vesicles downstream of EphB by interacting with syntenin-1. To test whether EphB-dependent presynaptic induction is caused by syntenin-1 PDZ domain interactions, we generated a syntenin-1 molecule lacking the second PDZ domain (syntenin-1ΔPDZ2). The second PDZ domain of syntenin-1 is required to bind ephrin-B (Grembecka et al., 2006; Grootjans et al., 2000; Ko et al., 2006; Lin et al., 1999), and we confirmed that syntenin-1ΔPDZ2 cannot bind ephrin-B1 by coimmunoprecipitation. Because this mutant cannot interact with ephrin-Bs, we predicted that it might act in a dominant negative fashion, similar to ephrin-B1ΔPDZ. We found that overexpression of syntenin-1ΔPDZ2 blocked the ability of EphB2-expressing HEK293T cells to induce an increase in syn-GFP in underlying axons (**Figure 2.2A and B**), suggesting that EphB-dependent presynaptic recruitment depends on PDZ domain interactions between ephrin-Bs and syntenin-1.

To confirm the role of PDZ proteins in EphB-dependent presynaptic induction, we generated shRNA constructs targeting syntenin-1 and GRIP1 (**Figure 2.2D**), a synaptically localized PDZ protein that can also interact with ephrin-B (Bruckner et al., 1999; Lin et al., 1999). Although GRIP1 is primarily thought to function postsynaptically, GRIP1 protein has also been identified in axons (Wyszynski et al., 1999). In axons expressing GRIP1 shRNA, EphB2-expressing HEK293T cells induced a significant increase in syn-GFP density,

suggesting that GRIP1 is not involved in this process (**Figure 2.2A and B**). However, in axons expressing either of two unique syntenin-1-targeting shRNAs, fEphB2-expressing HEK293T cells failed to induce an increase in syn-GFP density (**Figure 2.2A and B**). Knockdown of syntenin-1 had no effect on the ability of ephrin-B1 or ephrin-B2 to bind exogenously applied EphB2-Fc, suggesting that ephrin-Bs were still found at the cell surface (**Supplementary Figure 2.2**). However, syntenin-1 knockdown did cause a decrease in the colocalization of both ephrin-B1 and EphB2-Fc with syn-GFP, consistent with a model in which syntenin-1 links ephrin-Bs to the presynaptic complex (**Supplementary Figure 2.2**). The effects of syntenin-1 knockdown were rescued by transfecting an shRNA targeting syntenin-1 together with a knockdown-insensitive syntenin-1 molecule (**Figure 2.2A and C**), demonstrating that the effects of syntenin-1 shRNA constructs are specific. Taken together, these results demonstrate that EphB-dependent presynaptic development is likely mediated by ephrin-B1 and ephrin-B2, which can recruit presynaptic machinery through PDZ domain interactions with syntenin-1.

**Localization of Ephrin-B Subtypes and Syntenin-1 in Cultured Cortical Neurons.**

To begin to address how ephrin-Bs and syntenin function together to regulate synapse development, we immunostained mature DIV21–30 cultures for ephrin-B1, ephrin-B2, and syntenin-1 along with synaptic markers to determine the distribution of these molecules in cortical neurons. We have previously

reported that ephrin-B1 and ephrin-B3 are colocalized with excitatory presynaptic and postsynaptic markers (Kayser et al., 2006). To determine how this localization compares for ephrin-B2, we stained DIV21 cortical neurons for ephrin-B2 and the presynaptic and postsynaptic markers VGlut1 and SynGAP (Rao et al., 1998). Ephrin-B2 staining was found throughout cortical neuron cultures. However, in contrast to the highly synaptic staining observed for ephrin-B1 and ephrin-B3, the pattern of ephrin-B2 staining consisted of smaller puncta, some of which were colocalized with synaptic puncta (**Figure 2.3A**). Consistent with a previous report (Bundesen et al., 2003), we also observed a few cells with intense ephrin-B2 staining that were positive for the glial marker GFAP (**Figure 2.3B**). We next directly compared the synaptic localization of ephrin-B1 and ephrin-B2 by costaining DIV30 cultures for these molecules and VGlut1. Similar to previous observations, ephrin-B1 was highly colocalized with VGlut1 (≈45%), whereas ephrin-B2 was found in small puncta that were also colocalized with VGlut1 (≈23%; see **Supplementary Table 2.1, Figure 2.3C, and Supplementary Figure 2.3**). In addition, many synaptic puncta colocalized with both ephrin-B1 and ephrin-B2, and there was a significant association of these two molecules at presynaptic sites ($P < 0.0001$; Pearson's $\chi^2$ test) (**Figure 2.3C and Supplementary Table 2.1**). Interestingly, we often observed several small ephrin-B2 puncta surrounding and adjacent to ephrin-B1-positive VGlut1 puncta (**Figure 2.3C *Insets***). Thus, both ephrin-B1 and ephrin-B2 colocalize with synaptic markers, but the staining pattern is different from that for each ephrin-B protein.

The ephrin-B PDZ-binding domain can bind the tandem PDZ protein syntenin-1 (Grembecka et al., 2006; Grootjans et al., 2000; Ko et al., 2006; Koroll et al., 2001; Lin et al., 1999; Terashima et al., 2004; Torres et al., 1998), and our findings that knockdown of syntenin-1 blocks EphB-dependent presynaptic development suggests a model in which ephrin-Bs interact with the presynaptic machinery via syntenin-1. To further address the relationship between syntenin, ephrin-Bs, and the presynaptic machinery, we coimmunostained mature DIV21–30 neurons for syntenin-1, the excitatory presynaptic marker VGlut1, and either ephrin-B1 or ephrin-B2. Consistent with previous studies (Ko et al., 2006; Torres et al., 1998), we found that syntenin-1 is localized to presynaptic specializations (**Figure 2.3D and E**). In addition, we found that syntenin-1 is enriched at VGlut1-positive presynaptic puncta containing ephrin-B1 or ephrin-B2 ($P < 0.0001$; Pearson's $\chi 2$ test) (**Figure 2.3D and E and Supplementary Table 2.1**). These results demonstrate that ephrin-B1, ephrin-B2, and syntenin-1 are associated at presynaptic specializations.

**Presynaptic Ephrin-B1 and Ephrin-B2 Are Required for the Development of Synapses and Recruitment of Syntenin-1.**

To test whether ephrin-Bs regulate the formation of synaptic specializations, we examined the density of synapses in single axons after knockdown of ephrin-B1 or ephrin-B2 in the absence of exogenous stimulation with EphB2-expressing HEK293T cells. EphB-dependent synapse formation occurs between DIV7–14, and robust decreases in synapse number can be seen

by knocking down EphB2 from DIV3–21 (Kayser et al., 2008). Therefore, to identify the effects of ephrin-Bs on EphB-dependent synapse development, neurons were cotransfected with ephrin-B shRNA and syn-GFP constructs at DIV3, fixed at DIV21–23, and immunostained for GFP and the postsynaptic marker PSD-95. Synapses were identified as colocalization between syn-GFP and endogenous PSD-95 puncta. Our low transfection efficiencies allowed us to selectively examine the presynaptic role of ephrin-Bs during synapse development. Knockdown of ephrin-B1 or ephrin-B2 with either of two unique shRNA constructs for each led to a significant decrease in the density of both syn-GFP puncta and colocalized synaptic puncta (**Figure 2.4A-E and Supplementary Figure 2.4**). Together, these results demonstrate that reducing the expression of ephrin-B1 or ephrin-B2 results in fewer synapses.

To begin to investigate whether ephrin-B1 and ephrin-B2 function independently in the formation of synaptic contacts, we compared the effects of individual ephrin-B knockdown to simultaneous knockdown of ephrin-B1 and ephrin-B2 in the same axon. This approach is designed to mimic genetic experiments in which a single functional pathway is demonstrated by a more severe phenotype in double hypomorphic mutants than in the single mutants ((Boone et al., 2007; Mani et al., 2008) and see SI Text). To achieve this we used partial shRNA knockdown for both ephrin-B1 and ephrin-B2 in tandem.

To interpret double-knockdown experiments, knockdown of each molecule must be sufficient to create a sensitized background but not to an extent that further changes cannot be observed. Because shRNA-mediated knockdown is

incomplete, and the effects we observe on synapse number is partial, it is likely that the effects of single knockdown can be modified by double knockdown. Nevertheless, to ensure that knockdown levels were moderate, we first identified reduced amounts of ephrin-B1 and ephrin-B2 shRNA that generated similar, but decreased, levels of knockdown in non-neuronal cells (**Supplementary Figure 2.5** and SI Text). The expression of this reduced amount of ephrin-B1 shRNA resulted in a small, but significant, reduction in the number of syn-GFP puncta without a change in the number of colocalized synaptic puncta (**Figure 2.4F-H**), suggesting that this level of ephrin-B1 knockdown creates a sensitized background. The expression of ephrin-B2 shRNA at this reduced level resulted in a significant effect on the number of both syn-GFP puncta and colocalized synaptic puncta, which is also consistent with a sensitized background. Interestingly, the differences between the effects of ephrin-B knockdown suggest that synaptic specializations are more susceptible to changes in the expression level of ephrin-B2 than ephrin-B1. These findings suggest that knockdown of ephrin-B1 and ephrin-B2 with reduced levels of shRNA is suitable for the evaluation of double knockdown.

We next asked whether coexpression of these shRNAs might potentiate the effects on synapse density. When expressed together at these reduced levels, simultaneous knockdown of both ephrin-B1 and ephrin-B2 caused a decrease in synapse density similar to knockdown of ephrin-B2 alone (**Figure 2.4F and H**). Thus, the effects of ephrin-B1 and ephrin-B2 shRNAs do not

appear to be additive, consistent with ephrin-B1 and ephrin-B2 functioning nonredundantly in the formation of synaptic contacts.

Because syntenin-1 is required for EphB-dependent presynaptic development, and ephrin-Bs are enriched at synaptic specializations containing syntenin-1, we next asked how knockdown of ephrin-Bs specifically affects the localization of syntenin-1 to synapses. To address this question, we expressed ephrin-B1 and ephrin-B2 shRNA, alone or together, and determined the number of synapses that contain syntenin-1. We found that expression of reduced levels of ephrin-B2 shRNA, but not ephrin-B1 shRNA, led to a significant decrease in the number of synaptic puncta containing syntenin-1 (**Figure 2.4F**). However, simultaneous knockdown of ephrin-B1 and ephrin-B2 together resulted in a further significant reduction in the number of synapses containing syntenin-1 compared with either ephrin-B1 or ephrin-B2 alone (**Figure 2.4F**). These results suggest that both ephrin-B1 and ephrin-B2 are involved in normal syntenin-1 localization, and that ephrin-B1 and ephrin-B2 may function together during the formation of syntenin-1-containing synapses. Because decreases in the density of syntenin-1-containing synapses after ephrin-B knockdown might be caused by the overall loss in synapses number (**Figure 2.4H**), we asked how knockdown of ephrin-B1 and/or ephrin-B2 affected the ability of syntenin-1 to localize to the remaining synaptic contacts. For each axon, we determined the proportion of synapses that contain syntenin-1 by dividing the density of syntenin-1-containing synapses (**Figure 2.4I**) by the overall density of synaptic contacts (**Figure 2.4H**). We found that neither knockdown of ephrin-B1 nor ephrin-B2 led to a decrease in

the percentage of synaptic contacts containing syntenin-1 (**Figure 2.4F and J**), suggesting that ephrin-B1 and ephrin-B2 each can compensate for the loss of the other at the remaining synapses. However, simultaneous knockdown of ephrin-B1 and ephrin-B2 together resulted in a significant reduction in the percentage of synaptic puncta that contain syntenin-1 (**Figure 2.4F and J**). Thus, simultaneous knockdown of both ephrin-B1 and ephrin-B2 results in a synergistic effect on the ability of syntenin-1 to localize to synaptic contacts. Taken together, these results suggest that ephrin-B1 and ephrin-B2 are required for normal numbers of excitatory synapses and appear to function in a partially redundant fashion in the recruitment of syntenin-1 to synaptic specializations.

## Discussion

In this study we show that ephrin-B1 and ephrin-B2 are key regulators of EphB-dependent presynaptic development, likely through PDZ domain-dependent interactions with syntenin-1. Ephrin-B1, ephrin-B2, and syntenin-1 colocalize at synaptic contacts, and knockdown of ephrin-B1 or ephrin-B2 leads to a reduction in the number of synaptic contacts. Simultaneous knockdown of both ephrin-B1 and ephrin-B2 suggests that these molecules are required for the synaptic localization of syntenin-1, but function independently in the control of synapse formation. In sum, these results support a model in which excitatory synapse development occurs via a trans-synaptic interaction between postsynaptic EphB and specific presynaptic ephrin-Bs (**Supplementary Figure 2.6**).

Further study will be necessary to elucidate the mechanisms that determine specificity among different ephrin-B family members. Potential mechanisms include differences in signaling, localization, or affinity for EphBs. Differences in signaling or localization could be mediated by domains of the well-conserved juxtamembrane regions of ephrin-B1 and ephrin-B2, which diverges in ephrin-B3; affinity differences are possible given that ephrin-B3 has a slightly lower binding affinity for EphBs than ephrin-B1 or ephrin-B2 (Flanagan and Vanderhaeghen, 1998).

To study the role of ephrin-Bs in EphB-dependent presynaptic development, we have developed an assay that allows us to simultaneously manipulate both members of a trans-synaptic interaction pair. In previous

experiments using coculture assays (Biederer and Scheiffele, 2007), a single molecule of a potential interaction pair was expressed in heterologous cells, and the trans-synaptic binding partner was inferred. In contrast, our modified coculture system allows us to evaluate the effects of molecular interactions between pairs of cells that may occur in vivo. In addition, our assay allows us to study the intracellular events downstream of trans-synaptic interactions that induce presynaptic maturation. By coculturing heterologous cells expressing fEphB2 with neurons expressing shRNA constructs targeting ephrin-B family members, we provide direct evidence simultaneously implicating both members of a receptor–ligand pair in the trans-synaptic control of synapse formation. These findings are validated by our long-term knockdown experiments.

Presynaptic organization is supported by multidomain scaffolding molecules that regulate both structure and signaling at presynaptic terminals, including the PDZ domain-containing proteins Mint, CASK, Piccolo, RIM, and syntenin-1 (Jin and Garner, 2008). Syntenin-1 binds directly to the ephrin-B PDZ-binding domain (Grembecka et al., 2006; Grootjans et al., 2000; Ko et al., 2006; Koroll et al., 2001; Lin et al., 1999; Terashima et al., 2004; Torres et al., 1998) and is linked to presynaptic maturation via ERC2/CAST1 (Ko et al., 2006). ERC2/CAST1 associates with a number of other presynaptic molecules, including RIM, Piccolo, Bassoon, and liprin-α. RIM1 binds the synaptic vesicle protein Rab3A, and ERC2/CAST1 interacts with RIM1 and Piccolo/Bassoon to regulate synaptic transmission (Jin and Garner, 2008). Thus, syntenin-1 provides a directly link by which ephrin-B can associate with a protein complex involved in

the recruitment and regulation of presynaptic vesicles (**Supplementary Figure 2.6**).

The degree to which presynaptic development is mediated by specific interactions between synaptogenic factors and particular scaffolding proteins is not well established. The finding that disruption of syntenin-1 blocks EphB-dependent presynaptic development suggests that presynaptic development can be mediated by specific interactions between ephrin-Bs and syntenin-1. This pathway is likely distinct from those involving other PDZ domain interactions such as that between neurexin and Mint/CASK (Jin and Garner, 2008). Thus, these results suggest that presynaptic terminals may be organized by independent pathways.

Knockdown of ephrin-B1 or ephrin-B2 alone disrupts EphB-dependent presynaptic development and results in a decrease in the number of synaptic contacts. To test whether ephrin-B1 and ephrin-B2 function together or independently in synaptogenesis, we transfected neurons with shRNAs targeting both of these proteins to induce a partial loss in single neurons. Because we selected shRNA levels that generated a partial loss of function, results from these experiments are interpreted as analogous to genetic experiment using trans-heterozygous animals (Boone et al., 2007). However, while knockdown using shRNAs has often been described as generating a hypomorphic condition, it remains possible that simultaneous use of two shRNAs results in unexpected effects. Therefore, to fully resolve the roles of these proteins additional complex genetic experiments will be needed. Regardless, our simultaneous knockdown

experiments suggest that ephrin-B1 and ephrin-B2 likely function independently to control EphB-dependent synapse development. There are several possible explanations that account for these findings. While ephrin-B1 and ephrin-B2 share functional domains, they may coordinate synapse development through distinct pathways. Consistent with this idea, neurons display different sensitivities to the knockdown of ephrin-B1 versus ephrin-B2 for the formation of synaptic contacts, and the staining pattern of ephrin-B1 and ephrin-B2 is different at the level of individual synaptic puncta (**Figure 2.3C**). This specificity may be mediated by differences in trans-synaptic interactions or by distinct, currently unidentified, functional domains. Alternatively, while ephrin-B1 and ephrin-B2 colocalize at many synapses, they are often found alone. Thus, one mechanism for the function of the ephrin-Bs in synapse formation might be their localization to different synaptic puncta.

Ephrin-B1 and ephrin-B2 do appear to function together to recruit syntenin-1 to synapses. Evidence for this synergy comes from our findings that combined knockdown of ephrin-B1 and ephrin-B2 lead to a significant further reduction in density and percentage of synaptic specializations that colocalize with syntenin-1. One likely mechanism is the identical PDZ-binding domains found on ephrin-B1 and ephrin-B2, suggesting that they can both bind syntenin-1 with equal affinity. Although more work will be needed to resolve the different roles of ephrin-B1 and ephrin-B2 in synaptic development, our results provide evidence that ephrin-B1 and ephrin-B2 function to mediate EphB-dependent presynaptic maturation via syntenin-1.

## Materials and Methods

For detailed methods see SI Text.

### Cell Culture and Transfection.

Primary dissociated cortical neurons were prepared from embryonic day 17 (E17) to E18 rats and transfected at DIV0 or DIV3 as described (Kayser et al., 2006; Kayser et al., 2008). See SI Text for details on the culture conditions for the heterologous cell culture assay.

### Expression and shRNA Constructs.

Nineteen-nucleotide RNAi sequences were identified for ephrin-B1, ephrin-B2, and ephrin-B3. Sequences used for shRNAs and details for HA-ephrin-B1, HA-ephrin-B2, and FLAG-syntenin-1 constructs are in SI Text. Except when noted, 0.75 µg of shRNA construct per well (of 24-well plate) was transfected into neurons.

### Western Blot Analysis.

See SI Text for more details.

### Imaging and Analysis.

Cultures were fixed and immunostained using methods similar to those described in (Dalva et al., 2007). Significance between experimental conditions was determined by ANOVA, except where noted. Statistical measures were

conducted on a per-cell basis, collected from a minimum of three independent experiments. See SI Text for details.

**Acknowledgments**

We thank R. Balice-Gordon, G. Bashaw, T. Abel, T. Biederer, and members of M.B.D.'s lab for helpful advice; M. Lush and J. Raper (University of Pennsylvania) for syn-GFP; R. Huganir (The Johns Hopkins School of Medicine) for myc-GRIP1; and E. Kim (Korea Advanced Institute of Science and Technology) for FLAG-syntenin-1. This work was supported by Training Program in Developmental Biology Grant 5T32HD007516 (to A.C.M.), Vision Training Grant EY007035 (to S.I.S-C.), National Institutes of Health Ruth L. Kirschstein National Research Service Award NS051894-01 (to M.S.K.), the Whitehall Foundation (to M.B.D.), the Dana Foundation (to M.B.D.), National Institute of Mental Health Grant MH086425 (to M.B.D.), and National Institute of Drug Addiction Grant DA022727 (to M.B.D).

## Figure Legends

**Fig. 2.1. Ephrin-B1 and ephrin-B2 are required for EphB2-dependent presynaptic development.** (A) Representative images of DIV10 cortical neuron axons transfected with syn-GFP and shRNA constructs at DIV3 and cocultured with HEK293T cells transfected with RFP or FLAG-EphB2 (fEphB2). Arrowheads indicate syn-GFP puncta colocalized with HEK293T cells. (Scale bar: 3 μm.) (B) Quantification of fold increase in syn-GFP puncta density in axon segments contacting HEK293T cells expressing fEphB2 or control constructs compared with adjacent axon segments (syn-GFP induction) for neurons transfected with indicated shRNA constructs: vector control (RFP: n = 19; fEphB2: n = 29), ephrin-B1 shRNA#1 (RFP: n = 14; fEphB2: n = 29), ephrin-B3 shRNA (RFP: n = 21; fEphB2: n = 30). (C) Quantification of axonal syn-GFP induction: vector control (n = 40), ephrin-B1 shRNA#2 (n = 47), ephrin-B2 shRNA#1 (n = 24), or ephrin-B2 shRNA#2 (n = 20). (D) Quantification of axonal syn-GFP induction: vector control (n = 25), ephrin-B1 shRNA#1 (n = 26); HA-ephrin-B1ΔPDZ (n = 24). (E) Quantification of axonal syn-GFP induction: vector control (n = 50), ephrin-B1 shRNA#1 (n = 25), ephrin-B1 shRNA#1 + rescue (n = 27), ephrin-B2 shRNA#1 (n = 30), or ephrin-B2 shRNA#2 + rescue (n = 28). (F) Western blots of lysates from HEK293T cells transfected with HA-ephrin-B1 or HA-ephrin-B2 plus vector control, ephrin-B1 shRNA#1, ephrin-B1 shRNA#2, ephrin-B2 shRNA#1, or ephrin-B2 shRNA#2 and probed for HA and β-tubulin. Error bars indicate SEM. *, $P < 0.04$.

**Figure 2.2. Syntenin-1 is required for EphB-dependent presynaptic development.** (A) Representative images of DIV10 cortical neuron axons transfected with syn-GFP and indicated constructs and cocultured with HEK293T cells transfected with RFP or fEphB2. Arrowheads indicate syn-GFP puncta colocalized with HEK293T cells. (Scale bar: 3 μm.) (B) Quantification of axonal syn-GFP induction for neurons transfected with the indicated shRNA constructs: vector control (RFP: n = 76; fEphB2: n = 76), ephrin-B1 shRNA#2 (RFP: n = 26; fEphB2: n = 33), syntenin-1ΔPDZ2 (RFP: n = 32; fEphB2: n = 35), syntenin-1 shRNA#1 (RFP: n = 30; fEphB2: n = 29), syntenin-1 shRNA#2 (RFP: n = 27; fEphB2: n = 30), or GRIP1 shRNA (RFP: n = 43; fEphB2: n = 47). (C) Quantification of axonal syn-GFP induction: vector control (RFP: n = 27; fEphB2: n = 31), syntenin-1 shRNA#1 (RFP: n = 31; fEphB2: n = 32), or syntenin-1 shRNA#1 + rescue (RFP: n = 27; fEphB2: n = 30). (D) Western blots of lysates from HEK293T cells transfected with FLAG-syntenin-1 or myc-GRIP1 plus vector control, syntenin-1 shRNA#1, syntenin-1 shRNA#2, or GRIP1 shRNA and probed for FLAG or myc and β-tubulin. Error bars indicate SEM. **, $P < 0.002$; *, $P < 0.04$.

**Figure 2.3. Localization of ephrin-B1, ephrin-B2, and syntenin-1 in cultured cortical neurons.** (A) Representative image of DIV21 neurons stained for ephrin-B2 (green), SynGAP (blue), and VGlut1 (red). (Scale bar: 3 μm.) (B) Representative image of DIV21 neurons stained for ephrin-B2 (green) and GFAP (red). (Scale bar: 10 μm.) (C) Representative image of DIV30 neurons stained for

ephrin-B1 (green), ephrin-B2 (red), and VGlut1 (blue). See SI Text for staining details. Mask of merge is RGB image created from binary masks of the three individual channels. Image shown is of only the colocalized pixels with all other pixels removed. Colocalization in masks is indicated by: ephrin-B1 and ephrin-B2, yellow; ephrin-B1 and VGlut1, cyan; ephrin-B2 and VGlut1, magenta. (Scale bar: 3 μm.) (Inset) High-magnification image of boxed region. (Scale bar: 1 μm.) (D and E) Representative image of DIV21 neurons stained for syntenin-1 (green), VGlut1 (blue) and either ephrin-B1 (D) or ephrin-B2 (E) (red). Arrowheads indicate triple colocalization. (Scale bar: 3 μm.)

**Fig. 2.4. Presynaptic ephrin-B1 and ephrin-B2 are required for synapse formation and synaptic localization of syntenin-1.** (A) (Left and Center) Representative images of DIV21–23 axons transfected at DIV3 with syn-GFP and indicated shRNA construct costained for GFP (green) and PSD-95 (red). (Scale bar: 3 μm.) (Right) Mask of colocalization created by identifying colocalized puncta in binary masks from syn-GFP and PSD-95 images. (B–E) Quantification of density of syn-GFP puncta (B and D) and synaptic puncta defined by colocalized syn-GFP and PSD-95 (C and E) for vector control (n = 21) or ephrin-B1 shRNA#1 (n = 24) (B and C) and vector control (n = 19), ephrin-B1 shRNA#2 (n = 19), ephrin-B2 shRNA#1 (n = 12), or ephrin-B2 shRNA#2 (n = 19) (D and E). (F) (Left and Center) Representative images of DIV21 axons transfected at DIV3 with syn-GFP and indicated shRNA construct costained for GFP (green), syn-GAP (red), and syntenin-1 (blue). Arrowheads indicate

synaptic puncta identified colocalization of syn-GFP and SynGAP puncta. Arrows indicate colocalized SynGAP and syntenin-1 puncta. (Scale bar: 3 μm.) (Right) Schematic showing outlines of synaptic syn-GFP puncta and areas of colocalization with syntenin-1 in blue. (G–J) Quantification of syn-GFP puncta density (G), synaptic puncta identified by colocalization of syn-GFP and SynGAP (H), synaptic syntenin-1 (triple colocalized syn-GFP, SynGAP, and syntenin-1) puncta density (I), and percentage of synaptic puncta that colocalize with syntenin-1 for neurons transfected with vector control (n = 30), ephrin-B1 shRNA2 (n = 29), ephrin-B2 shRNA1 (n = 26), and ephrin-B1 shRNA2 + ephrin-B2 shRNA1 (n = 25) (J). Error bars indicate SEM. *, $P < 0.05$; **, $P < 0.003$.

**Supporting Information**

**SI Text**

**Ephrin-B3 Knockdown Validation.** To confirm that knockdown constructs targeting ephrin-B3 are effective in reducing the expression of ephrin-B3 in neurons, we evaluated ephrin-B3 immunostaining in neurons expressing ephrin-B3 knockdown constructs. DIV0 cortical neurons were transfected with GFP and ephrin-B3 shRNA or vector control. At DIV10, neurons were fixed and immunostained for GFP and ephrin-B3. We then measured both the number of endogenous ephrin-B3 puncta and the overall intensity of ephrin-B3 immunostaining. We found a significant decrease in both the intensity of ephrin-B3 immunostaining and the number of ephrin-B3 puncta (**Supplementary Figure 2.1**). Moreover, consistent with recent reports (Aoto and Chen, 2007), we found that expression of this ephrin-B3-targeting knockdown construct leads to a significant decrease in the number of postsynaptic specializations.

**Syntenin-1 Knockdown Does Not Affect Ephrin-B Surface Localization.** To address whether the effects of syntenin-1 knockdown on EphB-dependent presynaptic induction are caused by a role for syntenin-1in ephrin-B trafficking, we tested whether ephrin-B1 and ephrin-B2 could localize to the cell surface in the presence of syntenin-1 knockdown. To identify surface localized ephrin-B in knockdown axons, we cotransfected DIV3 neurons with syn-GFP and syntenin-1 shRNA or vector control. At DIV10, we treated live neurons with the extracellular

domain of EphB2 tagged to the human Fc fragment (EphB2-Fc) to label surface ephrin-B. Neurons were fixed and stained for GFP, the human Fc fragment to label EphB2-Fc, and ephrin-B1 or ephrin-B2. We then measured the percentage of ephrin-B puncta in syn-GFP positive axons that were labeled with EphB2-Fc. Consistent with a model in which syntenin links ephrin-Bs to presynaptic specializations, we found that syntenin-1 knockdown led to a decrease in the number of syn-GFP puncta colocalized with ephrin-B1 and EphB2-Fc (**Supplementary Figure 2.2C and G**). Interestingly, we did not detect a change in the density of ephrin-B2 colocalized with syn-GFP (**Supplementary Figure 2.2E**). When we evaluated the proportion of ephrin-B that was exposed to the surface, we found that the percentage of ephrin-B1 or ephrin-B2 puncta labeled with EphB2-Fc was unchanged with expression of syntenin-1 shRNA (**Supplementary Figure 2.2D and F**). These results suggest that the effects of syntenin-1 knockdown on EphB2-dependent presynaptic development are not caused by an effect on ephrin-B surface localization.

**Ephrin-B1 and Ephrin-B2 Co-immunostaining.** To simultaneously immunostain with anti-ephrin-B1 and anti-ephrin-B2 primary antibodies that were both raised in goat, we used rabbit anti-goat Fab fragments to convert the goat IgG epitope of the antiephrin-B2 antibody to rabbit. We confirmed that ephrin-B1 and ephrin-B2 recognize the target protein expressed in HEK293T cells and not other ephrin-B family members by Western blot, and the specificity of the ephrin-B2 antibody has been confirmed in mice lacking ephrin-B2 (Grunwald et al.,

2004). Before staining, goat antiephrin-B2 antibodies were preincubated with rabbit anti-goat Fab fragments at a ratio of 650:1 by weight. After fixation and blocking with standard conditions, cells were incubated with goat anti-ephrin-B2/Fab conjugates for 2 h at room temperature followed by goat anti-ephrin-B1 and guinea pig anti-VGlut1 primary antibodies overnight at 4 °C. Secondary labeling was performed with Cy2-conjugated donkey anti-goat, Cy3-conjugated donkey anti-rabbit, and Cy5-conjugated donkey anti-guinea pig (**Supplementary Figure 2.3A**). To validate the effectiveness of the Fab fragments, we evaluated two control conditions. First, we performed the identical staining as described above but without goat anti-ephrin-B1 primary antibody. In this condition, we observed normal staining of the goat anti-ephrin-B2/Fab conjugates with Cy3 anti-rabbit secondary antibodies, but we did not observe any labeling with Cy2 anti-goat antibodies, demonstrating that the Fab fragment effectively blocked the goat epitope of the ephrin-B2 antibody (**Supplementary Figure 2.3B**). Second, we performed the identical staining as described above but without the goat anti-ephrin-B1 antibody or the rabbit anti-goat Fab fragment (**Supplementary Figure 2.3C**). In this condition, the staining pattern for the Cy2 anti-goat secondary is identical to that as for the Cy3 anti-rabbit secondary in **Supplementary Figure 2.3A and B**, indicating that the Fab fragment accurate converts the goat epitope of the ephrin-B2 antibody to rabbit. In addition, we did not observe any labeling with the Cy3 anti-rabbit secondary, demonstrating that the Cy3 labeling in **Supplementary Figure 2.3A** was only caused by the Fab fragment labeling of the goat anti-ephrin-B1 antibody. Taken together, these results confirm that the

Fab fragment effectively blocks anti-goat secondary reagents and accurately converts the ephrin-B2 epitope into rabbit. Thus, the pattern observed with anti-rabbit and anti-goat secondary reagents after application of goat-ephrin-B2/Fab conjugates with goat anti-ephrin-B1 antibody accurately represents the staining pattern of these antibodies.

**Ephrin-B Knockdown at DIV9.** To confirm that the effects of ephrin-B shRNA constructs are caused by reduction in ephrin-B expression, we conducted experiments to determine whether the decreases in synaptic specializations induced by ephrin-B knockdown could be rescued by coexpressing ephrin-B1 shRNA constructs with an HA epitope-tagged ephrin-B1 with silent mutations in the region targeted by our shRNA construct (HAeB1R). In these experiments, DIV0 cortical neurons were cotransfected with syn-GFP and ephrin-B shRNA or vector control, and the density of syn-GFP was determined at DIV9. Compared with control conditions, axons of neurons expressing ephrin-B1 shRNA constructs had a ~25% decrease in the density of syn-GFP (**Supplementary Figure 2.4**). Coexpression of ephrin-B1 shRNA with HAeB1R constructs rescued the effects of ephrin-B1 knockdown, resulting in a syn-GFP puncta density similar to control (**Supplementary Figure 2.4**), suggesting that the effects we observed after transfection of shRNA are specific.

We also examined the effects of ephrin-B3 shRNA on the development of synaptic specializations. Consistent with the effect on EphB-dependent presynaptic induction, knockdown of ephrin-B3 did not lead to a decrease in syn-

GFP puncta density (**Supplementary Figure 2.4**). In contrast, knockdown of ephrin-B3 resulted in syn-GFP puncta that were smaller and less evenly distributed than in control conditions, resulting in an increased syn-GFP density (**Supplementary Figure 2.4**). It has previously been shown that loss of ephrin-B3 leads to a generalized increase in the expression of a number of synaptic proteins (Rodenas-Ruano et al., 2006), and this effect may lead to an increase in disorganized presynaptic clusters in ephrin-B3 knockdown conditions. In addition, as described, ephrin-B3 shRNA does not affect EphB-dependent presynaptic formation (**Figure 2.1**). These results suggest that knockdown of ephrin-B3 presynaptically leads to a phenotype that is consistent with that observed in mice lacking ephrin-B3, but ephrin-B3 does not appear to be required for EphB-induced presynaptic specializations. Taken together, these results demonstrate that knockdown of ephrin-B1 or ephrin-B2 in axons leads to a reduction in excitatory synapse number and disrupts the ability of EphB2 to induce presynaptic differentiation. Thus, ephrin-Bs appear to mediate EphB-dependent presynaptic development but not all ephrin-Bs participate in this process.

**Identifying Reduced Amounts of Ephrin-B shRNA Constructs for Double Knockdown.** To evaluate the potential redundancy of ephrin-B1 and ephrin-B2 knockdown, we used a double-knockdown approach modeled on genetic experiments in which interactions between genes are identified by a phenotype in a double mutant that cannot be accounted for by the effects of the single mutants alone (Mani et al., 2008). In these genetic experiments, the interpretation of an

identified interaction depends on the nature of the genetic manipulation. An interaction between two null alleles suggests that the two gene products function in parallel pathways that converge on a shared function; in contrast, an interaction between two hypomorphs suggests that the two gene products function in a single pathway (Boone et al., 2007). To replicate the latter condition in our double-knockdown experiments, we used reduced amounts of shRNA for ephrin-B1 and ephrin-B2 that were more similar to hypomorphs than nulls. To identify reduced amounts of ephrin-B1 and ephrin-B2 knockdown constructs that were suitable for use in double knockdown experiments, we evaluated the relationship between the amount of ephrin-B shRNA constructs transfected into cells and the amount of knockdown achieved. We transfected HEK293T cells with HA-ephrin-B1 or HA-ephrin-B2 and different amounts of ephrin-B1 shRNA2 or ephrin-B2 shRNA1, respectively. The total amount of shRNA construct transfected was maintained at 1 μg in each condition with corresponding amounts of empty control vector. We found that there is a steady decrease in knockdown effect from 1 μg per well (of a six-well plate) to 0.083μg per well (**Supplementary Figure 2.5**). Very little knockdown was observed at low amounts of shRNA constructs (0.017 μg per well; **Supplementary Figure 2.5**). Knockdown levels were similar at equivalent shRNA construct amount between ephrin-B1 and ephrin-B2 (**Supplementary Figure 2.5**). These results suggest that ephrin-B shRNA constructs are effective over a wide range of amounts, but that absolute level of knockdown is proportional to the amount of shRNA construct transfected. For double-knockdown experiments (**Figure 2.4 F-J**), we

reduced the amount of ephrin-B1 shRNA2 by 50% relative to other experiments (0.375 µg per well of a 24-well plate) and by 75% for ephrin-B2 shRNA2 (0.187 µg per well). To determine that our dual-knockdown assay could effectively measure increasing effects of simultaneous knockdown we considered and addressed possible limitations. As discussed in the main text, shRNA-mediated knockdown does not completely prevent protein expression; therefore, knockdown is likely to give a suitable background for measuring additive effects. To help to ensure this, we determined lower amounts of knockdown that could still generate effects (see **Figure 2.4H-J and Supplementary Figure 2.5**). An important potential concern arises from the fact that ephrin-B2 knockdown generates a larger effect on synapse number than ephrin-B1 knockdown, because the greater effect on synapse number of ephrin-B2 shRNA may represent the largest effect beyond which further decreases in synapse number are difficult to detect. However, this possibility is unlikely because the reduced level of knockdown results in only a partial knockdown of ephrin-B protein, and our assay has the sensitivity needed to detect larger decreases in synapse density (**Figure 2.4I-J**).

**Cell Culture and Transfection.** Neurons were cultured in neurobasal (Invitrogen), B27 supplement (Invitrogen), glutamine (Sigma), and penicillin–streptomycin (Sigma) on poly-D-lysine (BD Biosciences or Sigma) and laminin (BD Biosciences)-coated glass coverslips (12 mm; Bellco Glass) in 24-well plates (Costar). Cells were plated at 150,000 per well maintained in a humidified

incubator with 5% $CO_2$ at 37 °C. As indicated, neurons were transfected either with Lipofectamine 2000 (Invitrogen) in suspension immediately before plating (Takasu et al., 2002) or at 3 DIV using the calcium phosphate method (Xia et al., 1996).

**shRNA Constructs. Sequences used were:**

ephrin-B1 shRNA#1, 5'-GTTCCTAAGTGGGAAGGGC-3';

ephrin-B1 shRNA#2, 5'-CACTGTGCTTGATCCCAAT-3';

ephrin-B2 shRNA#1, 5'-GCAGACAGATGCACAATTA-3';

ephrin-B2 shRNA#2, 5'-GAGACAAATTGGATATTAT-3';

ephrin-B3 shRNA, 5'-GCCTTCGGAGAGTCGCCAC-3';

syntenin-1 shRNA#1, 5'-GTCTTTAAGTGAAGCTGAA-3';

syntenin-1 shRNA#2, 5'-CAGTGGACATGTTGGCTTT-3'; and GRIP1 shRNA, 5'-GAGAGTTCCGGAGCGATTA-3'. Forward and reverse oligonucleotides were synthesized (Integrated DNA Technologies) such that, when annealed, they generated a dsDNA insert consisting of the forward and reverse complement RNAi sequences separated by a hairpin region and flanked by restriction site overhangs. Inserts were subcloned into pSuper (Brummelkamp et al., 2002).

**Expression Constructs.** HA-ephrin-B2 was generated by cloning ephrin-B2 from mouse cDNA using sequence-specific primers and then QuikChange (Invitrogen) to insert the HA coding sequence flanked by unique restriction sites immediately downstream of the signal sequences. The HA-ephrin-B1, HA-ephrin-

B2, and FLAG-syntenin-1 rescue constructs were generated by creating seven to nine silent mutations within the sequence targeted by ephrin-B1 shRNA#1, ephrin-B2 shRNA#1, and syntenin-1 shRNA#1 sequences, respectively. HA-ephrin-B1ΔPDZ was created by amplifying the full-length HA-ephrin- B1 without the four terminal amino acids. Syntenin-1ΔPDZ2 was created by QuikChange to remove the second PDZ domain (amino acids 198–272). Synaptophysin-GFP in pFUGW vector was a generous gift from M. Lush and J. Raper. FLAG-syntenin-1 and myc-GRIP1 were kind gifts of E. Kim (Ko et al., 2006) and R. Huganir, respectively.

**Immunocytochemistry.** Cultures were fixed in 4% paraformaldehyde/2% sucrose for 8 min at room temperature. Cells were washed three times in PBS and blocked and permeabilized in 1% ovalbumin (Sigma)/0.2% cold water fish scale gelatin (Sigma)/ 0.1% saponin (Sigma) for 1 h at room temperature. Antibody incubations were conducted overnight at 4 °C for primary antibody and 1 h at room temperature in secondary antibody diluted in blocking reagents. Dilutions of each antibody used is reported below. For double labeling for ephrin-B1 and ephrin-B2, the goat IgG epitope of ephrin-B2 was converted to rabbit by preincubation with goat anti-rabbit Fab fragments (Jackson ImmunoResearch). Antibodies used were: chicken anti-GFP (Upstate; 1:2,500), mouse anti-FLAG M2 (Sigma; 1:2,000), rabbit anti-ephrin-B3 (Zymed, 1:50), goat anti-ephrin-B1 (R&D Systems; 1:500), goat anti-ephrin-B2 (R&D Systems; 1:500), mouse anti-PSD95 (Affinity BioReagents; 1:200), rabbit anti-SynGAP (Affinity BioReagents;

1:1,000), guinea pig anti-VGlut1 (Chemicon; 1:5,000), mouse anti-syntenin-1 (Synaptic Systems; 1:200), and mouse anti-GFAP (Boehringer Manheim; 1:500).

**Western Blot Analysis.** Lysates from HEK293T cells were separated by SDS/PAGE and transferred onto 0.45-μm PVDF membranes (Millipore). Immunoblots were blocked in 5% milk in TBST (150 mM NaCl/10 mM Tris, pH 8.0/0.05% Tween 20) and blotted for indicated proteins. Antibodies used were mouse anti-HA (Covance), mouse anti-Myc (DSHB; 9E10), mouse anti-FLAG M2 (Sigma), mouse anti-β-tubulin (DSHB; E19), and rabbit anti-actin (Sigma).

**Ephrin-B Surface Labeling.** Cultured cortical neurons were treated with EphB2-Fc (R&D Systems) preclustered with donkey antihuman Fc antibody (Jackson ImmunoResearch; see (Kayser et al., 2006)) for 60 min at 37 °C. Cultures were washed once in PBS and fixed as described.

**Imaging and Analysis.** Images of primary neuronal cultures were acquired by using confocal scanning microscopy (Leica). All images were acquired and subsequently analyzed with custom designed National Institutes of Health ImageJ macros blind to experimental condition. Significance between experimental conditions was determined by ANOVA, except where noted. Statistical measures were conducted on a per-cell basis, collected from a minimum of three independent experiments. For puncta analysis, images were

converted to binary scale, and puncta were identified as continuous groups of pixels corresponding to 0.5–7.5 μm. Colocalization between puncta was defined as >1 pixel overlap between channels. Linear density measurements were obtained by identifying puncta along at least 50 μm of axon per image.

For heterologous coculture experiments, synaptophysin-GFP puncta density was determined as described above for axon regions colocalized with HEK293T cells and for adjacent axon regions (starting >5μm away from HEK293T cell border). Syn-GFP induction was determined by dividing puncta density colocalized with HEK293T cells by density in adjacent regions.

To determine endogenous ephrin-B3 staining intensity in GFP-expressing neurons cotransfected with constructs encoding ephrin-B3 shRNA, the average intensity of pixels colocalized with a GFP mask in which the soma had been removed was measured in nonsaturated images of ephrin-B3 staining in neurons cotransfected with either vector control or ephrin-B3 shRNA collected with identical microscope settings.

**Supplementary Figure Legends**

**Supplementary Figure 2.1. Validation of endogenous ephrin-B3 knockdown.** (*a* and *b*) Representative images of DIV10 neurons expressing GFP plus vector control (*a*) or ephrin-B3 shRNA (*b*) and stained with anti-GFP (green) and anti-ephrin-B3 (red) antibodies. (*c* and *d*) Endogenous ephrin-B3 staining from *a* and *b*. (Scale bar: 10 μm.) (*e1–f2*) High-magnification views of boxed region of dendrite from neurons expressing GFP (green in *e2* and *f2*) plus vector control (*e1* and *e2*) or ephrin-B3 shRNA (*f1* and *f2*). (*e1* and *f1*) Endogenous ephrin-B3 staining (red in *e2* and *f2*). Arrows indicate ephrin-B3 puncta in transfected cells. Arrowheads indicate puncta in adjacent cells. (Scale bar: 3 μm.) (*g* and *h*) Quantification of ephrin-B3 staining intensity in arbitrary units (*g*) or ephrin-B3 puncta/μm (*h*) after transfection of vector control ($n$ = 37) or ephrin-B3 shRNA ($n$ = 41). Error bars indicate SEM. *, $P < 0.0001$.

**Supplementary Figure 2.2. Syntenin-1 knockdown does not affect ephrin-B surface localization.** (*a* and *b*) Representative images of DIV10 neurons transfected at DIV3 with syn-GFP plus syntenin-1 shRNA#2 or vector control, treated with clustered EphB2-Fc for 60 min, fixed, and stained for anti-GFP (green), human Fc fragment of IgG (blue), and ephrin-B1 (*a*) or ephrin-B2 (*b*) (red). Arrowheads indicate triple colocalization. (Scale bar: 3 μm.) (*c* and *d*) Quantification of puncta density for colocalized syn-GFP and ephrin-B1 puncta (*c*) and percentage of colocalized ephrin-B1 and syn-GFP puncta that are

positive for EphB2-Fc in neurons transfected with vector control (*n* = 31) or syntenin-1 shRNA#2 (*n* = 28) (*d*). (*e* and *f* ) Quantification of puncta density for colocalized syn-GFP and ephrin-B2 puncta (*e*) and percentage of colocalized ephrin-B2 and syn-GFP puncta that are positive for EphB2-Fc in neurons transfected with vector control (*n* = 30) or syntenin-1 shRNA2 (*n* = 30) ( *f*). (*g*) Quantification of puncta density for colocalized syn-GFP and EphB2-Fc puncta for vector control (*n*=31) or syntenin-1 shRNA2 (*n*=28). Error bars indicate SEM. *, $P < 0.02$.

**Supplementary Figure 2.3. Immunostaining controls.** (a) Representative images of DIV30 neurons stained with goat anti-ephrin-B1 antibodies recognized with Cy2 donkey anti-goat secondary antibodies (green), goat anti-ephrin-B2 antibodies preincubated with rabbit anti-goat Fab fragment and recognized with Cy3 donkey anti-rabbit secondary antibodies (red), and guinea pig anti-VGlut1 antibodies recognized with Cy5 donkey anti-guinea pig secondary antibodies (blue). (b) Representative images of DIV30 neurons stained identically to a, except anti-ephrin-B1 antibody was omitted. (c) Representative images of DIV30 neurons stained identically to a, except anti-ephrin-B1 antibody and preincubation of anti-ephrin-B2 with rabbit anti-goat Fab fragment was omitted. Goat anti-ephrin-B2 antibodies are labeled with Cy2 donkey anti-goat secondary antibodies (green). See SI Text for details. (Scale bar: 3 μm.)

**Supplementary Figure 2.4. Ephrin-B Knockdown at DIV9.** (a) Ephrin-B in presynaptic development Representative axons from DIV9 cortical neurons transfected at DIV0 with syn-GFP plus indicated shRNA constructs. (Scale bar: 3μm.) (b) Quantification of syn-GFP puncta density of axons transfected with vector control (n=77), ephrin-B1 shRNA#1 (n=93), ephrin-B1 shRNA#1 + rescue (n = 25), or ephrin-B3 shRNA (n = 77). Error bars indicate SEM. *, $P < 0.002$.

**Supplementary Figure 2.5. Titration of ephrin-B1 and ephrin-B2 knockdown in heterologous cells.** (*a* and *b*) Western blots of lysates from HEK293T cells transfected with HA-ephrin-B1 (*a*) or HA-ephrin-B2 plus vector control (*b*) and the indicated amounts of ephrin-B1 shRNA#2 (*a*) or ephin-B2 shRNA#1 (*b*). Control plasmid was transfected as needed so that the total amount of shRNA vector was 1 μg. Blots were probed for HA antibody, stripped, and reprobed for actin.

**Supplementary Figure 2.6. Model EphB-dependent presynaptic development.**

**Supplementary Table 2.1. Puncta analysis of DIV30 cortical neuron culture immunostained for ephrin-B1, ephrin-B2, syntenin-1, and VGlut1**

**Figure 2.1**

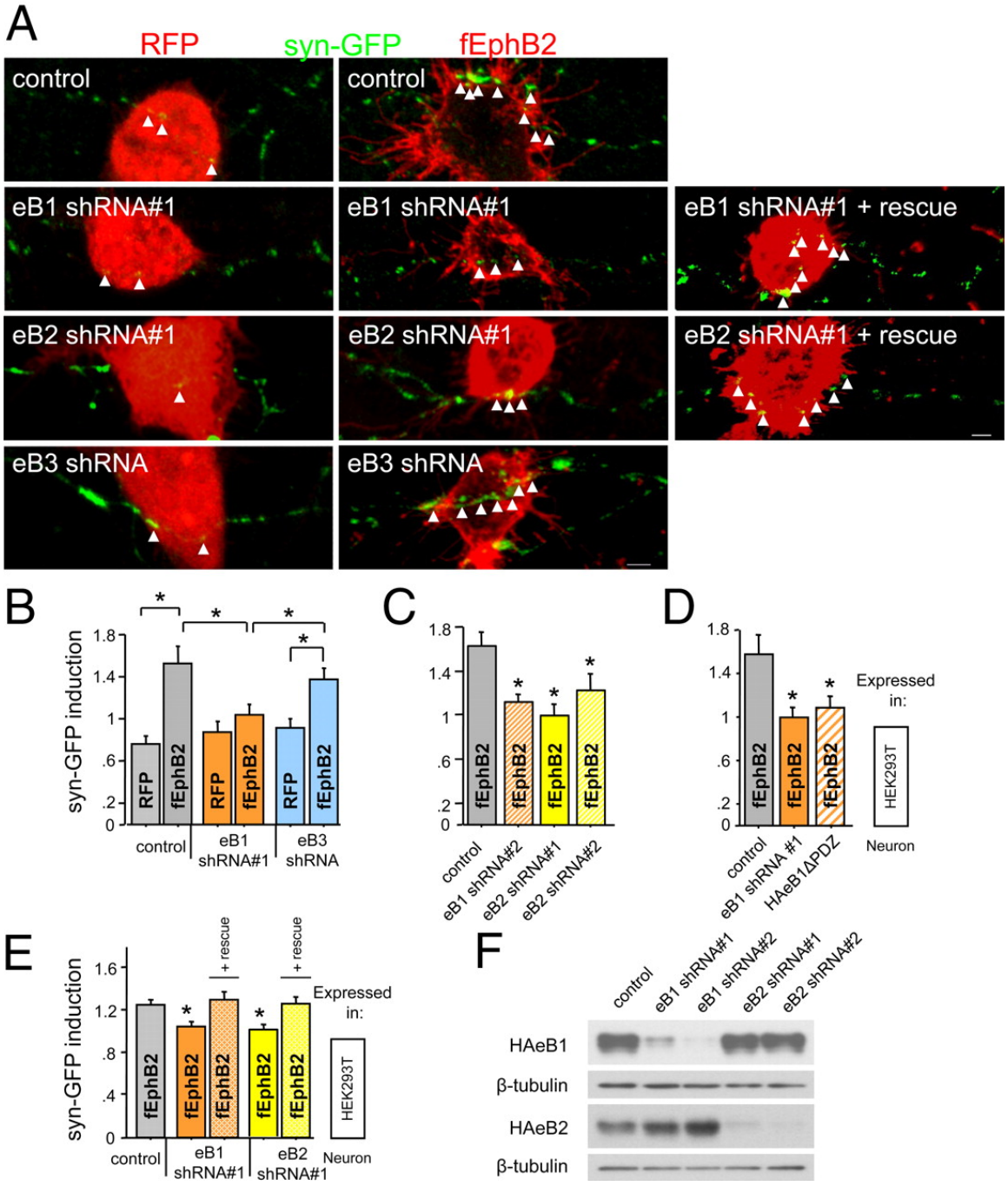
A
RFP
syn-GFP
fEphB2
control
control
eB1 shRNA#1
eB1 shRNA#1
eB1 shRNA#1 + rescue
eB2 shRNA#1
eB2 shRNA#1
eB2 shRNA#1 + rescue
eB3 shRNA
eB3 shRNA
B
syn-GFP induction
RFP
fEphB2
control
eB1 shRNA#1
eB3 shRNA
C
fEphB2
control
eB1 shRNA#2
eB2 shRNA#1
eB2 shRNA#2
D
fEphB2
Expressed in:
HEK293T
Neuron
control
eB1 shRNA #1
HAeB1ΔPDZ
E
syn-GFP induction
+ rescue
Expressed in:
HEK293T
Neuron
control
eB1 shRNA#1
eB2 shRNA#1
F
control
eB1 shRNA#1
eB1 shRNA#2
eB2 shRNA#1
eB2 shRNA#2
HAeB1
β-tubulin
HAeB2
β-tubulin

## Figure 2.2

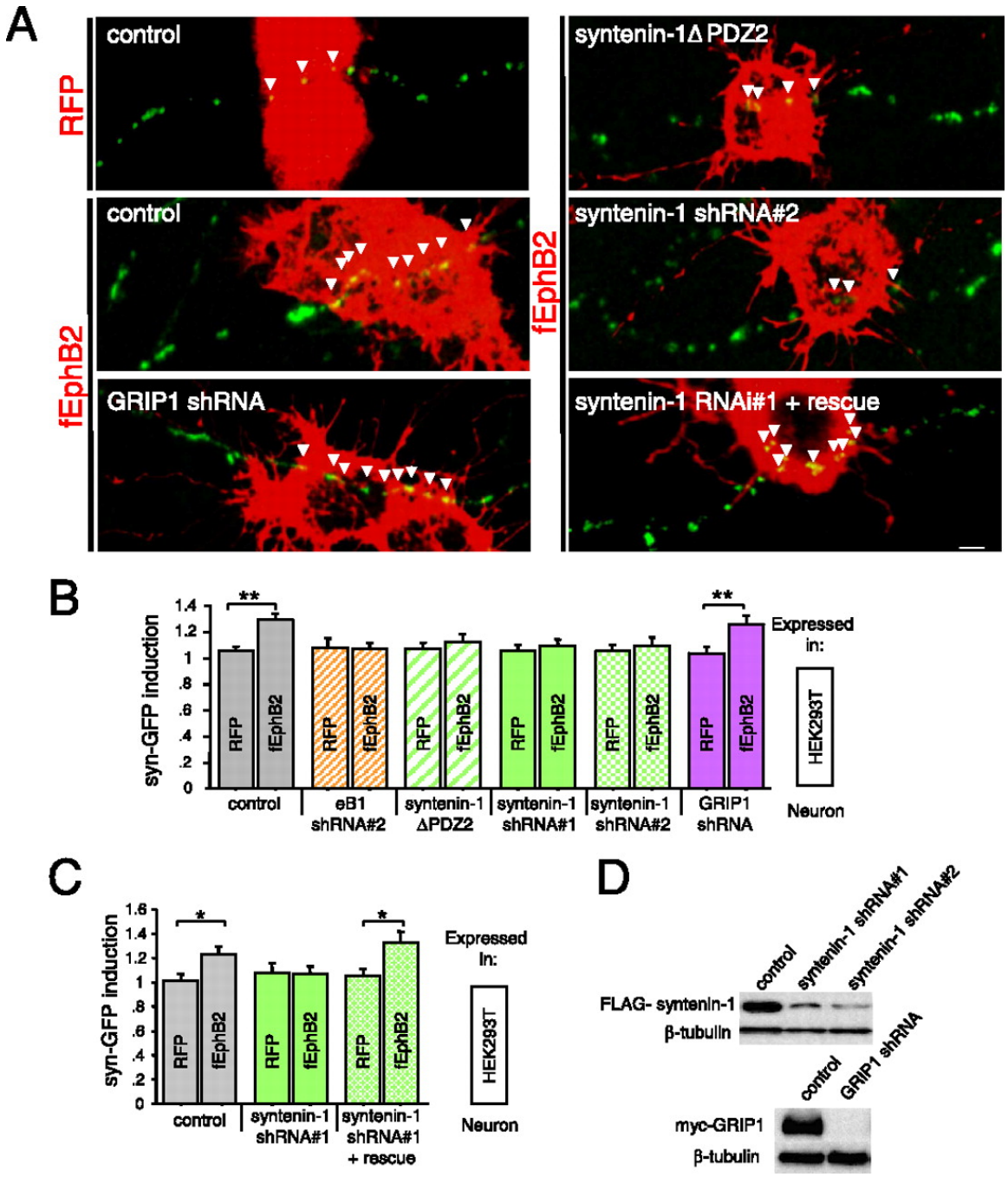
A
RFP
fEphB2
control
syntenin-1ΔPDZ2
control
syntenin-1 shRNA#2
GRIP1 shRNA
syntenin-1 RNAi#1 + rescue
B
syn-GFP induction
1.4
1.2
1
.8
.6
.4
.2
0
**
**
RFP
fEphB2
Expressed in:
HEK293T
Neuron
control
eB1 shRNA#2
syntenin-1 ΔPDZ2
syntenin-1 shRNA#1
syntenin-1 shRNA#2
GRIP1 shRNA
C
syn-GFP induction
1.6
1.4
1.2
1
.8
.6
.4
.2
0
*
*
RFP
fEphB2
Expressed In:
HEK293T
Neuron
control
syntenin-1 shRNA#1
syntenin-1 shRNA#1 + rescue
D
control
syntenin-1 shRNA#1
syntenin-1 shRNA#2
FLAG- syntenin-1
β-tubulin
control
GRIP1 shRNA
myc-GRIP1
β-tubulin

## Figure 2.3

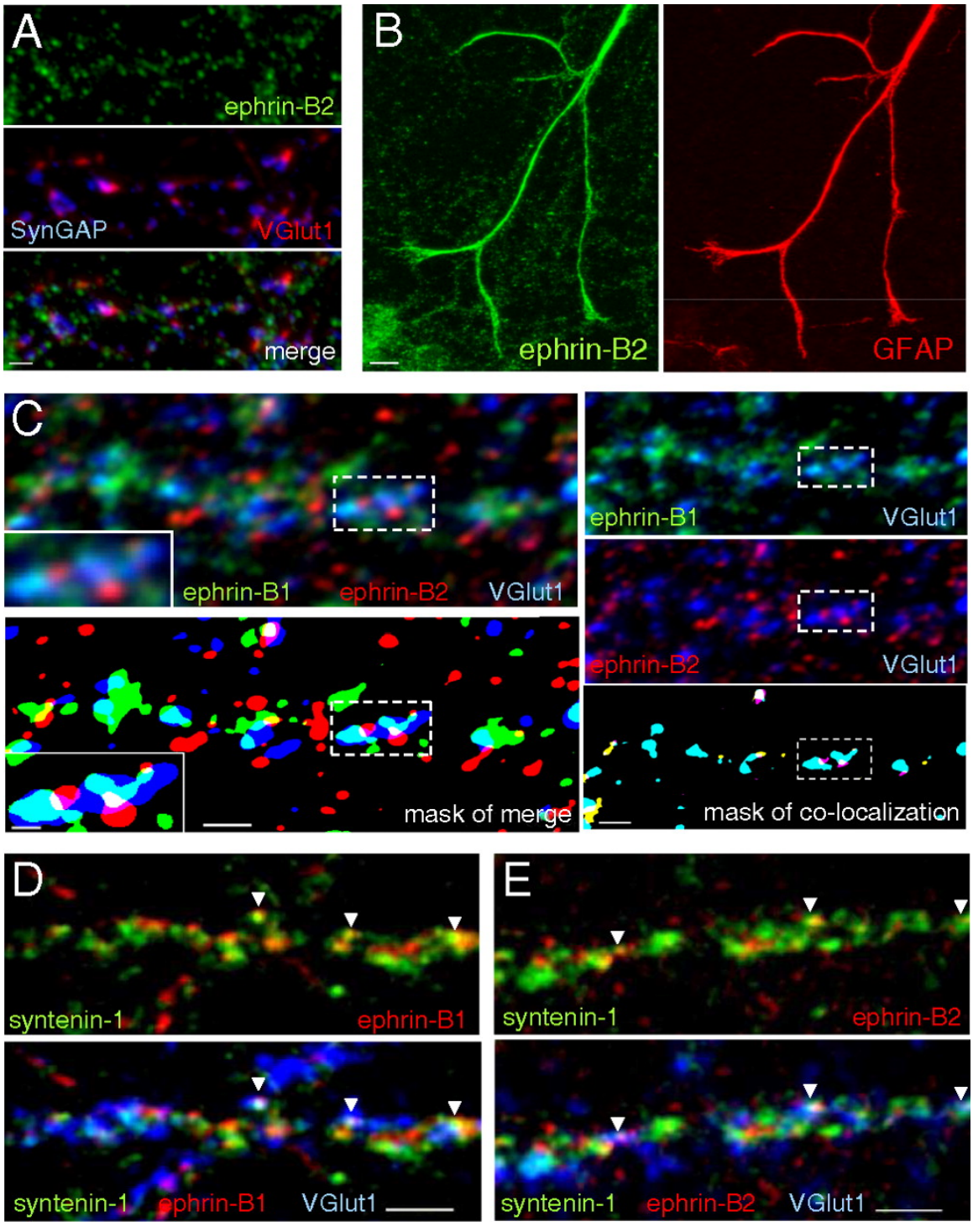
A
ephrin-B2
SynGAP
VGlut1
merge
B
ephrin-B2
GFAP
C
ephrin-B1
ephrin-B2
VGlut1
mask of merge
ephrin-B1
VGlut1
ephrin-B2
VGlut1
mask of co-localization
D
syntenin-1
ephrin-B1
syntenin-1
ephrin-B1
VGlut1
E
syntenin-1
ephrin-B2
syntenin-1
ephrin-B2
VGlut1

## Figure 2.4

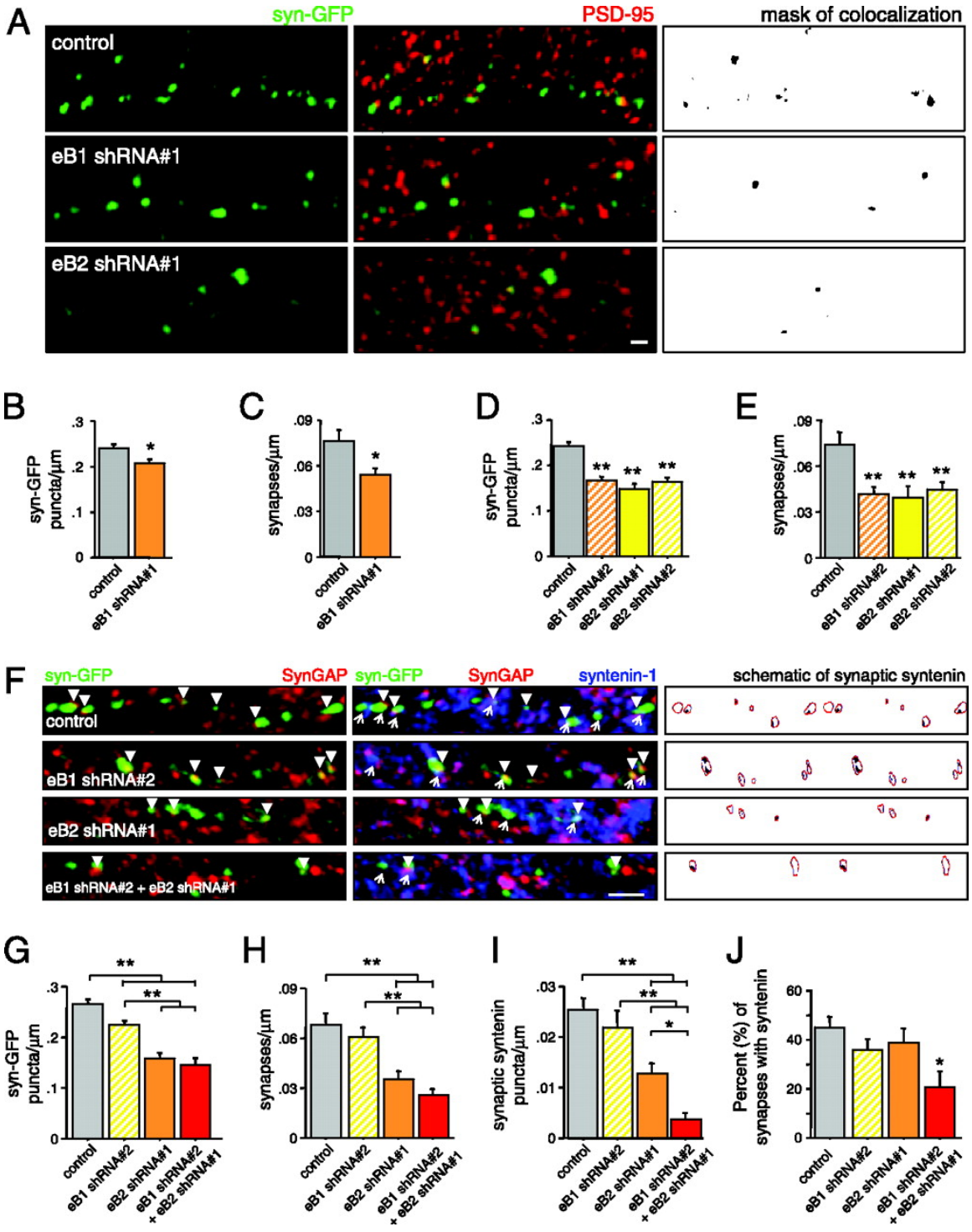
A
syn-GFP
PSD-95
mask of colocalization
control
eB1 shRNA#1
eB2 shRNA#1
B
syn-GFP puncta/µm
control
eB1 shRNA#1
C
synapses/µm
control
eB1 shRNA#1
D
syn-GFP puncta/µm
control
eB1 shRNA#2
eB2 shRNA#1
eB2 shRNA#2
E
synapses/µm
control
eB1 shRNA#2
eB2 shRNA#1
eB2 shRNA#2
F
syn-GFP
SynGAP
syn-GFP
SynGAP
syntenin-1
schematic of synaptic syntenin
control
eB1 shRNA#2
eB2 shRNA#1
eB1 shRNA#2 + eB2 shRNA#1
G
syn-GFP puncta/µm
control
eB1 shRNA#2
eB2 shRNA#1
eB1 shRNA#2 + eB2 shRNA#1
H
synapses/µm
control
eB1 shRNA#2
eB2 shRNA#1
eB1 shRNA#2 + eB2 shRNA#1
I
synaptic syntenin puncta/µm
control
eB1 shRNA#2
eB2 shRNA#1
eB1 shRNA#2 + eB2 shRNA#1
J
Percent (%) of synapses with syntenin
control
eB1 shRNA#2
eB2 shRNA#1
eB1 shRNA#2 + eB2 shRNA#1

## Supplementary Figure 2.1

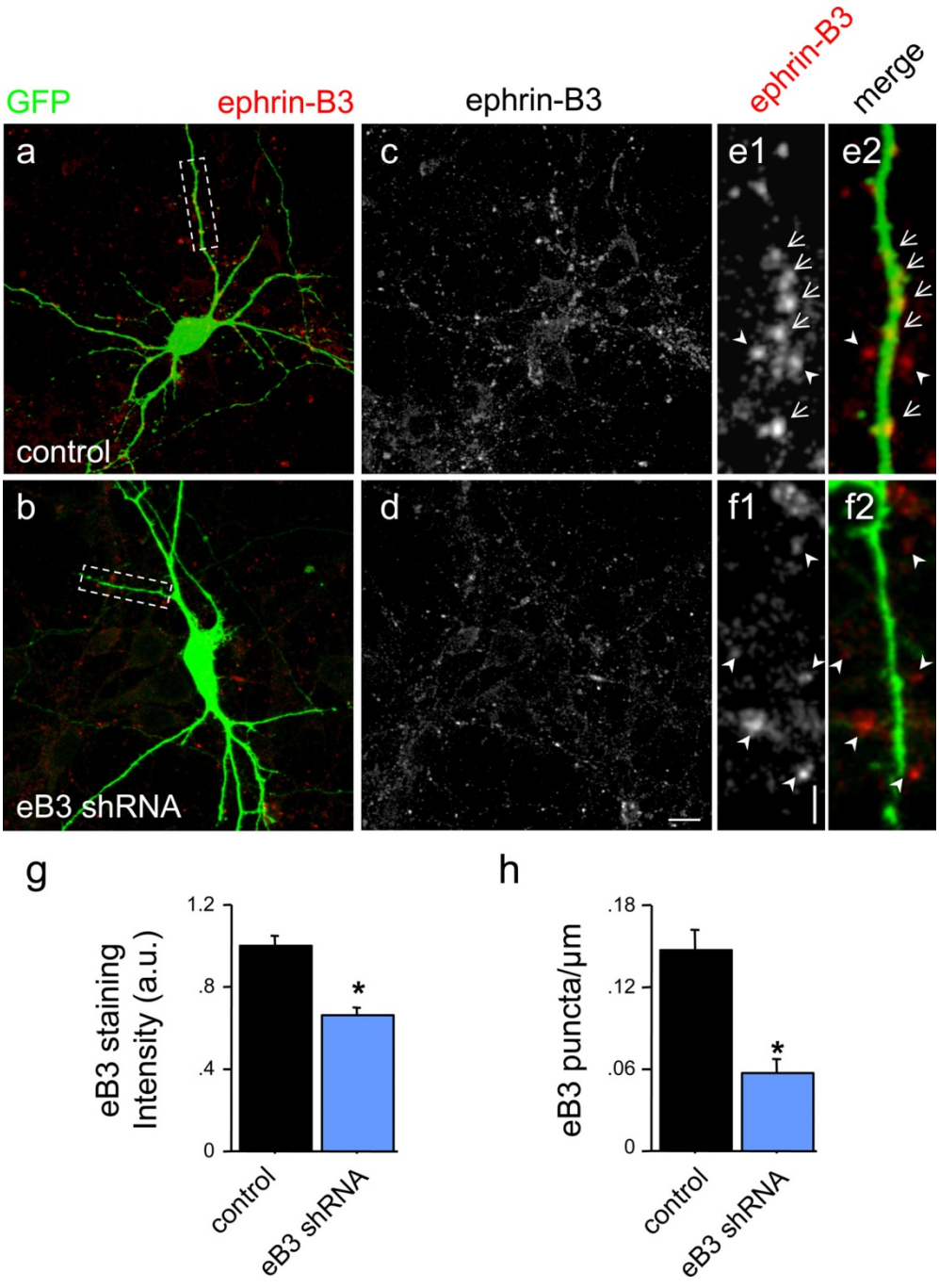

# Supplementary Figure 2.2

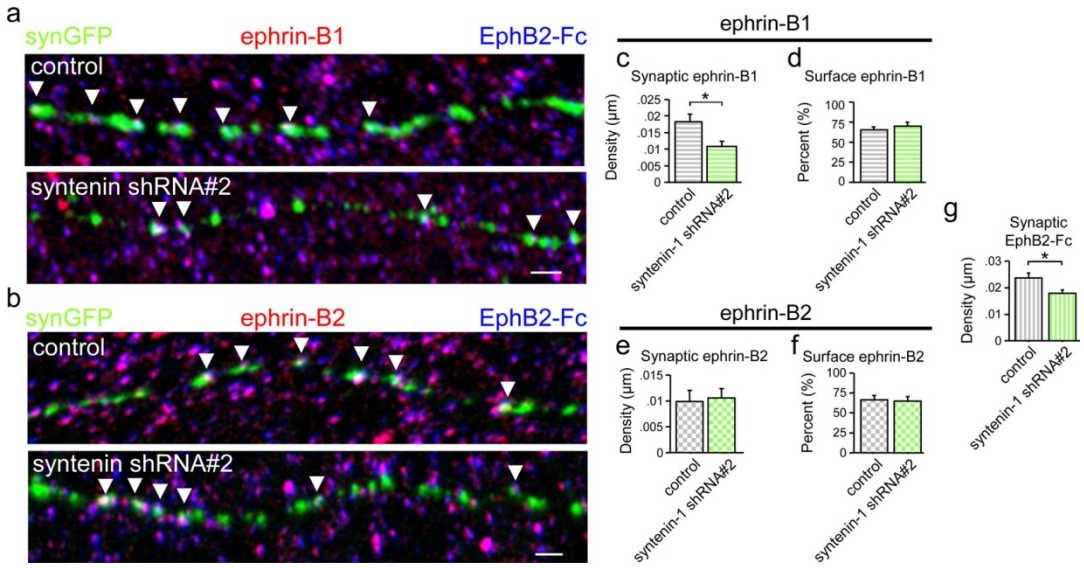

# Supplementary Figure 2.3

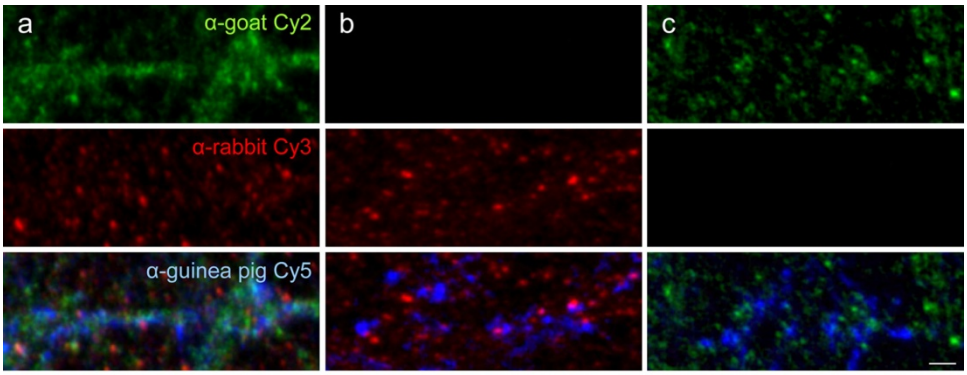


| a | b | c |
|---|---|---|
| 1°Antibody | 1°Antibody | 1°Antibody |
| Goat α-eB1 | | Goat α-eB2 |
| Rabbit α-goat Fab + Goat α-eB2 | Rabbit α-goat Fab + Goat α-eB2 | |
| Guinea Pig α-VGlut1 | Guinea Pig α-VGlut1 | Guinea Pig α-VGlut1 |
| 2°Antibody | 2°Antibody | 2°Antibody |
| Cy2 Donkey α-Goat | Cy2 Donkey α-Goat | Cy2 Donkey α-Goat |
| Cy3 Donkey α-Rabbit | Cy3 Donkey α-Rabbit | Cy3 Donkey α-Rabbit |
| Cy5 Donkey α-Guinea Pig | Cy5 Donkey α-Guinea Pig | Cy5 Donkey α-Guinea Pig |

## Supplementary Figure 2.4

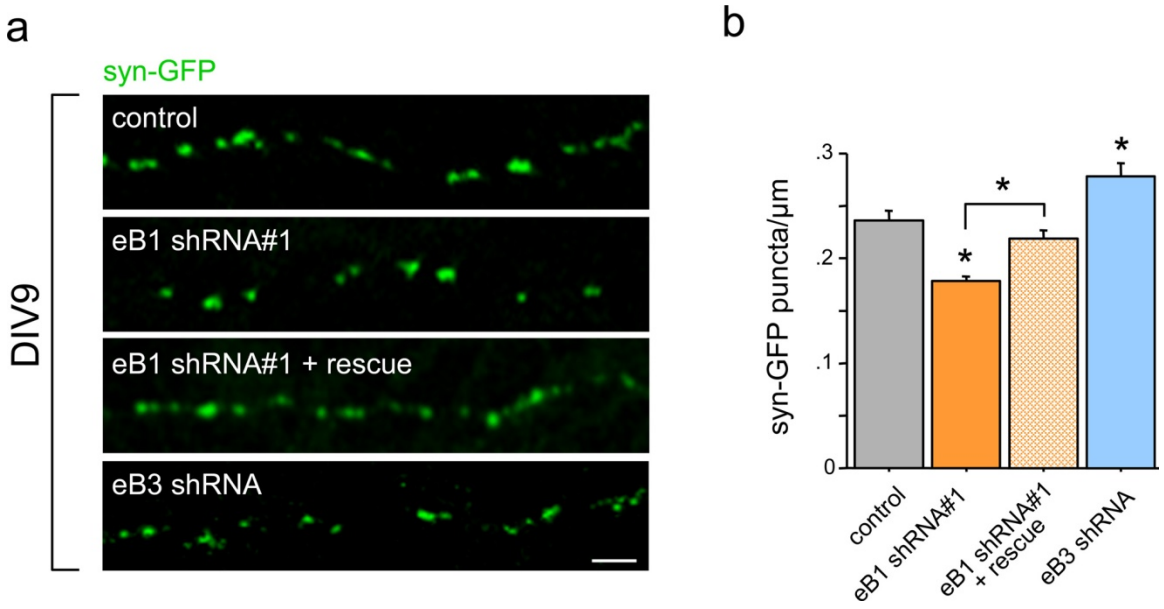

## Supplementary Figure 2.5

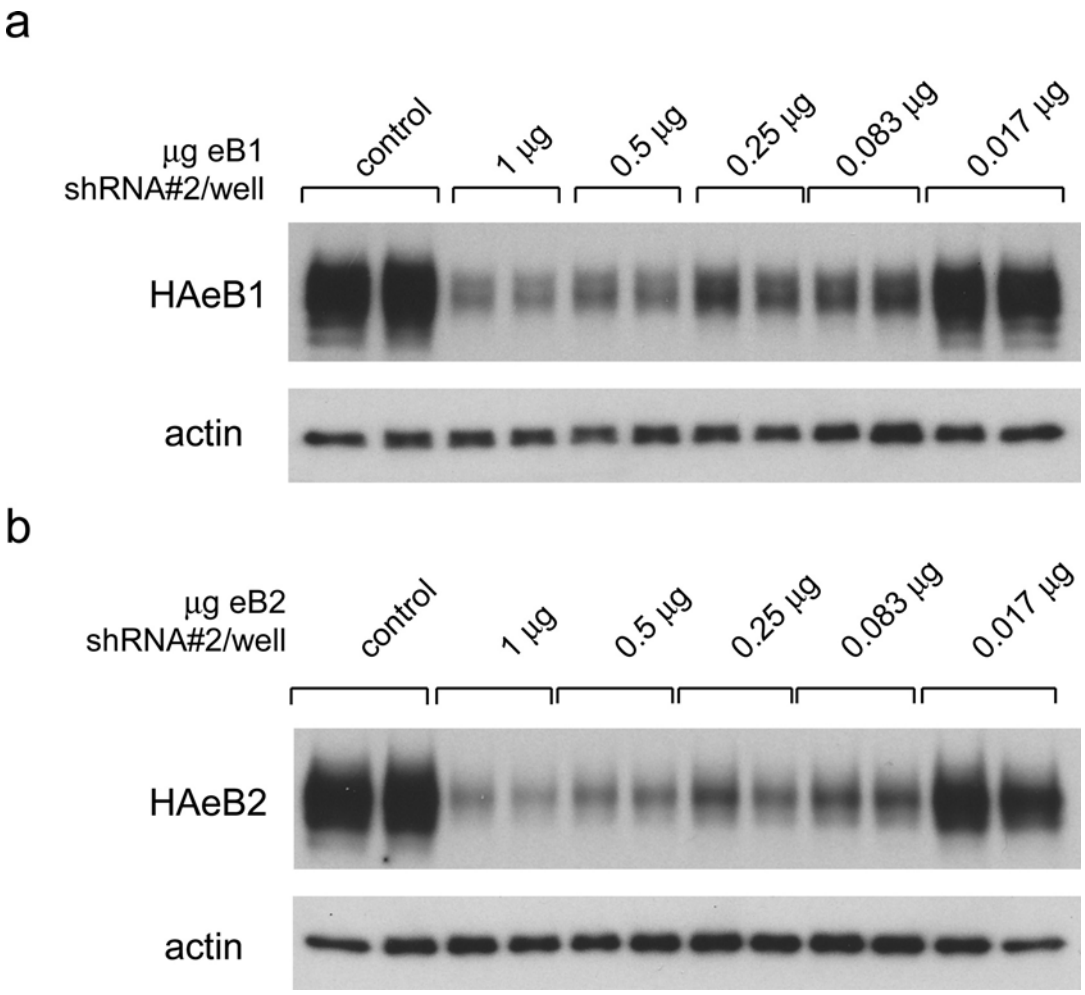

## Supplementary Figure 2.6

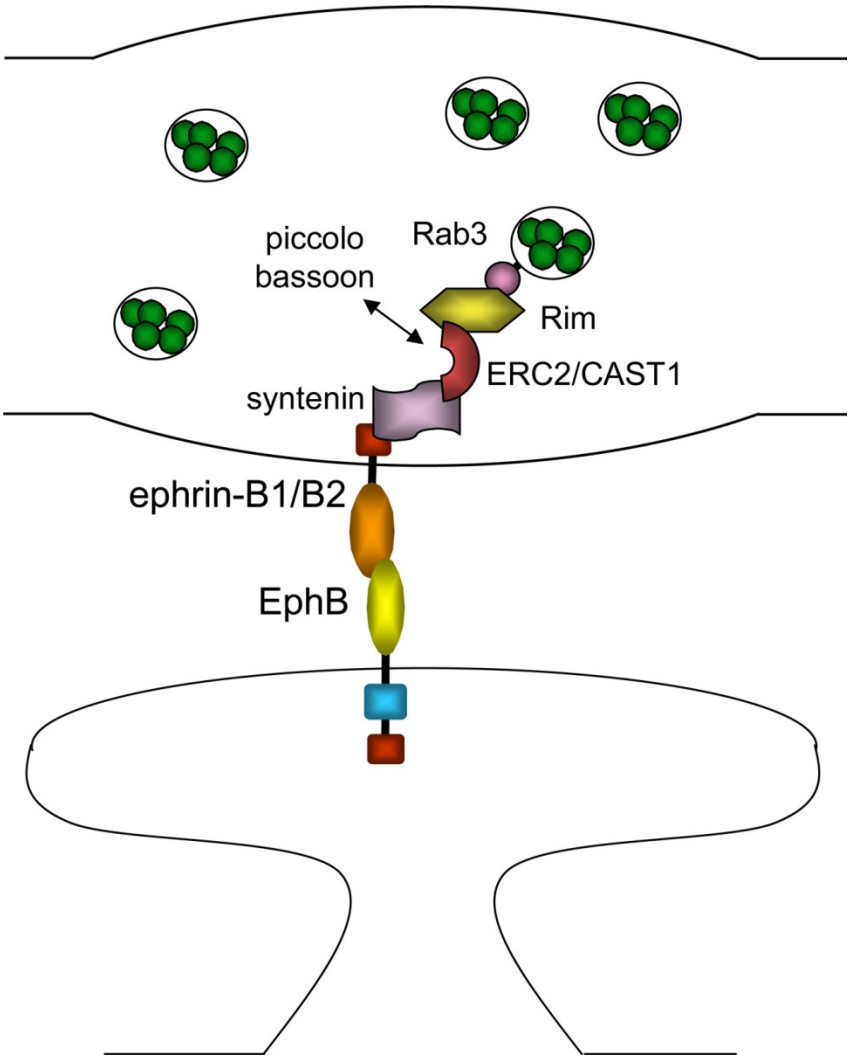

# Supplementary Table 2.1

**Table S1. Puncta analysis of DIV30 cortical neuron culture immunostained for ephrin-B1, ephrin-B2, syntenin-1, and VGlut1**

| | |
|---|---|
| VGlut1 puncta that colocalize with ephrin-B1 | Percentage |
| Total | 36.89 |
| Colocalized with ephrin-B2 | 54.15 |
| Colocalized with syntenin-1 | 62.65 |
| Glut1 puncta that colocalize with ephrin-B2 | |
| Total | 21.03 |
| Colocalized with ephrin-B1 | 27.93 |
| Colocalized with syntenin-1 | 42.14 |
| VGlut puncta that co-localize with syntenin-1 | |
| Total | 19.81 |
| Colocalized with ephrin-B1 | 39.49 |
| Colocalized with ephrin-B2 | 28.86 |
| VGlut puncta area colocalized with | |
| ephrin-B1 | 46.68 |
| ephrin-B2 | 21.52 |

CHAPTER 3

# A novel extracellular interaction mechanism controls the EphB-NMDAR interaction and synaptic function

Sean I. Sheffler-Collins[1, 3], Kenji Hanamura[1], Daniel S. Spellman[2], Thomas A. Neubert[2] and Matthew B. Dalva[1]

[1]Department of Neuroscience and Farber Institute for Neurosciences, Thomas Jefferson University, 900 Walnut Street, JHN Suite 462, Philadelphia, PA, 19107

[2]Department of Pharmacology and Kimmel Center for Biology and Medicine at the Skirball Institute, New York University School of Medicine, New York, NY 10016

[3]Neuroscience Graduate Group, University of Pennsylvania School of Medicine, Philadelphia, PA 19104

Contributions: S.I.S-C. generated constructs, performed and analyzed experiments, generated figures, and wrote the manuscript, except where noted below. D.S.S. performed all mass spectrometry experiments and generated figures (Figure 3.1A-B, Supplementary Figure 3.1 and 3.2). T.A.N. helped with mass spectrometry experimental design and analysis. M.B.D. performed all physiology and analysis for Figure 3.4A-D and the luciferase assay in Figure 3.4H. K.H. performed and analyzed experiments for Figure 4E-G. S.I.S-C. and M.B.D. designed all experiments except for mass spectrometry.

**Abstract**

Trafficking of NMDA receptors to synaptic sites is critical for synaptic function and plasticity in the mature brain. The type and number of NMDARs must be maintained and tightly regulated to enable changes in synaptic strength while preventing excitotoxicity. Increased content of NR2B-containing NMDARs at synaptic sites increases synaptic plasticity and improves behavioral tasks of learning and memory. In the mature brain, EphBs interact directly with NMDA receptors and regulate the synaptic localization of NR2B-containing NMDARs. EphB-dependent modulation of NMDARs promotes synaptic function, plasticity, and its misregulation results in disease. However, whether the interaction between EphBs and NMDARs is important for these events have not been tested. Here, we identify a single amino acid in the extracellular domain of EphB2 that is necessary and sufficient to mediate the EphB-NMDAR interaction. We define a novel molecular mechanism, where a specific extracellular tyrosine residue is phosphorylated after ephrin-B ligand binding, to induce the EphB-NMDAR interaction. Mutations at this site enhance or reduce synaptic currents of NR2B-containing NMDARs, receptor stabilization at the cell surface, and $Ca^{2+}$-dependent gene transcription. These findings indicate that in EphBs are critical regulators of NMDAR subunit composition, function, and synaptic localization to prevent disease in the mature brain.

During development and in the adult brain, the NMDAR is required for the generation of normal circuitry and synaptic function (Lau and Zukin, 2007; Perez-Otano and Ehlers, 2005). NR2B subunit-containing NMDARs have longer channel open time and increased calcium influx (Chen and Roche, 2007; Cull-Candy and Leszkiewicz, 2004; Prybylowski and Wenthold, 2004). Driving NR2B-containing NMDARs to synapses in the mature brain increases the plasticity of synapses and improves performance on behavioral tasks of learning and memory (Philpot et al., 2007; Tang et al., 1999). It appears that EphBs interact directly with NMDARs through their extracellular domains and cluster NMDARs at synaptic sites (Attwood et al., 2011; Dalva et al., 2000; Grunwald et al., 2001; Slack et al., 2008). The EphB-NMDAR interaction is implicated in numerous synaptopathies such as: Alzheimer's disease (Cisse et al., 2011; Simon et al., 2009), anxiety disorders (Attwood et al., 2011), and neuropathic pain (Liu et al., 2011; Liu et al., 2009; Slack et al., 2008; Song et al., 2008b). In mature neurons, EphB2 regulates synaptic localization and $Ca^{2+}$-dependent desensitization of NR2B-containing NMDARs (Nolt et al., 2011). After EphB activation, the EphB-NMDAR interaction results in enhanced calcium influx, tyrosine phosphorylation, and function of NMDARs (Dalva et al., 2000; Takasu et al., 2002). The EphB-NMDAR interaction induces phosphorylation of the NR2B subunit at intracellular Y1472, which can stabilize NR2B-containing NMDARs at synaptic sites (Dalva et al., 2000; Prybylowski et al., 2005; Takasu et al., 2002).

EphB receptors are cell-surface localized, single-pass transmembrane receptor tyrosine kinases that are activated by their clustered, membrane-

attached ephrin-B ligands (Egea and Klein, 2007). Ephrin-B/EphB signaling in the CNS controls axon guidance, dendritic filopodia motility, pre-and postsynaptic excitatory synapse formation, synapse maturation, glutamate receptor localization and function, and synaptic plasticity (Egea and Klein, 2007; Sloniowski and Ethell, 2011). For EphBs, the ability to coordinate these events requires tight regulation of receptor trafficking including EphB receptor cleavage, internalization, and degradation (Pitulescu and Adams, 2010). While the differences between these modes of trafficking are poorly understood, regulation of EphB receptor trafficking is clearly important for regulation of NMDA receptors at synaptic sites.

*EphB1*$^{-/-}$*, B2*$^{-/-}$*, B3*$^{-/-}$ (TKO) mice are defective in their ability to localize NR2B-containing NMDARs to synaptic sites (Henkemeyer et al., 2003; Kayser et al., 2006; Nolt et al., 2011). EphBs interact directly with NMDARs through an undefined region of their extracellular domains (Attwood et al., 2011; Dalva et al., 2000; Grunwald et al., 2001; Slack et al., 2008). We generated numerous EphB expression constructs, but were unable to identify a small subregion (<100 amino acids) that mediates the EphB-NMDAR interaction. Therefore, we undertook an unbiased mass spectrometry based approach to identify candidate interactions domains. We expressed the FLAG epitope-tagged EphB2 (fB2) receptor in NG108 cells. After 48 hours, cells were stimulated with clustered ephrin-B1-Fc for 45 minutes to activate the receptors (for verification see **Supplementary Figure 3.1**). Ephrin-B treatment was used because induction of the EphB-NMDAR interaction requires ephrin-Bs (Dalva et al., 2000). EphB2 receptors

were immunoprecipitated using anti-FLAG antibodies, proteins were separated using SDS-PAGE, digested in-gel with trypsin, and phosphopeptides were enriched using $TiO_2$ before LC-MS/MS (MW range 100-130kD). Three known phosphopeptides were identified in the juxtamembrane and kinase domains (**Supplementary Figure 3.2**) in addition two novel phosphorylation sites (ELSE**Y**NATAIK and AGAI**Y**VFQVR) were identified that correspond to regions in the extracellular portion of the receptor (**Figure 3.1A-C**). Due to the unusual nature of the location of these peptides Mascot results and MS/MS spectra were closely inspected. We found that each peptide was identified on four independent experiments and twice in each labeling state, with Mascot scores of 34 and 63 respectively and definable separation from the next peptide assigned to that spectrum. Manual inspection of the MS/MS spectrum confirmed that the signals present are accounted for and ions critical to localization at the site of phosphorylation are present.

The two phosphopeptides identified, ELSE**Y**NATAIK and AGAI**Y**VFQVR were each found in the C-terminal fibronectin type III repeat domains (cFN3; see **Figure 3.1C** for schematic) and correspond to tyrosine residues Y481 and Y504 respectively. Y504 and neighboring residues are well conserved (>51% identity in 15 of 18 neighboring amino acids) amongst the entire Eph family, whereas Y481 is less well conserved (>51% identity in 2 of 16 neighboring amino acids) in other Ephs (**Figure 3.1D**). These findings suggest that phosphorylation at Y504 may also be a common mechanism for regulation of other Eph family members. EphB receptors interact directly with NMDA-type glutamate receptors through an

undefined region of their extracellular domains (Attwood et al., 2011; Dalva et al., 2000; Grunwald et al., 2001; Slack et al., 2008). Since, both the EphB-NMDAR interaction and phosphorylation at Y481 and Y504 require activation by ephrin-B ligand; we hypothesized that one or more of these sites might play a role in the EphB-NMDAR interaction. To test this possibility, we generated phosphomimetic (fB2 Y481E and Y504E) and non-phosphorylatable (fB2 Y481F and Y504F) point mutants to the FLAG-tagged EphB2 receptor. We then transfected HEK293T cells with fB2 WT, fB2 Y481E, or fB2 Y481F, along with HA-NR1-GFP and NR2B constructs, to form a functional NMDAR that is trafficked to the cell surface. NR2B-containing receptors were used because their trafficking and function is specifically regulated at mature synapses by EphBs (Nolt et al., 2011). EphB2 receptors were immunoprecipitated using an anti-FLAG antibody, and then probed for the HA-tag of NR1. We find that neither EphB2 Y481E (**Figure 3.1E lane 3; Figure 3.1F quantification**) nor Y481F (**Figure 3.1E lane 4; Figure 3.1F quantification**) affect the ability of EphBs to bind NR1. These data suggest that Y481 does not play an important role in the EphB-NMDAR interaction. We next tested whether the Y504 site might modulate the EphB-NMDAR interaction. When co-expressed in HEK293T cells, we find that EphB2 Y504F significantly reduced NR1 binding compared to WT (**Figure 3.1G lane 4; Figure 3.1H quantification,** ANOVA test, $p < 0.05$), while mutation of Y504E significantly increased binding compared to WT and Y504F (**Figure 3.1G lane 3; Figure 3.1H quantification,** ANOVA test, $p < 0.05$). These findings suggest that Y504 may play an important role in the EphB-NMDAR interaction.

Next, we wanted to test whether Y504 mutant receptors affect the EphB-NMDAR interaction in neurons. Therefore, we generated lentiviruses transducing EphB2-YFP WT, EphB2-YFP Y504E, and EphB2-Y504F constructs into DIV2 cultured cortical neurons for co-IP experiments. At DIV7, expressed EphB2 receptors were enriched using an anti-GFP antibody and level of NR1 pull-down was assessed. Consistent with previous reports (Dalva et al., 2000), in neurons over-expressing WT EphB receptors the EphB-NMDAR interaction is induced by ephrin-B stimulation (**Figure 3.1I lanes 1 and 2; Figure 3.1J quantification**). Interestingly, in the phosphomimetic Y504E mutant, the EphB-NMDAR interaction is induced without ephrin-B treatment (**Figure 3.1I lane 3**). Furthermore, ephrin-B stimulation does not potentiate the EphB-NMDAR interaction further in Y504E mutants (**Figure 3.1I lane 4; Figure 3.1J quantification**). These data are consistent with phosphorylation at Y504 being sufficient for the EphB-NMDAR interaction to occur. Consistently, non-phosphorylatable Y504F mutants have little pull-down with NR1 in absence of ephrin-B treatment (**Figure 3.1I lanes 5; Figure 3.1J quantification**). Ephrin-B stimulation did not potentiate the EphB-NMDAR interaction in Y504F mutant receptors (**Figure 3.1I lanes 6; Figure 3.1J quantification**). Together, these data suggest that phosphorylation of Y504 is necessary and sufficient for the EphB-NMDAR interaction in neurons and HEK293T cells.

Although most protein kinases have been studied inside the cell, evidence suggests that phosphorylation of proteins can occur in the extracellular space (Redegeld et al., 1999). Both soluble and membrane attached kinases have

been found in numerous cell types including neurons (Chen et al., 1996; Fujii et al., 2000; Kumar et al., 2011). In neurons extracellular protein kinases regulate processes including synaptic plasticity (Chen et al., 1996; Fujii et al., 2000) and aggregation of amyloid β-peptides (Aβ) in mouse and human brain (Kumar et al., 2011). To begin to test whether Y504 is phosphorylated extracellularly, we first generated a polyclonal phospho-specific antibody to tyrosine 504. We tested this antibody in lysates from HEK293T cells transfected with FLAG-EphB2 constructs and found that full-length WT EphB2 receptors were recognized by this antibody at the appropriate molecular weight ~120 kD, but not Y504F non-phosphorylatable mutants nor untransfected lysates (**Figure 3.2A left**). To test whether Y504 might become phosphorylated in the extracellular space we next asked whether in HEK293T cells if a truncated fB2 construct lacking an intracellular domain (Kayser et al., 2006) would still be phosphorylated. We have previously shown this construct localizes to the plasma membrane and can recruit presynaptic markers (Kayser et al., 2006). We found that the truncated WT EphB2 receptor, but not Y504F mutant receptor was recognized by the pY504 antibody at the appropriate molecular weight ~75kD (**Figure 3.2A right**). These data suggest that the EphB tyrosine kinase is not required for phosphorylation of Y504. Next, we wanted to test that our pY504 antibody was phospho-specific and recognized synaptic EphB2 protein. Synaptosomes were prepared from two WT CD1 mouse brains before being subjected to SDS-PAGE in duplicate, and then immunoblots were cut in half. One blot was treated with Calf Intestinal Alkaline Phosphatase (CIP, 1:500; New England BioLabs)

overnight to de-phosphorylate all proteins. Blots were then probed with the pY504 antibody (**Figure 3.2B top**), then stripped and reprobed with an N-terminal commercial EphB2 antibody to verify non-phosphorylated protein was present, and that the phospho-band ran at the appropriate molecular weight (**Figure 3.2B bottom**). These data suggests our antibody recognizes a phospho-specific epitope.

Next, to test whether phosphorylation of Y504 might occur on the cell surface, we asked if blocking internalization of EphB2 might block phosphorylation of Y504. Since EphBs are internalized by clathrin-mediated mechanisms after ephrin-B stimulation (Irie et al., 2005; Litterst et al., 2007; Pitulescu and Adams, 2010; Vihanto et al., 2006), we blocked clathrin-mediated endocytosis using two pharmacological treatments (450mM hypertonic sucrose or 80 μM dynasore; Sigma-Aldrich) in DIV6-7 cultured cortical neurons in the presence or absence of ephrin-B stimulation. To examine the effects of drug treatment on EphB2 phosphorylation, we immunoprecipitated with an N-terminal anti-EphB2 antibody then probed with pY504 or intracellular EphB2 antibodies. We found that treatment with either hypertonic sucrose or dynasore did not block the induction of Y504 phosphorylation after ephrin-B2 treatment (**Figure 3.2C left**). To validate that drug treatments did not block intracellular kinase activity, we stripped and probed the same blots with an antibody against the EphB2 intracellular kinase domain (pY662; (Dalva et al., 2000)). Neither dynasore nor hypertonic sucrose blocked the ability for the EphB2 kinase activation. These

data supports the model (**Figure 3.2D**) that EphB2 pY504 gets phosphorylated in the extracellular space by an exo- or ecto-protein kinase.

We next tested whether inhibition of extracellular phosphorylation alone was sufficient to block the EphB-NMDAR interaction. To do this, we took advantage of the widely used, broad-spectrum extracellular kinase inhibitor k-252b (Chen et al., 1996; Fujii et al., 2000; Nguyen et al., 2008). In DIV6-7 cortical neurons, treatment with activated ephrin-B for 45 minutes induces the EphB-NMDAR interaction (**Figure 3.2E lanes 1 and 2; Figure 3.2F quantification**) and resulted in phosphorylation of Y504 (**Figure 3.2E lanes 1 and 2; Figure 3.2G quantification**). Following k-252b treatment (10μM; Sigma-Aldrich), ephrin-B stimulation failed to induce phosphorylation at Y504, although the kinase activity of the EphB receptor was unaffected (**Figure 3.2E lanes 3 and 4; Figure 3.2G quantification**). In addition, treatment of neurons with k-252b is sufficient to block the ephrin-B induced EphB-NMDAR interaction (**Figure 3.2E lanes 3 and 4; Figure 3.2F quantification**). Taken together, these results suggest that ephrin-B-dependent phosphorylation of EphB2 Y504 occurs in the extracellular space and is required for the EphB-NMDAR interaction.

The ability of EphB2 receptors to properly regulate NMDAR surface localization at synapses is required for normal brain functioning, and dysfunction of these events are implicated in numerous human diseases such as Alzheimer's disease (Cisse et al., 2011; Simon et al., 2009) and anxiety disorders (Attwood et al., 2011). Therefore we asked whether phosphorylation at Y504 might alter the trafficking of the EphB2 receptors (**Figure 3.3A**). We reasoned that since WT

EphB2 receptors are localized to the plasma membrane, mutation of Y504 to E should not stop insertion of mutant receptors into the plasma membrane. In support of this idea, we find that fB2 Y504E receptors do localize to the cell surface, although at significantly reduced levels compared to other EphB2 constructs (**Figure 3.3B; Figure 3.3C quantification**). Furthermore, when expressed alone in HEK293T cells, total expression levels of fB2 Y504E are reduced compared to WT or Y504F constructs (**Supplementary Figure 3.3).** These data suggest that phosphorylation of Y504 may also regulate EphB trafficking as well as the EphB-NMDAR interaction (**Figure 3.3A**). Furthermore, these data suggest the possibility that in the absence of the NMDAR, phosphorylation of Y504 may lead to the removal and proteolysis of EphB2

To test whether phosphomimetic Y504E mutant receptors were properly localized to the plasma membrane, but prematurely degraded, we blocked clathrin-mediated internalization using hypertonic sucrose (Heuser and Anderson, 1989) in HEK293T cells transfected with fB2 WT, Y504E, and Y504F constructs. Sucrose treatment for only 15 minutes increased total fB2 Y504E expression back to baseline levels, but did not affect WT or Y504F constructs (**Figure 3.3D lanes 5 and 6; Figure 3.3E quantification**). Because proper activation of the intracellular kinase domain in EphB2 is required for surface localization (Irie et al., 2005; Zimmer et al., 2003), we wanted to test if kinase activity was also required for Y504 surface localization. Therefore, we used constructs with a point mutation (fB2 K663R or fB2 KD) in the EphB2 ATP-binding domain that renders the kinase inactive (Dalva et al., 2000) to generate

both non-phosphorylatable and phosphomimetic double-point mutants with inactive kinases fB2 KD Y504E and fB2 KD Y504F respectively. Consistent with this model, fB2 KD Y504E mutants were expressed at similar levels to WT and Y504F constructs (**Figure 3.3D; Figure 3.3E quantification**). Together, these findings suggest that Y504E mutant EphB2 receptors are rapidly internalized by clathrin-mediated mechanisms that require EphB tyrosine kinase activity.

We next asked whether blocking endocytosis with dominant negative dynamin (K44A) constructs, which block the formation of clathrin-coated pits at the plasma membrane, might also rescue the expression level of EphB2 Y504E constructs (Conner and Schmid, 2003). Over-expression of WT dynamin should lead to a large increase in protein degradation in total lysates, whereas K44A over-expression should block clathrin-mediated endocytosis. We co-expressed these two dynamin constructs with fB2 WT, Y504E, and Y504F constructs in HEK293T cells. We find that co-expressing K44A dynamin causes a significant increase in EphB2 expression in the total lysate of WT and Y504E, but not non-phosphorylatable Y504F receptors (**Figure 3.3F-G**). Furthermore, there is significantly more fB2 expression in Y504E mutants than Y504F mutants (**Figure 3.3G**). These data support a model (**Figure 3.3A**) where Y504E mutants are trafficked to the plasma membrane, but rapidly degraded via clathrin-mediated mechanisms.

To test the idea that phosphomimetic Y504E receptors are degraded in the proteasome, we used lactacystin (5μM; Calbiochem), an irreversible inhibitor of the 20S proteasome, to block all protein degradation (Litterst et al., 2007;

Margolis et al., 2010). We reasoned that in the presence of lactacystin, there should be significantly more protein in the total lysate than under untreated conditions. As expected, in the presence of lactacystin, the level of expression of fB2 Y504E was rescued to control levels (**Figure 3.3H lanes 5 and 6; Figure 3.3I quantification**). These data is consistent with a model (**Figure 3.3A**) in which Y504E mutant receptors are rapidly internalized off the plasma membrane after ephrin-B activation.

To test whether a similar mechanism might function in neurons, we biotinylated surface-localized, endogenous EphB2 receptors in DIV7 cultured cortical neurons after ephrin-B activation. Consistent with previous reports (Irie et al., 2005; Zimmer et al., 2003), we find that EphB2 receptors are internalized after ephrin-B activation (**Supplementary Figure 3.4**). Furthermore, we find that these activated receptors move from the biotin-labeled surface fraction to an intracellular avidin fraction without affecting total expression (**Supplementary Figure 3.4**). These data confirm that similar to HEK293T cells, EphB2 receptors are internalized in neurons after ephrin-B activation.

Phosphorylation of Y504 induces the EphB-NMDAR interaction; therefore we asked whether the presence of NMDAR receptors would affect the instability of Y504E mutant receptors. To test this, we transfected fB2 WT, Y504E, and Y504F constructs alone, or with HA-NR1-GFP and NR2B in HEK293T cells before performing a steady-state cell surface biotinylation. We find that Y504E mutants have reduced surface localization compared to WT or Y504F receptors (**Figure 3.3J; Figure 3.3K quantification**). However, when co-expressed with

NMDARs, the levels of Y504E mutant receptors are rescued back to levels comparable to WT and Y504F receptors (**Figure 3.3J lanes 3 and 4; Figure 3.3K quantification**). These data suggests that the EphB-NMDAR interaction stabilizes EphB receptors on the plasma membrane. Moreover, a cell surface biotinylation in cultured cortical neurons infected with our EphB2-YFP lentiviruses resulted in no significant differences in surface localization between Y504E, WT, or Y504F receptors (**Supplementary Figure 3.5**). These data suggests that in the presence of endogenous NMDARs, over-expressed Y504E mutant receptors are stabilized on the membrane.

To test whether the EphB-NMDAR interaction might affect NR1 surface retention, we transfected fB2 WT, Y504E, and Y504F constructs with HA-NR1-GFP and NR2B, or NR1/2B alone in HEK293T cells before performing a steady-state cell surface biotinylation and probing for the HA-tag of NR1 (same lysates as in **Figure 3.3L-M**). We find that co-expression of fB2 Y504E significantly increased the fraction of NR1 receptors on the plasma membrane compared to all other conditions (**Figure 3.3L lane 3; Figure 3.3M quantification**). Interestingly, co-expression of non-phosphorylatable Y504F mutant receptors causes a significant decrease of NR1 receptors on the cell surface compared to WT EphB2 (**Figure 3.3L; Figure 3.3M quantification**). These data suggests that the EphB-NMDAR interaction stabilizes NMDA receptors on the plasma membrane.

Late in neuronal development (after DIV14), EphBs are not required to maintain synapse number (Kayser et al., 2008), but are instead key regulators of

NMDAR localization and functional at mature synapses (Nolt et al., 2011). To test whether the EphB-NMDAR interaction is required to maintain the normal number of NR2B-containing NMDARs at synapses, we asked if mutation to Y504 would alter the functional properties of synapses in mature cultured cortical neurons. Neurons were transfected at DIV14 with EGFP and vector control, EphB2-YFP-WT, Y504E, or Y504F constructs. Then at DIV21-23, spontaneous miniature EPSCs (mEPSCs) were recorded using whole-cell patch clamp at +50mV including tetrodotoxin and blockers of GABAergic channels to isolate NMDAR-mediated spontaneous currents. No changes on mEPSC frequency were observed between conditions (Control, n=9; WT, n=10; Y50E, n=10; Y504F n=13). However, EphB2 WT and EphB2 Y504E over-expression both caused a significant increase in amplitude compared to control or non-phosphorylatable Y504F mutants (**Figure 3.4A**). These changes in mEPSC amplitude are attributable specifically to NMDARs because treatment of the NMDAR antagonist D-APV (50μM) blocked these affects (**Figure 3.4A-B**: Control n=5 cells, 491 mEPSCs w/o APV, 421 mEPSCs w/ APV; WT, n=7 cells, 1182 mEPSCs w/o APV, 758 mEPSCs w/ APV; Y504E, n=6 cells, 705 mEPSCs w/o APV, 349 mEPSCs w/ APV; Y504F, n=9 cells, 912 mEPSCs w/o APV, 541 mEPSCs w/ APV: $p<0.001$). While there is a modest effect on Y504F mutants with APV treatment, a much larger effect is observed for Y504E mutants (**Figure 3.4B**). These data suggests that phosphorylation at Y504 is a functional regulator of NMDAR currents at mature synapses.

We have shown that EphB2 is a subunit-specific regulator of synaptic-NR2B containing NMDARs (Nolt et al., 2011) at mature synapses. Based on the finding that Y504 regulates the function of NMDAR currents at mature synapses (**Figure 3.4A-B**), we hypothesized that this change was due to recruitment of NR2B-containing NMDARs to synaptic sites. To test this, we treated neurons with Ro25-6981 (Ro25) the NR2B-selective antagonist (2.5 μM; Tocris Bioscience) and then measured mEPSC amplitude. We find that treatment with Ro25 caused a large decrease on mEPSC amplitude in cells expressing phosphomimetic Y504E mutant receptors (**Figure 3.4C**; Y504E, n=7 cells, 767 mEPSCs w/o Ro25, 456 mEPSCs w/ Ro25). However, no changes were observed in current amplitude from cells expressing Y504F mutant receptors after Ro25 treatment (**Figure 3.4D**; Y504F, n=6 cells, 457 mEPSCs w/o Ro25, 444 mEPSCs w/ Ro25). These data demonstrate that at mature synapses, phosphorylation of Y504 results in increased trafficking of NR2B-containing NMDARs to synaptic sites, which alters synaptic currents.

To confirm our physiological findings, we performed immunostaining experiments at the same developmental timepoints, using the same conditions, and looking at NR2B staining intensity at synapses. We looked at NR2B staining intensity at synaptic sites (positive for the presynaptic vesicle protein SV2; **Figure 3.4E-G:** Control, n=539 synapses; WT, n=516; Y504E, n=527; Y504F, n=539). In accordance with our physiological findings, we find that synaptic NR2B is significantly reduced in EphB2 Y504F expressing neurons compared to EphB2 Y504E (**Figure 3.4E-G**; ANOVA test, $p < 0.01$). Furthermore, neurons

expressing Y504F mutant receptors had significantly reduced synaptic NR2B compared to controls (**Figure 3.4E-F**; ANOVA test, $p < 0.05$). We find similar increases in EphB2 Y504E, as expected from our physiological experiments with Ro25 (**Figure 3.3C-D**).

EphB regulates NMDAR-dependent gene transcription by modulating calcium influx through NR2B-containing NMDARs (Takasu et al., 2002). To test whether the ability of EphB2 to recruit NR2B receptors to synaptic sites might impact NMDAR-dependent gene expression, we used a synaptic stimulation paradigm and asked if our EphB Y504 mutant receptors altered CREB-dependent reporter gene expression. We transfected DIV7 cultured cortical neurons with GFP control, EphB2 WT, EphB2 Y504E, or EphB2 Y504F constructs along with CRE-luciferase reporter construct or *Renilla* luciferase as a transfection control. Neurons were stimulated with 4-AP and BIC in the presence of nifedipine to block L-type calcium channels; and then some neurons were treated with Ro25-6981 (2.5 μM) to block NR2B-containing receptors. We find that expression of EphB2 Y504E constructs potentiates CREB-dependent gene transcription (**Figure 3.4H**). Furthermore, this effect is totally abolished with treatment of Ro25 (**Figure 3.4H**). Taken together, these results suggest that phosphorylation at Y504 potentiates calcium-dependent gene transcription through NR2B-containing NMDARs.

It was previously shown that the EphB-NMDAR interaction requires the EphB extracellular domain, but the specific residues required for this interaction have remained elusive for over a decade. Here, we report that EphB2 Y504 is

both necessary and sufficient for the EphB-NMDAR interaction to occur. Our findings support a model in which phosphorylation of extracellular domains of EphB2, in a ligand-dependent manner, alters the direct protein-protein interactions with NMDARs. Mislocalization of NMDARs from the cell surface and synaptic sites is a hallmark of the diseased brain. Specifically, deficits in EphB-dependent regulation of NMDAR localization is associated with synaptopathies including neuropathic pain (Slack et al., 2008; Song et al., 2008b), Alzheimer's disease (Cisse et al., 2011; Simon et al., 2009) and anxiety disorders (Attwood et al., 2011). Our data indicates that the EphB-NMDAR interaction in brain is responsible for modulating NMDARs at the surface and altering receptor function, signaling, and gene expression in a subunit specific manner.

Notably, we find that a broad-spectrum inhibitor of extracellular kinases, k-252b can block the EphB-NMDAR interaction and phosphorylation at Y504 in neurons. An extensive literature shows that in the spinal cord and periphery, blocking EphB1 signaling is sufficient to block hyperalgesia and NMDAR-dependent hyperexcitability in neuropathic and cancer-induced pain (Liu et al., 2011; Liu et al., 2009; Slack et al., 2008; Song et al., 2008b). Our data suggests that k-252b inhibits the phosphorylation of Y504 and suggests that extracellular inhibition of the EphB-NMDAR interaction could be a viable approach to treat neuropathic and cancer-induced pain.

While extracellular phosphorylation has previously been reported on serine and threonine residues (Chen et al., 1996; Fujii et al., 2000; Kumar et al., 2011; Redegeld et al., 1999), this is the first example of extracellular tyrosine

phosphorylation. One possible kinase that might mediate these events is a reported soluble form of the FGFR that lacks a transmembrane domain (Johnston et al., 1995; Katoh et al., 1992; Sturla et al., 2003). Our data define a new type of protein modification: phosphorylation of extracellular tyrosines that can enable novel forms of interactions at sites of cell-cell contact or give cells the ability to respond directly to their environment. Based on the conservation of Y504 amongst the EphB family, we expect that extracellular phosphorylation is an underappreciated mechanism for human disease. Taken together our finding suggests that extracellular phosphorylation of EphB2 at Y504 is a critical regulator of NMDAR synaptic localization and function with profound implications on synaptic plasticity and disease.

## Figure Legends

**Figure 3.1. Novel phosphorylation sites on the EphB2 receptor modulate the EphB-NMDAR interaction.** (A-B) MS/MS spectra of peptides (A) ELSEYNATAIK and (B) AGAIYVFQR are shown. Fragments critical for localization of phosphorylation sites are labeled in red. Most abundant signals are accounted for by sequence specific ions as indicated by labeling. (C) Schematic of the known functional domains of EphB2 receptor. LBD, Ligand-binding domain; Cys, cysteine-rich domain; FN3, Fibronectin type III repeat domain; TM, Transmembrane domain; JM, juxtamembrane domain; SAM, sterile-α-motif; PDZ, PSD-95/DLG1/ZO-1 domain. (D) Alignment of all mouse Eph family members cFN3 domains (Uniprot database) for 40 amino acids beginning at indicated site using ClustalW2 and Jalview software. EphB2 Y504 corresponds to a very well conserved tyrosine residue (red) whereas Y481 is not well conserved amongst the Eph family (yellow box). Blue color indicates % identity score with a threshold set at greater than 51%. Darker blue colors correspond to the most conserved residues. (E-F) HEK293T cells were co-transfected with HA-NR1-GFP and NR2B alone, or NR1/2B and fB2 WT, fB2 Y481E, or fB2 Y481F. EphB2 receptors were immunoprecipitated with anti-FLAG antibodies, and immunoblotted with anti-HA (NMDAR1) or EphB2 antibodies. *Right* Lysates from the same preparation as in E are shown immunoblotted with the same antibodies. (F) Quantification of relative amount of HA-NR1 immunoprecipitated compared to input (*$p < 0.05$, ANOVA test; n=5).

(G-H) As in E, HEK293T cells were co-transfected with NR1/2B construct alone, or with fB2 WT, fB2 Y504E, or fB2 Y504F mutants. EphB2 receptors were immunoprecipitated with anti-FLAG antibodies, and immunoblotted with anti-HA (NMDAR1) or EphB2 antibodies. *Right,* Lysates from the same preparation as in G are shown immunoblotted with the same antibodies. (H) Quantification of relative amount of HA-NR1 immunoprecipitated compared to input (*$p < 0.05$, ANOVA test; n=5). (G-H) DIV2 cultured cortical neurons were infected with EphB2-YFP WT, EphB2-YFP Y504E, or EphB2-YFP-Y504F constructs as indicated. At DIV7, neurons were stimulated for 45 minutes using ephrin-B2-Fc or Fc control as indicated. Infected EphB2 receptors were immunoprecipitated using an anti-GFP antibody. Resulting western blots were probed with anti-NMDAR1 or GFP (EphB2) antibodies. (H) Quantification of relative amount of NMDAR1 immunoprecipitated compared to input (*$p < 0.05$, ANOVA test; n=6).

**Figure 3.2. Extracellular phosphorylation modulates the EphB-NMDAR interaction and generation of a phospho-specific antibody to Y504**. (A-B) HEK293T cell lysates transfected with indicated FLAG-EphB2 constructs then probed with a phospho-specific polyclonal antibody generated against EphB2 Y504 (EphB2 pY504). (B) Pure synaptosome fractions from WT CD1 mice were subjected to SDS-PAGE. Resulting western blots were left untreated or were treated overnight with gentle shaking at 37°C with calf intestinal alkaline phosphatase (CIP; 1:500) as indicated then probed with EphB2 pY504 antibodies. Immunoblots were then stripped and reprobed with a commercial

antibody against the N-terminal domain of EphB2. (C) DIV6-7 cultured cortical neurons were treated as indicated with 450mM hypertonic sucrose for 15min at 37°C, or 30 min at 37°C with 80μM dynasore followed by 45 min of stimulation with Fc control or ephrin-B2-Fc (eB2). EphB2 receptors were immunoprecipitated with an N-terminal anti-EphB2 antibody, and immunoblotted against EphB2 pY504, EphB2, or the phosphorylated EphB2 kinase (EphB2 pY662). (D) Model of how extracellular phosphorylation at Y504 modulates the EphB-NMDAR interaction. (E-G) DIV6-7 cultured cortical neurons were treated as indicated with 10μM of the broad spectrum extracellular protein kinase inhibitor K-252b for 60 minutes, before 45 minutes of stimulation with Fc control or ephrin-B2-Fc. EphB2 receptors were immunoprecipitated with an N-terminal EphB2 antibody and resulting western blots were probed with anti-NMDAR1, anti-EphB2, anti-EphB2 pY504 extracellular, or anti-EphB2 pY662 intracellular kinase antibodies. (F) Quantification of relative amount of NMDAR1 immunoprecipitated compared to input (*$p < 0.05$, ANOVA test; n=5). (G) Quantification of relative amount of EphB2 pY504 phosphorylation immunoprecipitated compared to input (*$p < 0.05$, ANOVA test; n=5).

**Figure 3.3. Tyrosine 504 regulates EphB2 surface localization, degradation, and affects NMDAR surface retention.** (A) Model of how extracellular phosphorylation at Y504 modulates EphB receptor trafficking and the EphB-NMDAR interaction. (B-C) Mutation of Y504 to E causes decreased surface localization of EphB2 Receptors. (B) Representative immunoblots of biotinylated

EphB2 with no actin biotinylated. (C) Quantification of percent localized to the cell surface of total lysate. (*$p < 0.05$, ANOVA test; n=4). (D-E) Mutation of Y504 to E causes EphB2 internalization by a clathrin-mediated mechanism. (D) Western blots of lysates from HEK293T cells transfected with indicated constructs for 16-18 hours, then treated with 450mM sucrose for 15 minutes at 37°C before lysis. Lysates were probed for EphB2, or β-actin. (E) Quantification of fold change normalized to actin in total protein lysate after sucrose treatment (*$p < 0.05$, ANOVA test; n=4-5). (F-G) Expression of dominant negative (K44A) dynamin increases WT and Y504E EphB2 receptor expression, but not Y504F. (F) Western blots of lysates from HEK293T cells co-transfected with indicated fB2 constructs and either wild-type (WT Dyn) or dominant-negative dynamin K44A (DN Dyn) constructs. Blots were and probed for EphB2, dynamin-1, or β-actin. (G) Quantification of relative amount of EphB2 in the presence of DN K44A dynamin compared to when co-expressed with WT dynamin. (*$p < 0.05$, ANOVA test; n=5). (H-I) Mutation of Y504 to E causes EphB2 increased degradation in the proteasome. (H) Representation immunoblots from HEK293T cells transfected with indicated constructs for 16-18 hours, then treated with 5μM lactacystin for 4 hours at 37°C before lysis. Lysates were probed for EphB2, and β-actin. (I) Quantification of fold change normalized to actin in total protein lysate after lactacystin treatment. (*$p < 0.05$, ANOVA test; n=5). (J-M) Mutations at EphB2 Y504 modulates EphB2 and NMDAR1 trafficking. (J) Expression of NMDARs rescues EphB2 Y504 to E surface localization, and (L) co-expression of EphB2 Y504E increases NMDAR1 surface localization. (J, L) Representative

immunoblots of biotinylated EphB2 (J) or NMDAR1 (L) with no actin biotinylated from HEK293T cells. (K, M) Quantification of percent localized to the cell surface of total lysate. (*$p < 0.05$, ANOVA test; n=5). Error bars indicate SEM.

**Figure 3.4. Tyrosine 504 regulates the function of synaptic NR2B-containing NMDARs in mature neurons**. (A-D) Phosphomimetic mutants at Y504 regulate mEPSC amplitude in mature neurons in a subunit-specific manner. (A) Quantification of mean mEPSCs before and after the application of 50μM APV. An increase in mEPSC amplitude was observed with overexpression of EphB2 WT and Y504F, whereas NMDAR blockade using APV reduced mEPSC in all conditions. Control: n=5 cells, 491 mEPSCs w/o APV, 421 mEPSCs w/ APV; EphB2 WT: n=7 cells, 1182 mEPSCs w/o APV, 758 mEPSCs w/ APV; EphB2 Y504E: n=6 cells, 705 mEPSCs w/o APV, 349 mEPSCs w/ APV; EphB2 Y504F: n=9 cells, 912 mEPSCs w/o APV, 541 mEPSCs w/ APV. (ANOVA test, $p < 0.001$). Error bars indicate SEM. (B) Cumulative probability histogram of mEPSC amplitude for Y504E and Y504F mutants at ~20-35 ms before (dark shading) and after (light shading) NMDAR blockage with 50μM APV. *Inset,* Mean traces of mEPSCs after NMDAR blockage with APV. (C-D) Cumulative probability histogram of mEPSC amplitude for Y504E (C) and Y504F (D) mutants before and after application of NR2B-specific antagonist Ro25-6981 (2.5 μM). *Inset*, Mean traces of mEPSCs after treatment with Ro25. EphB2 Y504E: n=7 cells,767 mEPSCs w/o Ro25,456 mEPSCs w/ Ro25; EphB2 Y504F: n=6 cells, 457 mEPSCs w/o Ro25, 444 mEPSCs w/ Ro25. (E-G) Distribution of

synaptic NR2B-containing NMDARs. (E) Representative images of DIV21-23 cultured cortical neurons expressing EGFP and vector control (n=539), EphB2-YFP-WT (n=516), Y504E (n=527), or Y504F (n=539) constructs, immunostained for GFP (green), NMDAR2B (red), and SV2 (blue). Arrowheads indicate measurement site (Scale bar: 5 μm). (F) Quantification of average of normalized intensity for synaptic NR2B in spines. (*$p < 0.05$, **$p < 0.01$, ANOVA test). Error bars indicate SEM. (G) Cumulative probability histograms of normalized intensity of NR2B on synaptic spines for Y504E and Y504F receptors. ANOVA test, $p<0.001$ (H) CREB-dependent gene transcription is enhanced with synaptic NMDAR stimulation in Y504E mutants and blocked by NR2B antagonist Ro25. CRE-luciferase activity is reported as fold-induction (*$p<0.05$, ANOVA test), Error bars indicate 0.05 confidence.

**Acknowledgements**

We would like to thank E. Krizman-Genda and M. B. Robinson who were supported by the Institutional Intellectual and Developmental Disabilities Research Center (P30 HD26979) at the Children's Hospital of Philadelphia for assistance with antibody purification and biotinylation assays. We thank M. Hruska for synaptosome preparations. Dynamin WT and dominant negative (K44A) mutant constructs were generously provided by M. A. Lemmon at the University of Pennsylvania. We acknowledge the generous support of the National Institute on Drug Abuse (Grant DA022727), National Institute of Mental Health (Grant MH086425) and the Dana Foundation (M. B. D.), and the National Eye Institute Vision Training Grant (EY007035 to S. I. S-C.).

## Supplemental Online Material

### Materials and Methods

*Expression Constructs*

Full length FLAG-EphB2, truncated FLAG-EphB2 (fEphB2 Tr) and FLAG-tagged kinase dead (KD; K663R) EphB2 and truncated were previously described (Dalva et al., 2000). Single amino acid point mutations to Y481 and Y504 were introduced using sequence specific primers and site-directed mutagenesis (Strategene, La Jolla, CA). Sequences used were: EphB2 Y504F, 5'-GCCTCAAAGCCGGTGCCATCTTTGTCTTCCAGGTGCGG-3'; EphB2 Y504E, 5'-GCCTCAAAGCCGGTGCCATCGAAGTCTTCCAGGTGCGG-3'; EphB2 Y481F, 5'-ATGAGAAGGAGCTAAGTGAGTTCAACGCCACGGCCATA-3'; EphB2 Y481E, 5'-ATGAGAAGGAGCTAAGTGAGGAGAACGCCACGGCCATA-3'. Forward and reverse oligonucleotides were synthesized (Integrated DNA Technologies, Coralville, IA). Generation of EphB2-YFP was previously described (Kayser et al., 2006). AgeI and MfeI sites were added to EphB2-YFP using site-directed mutagenesis and sequence specific primers: EphB2-YFP_AgeI, 5'-AAACCGGTTTACCGTGGAAGAAACCCTGATG-3'; EphB2-YFP MfeI, 5'-TTAATCCAATTGGAGTGACAGAGCAGCAGGGAC-3'. Then point mutations at Y504 were introduced using site-directed mutagenesis. PCR products were ligated into the pFUGW vector using Age1 (bp3860) and EcoR1 (bp4609) sites. Lentivirus were produced and purified by the Gene Therapy Program Penn Vector Core Facility at the University of Pennsylvania.

*Generation of a phosphorylation-specific antibody*

The phosphorylated peptide Ac-CKGLKAGAI-pY-VGQVRA-$NH_2$ was conjugated to Keyhole Limpet Hemocynein (KLH) in position 1 (EZBiolab, Carmel, IN). This conjugated, phosphorylated peptide was injected into rabbits for polyclonal antibody production (Covance, Denver, PA). Antibody titer was assessed using an ELISA (Covance, Denver, PA) with a non-phosphorylated form of the injection peptide Ac-CKGLKAGAIYVGQVRA-$NH_2$ (EZBiolab, Carmel, IN). Serum from each animal was affinity purified using SulfoLink Coupling Resin (Thermo Scientific – Pierce Biotechnology, Rockford, IL) according to manufacturer's instructions and the phosphorylated peptide without KLH conjugation. Protein concentration was calculated using a Bradford assay (BioRad, Hercules, CA). Eluates were dialyzed overnight in Slide-A-Lyzer 10K Dialysis Cassettes (Thermo Scientific – Pierce Biotechnology, Rockford, IL), then aliquoted with a final concentration of 10% glycerol and stored at 4°C.

*Cell Culture and Transfection*

Dissociated cortical neurons were prepared from embryonic day 17 (E17) to E18 rats as previously described (Kayser et al., 2008; Nolt et al., 2011) on poly-*D*-lysine (BD Bioscience, Bedford, MA) and laminin (BD Biosciences, Bedford, MA) coated glass coverslips (12 mm; Bellco Glass, Vineland, NJ) in 24-well plates (Corning Life Sciences, Lowell, MA). For immunostaining and electrophysiology experiments neurons were transfected as indicated at either 7 or 14 *days in vitro* (DIV) using Lipofecatmine 2000 (Invitrogen, Carlsbad, CA) as

previously described (Kayser et al., 2008; Nolt et al., 2011). For biochemistry cortical neurons were plated at a density of $10 \times 10^6$ cells per 100 mm dishes (BD Bioscience, Franklin Lakes, NJ) pre-coated with poly-*D*-lysine and laminin.

*HEK293T Culture and Transfection*

HEK-293T cells were maintained in DMEM (Invitrogen), 10% Fetal Bovine Serum (Thermo Scientific – Hyclone, Logan, UT), penicillin-streptomycin (Sigma-Aldrich, Saint Louis, MO), and glutamine (Sigma-Aldrich, Saint Louis, MO). For transfection, HEK293T cells were plated in 6-well or 35mm culture plates (BD Bioscience, Franklin Lakes, NJ) and transfected with indicated EphB2, NR1, or NR2B constructs using the calcium phosphate method (Kayser et al., 2006; McClelland et al., 2009; Xia et al., 1996). 100 μm APV (Sigma-Aldrich, Saint Louis, MO) was added to the culture medium after NMDAR transfection to prevent excitotoxicity.

*Immunocytochemistry*

Cells were fixed in 4% paraformaldehyde/ 2% sucrose for 5 minutes followed by 10 minutes in 0.25% Triton X-100 at room temperature. Cells were washed three times in PBS then blocked and permeabilized in 1% ovalbumin (Sigma-Aldrich, Saint Louis, MO) / 0.2% cold water fish skin gelatin (Sigma-Aldrich, Saint Louis, MO) / 0.1% saponin (Sigma-Aldrich, Saint Louis, MO) for 1 hour at room temperature. Primary antibody was incubated overnight at 4°C in blocking reagents. Cells were again washed three times in PBS then incubated

with secondary antibody in blocking reagents for 45-60 minutes at room temperature. Cells were then washed three times in PBS before mounting using Aqua-Mount (Thermo Scientific -- Lerner, Kalamazoo, MI). Antibodies used were: chicken polyclonal anti-GFP (1:2500; Millipore, Temecula, CA), rabbit anti-NR2B polyclonal (1:1000; (Dalva et al., 2000)), mouse monoclonal anti-NMDAR1 (1:500; BD Pharmingen, San Diego, CA) and mouse monoclonal anti-synaptic vesicle protein 2 (SV2) (1:200; Developmental Studies Hybridoma Bank, University of Iowa, Iowa City, IA). Cy2, Cy3, and Cy5 secondary antibodies were used 1:250 (Jackson ImmunoResearch, West Grove, PA).

*Synaptosome Preparation*

Synaptosomes were prepared as previously described (Nolt et al., 2011). Briefly, whole brains from P30 WT CD1 mice were homogenized in HEPES-buffered sucrose. Centrifugation was used to remove the nuclear fraction and generate a S1 fraction. A crude membrane (P1) fraction was generated by centrifugation of the S1 fraction. The P1 fraction was resuspended in HEPES-buffered sucrose and centrifuged again to generate a crude synaptosome. The crude synaptosome was layered onto a sucrose gradient and found at the interface of buffer and 1.2 M sucrose. The interface was diluted and centrifuged again at 230,000 X *g* to obtain the final pure synaptosomal (Syn) pellet.

*Western Blot Analysis*

Lysates from HEK293T cells or neurons were separated using 8% SDS-polyacrylamide gels and transferred onto 0.45μM PVDF membranes (Millipore, Temecula, CA). Immunoblots were then blocked in 5% nonfat dry milk in TBS-T (150mM NaCl, 10mM Tris pH 8.0, 0.05% Tween-20). Indicated primary antibodies were presented in blocking solution for 2 hours at room temperature or overnight at 4°C: mouse monoclonal anti-GFP (1:1000; Roche, Mannheim Germany), mouse monoclonal anti-Dynamin (1:1000, BD Transduction Laboratories, Lexington, KY), goat polyclonal anti-EphB2 (1:500; R&D Systems; Minneapolis, MN), mouse monoclonal anti-NMDAR1 (1:500; BD Pharmingen, San Diego, CA), mouse monoclonal anti-FLAG (M2; 1:2500; Sigma-Aldrich, Saint Louis, MO), rabbit polyclonal anti-EphB2 (1:500; (Dalva et al., 2000)), rabbit polyclonal anti-EphB2 pY662 (1:1000; (Dalva et al., 2000)). HRP-conjugated secondary antibodies were used at 1:20,000 in blocking solution for 1 hour (EMD Biosciences – Calbiochem, San Diego, CA or Santa Cruz Biotechnology, Santa Cruz, CA) then visualized using ECL (PerkinElmer, Waltham, MA) and autoradiography film (Kodak, Rochester, NY or TruMark Scientific, Edison, NJ). Protein band immunoreactivity was quantified using NIH ImageJ software.

*Cultured Neuron Biotinylation and HEK293T Cell Biotinylation*

Biotinylations were preformed as previously described (Nolt et al., 2011). Briefly, cells were washed twice in ice-cold PBS-$Ca^{2+}$/$Mg^{2+}$ rinsing solution then cell surface proteins were bulk labeled using 1mg/mL Sulfo-NHS-SS-Biotin

(Thermo Scientific – Pierce Biotechnology, Rockford, IL). Unreacted biotin was quenched using rinsing solution with 100mM glycine. Cells were then washed and lysed using radioimmunoprecipitation assay (RIPA) buffer. Lysates were harvested and centrifuged to remove cellular debris. Biotinylated proteins were extracted using monomeric avidin agarose (Thermo Scientific – Pierce Biotechnology, Rockford, IL). Surface proteins were solubilized off the avidin beads using 2X-SDS sample buffer. Equal amounts of total cell lysate and biotinylated (surface) proteins were subjected to SDS-PAGE and western blot analysis.

*Immunoprecipitation*

Immunoprecipitations were performed as previously described with small changes (Dalva et al., 2000; Takasu et al., 2002). After treatment with clustered ephrin-B2-Fc or Fc control, cortical neuron cultures (or untreated HEK293T cells) were lysed in radioimmunoprecipitation assay (RIPA) buffer (750µl for 100mm dishes or 300µl per well for 6-well plates) containing protease inhibitors and agitated at 4°C for 15 minutes. Cell lysates were harvested and centrifuged at 13,000 rpm for 25 minutes to pellet cellular debris. A fraction of the resulting supernatant (100µl for 100mm dishes or 75 µl per well for 6-well plates) was removed as an input control. The remaining supernatant was incubated with appropriate antibody to conjugate on ice for 2 hours: rabbit polyclonal anti-GFP (ab290; Abcam, Cambridge MA), goat polyclonal anti-EphB2 (R&D Systems, Minneapolis, MN), or mouse monoclonal anti-FLAG (M2; Sigma-Aldrich, Saint

Louis, MO). Antibody bound proteins were then isolated using pre-blocked protein-G agarose beads (Invitrogen, Carlsbad, CA) 75µl for 100mm dishes or 50 µl per well for 6-well plates on a rotator for 60 minutes at 4°C. Samples were then centrifuged and beads were washed four times in RIPA lysis buffer and two times in TBS-V. Immunoprecipitates were eluted from the agarose beads by adding 25µl boiling 6X SDS-sample buffer and boiled for 5 minutes at 95°C.

*Inhibitors and Reagents*

K-252b and D(-)-2-Amino-5-phosphonopentanoic acid (D-APV) were obtained from Sigma-Aldrich (Saint Louis, MO). Lactacystin was obtained from Calbiochem (EMD Biosciences, San Diego, CA). Alkaline Phosphatase, Calf Intestinal (CIP) was purchased from New England BioLabs (Ipswich, MA). Ephrin-B2-Fc and Fc control were obtained from R&D Systems (Minneapolis, MN) and clustered using anti-Human IgG (Jackson ImmunoResearch, West Grove, PA) then used as previously described (Kayser et al., 2006; Nolt et al., 2011).

*Cre-luciferase transcription*

Cre-luciferase assay were performed as previously described with small changes (Takasu et al., 2002). Briefly, neurons were transfected at DIV7 by the lipofectamine method (Kayser et al., 2006; Nolt et al., 2011) with a ratio of 8:1 of CRE-luciferase reporter construct and *Renilla* luciferase as a transfection control. In this CRE-luciferase construct, there are four copies of somatostatine CRE

before firefly luciferase. EphB2-YFP-WT, EphB2-YFP-Y504E, EphB2-YFP-Y504F, and pFUGW vector control were co-transfected with EGFP to assess transfection efficiency, along with the CRE-luciferase reporter and the Renilla luciferase at the ratio previously described in (Takasu et al., 2002). At DIV10, neurons were silenced for 6 hours with TTX, before synaptic stimulation with a mixture of 4-aminopyridine (4-AP) and bicuculline (BIC) in the presence of nifedipine to block L-type Ca2+ channels for 3-4 hours before lysis (Kawashima et al., 2009). Lysates were then collected and analyzed for luciferase expression using the Dual Luciferase Reporter Assay System (Promega, Madison, WI).

*Imaging and Analysis*

Images of cultured cortical neurons were obtained using confocal scanning microscopy (Leica Microsystems, Wetzlar, Germany) as previously described (McClelland et al., 2009; Nolt et al., 2011). Briefly, images were acquired at 63X resolution, numerical aperture 1.4, and oil-immersion objective. Analysis was done using MetaMorph software (Molecular Devices, Sunnyvale, CA) blind to experimental condition. Images were collected from at least three independent experiments. Puncta were considered to be co-localized when there was greater than one pixel overlap between channels. During image collection all gain values were held constant. Amount of NR2B intensity were normalized to the maximum intensity observed from all three conditions for each experiment.

*Electrophysiology*

Recordings from DIV21-23 cultured rat cortical neurons were performed using whole-cell patch methods as previously described (McClelland et al., 2009; Nolt et al., 2011). Briefly, coverslips were moved into a recording chamber and bathed in a HEPES-buffered artificial CSF (ACSF) solution in mM: 140 NaCl, 5 KCl, 2 $CaCl_2$, 1 $MgCl_2$, 20 glucose, and 10 HEPES, pH 7.2). Tetrodotoxin (TTX) and picrotoxin were used at 1 and 10 μM, respectively (Sigma-Aldrich, St. Louis, MO). Bicuculline was used at 50 μM, D-APV was used at 10 μM, and (αR, βS)-α-(4-hydroxyphenyl)-β-methyl-4-(phenylmethyl)-1-piperidinepropanol maleate (Ro25-6981) was used at 2.5 μM (Tocris Bioscience, Ellisville, MO). All data were collected at 5 kHz and filtered at 1 kHz; events were detected in Clampfit 9.2 (Molecular Devices, Sunnyvale, CA). Event analysis and statistics were performed using Clampfit software (Molecular Devices, Sunnyvale, CA). To isolate the NMDAR component, neurons were held at +50 mV in the presence of TTX (1 μM), bicuculline (50 μM), and picrotoxin (10 μM).

## *SILAC Assay*

*Cell culture, metabolic labeling and stimulation*

Two NG108-15 (mouse neuroblastoma x rat glioma hybrid) cell lines were used, a “wild type” cell line without stable transfection and another stably overexpressing EphB2 (Holland et al., 1997). Both cell lines were maintained in Dulbecco’s modified Eagle’s medium (DMEM) (Invitrogen Corporation, Carlsbad, CA) or lysine and arginine depleted DMEM (Special Media, Philipsburg, NJ) and

supplemented with 10% dialyzed fetal bovine serum (Invitrogen Corporation, Carlsbad, CA), HAT (Sigma-Aldrich, St. Louis, MO), 100 units/ml of penicillin / streptomycin, and either normal or $^{13}C_6$ lysine and $^{13}C_6$ arginine (Cambridge Isotope Labs, Andover, MA). In experiments that employed metabolic labeling cells were grown for at least 6 doublings to allow full incorporation of labeled amino acids.

*Transient Transfection of FLAG-EphB2*

FLAG-EphB2 plasmid was amplified and purified according to manufactures instructions using Plasmid Midi kit (Qiagen, Valencia, CA). Cells were cultured to approximately 50% confluence and transiently transfected using Superfect (Qiagen, Valencia, CA) according to manufactures instructions. Briefly, 10µg of vector was diluted in 298µL of DMEM and incubated with 60µL of superfect reagent for10 minutes at RT. 7mL of pre-condition media (media removed directly from the cells that were to be transfected) was added to superfect/plasmid mixture. Cells were then washed with sterile PBS and the mixture was then added to cells, incubated for 3 hours at 37°C, removed and replaced with fresh culture media. 24 hours later media was removed, cells were washed with PBS and media was replaced with above mentioned formulation without FBS. At 48hrs cells were stimulated and lysed.

*Starvation, ephrin stimulation, and phosphatase treatment*

For all experiments that involved ephrin stimulation, cells were subjected to 24hrs of serum starvation before treatment with 2 μg/mL pre-clustered ephrinB1-Fc (Sigma-Aldrich, Saint Louis, MO) for 5 or 45 minutes. The clustering procedure consisted of incubation of 250 μg/mL ephrinB1-Fc with 65 μg/ml anti-human Fc (Jackson ImmunoResearch, West Grove, PA) at RT for 1 hr. In a separate experiment cells received a general phosphatase inhibitor solution (1:75 phos. inhib. solution: culture media) containing 1mM pervanadate and 50nM calyculin A for 1 hr.

*Cell lysis, anti-FLAG immunoprecipitation and Western Blot*

Cells were lysed in lysis buffer containing 1% Triton X-100, 150 mM NaCl, 20 mM Tris, pH8, 0.2mM EDTA, pH8, 2 mM $Na_3VO_4$, 2mM NaF, and protease inhibitors (Complete tablet; Roche, Mannheim, Germany). For SILAC experiments lysates were mixed in a 1:1 ratio (v:v) and incubated with agarose-conjugated anti-FLAG M2 antibody (Sigma-Aldrich, Saint Louis, MO) overnight. After incubation the beads were spun down in a bench top Megafuge 1.0R basket centrifuge (Thermo Scientific – Heraeus Instruments, Asheville, NC) at 2000 RPM for 1 min and the supernatant was removed. Beads were then washed in ~25mL lysis buffer 4 times in a similar fashion. Precipitated proteins were eluted by boiling in SDS-PAGE sample buffer for 5 min. After elution sample volume was reduced by ½ by vacuum centrifugation. Phosphatase inhibitor treated cell lysates were also mixed 1 to 1 with SDS-PAGE sample

buffer and boiled for 5 min. Samples were separated on a 7.5% (receptor IPs) or 10% (Phos. treated lysates) Tris-HCl gel (BioRad, Hercules, CA). Gels were stained with Coomassie Blue and EphB2 band was excised (receptor IPs) or the gel lane was cut horizontally into 6 sections (Phos. treated lysates).

*In-gel and in-solution tryptic digestion*

For in-gel digestions excised gel bands were cut into small pieces and destained in 50 mM ammonium bicarbonate / 50% acetonitrile, dehydrated with acetonitrile and dried. The gel pieces were rehydrated with 10 ng/µl trypsin solution in 50 mM ammonium bicarbonate and incubated overnight at 37°C. Peptides were extracted twice with 5% formic acid / 50% acetonitrile followed by a final extraction with acetonitrile (Shevchenko et al., 1996). For in-solution digests samples were dried in vacuum centrifuge, resuspended in 50mM ammonium bicarbonate and denatured at 55°C for 30 minutes. Trypsin was added at a 1:100 trypsin:sample ratio and incubated overnight at 37°C. After either in-gel or in-solution digestion samples were dried by vacuum centrifugation.

*Enrichment by peptide-pipette tip TiO2 chromatography*

TiO2 tips (NuTip, 1-10µL for affinity purified proteins and 10-100uL for complex mixtures, (Glygen Corp., Columbia, MD) were conditioned TiO2 tips by pipetting 1̣0 (purified protein) or 100µL (complex mixture) of 1.0% TFA in 80% acetonitrile loading buffer through the tip 10 times. Peptides were dissolved in 1̣0

or 100µL of loading buffer and loaded on to tip by pipetting peptide solution through the tip at least 10 times. The tip was then washed with an additional 10 or 100 µL of loading buffer by pipetting the solution through the tip at least 10 times. The tip was washed a second time with 10 or 100 µL of 0.1% TFA in 80% acetonitrile by pipetting the solution through the tip at least 10 times. Bound peptides were eluted by pipetting 3.5-10 or 25-100µL of 500 mM $NH_4OH$ through the tip 10 times. Solvent was removed by vacuum centrifugation and stored at -20°C until MS analysis.

*Analysis of methyl esterified peptides by MALDI-TOF/TOF MS*

Methanolic HCl solution was prepared by dropwise addition of 160 µl of acetyl chloride to 1 ml of dry methanol (Ficarro et al., 2002). Phosphopeptide standards and tryptic digests were redissolved in 50 µl of 2 M methanolic HCl reagent. Methyl esterification was allowed to proceed for 2–3 h at room temperature. Solvent was removed by lyophilization, and peptide mixtures were resuspended in 0.2% TFA, 30% acetonitrile. MALDI matrix was prepared by dissolving 5mg/mL of α-cyano-4-hydroxycinamic acid (HCCA) in 900 uL of a 50/50 mix 0.1% TFA: ACN to which 100 uL of 0.1M solution of Ammonium Phosphate was added. Sample was then mixed with MALDI matrix 1:1 (v/v), 1.2 µl was spotted onto MALDI sample stage and allowed to air dry. Positive and negative ion mode MALDI MS spectra were obtained using an Applied Biosystems 4700 Proteomics Analyzer with TOF/TOF ion optics (Applied Biosystems, Wilmington, DE); in MS/MS mode the instrument was always

operated with the collision gas off. A diode pumped Nd:YAG laser with a 600 ps pulse length was used. The instrument was controlled by ABI 4700 Series Explorer (version 3.0). The ABI calibration mixture was used to calibrate the instrument in MS mode and MS/MS mode was calibrated using the y-series fragment ions of Glu-fibrinogen peptide, m/z 1570.677. An additional internal calibrant of the N-terminal y1 fragment (either K or R) m/z 147.113 or 175.119 was applied in MS/MS mode. Spectra were obtained for each sample using 500 laser shots in MS mode and 3500 shots in MS/MS. Precursor ions were fragmented by accelerating to 8 keV, selecting them with the timing gate set to a resolution of 50 and then accelerating fragment ions to 14 keV before entering the reflector. Positive and negative ion mode MS spectra where acquired for in-solution digests of 100fmol of Beta casein with or without methyl esterification. All MS/MS spectra were acquired in positive ion mode and sequenced manually.

*SILAC ratio determination and assignment of EphB2 phosphorylation Sites*

Quantification was carried out using the open-source software MSQuant (Peter Mortensen and Matthias Mann, http://msquant.sourceforge.net/). To identify the most likely sites of phosphorylation for EphB2 observed peptides, spectra identified as phosphopeptides by Mascot were processed and validated using MSQuant software. MSQuant calculated the probabilities for phosphorylation at each potential site and generated PTM scores as described previously (Olsen et al., 2006).

## Supplementary Figure Legends

**Supplementary Figure 3.1. Activity of FLAG-EphB2.** FLAG and pY99 IPs followed by anti-FLAG and pY99 Western blotting verified that transfected construct was tyrosine phosphorylated in an ephrin-dependent fashion. Also observed in a general increase in overall tyrosine phosphorylation after ligand treatment suggesting the FLAG-tagged receptor is signaling properly.

**Supplementary Figure 3.2. Phosphorylation Sites and Individual Ratios**

**Supplementary Figure 3.3. Mutation of amino acid Y504 to glutamic acid (E) in HEK293T cells generates receptors with reduced expression.** *Left,* Western blots of lysates from HEK293T cells transfected with 1µg of indicated fEphB2 constructs and probed for EphB2, or β-actin. *Right.* DNA titration for indicated amount of fEphB2 constructs cDNA transfected into HEK293T cells and immunoblotted for EphB2, or β-actin.

**Supplementary Figure 3.4. Clustered ephrin-B2-Fc treatment causes internalization of EphB2 receptors in neurons.** (A-C) DIV 7 cultured cortical neurons were stimulated as indicated with either Fc control (Control), unclustered ephrin-B2-Fc (inactivating eB2), or clustered ephrin-B2-Fc (activating eB2). (A) Representative immunoblot of biotinylated EphB2 from DIV7 cultured cortical neurons with no actin biotinylated. (B) Quantification of percent localized to the

cell surface compared to Fc treated control. (C) Quantification of percent in intracellular avidin fraction compared to Fc treated control. Error bars indicate SEM. (*$p < 0.05$, ANOVA test; n=4).

**Supplementary Figure 3.5. EphB2 Y504E mutants in cultured cortical neurons are retained on the plasma membrane.** (A-B) DIV2 cultured cortical neurons were infected with indicated YFP-EphB2 lentiviral constructs, then at DIV7 cell surface EphB2 receptors were biotinylated. (A) Representative immunoblot of biotinylated infected EphB2 with no actin biotinylated. (B) Quantification of percent localized to the cell surface compared to YFP-EphB2 WT. Error bars indicate SEM. ($p > 0.5$, ANOVA test; n=3).

# Figure 3.1

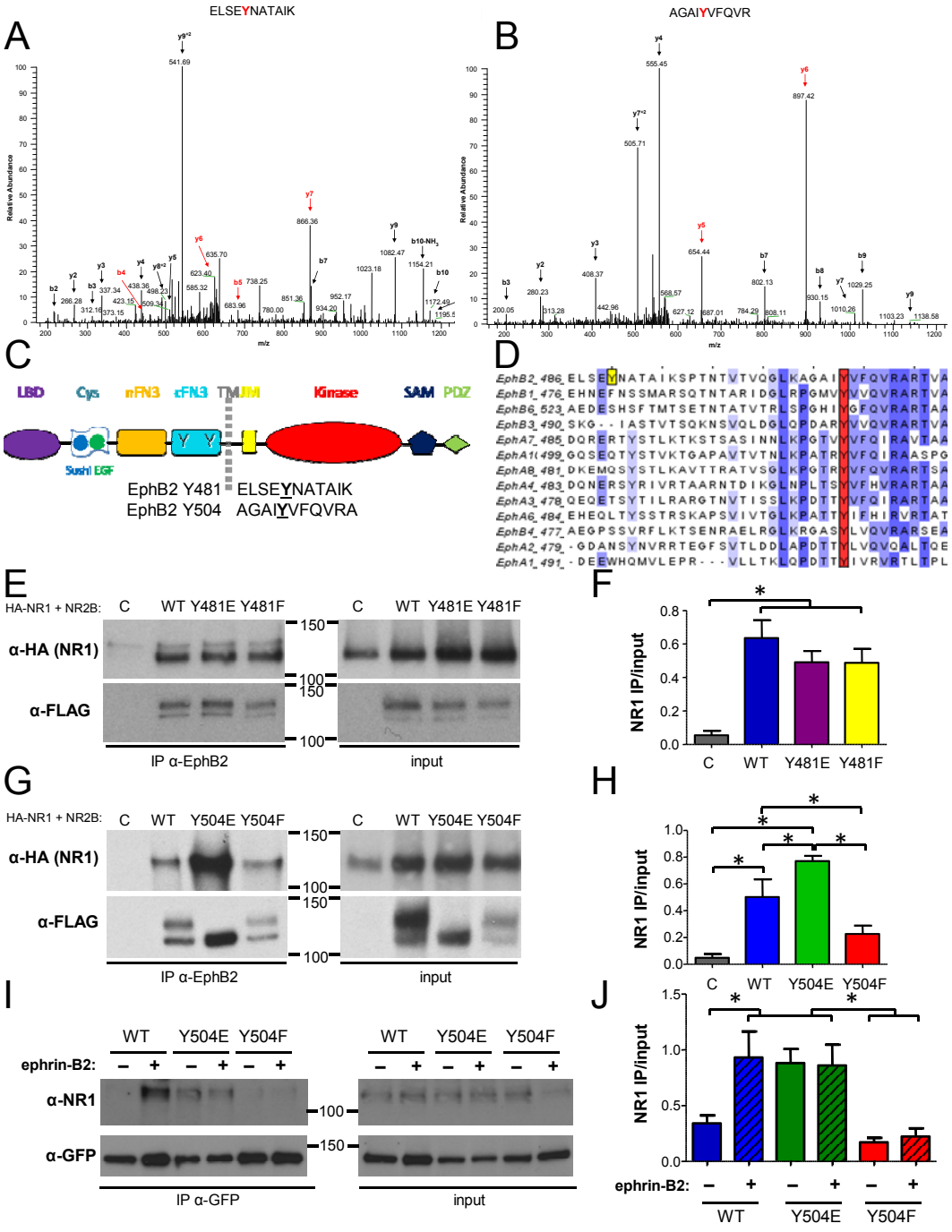
A
ELSEYNATAIK
B
AGAIYVFQVR
C
LBD
Cys
nFN3
cFN3
TM
JM
Kinase
SAM
PDZ
Sushi
EGF
EphB2 Y481 ELSEYNATAIK
EphB2 Y504 AGAIYVFQVRA
D
E
HA-NR1 + NR2B:
C
WT
Y481E
Y481F
α-HA (NR1)
α-FLAG
IP α-EphB2
input
F
NR1 IP/input
G
Y504E
Y504F
H
I
ephrin-B2:
α-NR1
α-GFP
IP α-GFP
J

# Figure 3.2

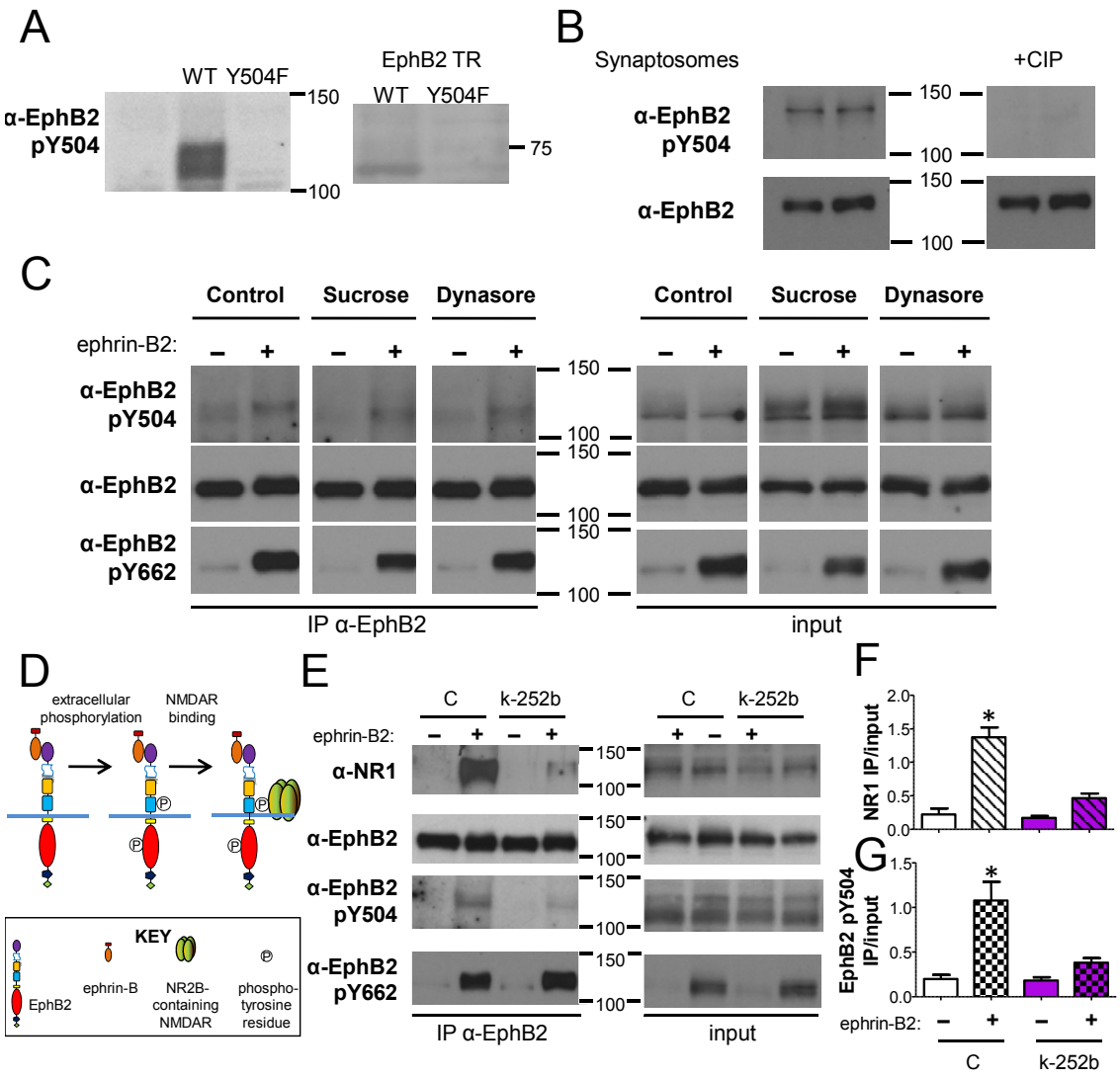
A
WT Y504F
EphB2 TR
WT Y504F
α-EphB2 pY504
150
100
75
B
Synaptosomes
+CIP
α-EphB2 pY504
α-EphB2
150
100
C
Control
Sucrose
Dynasore
ephrin-B2:
α-EphB2 pY504
α-EphB2
α-EphB2 pY662
IP α-EphB2
input
D
extracellular phosphorylation
NMDAR binding
KEY
EphB2
ephrin-B
NR2B-containing NMDAR
phospho-tyrosine residue
E
C
k-252b
α-NR1
α-EphB2
α-EphB2 pY504
α-EphB2 pY662
F
NR1 IP/input
G
EphB2 pY504 IP/input

# Figure 3.3

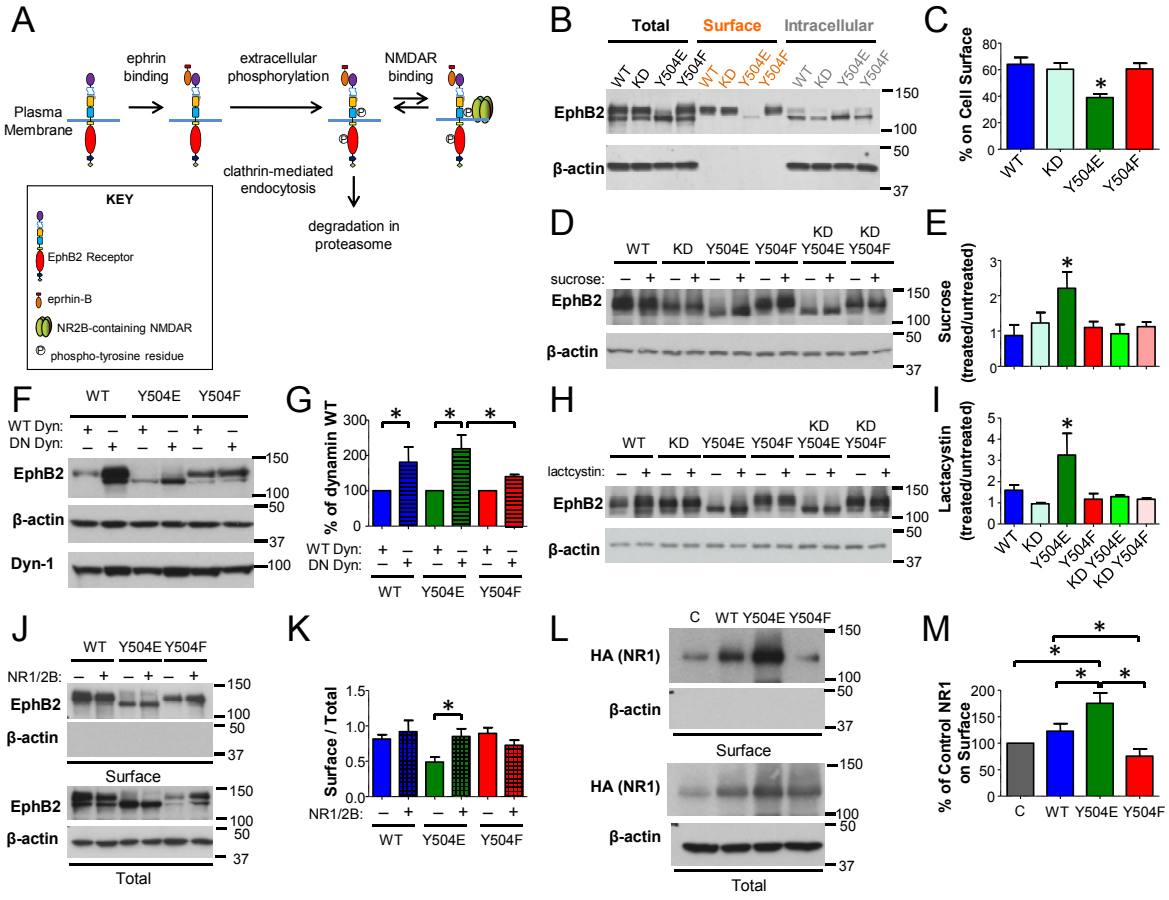
A
ephrin binding
extracellular phosphorylation
NMDAR binding
Plasma Membrane
clathrin-mediated endocytosis
degradation in proteasome
KEY
EphB2 Receptor
ephrin-B
NR2B-containing NMDAR
phospho-tyrosine residue
B
Total
Surface
Intracellular
WT
KD
Y504E
Y504F
EphB2
β-actin
C
% on Cell Surface
D
sucrose:
E
Sucrose (treated/untreated)
F
WT Dyn:
DN Dyn:
Dyn-1
G
% of dynamin WT
H
lactcystin:
I
Lactacystin (treated/untreated)
J
NR1/2B:
Surface
Total
K
Surface / Total
L
C
HA (NR1)
M
% of Control NR1 on Surface

# Figure 3.4

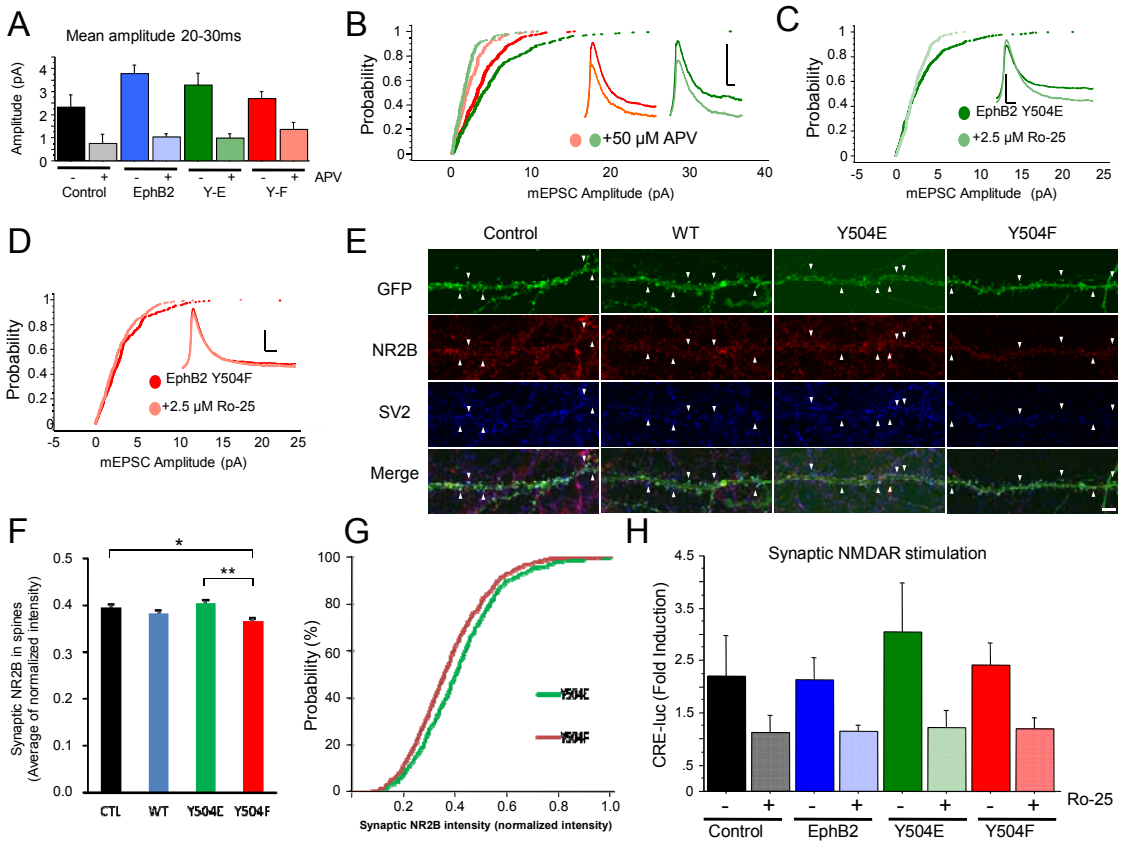
A
Mean amplitude 20-30ms
Amplitude (pA)
Control
EphB2
Y-E
Y-F
APV
B
Probability
+50 μM APV
mEPSC Amplitude (pA)
C
Probability
EphB2 Y504E
+2.5 μM Ro-25
mEPSC Amplitude (pA)
D
Probability
EphB2 Y504F
+2.5 μM Ro-25
mEPSC Amplitude (pA)
E
Control
WT
Y504E
Y504F
GFP
NR2B
SV2
Merge
F
Synaptic NR2B in spines
(Average of normalized intensity)
CTL
WT
Y504E
Y504F
G
Probability (%)
Synaptic NR2B intensity (normalized intensity)
H
Synaptic NMDAR stimulation
CRE-luc (Fold Induction)
Control
EphB2
Y504E
Y504F
Ro-25

# Supplementary Figure 3.1

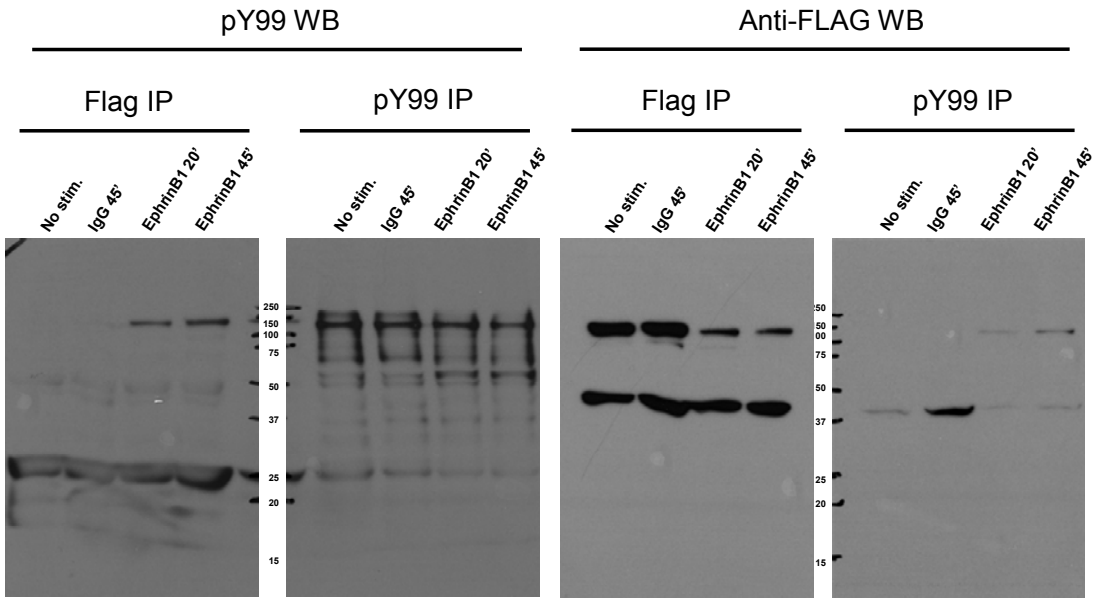

# Supplementary Figure 3.2

**Phosphopeptide Quantitation**

| Sequence | Modifications | Mass [Da] | Mascot Score | SILAC Ratio | SD | SIM XIC Ratio | Phos localized |
|---|---|---|---|---|---|---|---|
| ADSEYTDK | 1pT | 1007.35, 1013.37 | 21 | N/D | N/D | >10.0 | Y |
| ADSEYTDK | 1p(ST) | 1007.35, 1013.37 | 29 | 1.43 | 0.56 | N/D | N |
| ADSEYTDK | 1pS | 1007.35, 1013.37 | 50 | N/D | N/D | 1.15 | Y |
| ADSEYTDK | 1pY | 1007.35, 1013.37 | 42 | N/D | N/D | 0.89 | Y |
| AGAIYVFQVR | 1pY | 1202.58, 1208.60 | 63 | 1.01 | 0.35 | 0.98 | Y |
| ELSEYNATAIK | 1pY | 1317.59, 1323.61 | 34 | 1.26 | 0.28 | 1.14 | Y |
| *FLEDDTSDPTYTSALGGK* | | 1915.88, 1921.89 | 114 | 0.88 | 0.21 | N/O | |
| FLEDDTSDPTYTSALGGK | 1pY | 1995.84, 2001.85 | 128 | 1.19 | 0.23 | 1.09 | Y |
| FLEDDTSDPTYTSALGGK | 1p(ST) | 1995.84, 2001.85 | 100 | N/D | N/D | N/D | N |
| FLEDDTSDPTYTSALGGK | 1pT | 1995.84, 2001.85 | 43 | N/D | N/D | 7.98 | Y |
| FLEDDTSDPTYTSALGGK | 1pT 1pY | 2075.80, 2081.83 | 51 | N/D | N/D | 1.46 | Y |
| FLEDDTSDPTYTSALGGK | 1pS 1pY | 2075.80, 2081.83 | 71 | N/D | N/D | 1.87 | Y |
| FLEDDTSDPTYTSALGGK | 1p(ST) 1pY | 2075.80, 2081.83 | 71 | 1.76 | 0.61 | 1.60 | N |
| IYIDPFTYEDPNEAVR | 1pY | 2020.88, 2026.91 | 112 | 1.33 | 0.19 | 1.42 | Y |
| IYIDPFTYEDPNEAVR | 1pY | 2020.88, 2026.91 | 79 | N/D | N/D | 1.31 | Y |
| IYIDPFTYEDPNEAVR | 1pT | 2020.88, 2026.91 | 23 | N/D | N/D | 1.07 | Y |
| IYIDPFTYEDPNEAVR | 1pY 1pT | 2100.85, 2106.87 | 45 | N/D | N/D | 1.18 | Y |
| IYIDPFTYEDPNEAVR | 2pY | 2100.85, 2106.87 | 77 | 1.51 | 1.13 | 1.87 | Y |
| *QLGLTEPR* | | 912.51, 918.52 | 36 | 0.98 | 0.21 | | |
| *SPTNTVTVQGLK* | | 1243.68, 1249.69 | 62 | 1.08 | 0.28 | | |
| *VDTIAADESFSQVDLGGR* | | 1878.90, 1884.92 | 124 | 1.09 | 0.46 | | |
| *VSDFGLSR* | | 879.45, 885.47 | 26 | 0.92 | 0.15 | | |

**BOLD RED** - indicates localized phosphorylation site, **BOLD BLUE** - indicates possible sites of unlocalized phosphorylation, *ITALICS* - indicates non-phosphopeptide, N/D - not determined, N/O - not observed

## Supplementary Figure 3.3

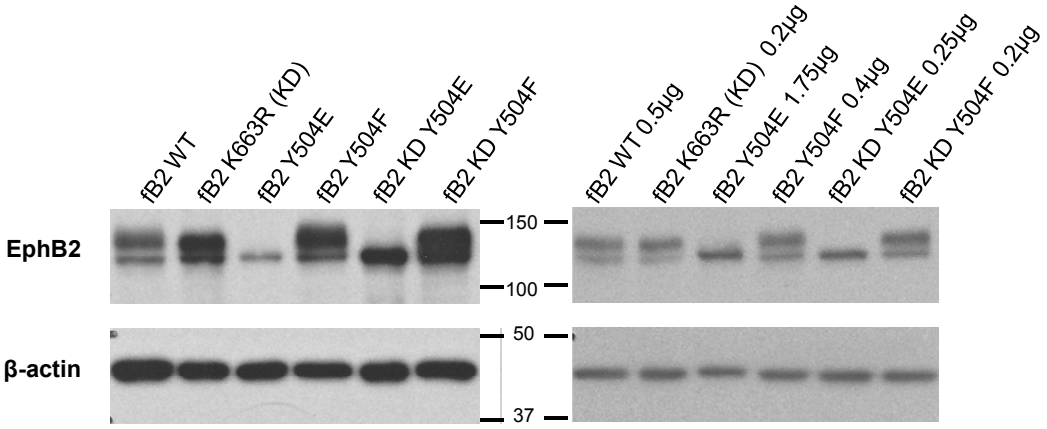

## Supplementary Figure 3.4

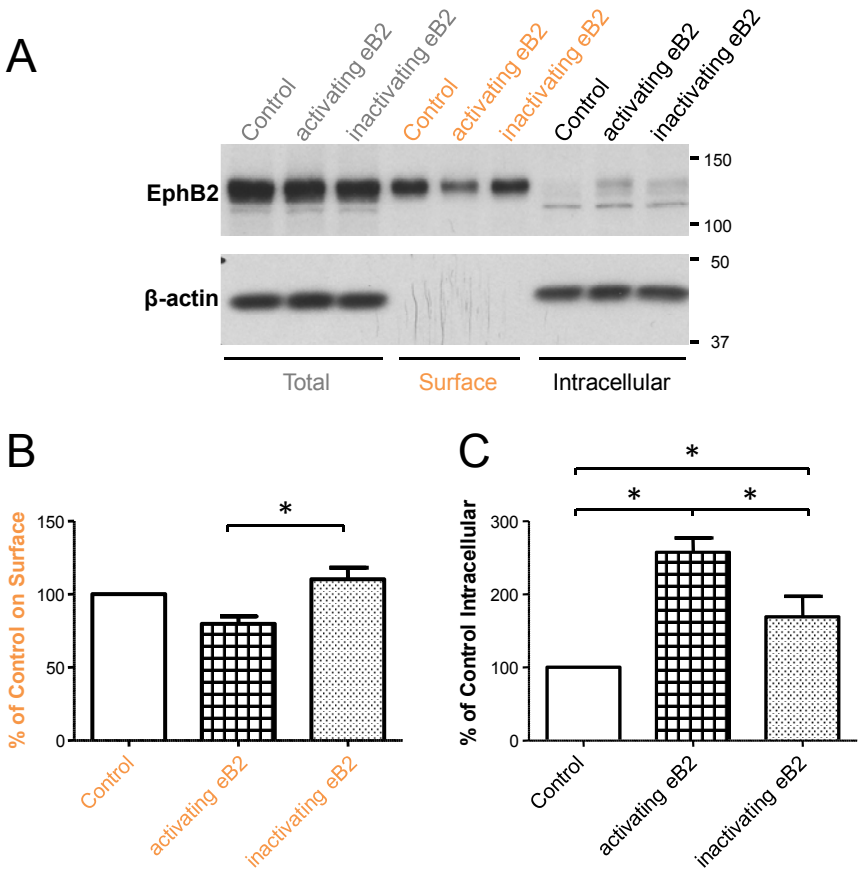

## Supplementary Figure 3.5

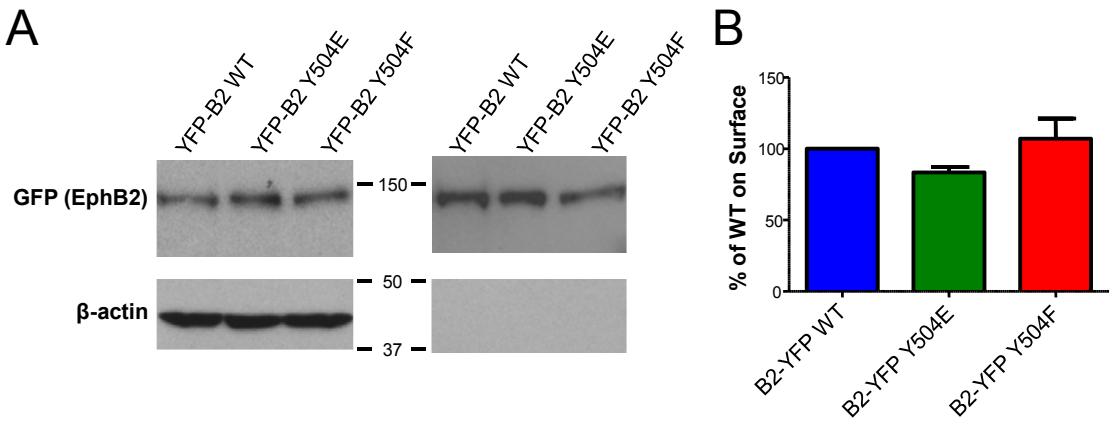

# CHAPTER 4

# DISCUSSION

Since the identification of the EphB receptor tyrosine kinase as a regulator of excitatory synapse formation and NMDA receptor synaptic localization, our laboratory has been striving to understand how these processes work at a molecular level. Of particular interest was how postsynaptic EphBs mediate formation of presynaptic specializations through cognate ephrin-B ligands and how signaling occurs at the molecular level; and the specific binding domain and mechanism for the direct EphB-NMDAR interaction. Synaptopathies, or disruption of synaptic structure and function, have been described as key features of neurodevelopmental, neurodegenerative, and psychiatric diseases. The research presented in this dissertation improves our understanding of the roles of EphB receptor tyrosine kinases in synapse formation, function, and mechanisms of disease.

**Summary of main results**

There are several main findings of these studies. First, from Chapter 2 focusing on ephrin-B-dependent presynaptic formation, it was found that: 1) Postsynaptic EphBs induce formation of presynaptic specializations via ephrin-B1 and ephrin-B2 early in neuronal development. 2) Presynaptic ephrin-B1 and ephrin-B2 are able to recruit the machinery required for neurotransmitter release through a PDZ-domain dependent interaction with syntenin-1. Second, Chapter

3 of this dissertation focused specifically on the EphB-NMDAR interaction and found that: 1) The extracellular domain of postsynaptic EphB2 receptors undergoes phosphorylation at tyrosine residue 504 after binding ephrin-B ligands. 2) Phosphorylation at Y504 promotes the EphB-NMDAR direct interaction stabilizing both receptors on the plasma membrane. 3) Mutations at Y504 affect the synaptic function of NR2B-containing NMDARs late in neuronal development altering synaptic currents and gene transcription. In this chapter, I will discuss the results from both Chapter 2 and Chapter 3 separately, focusing on the consequences and future directions for the EphB research field.

**EphBs in formation of presynaptic specializations**

Prior to the work presented in Chapter 2 of this dissertation, it was shown that EphBs can induce the formation of both pre- and postsynaptic specializations (Kayser et al., 2006). This is accomplished through bi-directional EphB signaling; both “forward” signaling in the EphB receptor expressing cell or “reverse” signaling in the ephrin-B expressing cell (Egea and Klein, 2007). While EphB signaling was well characterized, the roles for different membrane attached ephrin-B (B1-3) ligands were poorly understood. In the hippocampus, a postsynaptic role began to emerge for ephrin-B2 (Essmann et al., 2008; Grunwald et al., 2004) and ephrin-B3 (Aoto and Chen, 2007; Rodenas-Ruano et al., 2006). Interestingly, it was shown in *Xenopus* retinotectal system that ephrin-B1 controlled presynaptic formation (Lim et al., 2008). Therefore, the roles of ephrin-B1, ephrin-B2, and ephrin-B3 on the development of EphB-dependent

presynaptic formations were investigated in cultured cortical neurons. As this work began, some of the known intracellular signaling domains including Grb4 and GIT1 on ephrin-Bs were reported (Segura et al., 2007). Therefore, I also sought to identify the molecular mechanisms that mediate EphB-dependent development of presynaptic specializations via ephrin-Bs.

This work moved the fields of synapse formation and EphB receptor biology forward in several important ways. First, this work demonstrates that postsynaptic EphB2 interacts *trans-synaptically* with presynaptic ephrin-B1 or ephrin-B2, but not ephrin-B3, and that this interaction is necessary and sufficient for formation of a functional synapse. Second, knockdown of the adaptor protein syntenin-1 is sufficient to block EphB-dependent presynaptic formation. Based on this work and others, a model emerges (**Supplementary Figure 2.6**) where postsynaptic EphB binds presynaptic ephrin-B1/2, recruiting the adaptor protein syntenin-1, through its PDZ domain 2, which binds ERC2/CAST1 (Ko et al., 2006), that is directly linked to vesicles of neurotransmitter through Rim and the synaptic vesicle protein Rab3a (Jin and Garner, 2008). Thus, the *trans*-synaptic interaction between EphBs and ephrin-B1/2 can recruit the necessary machinery including receptors and changes in the actin cytoskeleton for presynaptic neurotransmitter release via syntenin-1. In support of this model, syntenin-1, ephrin-B1, and ephrin-B2 are co-localized at synaptic sites. However, it is important to note that ephrin-Bs are not responsible for formation of all presynaptic specializations. Therefore, our data are consistent with EphB/ephrin-B signaling directing a subset (~45% co-localization with VGLUT1 for ephrin-B1

and ~23% for ephrin-B2; **Supplementary Table 2.1**) of excitatory presynaptic specializations.

There are a number of interesting future directions that come out of this work. One of the most intriguing results from these studies was that simultaneous knockdown of both ephrin-B1 and ephrin-B2 does not further reduce synapse number, but does increase the amount of syntenin-1 at synaptic sites. However, the differences between the ephrin-B1 and ephrin-B2 signaling pathways were never identified. Therefore, I hypothesize that ephrin-B1 and ephrin-B2 are members of distinct signaling pathways for formation of presynaptic specializations and cannot compensate for the loss of the other. One way to test this hypothesis would be to generate double knockout mice for both ephrin-B1 and ephrin-B2 and then perform immunostaining experiments comparing the number of presynaptic specializations between homozygous and heterozygous animals. However, both ephrin-B1$^{-/-}$ and ephrin-B2$^{-/-}$ null mice are embryonic lethal. Therefore, I would need to breed together the conditional knockout lines for both ephrin-B1 and ephrin-B2. I could then directly inject *Cre-recombinase* into these double conditional knockout mice to delete *efnb1* and *efnb2* gene expression. Brains from these animals could sectioned and immunostained for presynaptic marker SV2, postsynaptic marker SynGAP, and syntenin-1. Based on our knockdown experiments using ephrin-B1 and ephrin-B2 shRNAs (Chapter 2), I would expect that double knockout mice would not have fewer synapses than animals lacking either ephrin-B1 or ephrin-B2.

However, synaptic syntenin-1 levels should be reduced in the double knockout mice compared to mice lacking either ephrin-B1 or ephrin-B2.

Another interesting future direction would be to follow-up on our observation that ephrin-B2 is expressed in glial cells. These data leads to the intriguing hypothesis that ephrin-B2 might be involved in neuron-glial communication at synapses (Filosa et al., 2009; Murai and Pasquale, 2011; Zhuang et al., 2010). Glial glutamate transporters are known to modulate synaptic transmission by clearing glutamate from the synaptic cleft (Tzingounis and Wadiche, 2007). At the CA3-CA1 synapse, the loss of presynaptic ephrin-A3 caused deficits in synaptic plasticity and overexpression of ephrin-A3 in astrocytes reduced levels of glutamate transporters (Filosa et al., 2009). Therefore, I hypothesize that ephrin-B2 would be a regulator of glial glutamate transporters in the cerebral cortex. To test this hypothesis, cortical lysates from wild-type and conditional ephrin-B2 knockout mice could be probed for levels of the glial glutamate/aspartate transporter (GLAST) and glutamate transporter subtype-1 (GLT-1). Based on the findings of (Filosa et al., 2009), I would expect an upregulation in either GLAST or GLT-1 proteins in mice where ephrin-B2 gene expression was removed. Alternatively, ephrin-B2 constructs could be generated with a GFAP promoter for overexpression studies in cortical neuron culture and density of presynaptic specializations could be assessed. I would expect that glial over-expression of ephrin-B2 would increase density of presynaptic specializations.

**Role of the EphB-NMDAR interaction at mature synapses**

Prior to the work presented in Chapter 3 of this thesis, it was shown that EphBs directly bind NMDA-type glutamate receptors in an unknown region of their extracellular domains (Dalva et al., 2000). The EphB-NMDAR interaction is dependent on binding of ephrin-B ligand, but does not require activation of the EphB intracellular kinase (Dalva et al., 2000). The EphB-NMDAR interaction changes cellular signaling by causing changes in $Ca^{2+}$ influx, phosphorylation of NMDARs by Src kinases, and changes in NMDAR-dependent gene transcription (Takasu et al., 2002). Furthermore, EphBs are required for synapse formation early in neuronal development (DIV7-14), but not after DIV21 (Kayser et al., 2008). Late in neuronal development (DIV14-23), EphBs specifically regulate the expression levels, $Ca^{2+}$-dependent desensitization, and synaptic currents of NR2B-containing NMDARs (Nolt et al., 2011). However, for the EphB-NMDAR interaction; the specific binding domain, mechanism, and pharmacological agents that modulate the interaction remained unknown.

We have identified a single amino acid, tyrosine residue 504, in the extracellular domain of EphB2 that is necessary and sufficient for the EphB-NMDAR interaction to occur. Presynaptic ephrin-B binding to EphB2 leads to Y504 phosphorylation, which is required to induce the EphB-NMDAR interaction. Furthermore, the EphB-NMDAR interaction stabilizes both receptor proteins on the plasma membrane and blocks their internalization. We also show that late in neuronal development, mutations at Y504 affect synaptic regulation and function including; synaptic currents and gene transcription of NR2B-containing NMDARs.

Finally, I have identified a non-membrane permeable extracellular kinase inhibitor k-252b, which inhibits the EphB-NMDAR interaction.

This work moves the fields of EphB receptor biology, synapse maturation and function, and potentially treatment for synaptopathies forward in several important ways. In the sections below, I will specifically discuss how this work resolves between different receptor fates at the plasma membrane (including a model summarizing EphB2 Y504 in terms of receptor trafficking and the EphB-NMDAR interaction), how the EphB-NMDAR interaction can be targeted to treat neuronal disease, and future directions for this work.

**EphB Receptor Fates at the Plasma Membrane**

Ephrin-B binding to EphB receptors regulates a diverse number of receptor trafficking events from cleavage by γ-secretase / MMP system (Lin et al., 2008; Litterst et al., 2007; Xu et al., 2009), internalization by clathrin-mediated mechanisms (Andersson, ; Irie et al., 2005; Nishimura et al., 2006; Pitulescu and Adams, 2010), trans-endocytosis of the receptor-ligand complex (Marston et al., 2003; Zimmer et al., 2003), to EphB ubiquitination and degradation by the proteasome (Fasen et al., 2008; Margolis et al., 2010), or direct binding to NMDA receptors (Dalva et al., 2000; Takasu et al., 2002). However, what differentiates between these trafficking events at the plasma membrane is a major gap in the literature. One intriguing idea from this thesis work (Chapter 3), is that extracellular phosphorylation at Y504 might direct EphBs towards internalization and NMDAR binding, but away from cleavage events. Interestingly, it appears in

an environment without NMDARs present like HEK293T cells (Chapter 3); a negative charge at Y504 is a signal for receptor internalization and subsequent degradation. In this system, I was unable to detect the EphB2 receptor ectodomain in the supernatant (S.I.S-C and M.B.D., *unpublished observations*). However, in cortical neuron cultures where endogenous NMDAR are widely expressed or HEK293T cells over-expressing NMDARs, a negative charge at Y504 acts as a signal to promote the EphB-NMDAR interaction stabilizing both proteins at the plasma membrane and therefore inhibiting their internalization (Chapter 3).

These observations are summarized into a working model (**Figure 4.1**) to explain the role of extracellular phosphorylation of EphB2 on EphB receptor internalization and NMDAR density at the plasma membrane. Briefly, ephrin-B binding to EphB2 receptors at the plasma membrane leads to extracellular phosphorylation of Y504 and activation of the EphB kinase domain (including intracellular phosphorylation at Y662). Next, comes the main decision point for this signaling pathway, which depends on whether NMDARs are closely localized to EphB receptors after ligand binding and extracellular phosphorylation at Y504. Once EphB receptors are phosphorylated and unbound to NMDARs, (**Figure 4.1 bottom**) they are internalized by clathrin-mediated mechanisms, and degraded through ubiquitin-dependent mechanisms in the proteasome (Fasen et al., 2008; Margolis et al., 2010). However, if NMDARs are present (**Figure 4.1 top**), phosphorylated EphBs bind NMDARs blocking internalization of both proteins. The EphB-NMDAR interaction starts a number of signaling events including

# Figure 4.1

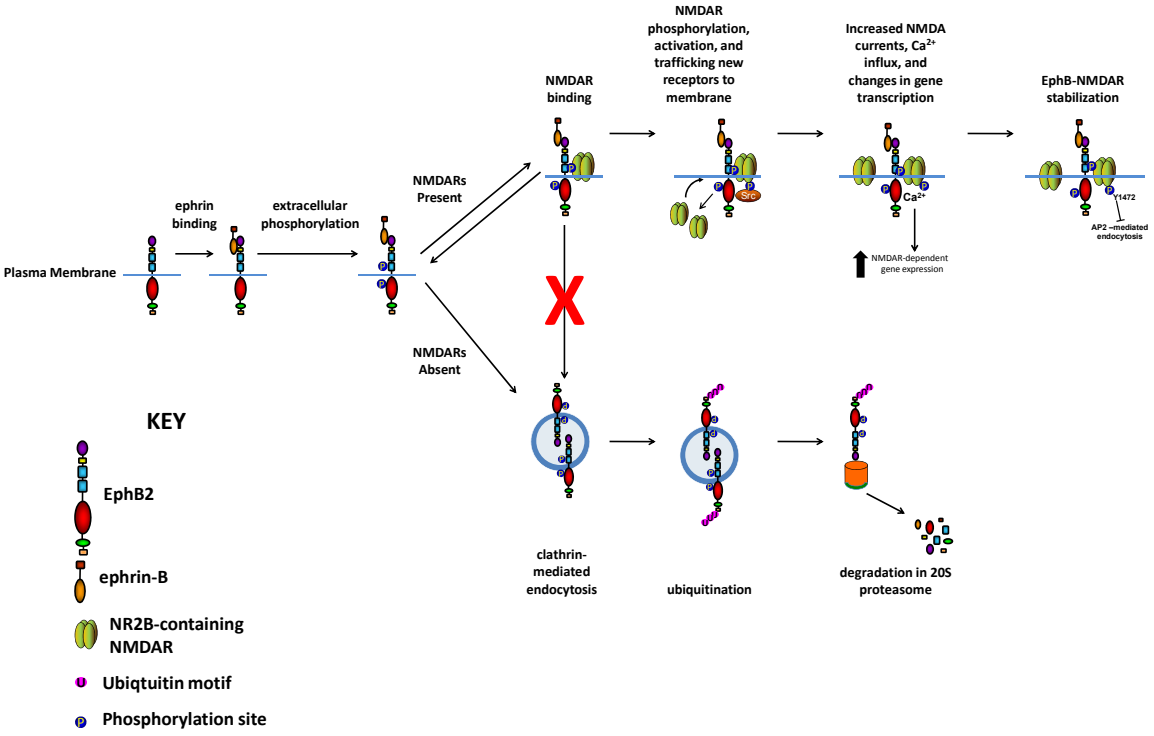
Plasma Membrane
ephrin binding
extracellular phosphorylation
NMDARs Present
NMDARs Absent
NMDAR binding
NMDAR phosphorylation, activation, and trafficking new receptors to membrane
Increased NMDA currents, Ca2+ influx, and changes in gene transcription
EphB-NMDAR stabilization
Src
Ca2+
NMDAR-dependent gene expression
Y1472
AP2 –mediated endocytosis
clathrin-mediated endocytosis
ubiquitination
degradation in 20S proteasome
KEY
EphB2
ephrin-B
NR2B-containing NMDAR
Ubiqtuitin motif
Phosphorylation site

src-mediated phosphorylation of NR2B-containing NMDARs (Takasu et al., 2002), trafficking of more NR2B-containing receptors to synaptic sites, increased NMDAR currents, calcium influx (Nolt et al., 2011; Takasu et al., 2002), and changes in gene expression.

A number of intriguing future directions arise from the observation that when NMDARs are absent, EphBs that are phosphorylated at Y504 are rapidly degraded. First, one attractive hypothesis is that phosphorylation at Y504 may allow for the developmental switch between axon guidance and synapse formation. The role of EphB/ephrin-B signaling is well established in both of these processes, but involves different molecular mechanisms. During axon guidance (DIV0-7), ephrin-Bs act as repulsive cues. Upon binding ephrin-Bs, EphB activation leads to receptor internalization and eventually growth cone collapse (Fasen et al., 2008; Marston et al., 2003; Zimmer et al., 2003). In contrast, at DIV7-14, EphB activation is not repulsive anymore but acts as an adhesion molecule promoting synapse formation (Kayser et al., 2008). This switch in EphB function could result from differences in NMDAR expression. Thus, low NMDAR expression such as seen in growth cones (Wang et al., 2011) would induce ephrin-B-dependent internalizations of EphBs and growth cone collapse; whereas higher levels of NMDARs, as observed in dendritic filopodia, would favor EphB-NMDAR interaction, and EphB-NMDAR retention at the surface.

One way to test the hypothesis that ephrin-B-dependent phosphorylation at EphB Y504 promotes growth cone collapse is to make retinal explants cultures

from retinal ganglion cell (RGC) neurons which endogenously express EphBs (Petros et al., 2010). Then, growth cone collapse could be assessed using live imaging or immunostaining after bath pretreatment with ephrin-B2 or Fc-control in the presence or absence of k-252b the broad spectrum, membrane impermeable, extracellular kinase inhibitor. If phosphorylation at Y504 is critical to ephrin-B-mediated growth cone collapse, then collapse should be blocked by k-252b treatment. Similarly, I would expect that over-expression of Y504F mutants would prevent growth cone collapse.

To assess the hypothesis that the presence of NMDARs blocks repulsion through Y504, RGC explants could be transfected with EphB2 WT and Y504 mutant constructs in the presence or absence of NR1/2B constructs. I would predict that because binding NMDARs stabilizes EphBs that over-expression of NR1/2B receptors would block growth cone collapse. We have shown in Chapter 3 that over-expression of Y504F mutant receptors decreases synaptic currents and NMDARs at postsynaptic specializations. Alternatively, it is also possible that the change from repulsive signaling during axon guidance at growth cones, to stabilization during synaptogenesis at dendritic filopodia is mediated by intracellular signaling events through different GEFs. Rho-GEF Vav2 is required for internalization during growth cone collapse (Cowan et al., 2005); whereas Rho-GEF intersectin-1 (Irie and Yamaguchi, 2002), Rac-GEF Tiam1 (Tolias et al., 2007), and Rho/Rac1-GEF Kalirin-7 (Penzes et al., 2003) help EphBs associate with NMDAR at synaptic sites to form dendritic spine synapses. Unfortunately, the differences in signaling mechanisms amongst GEFs remains

poorly understood. However, shRNAs could be generated against each individual GEF, and co-expressed with EphB WT and Y504 mutant constructs in cultured cortical neurons. Then dendritic filopodia motility and density of postsynaptic specializations could be assessed as previously described in (Kayser et al., 2008).

**Targeting the EphB-NMDAR interaction to treat CNS disease**

A number of recent reports have specifically implicated the EphB-NMDAR interaction as a critical regulator of the deleterious effects of both Alzheimer's disease and neuropathic pain. In this thesis (Chapter 3), I have identified a specific amino acid (Y504) that mediates the EphB-NMDAR interaction and a pharmacological agent (k-252b) that blocks this interaction. Therefore, the most exciting future direction for this thesis work is to test whether modulating EphB2 Y504 phosphorylation and the EphB-NMDAR interaction with k-252b can ameliorate either of these devastating diseases. While EphBs are not required for localization of NMDARs or NR2B-conatining NMDARs at all synaptic sites, our data suggests they are at a substantial fraction (~50%) of mature synapses (Kayser et al., 2006; Nolt et al., 2011). Here, I will discuss future directions to test the hypothesis that EphB2 Y504 is a critical regulator of Alzheimer's disease and neuropathic pain.

A strong link has emerged between EphBs and Alzheimer's disease (AD) through Amyloid-β (Aβ) including *in vitro*, *in vivo*, and clinical reports (Chen et al.). Furthermore, EphB2 expression levels are reduced in AD patients (Simon et

al., 2009). Aβ appears to bind directly to EphB2 in its extracellular FnIII domains (which contains Y504) promoting EphB receptor degradation (Cisse et al., 2011). Thus, viral overexpression of EphB2 can rescue LTP, NMDAR current deficits, and cognitive abilities in a mouse model of AD (Cisse et al., 2011). Therefore, it is intriguing to propose that EphB2, and modulation of the EphB-NMDAR interaction through phosphorylation at Y504 could yield a therapeutic target for Alzheimer's disease.

Based on the work of Cisse et al., (2011), it has been suggested that EphB binding directly to Aβ is a critical event to AD progression. First, it would be important to test the hypothesis that Y504 is the binding domain for EphBs and Aβ. This hypothesis could be tested *in vitro* using the human amyloid-beta (hAβ) protein precursor mouse model of AD (Cisse et al., 2011; Simon et al., 2009) and performing co-immunoprecipitation experiments. Cortical neurons from the hAPP mouse could be cultured, and then infected with EphB2-YFP WT, Y504E, and Y504F lentiviruses (Chapter 3). Over-expressed EphB2 receptors could be pulled down using an anti-GFP antibody, and then probed with an antibody against Aβ. Furthermore, these blots could be stripped and reprobed with anti-NMDAR antibodies to see if the EphB-NMDAR interaction is affected. If EphB2 Y504 is the binding domain for Aβ-binding, one would expect that due to the change in charge, EphB2 Y504E mutants would have decreased Aβ-binding, and more EphB-NMDAR interactions. Next, it would be important to see if infection of the EphB-YFP lentiviruses into the hAPP mice could rescue the deficits in LTP, NMDAR currents, and behavior as described by (Cisse et al.,

2011). If Y504 is the critical residue for EphB-Aβ-binding, I would expect that infection of EphB2 Y504F receptors would not rescue the deficits in hAPP mice because it would preferentially bind Aβ over NMDARs. However, it is possible that the Aβ-binding domain is not located at Y504, but somewhere else in the FnIII repeat domains. If Y504 were not the Aβ-binding domain, it would be interesting to see if the other extracellular phosphorylation site identified by our mass spectrometry experiments (Y481) is involved in this process.

In addition to a role of EphB in AD, a robust literature links EphB1/ephrin-B signaling to regulate neuropathic pain in the spinal cord and periphery through modulation of NMDAR signaling. Specifically, EphB1 and ephrin-Bs are upregulated in the spinal cord and periphery after injury (Kobayashi et al., 2007; Song et al., 2008a; Song et al., 2008b). The upregulation of EphB1/ephrin-Bs leads to hyperexcitable NMDARs with lower LTP thresholds (Battaglia et al., 2003; Cao et al., 2008; Guan et al., 2010; Ruan et al., 2010; Slack et al., 2008; Song et al., 2008b) and NR2B phosphorylation by src kinase (Battaglia et al., 2003; Slack et al., 2008; Song et al., 2008b). Therefore, it is hypothesized that the EphB-NMDAR interaction plays a critical role in the enhancement of pain sensitivity. EphB1 Y502 is the structurally homologous interaction domain on EphB1 that should modulate NMDAR binding. Based on our findings that k-252b is necessary and sufficient to block the EphB-NMDAR interaction, I hypothesize that k-252b injection could ameliorate neuropathic pain. To test this hypothesis, hyperalgesia could be induced by intrathecal injection of ephrin-B2-Fc (Battaglia et al., 2003; Slack et al., 2008; Song et al., 2008b) in the presence or absence of

k-252b pre-injection. Thermal hyperalgesia or mechanical allodynia models could be used to assess the behavioral affects of k-252b on pain, and the EphB-NMDAR interaction could be assessed biochemically in spinal tissues from injected rats. If EphB1 Y502 phosphorylation is required for neuropathic pain, then k-252b should block the induction of neuropathic pain mediated by ephrin-Bs by inhibiting the EphB-NMDAR interaction in behavioral and biochemical assays.

Alternatively, if we knew the kinase that phosphorylates Y504, antagonism of that receptor would also have large therapeutic potential because it may have fewer side effects than k-252b. While no extracellular tyrosine kinases have been reported, extracellular serine/threonine kinases have been found in numerous cell types including neurons (Chen et al., 1996; Fujii et al., 2000; Kumar et al., 2011; Redegeld et al., 1999). Three soluble FGFR splice variants have been reported with kinase domains intact, but lacking transmembrane domains (Johnston et al., 1995; Katoh et al., 1992; Sturla et al., 2003). Another possibility is known extracellular kinase Casein Kinase 2 (CK2) (Bohana-Kashtan et al., 2005; Maik-Rachline et al., 2005; Nguyen et al., 2008; Zimina et al., 2007) which has been reported to phosphorylate tyrosine residues in addition to its known function on serine/threonine residues (St-Denis and Litchfield, 2009).

There a few different ways to determine which kinase phosphorylates EphB2 Y504. A first approach, currently being taken by Dr. Kenji Hanamura a postdoc in the laboratory, is to use pharmacological inhibitors of known tyrosine kinases to find ones that inhibit phosphorylation of Y504, but not other

intracellular phospho-tyrosine residues. Then, effective inhibitors could be used to see if they can block the EphB-NMDAR interaction. Using a variety of inhibitors would narrow down the list to a few known kinases. Then, these kinases could be tested individually in *in vitro* kinase assays and in neuron culture for the EphB-NMDAR interaction. Preliminary experiments suggest that PD161570 an FGFR antagonist; and PD166285 an antagonist of FGFR, PDGFR, and src kinases blocks phosphorylation of EphB2 at Y504 (K.H., S.I.S-C, and M.B.D., *unpublished observations*). To build on the first approach, Dr. Hanamura is also performing an *in vitro* kinase assay with only the extracellular domain of EphB2 (EphB2-Fc). Commercially available soluble receptor tyrosine kinases like FGFRs, CK2, EphB, EGFR, and other RTKs are combined in the presence or absence of ATP. The EphB2-Fc is then immunoprecipitated using anti-human IgG antibodies and lysates are probed using the anti-EphB2 pY504 antibody.

A final approach based on mass spectrometry (similar to Y504 identification) would express EphB2 TR (extracellular domain only) constructs in cell lines. Then, the cells could be treated with ephrin-B2 ligand to induce Y504 phosphorylation. Next, a chemical cross-linking reagent like Dithiobis(succinimidyl propionate) (DSP) (Sinz, 2006; Wiseman et al., 2009) or formaldehyde (Sutherland et al., 2008) could be used to crosslink kinase and substrate. This cross-linking would need to be done at different timepoints including 5, 7.5, 15, and 30 minutes to makes sure to catch receptor and kinase together. Then, phospho-tyrosine residues could be immunoprecipitated using

PY99, and tryptic peptides identified could be bioinformatically linked to known tyrosine kinases (Sinz, 2006).

## Conclusion

The work presented in this thesis has strived to understand basic mechanisms of EphB receptor biology with the goal of understanding how to better understand synaptopathies. These findings move the field of EphB receptor biology, synapse formation, and synapse maturation forward in four important ways. First, the mechanisms for EphB-dependent presynaptic signalling have been elucidated from ephrin-B adhesion molecule to vesicles of glutamate. Second, this dissertation is the first report of extracellular tyrosine phosphorylation of any protein, and a significant advance for the field of EphB receptor biology by revealing new signalling mechanisms. Thirdly, it has shown a single residue that is necessary and sufficient for the EphB-NMDAR interaction to occur. Finally, a novel mechanism of extracellular tyrosine phosphorylation for regulating protein-protein interactions has emerged with the potential to treat diseases of the central nervous system and beyond. Future studies will address which specific tyrosine kinase is responsible for this extracellular phosphorylation event and whether inhibiting this phosphorylation event, using k-252b, to block the EphB-NMDAR interaction could have therapeutic potential for treating neuropathic pain. Also, potentiating the EphB-NMDAR interactions could be protective against Alzheimer's disease. Therefore, it is hoped that this

dissertation research moves the field of synapse formation and EphB receptor biology towards the goal of treating human disease.

# APPENDIX 1

## EphB Controls NMDA Receptor Function and Synaptic Targeting in a Subunit-Specific Manner

Mark J. Nolt[1, *], Ying Lin[2, *], Martin Hruska[1], Jessica Murphy[2], Sean I. Sheffler-Collins[1], Matthew S. Kayser[1], Joel Passer[1], Michael V. L. Bennett[2], R. Suzanne Zukin[2], and Matthew B. Dalva[1, **]

[1]Department of Neuroscience, University of Pennsylvania Medical School, Philadelphia, Pennsylvania 19104, and

[2]Dominick P. Purpura Department of Neuroscience, Albert Einstein College of Medicine, Bronx, New York 10461

*M.J.N. and Y.L. contributed equally to this work.

**** Correspondence should be addressed to Matthew B. Dalva, Department of Neuroscience, University of Pennsylvania Medical School, 1127 BRB II/III, 421 Curie Boulevard, Philadelphia, PA 19104. dalva@mail.med.upenn.edu

Contribution: I designed, carried out, and analyzed all experiments to generate Figure 5.5. I also wrote the figure legend and methods section for these experiments, and edited the paper.

**Abstract**

Dynamic regulation of the localization and function of NMDA receptors (NMDARs) is critical for synaptic development and function. The composition and localization of NMDAR subunits at synapses are tightly regulated and can influence the ability of individual synapses to undergo long-lasting changes in response to stimuli. Here, we examine mechanisms by which EphB2, a receptor tyrosine kinase that binds and phosphorylates NMDARs, controls NMDAR subunit localization and function at synapses. We find that, in mature neurons, EphB2 expression levels regulate the amount of NMDARs at synapses, and EphB activation decreases $Ca^{2+}$-dependent desensitization of NR2B-containing NMDARs. EphBs are required for enhanced localization of NR2B-containing NMDARs at synapses of mature neurons; triple EphB knockout mice lacking EphB1–3 exhibit homeostatic upregulation of NMDAR surface expression and loss of proper targeting to synaptic sites. These findings demonstrate that, in the mature nervous system, EphBs are key regulators of the synaptic localization of NMDARs.

## Introduction

The NMDA receptor (NMDAR) is essential for neuronal development and function, synaptic plasticity, and adaptive responses to sensory experience (Cull-Candy and Leszkiewicz, 2004; Lau and Zukin, 2007; Perez-Otano and Ehlers, 2005). These functions require glutamate-dependent calcium influx into neurons through the NMDAR. The NMDAR is a heteromeric protein complex of two obligate NR1 subunits and typically two NR2 subunits, which each convey distinct functional properties to the receptor (Cull-Candy and Leszkiewicz, 2004). NR2A is the principal subunit at mature cortical and hippocampal synapses. Although NR2B subunits are more prevalent at these synapses during development, they are still expressed in the mature brain (Monyer et al., 1994; Sheng et al., 1994; Tovar and Westbrook, 1999). NR2B-containing NMDARs have a slower inactivation rate and longer decay times compared with NR2A subunits (Cull-Candy and Leszkiewicz, 2004). Thus, synapses with higher proportions of NR2B can integrate synaptic currents across broader time intervals than those with more NR2A. In addition, NR2B-containing NMDA receptors carry more $Ca^{2+}$ current per unit charge (Sobczyk et al., 2005), are preferentially tethered to the plasticity protein CaMKII (calcium/calmodulin-dependent protein kinase II) (Barria and Malinow, 2005), and exhibit a lower threshold to undergo potentiation of synaptic responses (Philpot et al., 2007; Philpot and Zukin, 2010). Thus, understanding the molecular mechanisms that direct trafficking of NR2B subunits to and from synapses will provide insights into synaptic plasticity.

NMDARs are recruited to and retained at synapses through well studied mechanisms (Chen and Roche, 2007; Kim and Sheng, 2004; Lau and Zukin, 2007, including postsynaptic density-95/Discs large/zona occludens-1 (PDZ) binding domain interactions and phosphorylation of the receptor itself {Prybylowski, 2005 #112; Perez-Otano and Ehlers, 2005). Activation of EphB leads to a Src kinase-dependent phosphorylation of the NR2B subunit at three tyrosine residues (Antion et al., 2010; Takasu et al., 2002). One of these residues, Y1472, is important for regulating NMDAR surface and synaptic localization (Salter and Kalia, 2004), suggesting that EphBs might play a role in the synaptic targeting/retention of NMDARs.

The EphB family of receptor tyrosine kinases is enriched at excitatory synapses and is important during synapse and spine formation and maintenance (Aoto and Chen, 2007; Klein, 2009; Shi et al., 2009; Tolias et al., 2007). Triple knock-out mice lacking EphB1–3 have fewer excitatory synapses (Henkemeyer et al., 2003; Kayser et al., 2006), whereas animals lacking only EphB2 have reduced NMDAR content at synapses (Henderson et al., 2001). In addition to modulating NMDAR-mediated calcium influx, activation of EphBs leads to a direct association between EphB and the NMDAR NR1 subunit (Dalva et al., 2000); EphBs also associate with and regulate trafficking of AMPA receptors (AMPARs) (Irie et al., 2005; Kayser et al., 2006). We examined whether EphBs impact synaptic NMDAR function and contribute to subunit-specific synaptic localization of NMDARs. We find that expression levels of EphB2 control the amount of NMDAR at synapses, and that EphB2 kinase activity regulates the

calcium inactivation rate of NR2B-containing NMDARs. EphB2 activation also preferentially targets and stabilizes NR2B-containing NMDARs at synapses. These results suggest that EphBs may be important regulators of NMDAR targeting, subunit composition, and function at mature synapses.

## Materials and Methods

**Cell culture and transfection.** Dissociated cortical neurons were prepared from embryonic day 17 (E17) to E18 rats of either sex and cultured as described previously (Kayser et al., 2006). Briefly, neurons were cultured in Neurobasal (Invitrogen), B27 supplement (Invitrogen), glutamine (Sigma-Aldrich), and penicillin–streptomycin (Sigma-Aldrich) on poly-d-lysine (BD Biosciences or Sigma-Aldrich) and laminin (BD Biosciences)-coated glass coverslips (12 mm; Bellco Glass) in 24-well plates (Corning Life Sciences). Cells were plated at 150,000 per well and maintained in a humidified incubator with 5% $CO_2$ at 37°C. Neurons were transfected with Lipofectamine 2000 (Invitrogen) at 14 d *in vitro* (DIV) using methods described previously (Kayser et al., 2008).

**HEK-293 cell culture and transfection.** HEK-293 cells were maintained as described (Lin et al., 2004). For transfection, HEK-293 cells were plated at a density of $1 \times 10^6$ cells per milliliter on 12 mm glass coverslips coated with poly-d-lysine (10 μg/ml) in 24-well culture plates and transfected with NR1, NR2A, or NR2B and green fluorescent protein (GFP) or EphB2-YFP plasmid (1 μg of plasmid cDNA per 12 mm coverslips in 1:1:1 ratio) using the calcium phosphate method according to the manufacturer's protocol (Invitrogen). For the EphB2-KD experiment, we transfected YFP-NR1, NR2B, and EphB2-KD into HEK-293 cells in 1:1:1 ratio.

**Immunocytochemistry.** Cultures were fixed in 4% paraformaldehyde/2% sucrose for 8 min at room temperature. Cells were washed three times in PBS and blocked and permeabilized in 1% ovalbumin (Sigma-Aldrich)/0.2% coldwater fish scale gelatin (Sigma-Aldrich)/0.1% saponin (Sigma-Aldrich) for 1 h at room temperature. Antibody incubations were conducted overnight at 4°C for primary antibody and 1 h at room temperature in secondary antibody diluted in blocking reagents. Antibodies used were as follows: chicken anti-GFP (Millipore; 1:2500), guinea pig anti-VGlut1 (Millipore Bioscience Research Reagents; 1:5000), and mouse anti-NR1 (Millipore Bioscience Research Reagents; 1:1000). Cy2, Cy3, and Cy5 secondary antibodies were obtained from Jackson ImmunoResearch and used at 1:250.

**cDNA and short hairpin RNA constructs.** EphB2 short hairpin RNA (shRNA) was described previously (Kayser et al., 2006). The EphB2 rescue construct was generated and described previously (Kayser et al., 2006; Kayser et al., 2008). Full-length FLAG-tagged EphB2 and FLAG-tagged kinase inactive EphB2 were described previously (Dalva et al., 2000).

**Imaging and analysis.** Images of primary neuronal cultures were acquired by confocal scanning microscopy (Leica) using methods described previously (Kayser et al., 2006; Kayser et al., 2008). Briefly, all images were acquired using a 63×, numerical aperture 1.4, oil-immersion objective with *z*-steps of 0.5 μm and subsequently analyzed with custom-designed NIH ImageJ macros blind to

experimental condition. Images were collected from at least three independent experiments. For puncta analysis, images were converted from maximum projections to binary scale, and puncta were identified as continuous groups of pixels corresponding to 0.5–7.5 $\mu m^2$. Colocalization between puncta was defined as >1 pixel overlap between channels. To determine amount of NR1 at the synapse, images were collected for each condition with the same gain values. Intensity of NR1 staining at the synapse was then calculated for each condition. Amounts for each condition were normalized to the maximum intensity observed from all three conditions.

**Electrophysiology.** Whole-cell recordings were made from 21–23 DIV rat cortical neurons. Coverslips were moved into a recording chamber and bathed in a HEPES-buffered artificial CSF (ACSF) solution (in mm: 140 NaCl, 5 KCl, 2 $CaCl_2$, 20 glucose, and 10 HEPES, pH 7.2). GFP-positive pyramidal neurons were chosen for recording. The internal solution contained the following (in mm): 125 CsGlu, 5 EGTA, 2 $MgCl_2$, 1 $CsCl_2$, 2 $K_2$-ATP, 10 HEPES, and 0.42 Na-GTP, pH 7.2. Pipettes were pulled to a 6–9 MΩ resistance, and recordings were made for 2–5 min at −65 mV before bath application of APV. After application of APV, the cell was again recorded for 2–5 min. For experiments conducted at +50 mV, similar recording conditions were used except that coverslips were moved into a recording chamber and bathed in a HEPES-buffered ACSF solution (in mm: 140 NaCl, 5 KCl, 2 $CaCl_2$, 1 $MgCl_2$, 20 glucose, and 10 HEPES, pH 7.2). Tetrodotoxin (TTX) and picrotoxin were used at 1 and 10 μm, respectively (Sigma-Aldrich).

Bicuculline was used at 50–100 μm, APV was used at 10 μm, and (α*R*,β*S*)-α-(4-hydroxyphenyl)-β-methyl-4-(phenylmethyl)-1-piperidinepropanol maleate (Ro25-6981) was used at 1–2 μm (Tocris Bioscience). All data were collected at 5 kHz and filtered at 1 kHz; events were detected in Clampfit 9.2 (Molecular Devices). Event analysis and statistics were performed using Matlab (The MathWorks) and Clampfit software (Molecular Devices). Decay time was calculated as the time from peak amplitude of the current to 30% of the peak amplitude.

**Whole-cell recording from HEK-293 cells.** Electrophysiological recordings were performed 1–2 d after transfection. Once whole-cell-recording configuration was obtained, NMDA plus glycine was applied several times for 5 s periods separated by □25 s recovery intervals. Rapid agonist application was achieved by placing cells in a laminar solution stream that was delivered from a multibarrel array fed by gravity. Currents activated by NMDA (300 μm) in the presence of glycine (10 μm) were recorded in the whole-cell mode at a holding potential of −60 mV, filtered at 2 Hz, and digitized on-line at 1 kHz. Importantly, we did not observe an increase in desensitization during the few minutes of recording. Electrodes with open-tip resistances of 2–5 MΩ were used. Data were acquired and analyzed using pClamp 9 software and AxoPatch-1D amplifier (Molecular Devices). The internal pipette solution was composed of the following (in mm): 145 KCl, 4 Mg-ATP, 10 HEPES, and 5.5 EGTA, adjusted to pH 7.25 with KOH. External solution contained the following (in mm): 145 NaCl, 5.4 KCl, 2 $CaCl_2$, 11 glucose, and 10 HEPES, adjusted to pH 7.3 with NaOH.

**Cultured neuron biotinylation.** After treatment with clustered ephrin-B2-Fc or Fc control, cortical neuron cultures were placed on ice and rinsed twice with ice-cold rinsing solution (PBS, pH 7.5, containing 0.1 mm $CaCl_2$ and 1 mm $MgCl_2$). Clustering of ephrin-B2-Fc and human-Fc control proteins (R&D Systems) was achieved by incubation with anti-human IgG (Jackson ImmunoResearch) using methods described previously (Dalva et al., 2000). Cells were incubated in rinsing solution containing 1 mg/ml Sulfo-NHS-SS-Biotin (Pierce Protein Research Products; Thermo Fisher Scientific) with gentle agitation at 4°C for 30 min. Cells were then washed in quenching solution (rinsing solution with 100 mm glycine) and incubated in this solution with gentle agitation at 4°C for 30 min to quench unbound biotin. Cells were washed in rinsing solution, and then agitated at 4°C for 60 min using radioimmunoprecipitation assay (RIPA) buffer containing protease inhibitors for cell lysis. Cell lysates were harvested and centrifuged at 13,000 rpm for 20 min at 4°C. Aliquots were taken for total lysate fraction, for Bradford protein assay analysis (Bio-Rad), and for incubation with monomeric avidin agarose (Pierce Protein Research Products; Thermo Fisher Scientific) at 25°C for 60 min. After incubation, lysates were centrifuged at 13,000 rpm for 15 min, and the supernatant (intracellular fraction) was removed. The 4× sample solubilizing buffer was added to the total and intracellular fractions. Avidin beads were then washed three times with RIPA buffer, before incubation in 2× solubilizing buffer at 37°C for 30 min. Samples were then centrifuged for 5 min at 14,000 rpm, and the supernatant (surface fraction) was extracted. Five to 10 μg

of surface and total lysate fraction were subjected to SDS-PAGE and Western blot analysis. Experiments were excluded from additional analysis if Western blots of the biotinylated fractions were positive for the cytosolic protein β-actin. Band intensities were quantified by densitometric analysis using NIH ImageJ software, and comparisons were made between total and biotin labeled fractions.

**Biotinylation assay for surface NMDARs from slices.** Hippocampal or cortical slices were prepared from postnatal day 21 (P21) to P28 mice of either sex. After washing twice in ice-cold ACSF, slices were incubated in 1 mg/ml NHS-SS-biotin (Pierce) for 30 min at 4°C to biotinylate surface proteins as described previously (Huang et al., 2009). After removing nonspecifically bound NHS-SS-biotin, the tissue was homogenized and sonicated in PBS-based lysis buffer containing protease and phosphatase inhibitors (in mm: 1 EDTA, 1 EGTA, and 1% Triton X-100, 0.1% SDS, pH 7.4), followed by end-to-end rotating for 30 min at 4°C. After centrifugation at 13,000 rpm for 30 min at 4°C, the supernatant was incubated with Neutravidin beads (Thermo Fisher Scientific) to capture biotinylated surface proteins. After washing three times with lysis buffer, the surface proteins were eluted with protein sample buffer containing DTT and subjected to Western blotting. Membranes were probed with polyclonal anti-NR2A (1:1000; Millipore), with monoclonal anti-NR2B (1:2000; Millipore), monoclonal anti-NR1 (1:2000; 54.1; a generous gift from J. Morrison, Mount Sinai School of Medicine, New York, NY), and with anti-β-actin (1:5000; Sigma-Aldrich). Samples with actin labeling in the surface fraction were excluded from additional analysis.

Membranes were stripped with Restore reagent (Thermo Fisher Scientific) to reprobe the membranes with a different antibody. Band intensities were quantified by densitometric analysis using NIH ImageJ software.

**Synaptosome preparation.** This protocol was adapted from previous work (Blackstone et al., 1992; Lau et al., 1996). Briefly, whole brains from male and female P30 wild type (WT), EphB double knock-out (DKO), and triple knock-out (TKO) mice were homogenized in HEPES-buffered sucrose [0.32 m sucrose, 4 mm HEPES, pH 7.4, and protease inhibitor mixture (Sigma-Aldrich)]. The nuclear fraction was removed from the homogenate by centrifugation at 1000 × *g* for 15 min. The resulting supernatant (S1) was then centrifuged at 10,000 × *g* for 15 min to yield the crude membrane fraction (P1). The P1 pellet was resuspended in 10 vol of HEPES-buffered sucrose and spun again at 10,000 × *g* for 15 min to yield washed crude synaptosomal fraction (P2). The P2 fraction was layered onto 4 ml of 1.2 m sucrose containing protease inhibitors (Sigma-Aldrich) and centrifuged at 230,000 × *g* for 15 min. The interface was collected and diluted into final volume of 6 ml with HEPES-buffered 0.32 m sucrose and layered onto 0.8 m sucrose containing protease inhibitors. The sample was centrifuged at 230,000 × *g* for 15 min to obtain a pure synaptosomal (Syn) pellet. The intensities of glutamate receptors from each fraction were determined by densitometric analysis using ImageJ software. The raw intensities were then normalized to actin intensities in each fraction. The relative levels of synaptic versus membrane-associated glutamate receptors were calculated by taking a

ratio of normalized synaptic fraction values (Syn) to normalized crude membrane fraction values (P1). Statistical significance was assessed by ANOVA.

## Results

Early in development, the EphB receptor couples filopodia motility to synaptogenesis (Kayser et al., 2008). As neurons and synapses mature, EphB is no longer required to maintain normal numbers of established synapses (Kayser et al., 2008). However, EphB2 is still highly expressed in the adult nervous system (Bouvier et al., 2008), suggesting that it likely has an active role in mature neurons. We examined the impact of EphB2 on NMDAR surface and synaptic localization in the mature nervous system. We used an shRNA that targets EphB2 and has been extensively characterized previously in the following ways: (1) it has no detectable effects on neurons from EphB1-3 triple knock-out mice; (2) it causes selective inhibition of EphB2-dependent synapse formation; (3) it knocks down EphB2 expression with high efficacy in neurons and non-neuronal cells; and (4) the effects of expressing it can be reversed with expression of EphB2 constructs rendered insensitive to the shRNA by the introduction of silent mutations (Kayser et al., 2006; Kayser et al., 2008). Previous work using this shRNA has shown that knockdown of EphB2 in cortical neurons at either 3 or 10 DIV leads to a robust decrease in synapse number at 21 DIV, whereas later knockdown of EphB2 from 14–21 or 14–24 DIV has no effect on synapse number (Kayser et al., 2008). Importantly, knockdown at each of these times leads to similar decreases in EphB2 expression.

To selectively determine how changes in EphB2 expression later in neuronal development affect NMDAR localization in mature neurons, we first used immunohistochemical methods in cultured cortical neurons. Neurons were

transfected with enhanced green fluorescent protein (eGFP) and shRNA vector (control), EphB2.1 shRNA, or EphB2.1 shRNA with rescue at 14 DIV. We rescued EphB2 knockdown with a shRNA-insensitive EphB2 construct—an approach that generates functional overexpression (McClelland et al., 2010; McClelland et al., 2009). We used this approach to control the amount of EphB2 expressed in neurons. At 21 DIV, neurons were processed to determine the amount of NR1 labeling at synapses. In these experiments, we focused on NR1 immunolabeling because (1) this subunit is present in all NMDARs (Cull-Candy and Leszkiewicz, 2004), (2) EphB directly binds NR1 through an interaction involving extracellular domains (Dalva et al., 2000), and (3) the anti-NR1 antibody most reliably colocalizes with other presynaptic and postsynaptic marker proteins (data not shown). Synapses were defined as locations where NR1 puncta (red) colocalized with GFP-positive dendrites (green) within <1 μm of anti-vGlut1-positive puncta (blue) (**Figure 5.1A-C**). We determined the size and intensity of NMDAR staining at each synapse. Although there were no effects on the size of the NMDAR puncta, functional overexpression and knockdown of EphB2 did alter the amount of NMDAR localized at synapses as measured by the normalized intensity of synaptic puncta. We plotted the cumulative probability distribution of the amount of NMDAR staining at synaptic sites and found that knockdown of endogenous EphB2 caused a decrease in the amount of NR1 at synapses, whereas functional overexpression of EphB2 in the context of EphB2 knockdown resulted in a marked increase in synaptic NR1 (**Figure 5.1D**) [Kolmogorov–Smirnov (K-S) test, $p < 0.001$]. More specifically, EphB2

knockdown caused a preferential reduction in the number of synapses with large amounts of NR1. Conversely, functional overexpression of EphB2 resulted in a preferential increase in the number of synapses with smaller amounts of NR1. We next determined whether there were any differences between the effects of EphB2 manipulation on shaft and spine synapses. Analysis revealed that EphB2 knockdown or overexpression resulted in similar changes in the amount of NMDAR content at both shaft and spine synapses (**Figure 5.1E, F**) (K-S test, $p < 0.001$). Consistent with the role of EphB2 in control of dendritic spine shape in mature neurons, changes in the amount of NR1 at spine synapses were larger after EphB2 overexpression than the changes seen at shaft synapses. Together, these results suggest a role for EphB2 in directing or maintaining NMDARs at mature synapses.

To examine the functional significance of these immunohistochemical findings, we next measured spontaneous miniature EPSC (mEPSC) frequency in cultured cortical neurons at 21 DIV after endogenous EphB2 knockdown with or without expression of our EphB2 rescue construct at 14 DIV. As expected from previous work (Kayser et al., 2008), knockdown or functional overexpression of EphB2 at 14–21 DIV resulted in no change in mEPSC frequency (**Figure 5.2A, C**), confirming that EphBs are not likely to be important for the maintenance of overall excitatory synapse number in mature neurons. To determine whether modulation of EphB2 expression levels impacts synaptic receptor content, we studied mEPSC amplitude. To isolate glutamatergic mEPSCs, whole-cell patch-clamp recordings were conducted in $Mg^{2+}$-free solutions to increase NMDAR-

mediated currents in the presence of tetrodotoxin and blockers of GABAergic channels (see Materials and Methods). Although neither knockdown nor functional overexpression of EphB2 changed excitatory synapse number, functional overexpression of EphB2 did result in a significant increase in mEPSC amplitude (**Figure 5.2B, D, E**) (control, −15.45 ± 0.14 pA; EphB2, −22.79 ± 0.37; K-S test, $p < 0.001$). Similar changes in mEPSC amplitude were found in an independent series of experiments in which we overexpressed wild-type EphB2 without knockdown, in the presence of the endogenous protein (**Figure 5.3**). The small size of the NMDAR-dependent component of mEPSCs in cultured neurons (2–3 pA) prevents reliable isolation of this current alone. Therefore, to examine whether EphB-dependent changes in mEPSC amplitude are attributable to increased recruitment of NMDARs to synapses, we recorded from neurons in the presence or absence of the NMDAR antagonist APV (50–100 μm), applied via the bath perfusate. We found that NMDAR blockade significantly reduced mEPSC amplitude in all conditions (control, EphB2.1 shRNA, or functional EphB2 overexpression). To estimate the average NMDAR component of the mEPSC, we measured the difference between mean mEPSC amplitude before and after APV blockade. The estimated NMDAR component was 60% larger than control when EphB2 was functionally overexpressed [control, 3.13 pA; EphB2 overexpression (OE), 4.98 pA] (**Figure 5.2B, D**), indicating that the level of EphB2 expression might determine the amount of NMDARs at synapses. These findings were confirmed by cumulative probability histograms of mEPSC amplitude demonstrating that functional overexpression of EphB2 results in an

increase in the NMDAR-dependent component of mEPSCs (**Figure 5.2E**). Functional overexpression of EphB2 also appeared to increase the AMPAR-dependent component of mEPSCs, assessed by measuring mEPSCs in the presence of APV for all three conditions. These findings are consistent with previous work showing that EphB2 can regulate AMPAR retention in the recycling pool through its PDZ binding domain (Kayser et al., 2006). Although there appears to be a change in the AMPAR component, we focused on the role of EphB2 in the regulation of the NMDAR in this study because of the importance of this interaction in human disease (Cisse et al., 2011).

NMDARs contribute significantly to the decay component of synaptic currents, and thus measuring changes in these currents provides a sensitive measure for the presence of these channels at synapses. We found that, compared with controls, the average decay time (from peak to 30% amplitude) in neurons where EphB2 was functionally overexpressed was significantly longer, whereas knockdown of EphB2 resulted in a significant shortening of the average decay time. After blocking NMDARs with the antagonist APV, significantly shorter decay times were seen for all conditions (**Figure 5.3C**) (control, 5.88 ± 0.06 ms; control plus APV, 4.66 ± 0.05; EphB2.1 shRNA, 5.60 ± 0.06; EphB2.1 plus APV, 4.96 ± 0.06; functional EphB2 OE, 7.32 ± 0.10; functional EphB2 OE plus APV, 6.17 ± 0.08; ANOVA, $p < 0.001$). To further examine these data, we plotted cumulative probability distributions of the decay times for mEPSCs in control, knockdown, and functional overexpression conditions that represent all the measured decay times in our data set (**Figure 5.3D, E**). We found that before

blocking NMDARs with the antagonist APV, control and EphB2-overexpressing cells exhibit a larger proportion of mEPSCs with longer decay times, whereas EphB2 knockdown substantially reduces the fraction of events with longer decay times (**Figure 5.3C-E**). Specifically, in neurons expressing EphB2 shRNA, □5% of events have decay times of >10 ms; in control neurons, □10% fall into this group; in neurons overexpressing EphB2, □15% of events have decay times of >10 ms (**Figure 5.3D, E**). The difference between decay times in the control and EphB2 knockdown conditions were mostly eliminated by pharmacologic NMDAR blockade. Interestingly, the decay times of mEPSCs recorded from neurons functionally overexpressing EphB2 were longer than those of events in control or EphB2 knockdown neurons even in the presence of NMDAR blockade. These effects are most consistent with a change in AMPAR subunit composition at synapses, although additional work will be needed to determine whether this is the case. Regardless, our findings indicate that EphB2 expression levels might bidirectionally modulate the synaptic localization of NMDARs.

To further examine the role of EphB2 in the control of NMDAR trafficking, we recorded from neurons held at +50 mV to remove $Mg^{2+}$ voltage-dependent blockade of the NMDAR. In these experiments, we overexpressed EphB2 alone, without expression of shRNAs targeting EphB2. Consistent with our findings from functional overexpression of EphB2 in the presence of EphB2 shRNA (**Figure 5.2**), overexpression of EphB2 without knockdown resulted in a significant increase in mEPSC amplitude, whereas knockdown resulted in a reduction in mEPSC amplitude (control, 12.35 ± 0.23 pA, *n* = 957 events/9 neurons; EphB2

shRNA, 11.53 ± 0.19 pA, *n* = 1189/11; EphB2 OE, 15.44 ± 0.29 pA, *n* = 795/5; ANOVA, $p < 0.01$). To isolate the NMDAR component, neurons were held at +50 mV in the presence of TTX (1 μm), bicuculline (50 μm), and picrotoxin (10 μm). Using established methods (Myme et al., 2003), we examined the NMDAR component of mEPSCs by taking the average current 10–15 ms after the initial rise phase of each mEPSC (a time when the AMPAR-dependent current has already decayed). We found that knockdown of EphB2 resulted in a significant decrease in the NMDAR-dependent component of the mEPSCs, whereas overexpression of EphB2 resulted in a significant increase (**Figure 5.3F, G**) (control, 2.09 ± 0.13 pA, *n* = 368 events/6 cells; EphB2 shRNAi, 1.74 ± 0.11 pA, *n* = 744/11; OE, 2.83 ± 0.08 pA, *n* = 1247/9; ANOVA, $p < 0.01$). To test whether the effects of EphB2 overexpression might be linked to the recruitment of a specific NMDAR subunit, we treated neurons with an NR2B-selective NMDA receptor antagonist, Ro25-6981 (1–2 μm), and measured the percentage change in mEPSC amplitude. The NMDAR-dependent component of mEPSCs was reduced significantly (□25%) by the selective antagonist in neurons transfected with EphB2 compared with control transfected neurons (control, *n* = 5 cells; EphB2 OE, *n* = 5 cells; ANOVA, $p < 0.03$) (data not shown), suggesting that EphB2 overexpression increases the amount of NR2B-containing NMDARs found at synapses. We also conducted analysis of the decay times of mEPSCs recorded at +50 mV. Consistent with the effects observed at −65 mV, we found that EphB2 knockdown reduces the decay time, whereas overexpression of EphB2 causes a marked increase in the decay time of mEPSCs (control, 6.36 ±

0.19; EphB2.1 shRNA, 5.52 ± 0.14; EphB2 OE, 7.35 ± 0.16; ANOVA, $p < 0.001$) (data not shown). Together, our experiments demonstrate that, in mature neurons, EphB2 expression levels regulate the localization of NMDARs at synapses and their contribution to synaptic currents.

We investigated whether EphB signaling might modulate NMDAR function and localization in a subunit-specific manner. Activation of endogenous EphB receptors with soluble ephrin-B ligand results in an interaction between EphBs and NMDARs followed by phosphorylation of the NR2B subunit and increased NMDAR-dependent $Ca^{2+}$ influx (Takasu et al., 2002). The mechanism through which this increased calcium influx occurs is unknown. To both test whether this functional modification is subunit specific and determine the underlying mechanism, we coexpressed EphB2 with NR1-1a and either NR2A or NR2B subunits in HEK-293 cells (Zukin and Bennett, 1995). We examined whether the EphB–NMDAR interaction specifically alters NMDAR channel function by recording NMDA-evoked currents from transfected HEK-293 cells using the whole-cell patch-clamp method described in detail previously (Skeberdis et al., 2006; Zheng et al., 1997). Briefly, in control cells held at −60 mV, application of NMDA (300 μm) with glycine (10 μm) for 5 s by laminar flow elicited an inward current that rapidly declined to a steady-state value (Legendre et al., 1993; Skeberdis et al., 2006; Tong et al., 1995; Zheng et al., 1997; Zorumski et al., 1989). Measurements were made from the average of two to three trials per cell. In cells transfected with EphB2, NR1-1a, and NR2B, the peak amplitude was not significantly altered but the desensitization/inactivation in the NMDA response

was greatly reduced (**Figure 5.4A**). These effects required EphB kinase activity, as NMDAR currents in HEK-293 cells cotransfected with a kinase-dead form of EphB2 were normal. The absence of an effect with the kinase-dead mutant is not simply attributable to a disrupted interaction between EphB and NMDARs, as previous work has shown this mutant and the NMDAR still interact through their extracellular domains (Dalva et al., 2000). In cells transfected with EphB2, NR1-1a, and NR2A, we found no significant difference in NMDA-evoked currents compared with control cells transfected with only NR1 and NR2A (**Figure 5.4B**). These results suggest that EphB2 preferentially modulates desensitization/inactivation of NMDARs containing NR2B subunits, and that the enhanced $Ca^{2+}$ influx through NMDARs occurs by altering the kinetics of the channel in a kinase-dependent manner.

Activation of EphBs results in phosphorylation of the NR2B subunit at Y1472 (Takasu et al., 2002), which in turn controls the internalization and localization of NR2B-containing NMDARs (Chen and Roche, 2007; Lavezzari et al., 2003; Prybylowski et al., 2005). Given the subunit-specific modulation of $Ca^{2+}$ desensitization/inactivation in NR2B-containing NMDARs by EphB2, we examined whether EphB2 activation might preferentially control NR2B surface localization. We studied NMDAR subunit trafficking/localization with surface biotinylation experiments in cultured cortical neurons after treatment with control or activated ephrin-B2 at different times during development. Biotinylated surface proteins were pulled down and the fraction of the total protein labeled with biotin determined by Western blot analysis. Only samples lacking detectable actin in

the biotinylated fraction were included for additional analysis. We conducted these experiments at 7, 14, and 21 DIV—times when cultured cortical neurons have just entered a period of rapid EphB-dependent synapse addition (7 DIV), just ended the period of rapid synapse addition (14 DIV), or when synapses have matured (21 DIV) (Kayser et al., 2006). At each time point, NR2B was found on the cell surface under control conditions (**Figure 5.5**). We then asked whether 45 min to 1 h of ephrin-B2 treatment might alter the surface localization of the NMDAR. We compared the fraction of total NR2B with biotin before and after ephrin-B2 treatment. At 7 DIV, ephrin-B2 treatment failed to induce a significant increase in the surface localization of NR2B. In contrast, at 14 and 21 DIV, when EphB is no longer required for synapse addition or to maintain normal numbers of functional synapses, ephrin-B2 treatment induced a significant increase in NR2B surface expression (**Figure 5.5**). These results show that activation of EphB2 increases NR2B on the cell surface of neurons and confirm that EphB2 undergoes an age-dependent change in the control of NR2B trafficking.

To determine whether EphB also controls the localization of specific NMDAR subunits in organized neural tissue, we examined the surface expression of the NMDAR in acute brain slices from TKO mice lacking EphB1–3. We chose to examine TKO animals because the presence of any EphB family members often masks the effects of genetic loss of one or two EphBs {Henkemeyer, 2003 #32; Kayser, 2006 #7. Indeed, throughout our experiments, we failed to detect effects on NMDAR localization in DKO mice lacking EphB1 and 3, which maintain normal EphB2 function (**Figures 5.6-5.9**). To investigate if

the trafficking and localization of NMDARs is disrupted after the loss of EphB expression, we made hippocampal or cortical brain slices from wild-type, DKO, or TKO mice. The brain slices were then incubated live with Sulfo-NHS-SS-biotin (Pierce Protein Research Products; Thermo Fisher Scientific) on ice, and tissue was processed to determine the surface fraction of the NMDAR using methods similar to those for the cultured cortical neurons.

Cortical and hippocampal brain slices were collected and labeled in parallel. Surprisingly, surface and total expression of the NR2B subunit of the NMDAR was increased significantly in TKO mice compared with controls (**Figure 5.6A, E-G**). NR2A and NR1 expression were unchanged in cortex in the absence of EphBs, although the variability in this data set was large for NR1 (**Figure 5.6A-D, Figure 5.8**). These findings were not mirrored in hippocampus, where total NR2A levels were reduced and surface NR2B increased in TKO compared with WT (**Figure 5.7**); surface levels of NR1 were also significantly reduced in hippocampus of TKO mice (**Figure 5.8**). These effects suggest that the role of EphBs may differ between different brain regions and that the interaction between EphBs and NMDARs is more complex than simple recruitment or retention of NMDARs on the cell surface, in which case we would expect NR2B surface localization to be decreased in the absence of EphBs.

One possible explanation for the paradoxical increase in NR2B total and surface expression in the absence EphBs is that homeostatic mechanisms lead to upregulated expression and surface delivery because of a specific deficiency of NR2B at synapses. EphBs are localized to the postsynaptic complex at mature

synapses, and we have shown that increased expression or activation of EphB2 increases the amount of NR2B on the cell surface and NMDARs at the synapse *in vitro* (**Figures 5.1-5.3**). Thus, we tested whether EphBs might help to direct NMDARs to synaptic sites *in vivo*. Using fractionation experiments, we compared the normalized amount of NMDAR found in the crude membrane fraction (P1) and at synaptosomes (Syn) from EphB DKO, TKO, and control WT mice by quantifying the amount of specific proteins by Western blot. The P1 fraction is enriched for all membranes, whereas the synaptosomal fraction is enriched for synaptic components. As expected, synaptic proteins such as NR1, GluR1, PSD-95, and EphB2 were enriched in the Syn versus the P1 fraction from WT mice (**Figure 5.9A**). We then asked whether loss of the EphB proteins would disrupt the synaptic localization of the NMDAR. In the DKO mice lacking EphB1 and 3, NR2B expression and synaptic localization did not differ from wild-type animals, and we did not detect changes in the other synaptic proteins examined. However, TKO brains showed a significant decrease in the fraction of NR2B subunits at synapses (**Figure 5.9A, D**). Interestingly, there was also reduced localization of NR2A subunits at synapses in TKO brains (**Figure 5.9A, C**). Consistent with the direct nature of the EphB–NMDAR interaction, the loss of EphBs did not alter the localization of other synaptic components such as PSD-95 and GluR2 (**Figure 5.9A, E**). Together with the biotinylation experiments, these findings suggest that EphBs direct the NR2B subunit to synaptic sites, and in the absence of EphBs, neurons unsuccessfully attempt to compensate,

resulting in increased overall expression and nonsynaptic surface expression of the NR2B subunit.

## Discussion

Multiple mechanisms contribute to the tightly regulated yet dynamic control of NMDAR trafficking. Here, we provide evidence that the EphB2 receptor tyrosine kinase is also an important regulator of synaptic NMDAR localization, but preferentially at mature contacts. Our results indicate that expression levels of EphB2 in mature cells can determine NMDAR content at synapses without impacting synapse number. We also find that EphB2 kinase activity specifically reduces the temporal decline of the NR2B subunit-mediated currents, resulting in prolonged currents and increased $Ca^{2+}$ influx. In the absence of EphBs, total NR2B abundance and surface NR2B expression is increased, whereas synaptic expression is decreased, indicating mistargeting of this subunit without EphB signaling. These findings extend previous work demonstrating that EphB2 binds, clusters, and increases $Ca^{2+}$ flux through NMDARs in young neurons {Dalva, 2000 #9; Takasu, 2002 #8}, and suggest that the EphB–NMDAR interaction is significant throughout multiple phases of development and particularly in the mature brain.

We find an age-dependent change in how EphBs modulate NMDAR activity. Early in development, EphBs are essential for the formation of normal numbers of excitatory synaptic connections made on dendritic spines (Kayser et al., 2008). During this time period, activation of EphB does not appear to increase recruitment of NR2B subunits to the cell surface. As neurons mature, EphBs are no longer required to maintain normal numbers of functional excitatory synapses but function to control the number of NMDARs localized to synaptic

sites. These results begin to answer the question posed by *in vitro* work indicating distinct mechanisms of NMDAR recruitment at differing neuronal ages (Bresler et al., 2004; Washbourne et al., 2002). Moreover, our data indicate that EphB specifically regulates trafficking of NR2B subunits in mature neurons, although our results do not exclude the possibility that EphBs play some role in NR1 and NR2A localization as well. Localization of the NR2B subunit of the NMDAR is of particular interest, as the proportion of NR2B-containing receptors can affect NMDAR channel open time and $Ca^{2+}$ flux. Recent work has shown that phosphorylation of NR2B by casein kinase 2 (CK2) at a distinct site from EphB-dependent phosphorylation leads to NR2B endocytosis and increased NR2A expression (Sanz-Clemente et al.). The interplay between CK2 and EphB2 activity on NR2B, leading to endocytosis or retention, respectively, would be a sensitive mechanism for determining NR2B content at synapses. Functional consequences of increased NR2B content at synapses in certain areas of brain are known to include improved performance on memory tasks and enhanced visuocortical plasticity (Philpot et al., 2007; Tang et al., 1999). During normal development, the ratio of NR2A/NR2B at synapses increases over time ((Sheng et al., 1994), raising the threshold for long-lasting changes in synaptic strength in response to external stimuli (Philpot et al., 2007). Given that EphBs serve to drive NR2B into synapses only later in development, one interpretation of our data is that EphBs define mature synapses with a relatively low NR2A/NR2B ratio. These inputs would remain more plastic in the adult brain, with a lower threshold for long-term potentiation (LTP). Consistent with this role for EphBs in

maintaining or generating plastic synapses, EphB2 knock-out mice have reduced LTP, long-term depression (LTD), and quality of performance in the Morris water maze (Grunwald et al., 2001; Henderson et al., 2001). Although one feature of mature neurons by virtue of a higher NR2A/NR2B ratio is an increased selectivity for specific stimuli, it is clear that, even in the adult CNS, some inputs remain remarkably malleable (Holtmaat and Svoboda, 2009). Future work will need to specifically examine whether and how EphBs contribute to this sustained plasticity.

Two likely mechanisms mediating EphB-dependent control of synaptic localization of NMDARs are the direct EphB–NMDAR interaction and EphB-dependent phosphorylation of NR2B. We showed previously that ephrin-B activation of EphB2 results in the direct interaction of the NMDAR with EphB2 and the phosphorylation of three tyrosine residues on the NMDAR (Dalva et al., 2000; Takasu et al., 2002). One of the phosphorylated residues, Y1472, has since been shown to be important for the synaptic localization and retention of NMDARs, acting to prevent binding of AP-2 that in turn targets proteins for internalization by clathrin-mediated endocytosis (Chen and Roche, 2007; Lavezzari et al., 2003). Notably, there is a significant reduction in the level of NR2B phosphorylated at Y1472 found at synapses in EphB TKO brains compared with controls (data not shown). Although the magnitude of this change is matched by the decrease in total NR2B at synapses in TKOs, these data are consistent with a model in which EphB2 regulates retention of the NMDAR at synapses by phosphorylating the NR2B subunit at Y1472. In the absence of

EphBs, more NR2B is endocytosed, triggering the homeostatic drive of neurons to deliver more NR2B to synapses. This drive appears to fail in the absence of EphBs, as NR2B total and surface expression increase without effective synaptic delivery. Thus, the EphB–NMDAR interaction likely has a role in synaptic targeting of NMDARs in addition to retention. The loss of EphBs also results in decreased NR2A at synapses. This effect could be attributable to the direct interaction between EphB2 and the NMDAR or to the previously described phosphorylation of the NR2A subunit. Importantly, we cannot rule out a role for the direct EphB–NMDAR interaction in the synaptic localization of the NMDAR. In fact, the EphB–NMDAR interaction is likely to be central to the ability of EphB2 to specifically phosphorylate NR2 subunits, making it difficult to distinguish effects of the physical interaction and kinase activation.

Although EphBs are important for the proper localization of NMDARs to synapses, they are not essential for all NMDARs to localize properly, nor for all facets of NR2B trafficking. These conclusions are consistent with the observation that EphBs direct formation of a subset of excitatory synapses (Kayser et al., 2006) and our new findings that EphBs control a substantial fraction (□50%) of NMDAR localization to mature contacts. Although additional research is needed to characterize the significance of this subpopulation, loss of EphB2 causes abnormal LTP and LTD in mouse hippocampus (Grunwald et al., 2001; Henderson et al., 2001), suggesting a functionally important role. Other proteins are undoubtedly required in these events as well, however, and synaptic transmission still occurs. For example, neuroligins (NLGs) cluster NMDARs and

signal to regulate excitatory synapse maturation (Chih et al., 2005; Graf et al., 2004); more recent work suggests that loss of NLG1 results in reduced NMDAR expression and NMDAR-mediated synaptic transmission in hippocampus (Chubykin et al., 2007). These findings are similar to those for EphBs and suggest that both EphBs and NLGs, and very likely others, impact NMDAR localization at synaptic sites.

In addition to the effects that we observe on NMDAR localization and function, our analysis of mEPSCs reveals a change in the AMPAR-dependent component of synaptic currents (**Figures 5.2, 5.3**). This finding is consistent with previous work showing that EphB2 activation can increase the surface localization of the AMPAR via PDZ domain-dependent interactions (Irie et al., 2005; Kayser et al., 2006). However, our biotinylation and fractionation experiments in EphB TKO mice failed to detect changes in the localization of the GluR2 subunit of the AMPAR compared with controls. Thus, it appears possible that, although EphB2 overexpression results in increased AMPAR-dependent currents at synapses, mice lacking EphBs fail to show changes in the synaptic localization of GluR2. EphBs are therefore unlikely to regulate AMPAR function by simply controlling the overall amount of AMPARs at synapses. EphB2 associates with AMPAR-interacting proteins PICK1 and GRIP (Torres et al., 1998), which are important for trafficking of specific AMPAR subunits to synapses (Gardner et al., 2005; Liu and Cull-Candy, 2005). As with NMDARs, different AMPAR subunit combinations confer distinct channel properties (Greger and Esteban, 2007; Isaac et al., 2007). Thus, one interesting possibility is that

the EphB2-dependent changes in AMPAR current we observe (**Figures 5.2, 5.3**) are attributable to modulation of AMPAR subunit ratios at synapses rather than changes in overall AMPAR content. Additional work will be needed to determine the mechanisms by which EphBs regulate AMPAR synaptic currents.

In addition to their role in the localization of NMDARs, EphBs modulate NMDAR-mediated calcium flux through Src family kinase-dependent phosphorylation of NR2B. This enhanced calcium influx is likely mediated by a reduction in the rate of calcium-dependent inactivation in NMDAR channels that contain the NR2B subunit, although in our current analysis we cannot rule out a role for glycine-independent desensitization. Importantly, the effects of EphB2 appear selective for NR2B, as a similar change in time course is not found in NMDAR channels containing the NR2A subunit. Yet previous work has suggested that ephrin-B activation of EphB may increase tyrosine phosphorylation of not only NR2B subunits but also NR2A subunits (Grunwald et al., 2001; Takasu et al., 2002). The functional significance of EphB2/NR2A interactions has yet to be extensively examined, but given that EphB2 does bind to NR2A (Dalva et al., 2000), future investigation into whether EphBs modulate NR2A function will be of interest.

The expression level of EphBs has recently been shown to be downregulated in models of Alzheimer's disease (Simon et al., 2009), and phosphorylation of NMDARs is reduced in brains of Alzheimer's disease patients relative to controls (Sze et al., 2001). One intriguing possibility is that the late function of EphBs in synaptic localization of NMDARs may be relevant to

neurodegenerative diseases. Consistent with this hypothesis, both ephrin-Bs and EphBs undergo posttranslational modification via γ-secretase activity (Litterst et al., 2007; Tomita et al., 2006), and overexpression of EphB2 has recently been shown to rescue cognitive defects in a mouse model of Alzheimer's disease (Cisse et al., 2011). Additional work will be needed to determine how EphBs and their ligands are linked to Alzheimer's and other diseases, but the recruitment to and modulation of NMDARs at synapses is likely a key part of any potential role.

**Acknowledgements:**

Drs. Nolt, Lin, Hruska and Murphy, and Mr. Sheffler-Collins designed and carried out experiments and analyzed data; Drs. Kayser, Bennett and Zukin designed experiments and wrote the paper; Mr. Joel Passer carried out experiments; and Dr. Dalva designed and carried out experiments, analyzed data and wrote the paper. Dr. Lin was supported by postdoctoral fellowship from International Rett Syndrome Foundation. Mr. Sheffler-Collins was supported by the Vision Training Grant (EY007035). Dr. Bennett is the Sylvia and Robert S. Olnick Professor of Neuroscience and Distinguished Professor and is supported by NIH grant NS45287. Dr. Zukin is the F.M. Kirby Professor in Neural Repair and Protection and NIH grant NS46742 and a generous grant from the F.M. Kirby Foundation supported this work. NIH grants from NIDA (DA022727) and the NIMH (MH086425) and a grant from the Dana Foundation to Dr. Dalva supported this work.

**Figure Legends.**

**Figure 5.1. EphB2 regulates localization of NMDAR receptors to synapses in mature cortical neurons.** *A–C*, Confocal microscopy maximum projection images of cultured cortical neurons at 21 DIV expressing eGFP and shRNA vector (control), EphB2.1 shRNA, or EphB2.1 shRNA plus "rescue" EphB2 (functional EphB2 OE), immunostained for GFP (green), NR1 (red), and the presynaptic marker vGlut (blue). The magnified sections (top) of high-contrast image with arrows show spine (yellow arrows) and shaft (white arrows) synapses, defined as the locations where NR1, GFP, and vGlut immunostaining colocalize. The bottom panels show same region with anti-NR1 staining in red. *D–F*, Cumulative probability histograms of synaptic NR1, NR1 at spine synapses, and NR1 at shaft synapses. Functional EphB2 OE using a rescue construct in the context of endogenous EphB2 knockdown caused a significant increase in the amount of NR1 colocalizing with vGlut, whereas knockdown of EphB2 resulted in a decrease (Kolmogorov–Smirnov test, $p < 0.001$). Amount of NR1 for each condition is normalized to the maximum intensity observed from all three conditions. Control, $n$ = 27 cells, 432 synapses; EphB2.1 shRNA, $n$ = 27, 359; functional EphB2 OE, $n$ = 21, 319.

**Figure 5.2. EphB2 expression regulates mEPSC amplitude but not frequency in mature cortical neurons.** Whole-cell patch-clamp recordings were made from 21–23 DIV cultured rat cortical neurons expressing eGFP and

shRNAi vector (control; blue), EphB2 shRNA (EphB2.1 shRNA; red), or EphB2.1 shRNA plus “rescue” EphB2 (functional EphB2 OE; green). Recordings were at −65 mV in $Mg^{2+}$-free solution. *A*, Example whole-cell patch-clamp recordings from cortical neurons in each condition; functional EphB2 OE neurons (row 3) show occasional miniature synaptic events at higher amplitude (left) that are blocked by the NMDAR antagonist APV (right). *B*, Mean traces of mEPSCs after NMDAR blockade with APV. Control: $n = 5$ cells without APV, 2298 mEPSCs; $n = 5$ cells with APV, 2490 mEPSCs; EphB2 shRNA: $n = 5$ cells without APV, 2528 mEPSCs; $n = 5$ cells with APV, 2040 mEPSCs. Functional EphB2 OE: $n = 3$ cells without APV, 1037 mEPSCs; $n = 3$ cells with APV, 1052 mEPSCs. *C*, No change in mEPSC frequency was observed for any condition (ANOVA, $p > 0.05$). *D*, Quantification of mean mEPSC amplitude before and after application of 50–100 μm APV. An increase in mEPSC amplitude was observed with functional overexpression of EphB2, whereas NMDAR blockade with APV significantly reduced mEPSC amplitude for all conditions (ANOVA, $*p < 0.01$, $**p < 0.001$). *E*, Cumulative probability histograms of mEPSC amplitude for each condition. Error bars indicate SEM.

**Figure 5.3. EphB2 regulates synaptic localization of functional NMDARs in mature cortical neurons.** Whole-cell patch-clamp recordings were made from 21–23 DIV cultured rat cortical neurons expressing eGFP and shRNA vector (control; blue), EphB2 shRNA (EphB2.1 shRNA; red), or EphB2 shRNA plus “rescue” EphB2 (functional EphB2 OE; green) (*A*–*E*). *A*, Mean traces of EPSCs

for each condition. *B*, Sample trace of whole-cell patch-clamp recording illustrating decay time. Decay time was calculated as the time from peak amplitude of the current to 30% of the peak amplitude, indicated by the arrows. *C*, Quantification of average decay time for each condition. *D*, *E*, Cumulative probability histograms of mEPSC decay times for each condition, plotted together (*D*) and individually for clarity (*E*). Control/EphB2.1 shRNA, $p < 0.05$; EphB2.1 shRNA/functional EphB2 OE, $p < 0.0001$; without APV/with APV, $p < 0.0001$ for all conditions; control with APV/functional EphB2 OE with APV, $p < 0.0001$; EphB2.1 shRNA with APV/functional EphB2 OE with APV, $p < 0.0001$; K-S tests; *N* as in Figure 5.1. These findings indicate that the slow NMDAR component of mEPSCs is reduced by EphB2 knockdown (EphB2.1 shRNA) and increased when EphB2 is functionally overexpressed (EphB2.1 shRNA plus "rescue" EphB2). *F*, Whole-cell patch-clamp recordings were made from 21–23 DIV cultured rat cortical neurons expressing eGFP and vector (control; blue), EphB2.1 shRNA (red), or EphB2 (EphB2 OE; green). Normalized amplitude plot of the mean mEPSCs recorded at +50 mV in control, EphB2 shRNA, and EphB2 OE neurons. *G*, Quantification of NMDAR component of the mEPSCs recorded at +50 mV in the presence of $Mg^{2+}$ (control, $n = 368$ events/6 cells; EphB2 shRNAi, $n = 744/11$; EphB2 OE, $n = 1247/9$). $^{*}p < 0.05$, $^{**}p < 0.001$, ANOVA. Error bars indicate SEM.

**Figure 5.4. EphB2 attenuates $Ca^{2+}$-dependent desensitization of NR2B- but not NR2A-containing NMDARs.** *A*, Top, NMDA-elicited currents recorded from

HEK-293 cells expressing NR1-1a/NR2B receptors in the absence (left) or presence of EphB2 (center), or the kinase-dead mutant EphB2-KD (right). Recordings at −60 mV in $Mg^{2+}$-free solution. Bottom, Summary data showing peak current, steady-state current, and $Ca^{2+}$-dependent desensitization of NMDA current (quantified as 1 − steady-state current/peak current × 100) (*n* = 8, 9, and 7 for cells in the absence of cotransfected EphB2, presence of EphB2, or EphB2-KD, respectively). *B*, Top, NMDA-elicited currents recorded from HEK-293 cells expressing NR1-1a/NR2A receptors in the absence (left) or presence (right) of EphB2. Bottom, Summary data showing peak current, steady-state current, and $Ca^{2+}$-dependent desensitization of NMDA current [*n* = 10 and 8 cells (3 independent experiments) in the absence or presence of EphB2, respectively]. **p* < 0.05, ***p* < 0.01. Error bars indicate SEM.

**Figure 5.5. Ephrin-B2 activation of EphB2 increases NR2B surface localization.** *A*–*C*, Cortical neurons at 7 DIV (*A*), 14 DIV (*B*), or 21 DIV (*C*) were treated for 45 min with control Fc (*C*) or activated ephrin-B2-Fc (eB2). Biotinylated (surface) and total NR2B protein was visualized by immunoblotting with specific antibodies (top gels). β-Actin was used as a loading control for total protein (bottom gels). Absence of actin in surface (biotinylated) gels indicates validity of surface labeling. Representative immunoblots show no actin immunolabeling in the biotinylated surface fraction. The bottom bar graphs show the ratio of amount of surface NR2B to total NR2B at 7 DIV (*n* = 5 experiments), 14 DIV (*n* = 6 experiments), or 21 DIV (*n* = 6 experiments). Ephrin-B2-Fc versus

Fc (control) conditions were analyzed by an unpaired *t* test. **p* < 0.05. Error bars indicate SEM.

**Figure 5.6. Surface and total NR2B expression levels are increased in the cortex of EphB1$^{-/-}$, 2$^{-/-}$, 3$^{-/-}$ TKO mice.** *A*, Representative Western blots depicting NR2A and NR2B surface expression (left) and total expression (right) in WT, EphB1$^{-/-}$, 3$^{-/-}$ DKO, and TKO mice. *B*–*D*, Quantification of NR2A surface, total, and surface/total expression. *E*–*G*, Quantification of NR2B surface, total, and surface/total expression. Values were normalized to DKO (*n* = 6, 9, and 7 animals for WT, DKO, and TKO, respectively). **p* < 0.05, ***p* < 0.01. Error bars indicate SEM.

**Figure 5.7. NR2B surface expression is increased and total NR2A levels are decreased in the hippocampus of TKO mice.** *A*, Left, Representative Western blots depicting NR2A and NR2B surface expression in WT, EphB DKO, and EphB TKO mice. Right, Western blots showing total expression of NR2A and NR2B in WT, EphB DKO, and EphB TKO mice. Actin was used as a loading control in total protein fraction and as a control for surface staining in surface fraction. *B*, Quantification of NR2A and NR2B surface, total, and surface/total expression. Values are normalized to DKO (*n* = 6, 9, and 7 animals for WT, DKO, and TKO, respectively). **p* < 0.05, ***p* < 0.01, ANOVA. Error bars indicate SEM.

**Figure 5.8. NR1 surface expression is decreased in hippocampus of TKO mice.** Top left, Western blot illustrating surface and total NR1 expression in cortex of WT, EphB DKO, and EphB TKO mice. Top right, Western blot depicting surface and total NR1 levels in hippocampus of WT, EphB DKO, and EphB TKO mice. Actin is shown as a loading control in total protein fraction and as a control for surface staining in surface fraction. Below, Quantification of NR1 surface, total, and surface/total levels in cortex and hippocampus of WT, EphB DKO, and EphB TKO mice. Values are normalized to WT ($n$ = 2 animals each for WT, DKO, and TKO, samples were then divided and labeled with two independent reactions). *$p < 0.05$, ANOVA. Error bars indicate SEM.

**Figure 5.9. EphB TKO brains exhibit reduced synaptic expression of NR2A and NR2B.** *A*, Lysates from brains of WT, EphB DKO, and EphB TKO animals were fractionated to isolate supernatant (S1), crude membrane (P1), and pure synaptosome (Syn) fractions. Western blots were probed with indicated antibodies and show enrichment of glutamate receptor subunits in the synaptosome fraction of all animals. PSD-95 and EphB2 are enriched in the same fraction. *B*–*E*, Syn/P1 ratio was used to compare synaptic versus nonsynaptic expression of NMDA and GluR2 glutamate receptors subunits. Compared with the WT and EphB DKO brains, EphB TKO animals exhibit reduced synaptic expression of NR2A (*C*) and NR2B (*D*) subunits of the NMDAR. There is no change in synaptic expression the GluR2 subunit (*E*) of AMPA

receptors between different genotypes. ANOVA, *$p < 0.005$; $n = 3$ animals for each condition. Error bars indicate SEM.

# Figure 5.1

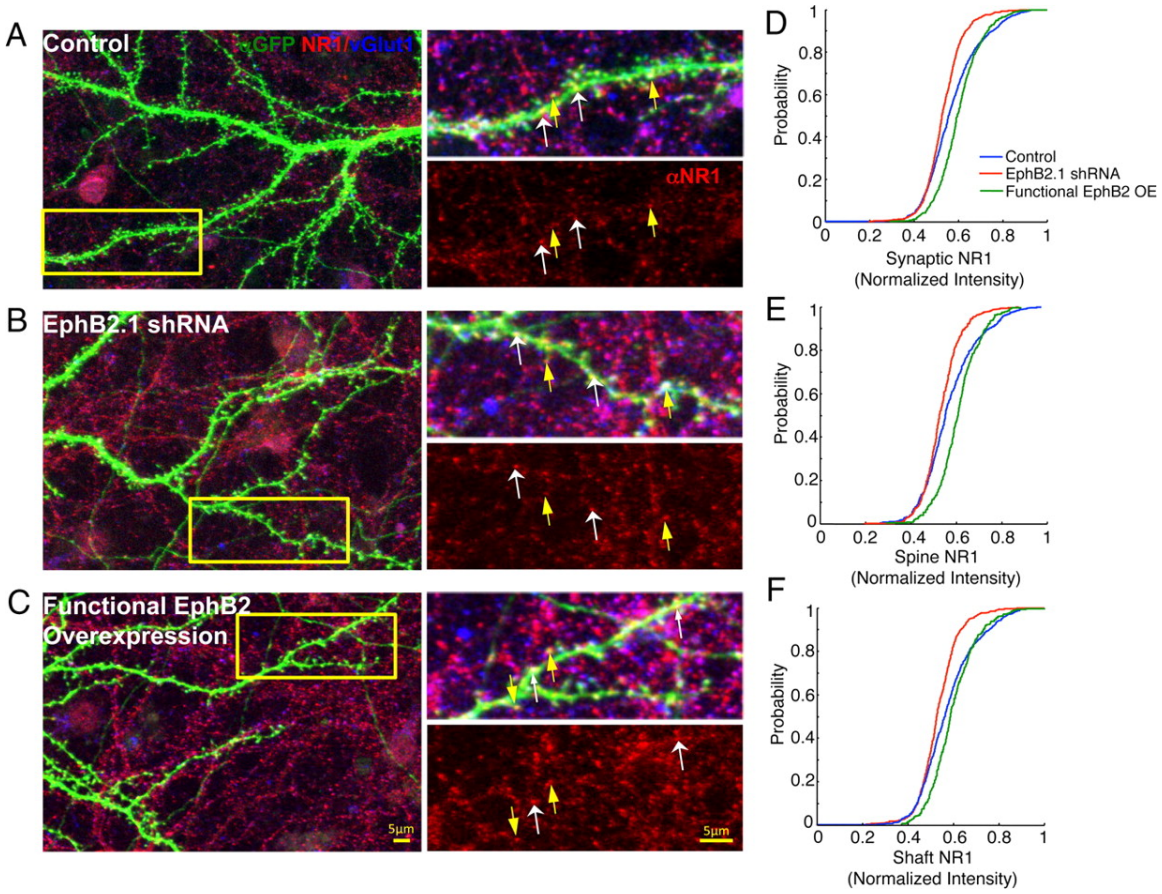
A
Control
αGFP NR1/αGlut1
αNR1
B
EphB2.1 shRNA
C
Functional EphB2
Overexpression
5μm
5μm
D
Probability
Synaptic NR1
(Normalized Intensity)
Control
EphB2.1 shRNA
Functional EphB2 OE
E
Probability
Spine NR1
(Normalized Intensity)
F
Probability
Shaft NR1
(Normalized Intensity)

# Figure 5.2

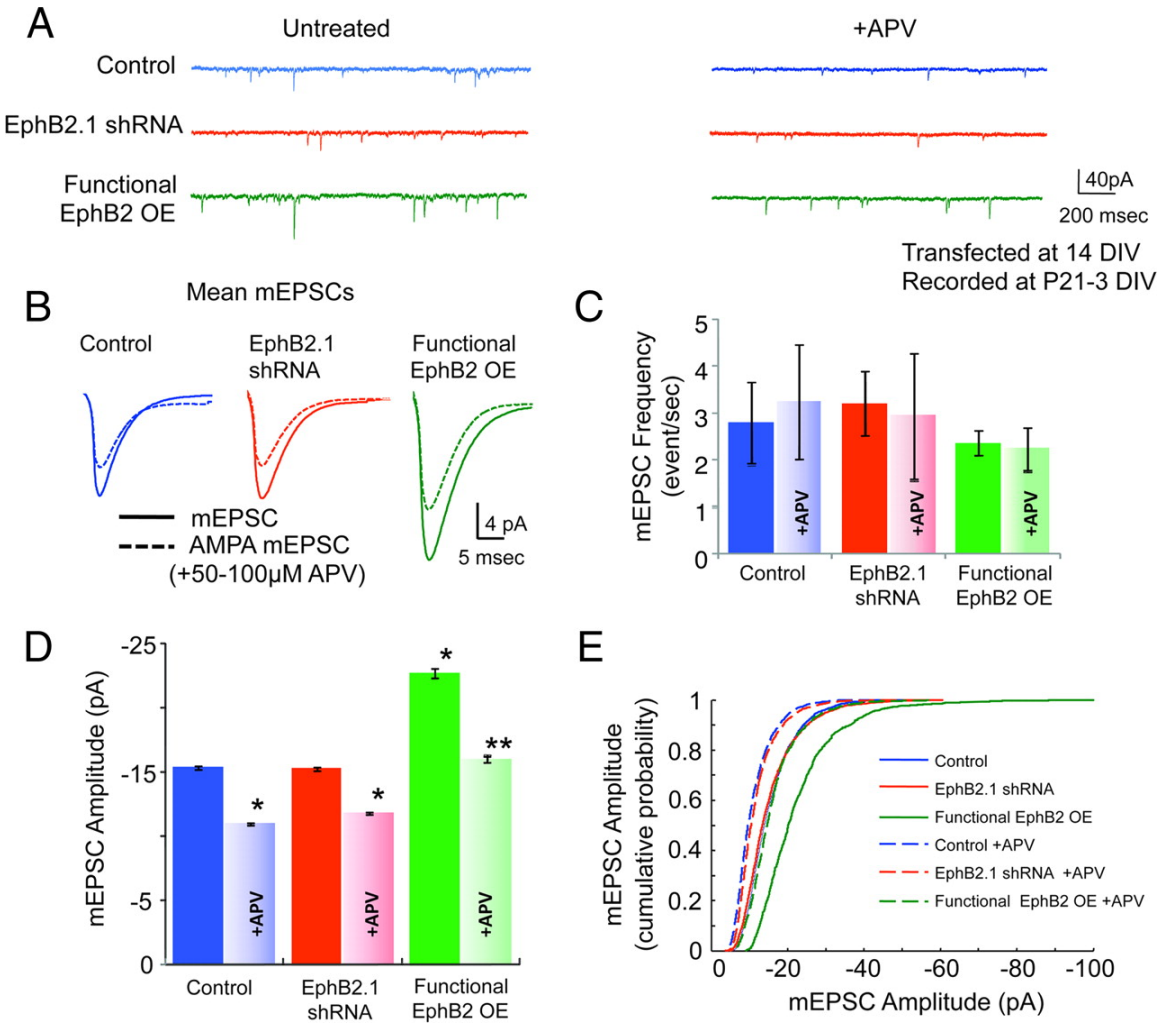
A
Untreated
+APV
Control
EphB2.1 shRNA
Functional EphB2 OE
40pA
200 msec
Transfected at 14 DIV
Recorded at P21-3 DIV
B
Mean mEPSCs
Control
EphB2.1 shRNA
Functional EphB2 OE
mEPSC
AMPA mEPSC
(+50-100μM APV)
4 pA
5 msec
C
mEPSC Frequency (event/sec)
+APV
Control
EphB2.1 shRNA
Functional EphB2 OE
D
mEPSC Amplitude (pA)
+APV
Control
EphB2.1 shRNA
Functional EphB2 OE
E
mEPSC Amplitude (cumulative probability)
Control
EphB2.1 shRNA
Functional EphB2 OE
Control +APV
EphB2.1 shRNA +APV
Functional EphB2 OE +APV
mEPSC Amplitude (pA)

## Figure 5.3

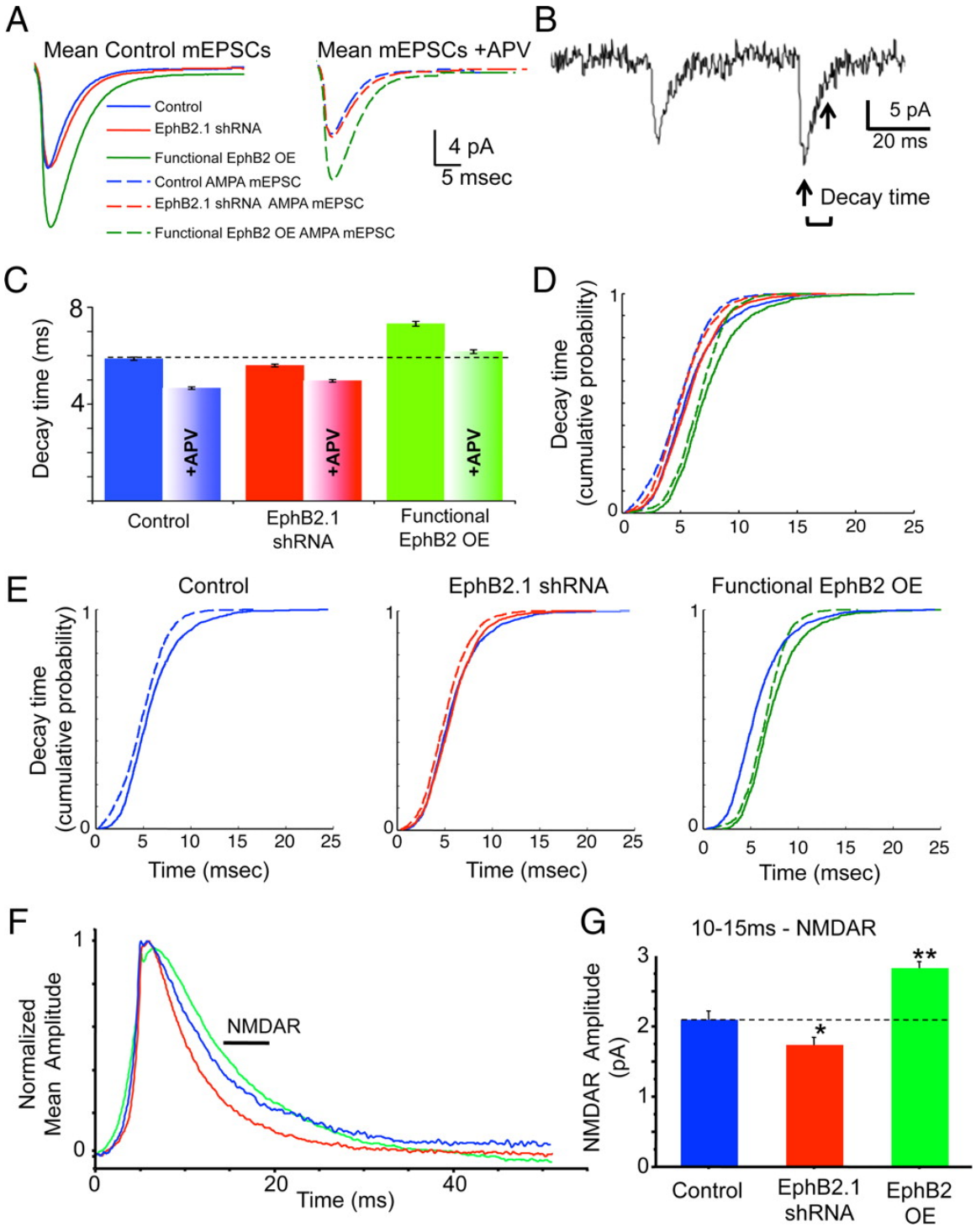
A
Mean Control mEPSCs
Mean mEPSCs +APV
Control
EphB2.1 shRNA
Functional EphB2 OE
Control AMPA mEPSC
EphB2.1 shRNA AMPA mEPSC
Functional EphB2 OE AMPA mEPSC
4 pA
5 msec
B
5 pA
20 ms
Decay time
C
Decay time (ms)
+APV
Control
EphB2.1 shRNA
Functional EphB2 OE
D
Decay time (cumulative probability)
E
Control
EphB2.1 shRNA
Functional EphB2 OE
Decay time (cumulative probability)
Time (msec)
F
Normalized Mean Amplitude
NMDAR
Time (ms)
G
10-15ms - NMDAR
NMDAR Amplitude (pA)
Control
EphB2.1 shRNA
EphB2 OE

## Figure 5.4

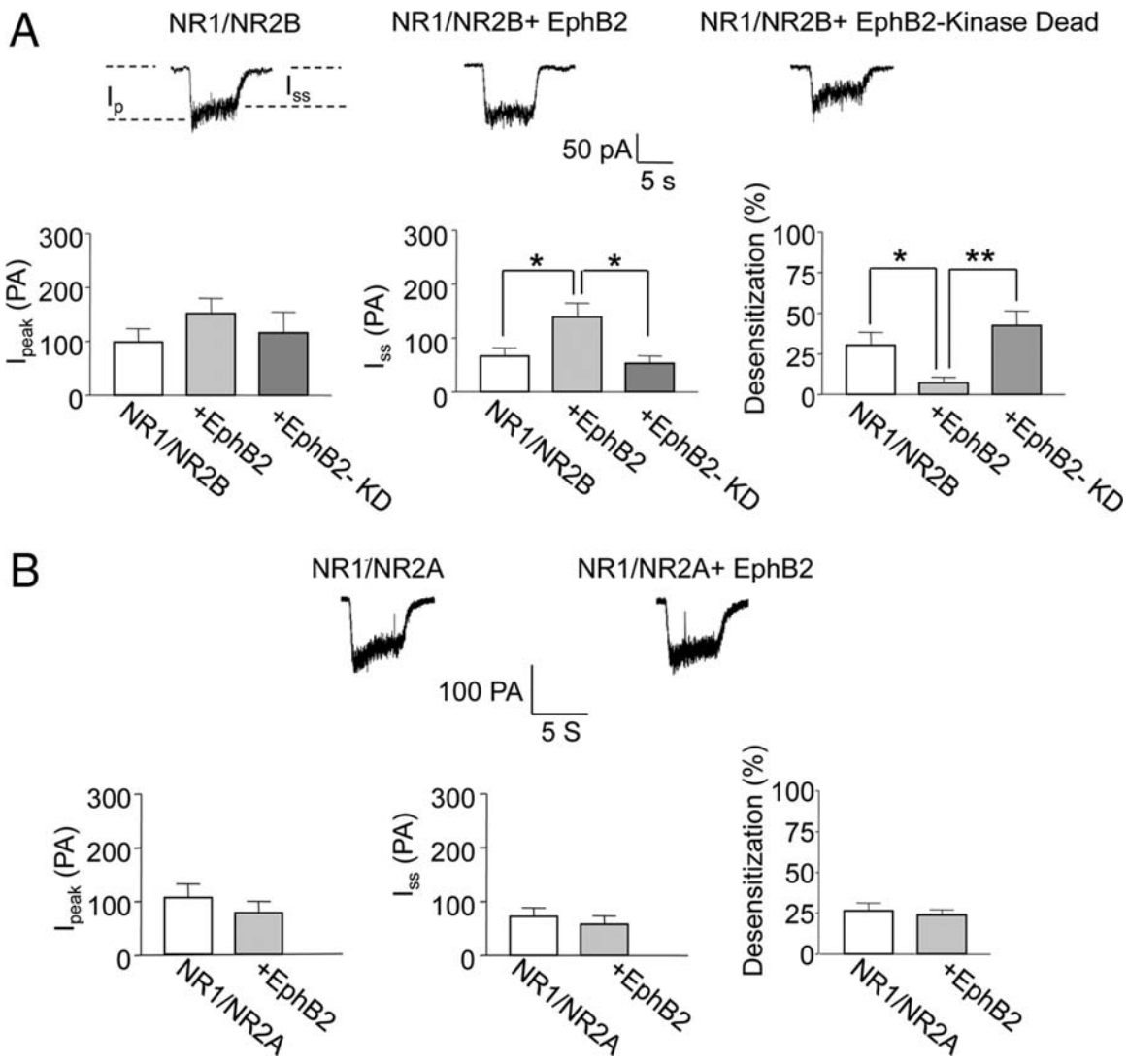
A
NR1/NR2B
NR1/NR2B+ EphB2
NR1/NR2B+ EphB2-Kinase Dead
$I_p$
$I_{ss}$
50 pA
5 s
$I_{peak}$ (PA)
$I_{ss}$ (PA)
Desensitization (%)
300
200
100
0
100
75
50
25
0
*
*
*
**
NR1/NR2B
+EphB2
+EphB2- KD
B
NR1/NR2A
NR1/NR2A+ EphB2
100 PA
5 S
$I_{peak}$ (PA)
$I_{ss}$ (PA)
Desensitization (%)
NR1/NR2A
+EphB2

## Figure 5.5

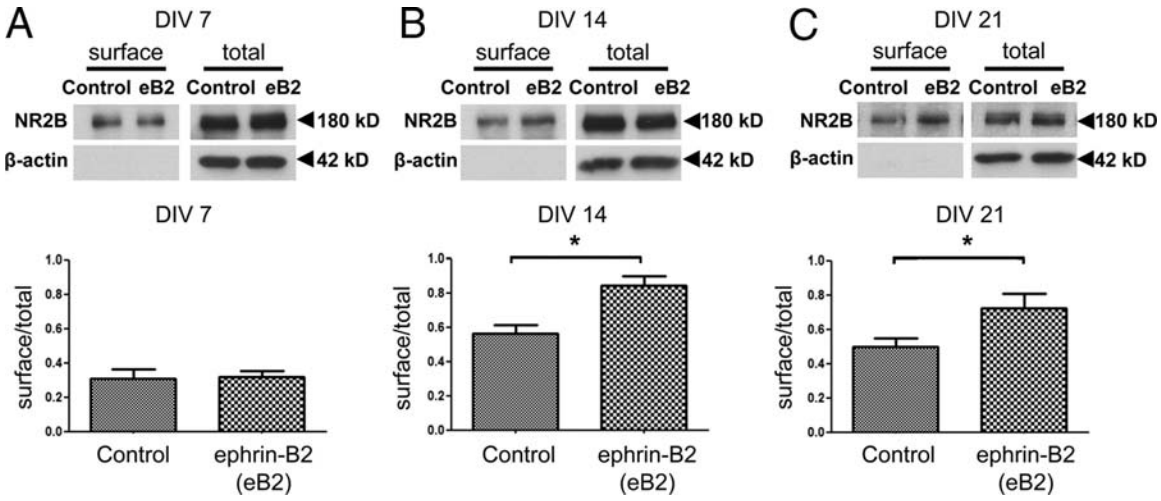
A
DIV 7
surface
total
Control eB2 Control eB2
NR2B
β-actin
180 kD
42 kD
B
DIV 14
C
DIV 21
DIV 7
DIV 14
DIV 21
surface/total
*
Control
ephrin-B2
(eB2)

## Figure 5.6

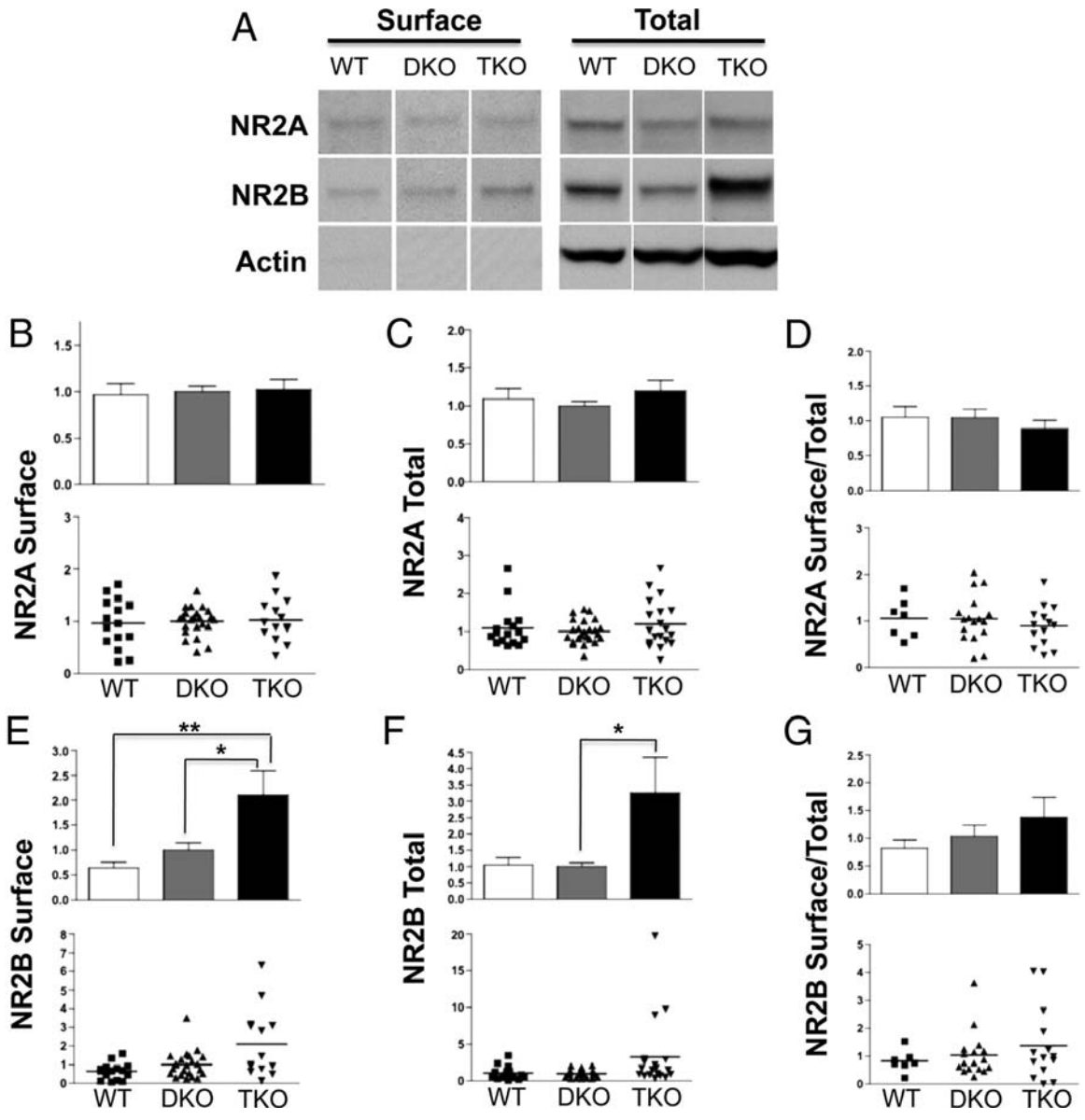
A
Surface
Total
WT
DKO
TKO
WT
DKO
TKO
NR2A
NR2B
Actin
B
NR2A Surface
C
NR2A Total
D
NR2A Surface/Total
E
NR2B Surface
F
NR2B Total
G
NR2B Surface/Total
**
*
*

## Figure 5.7

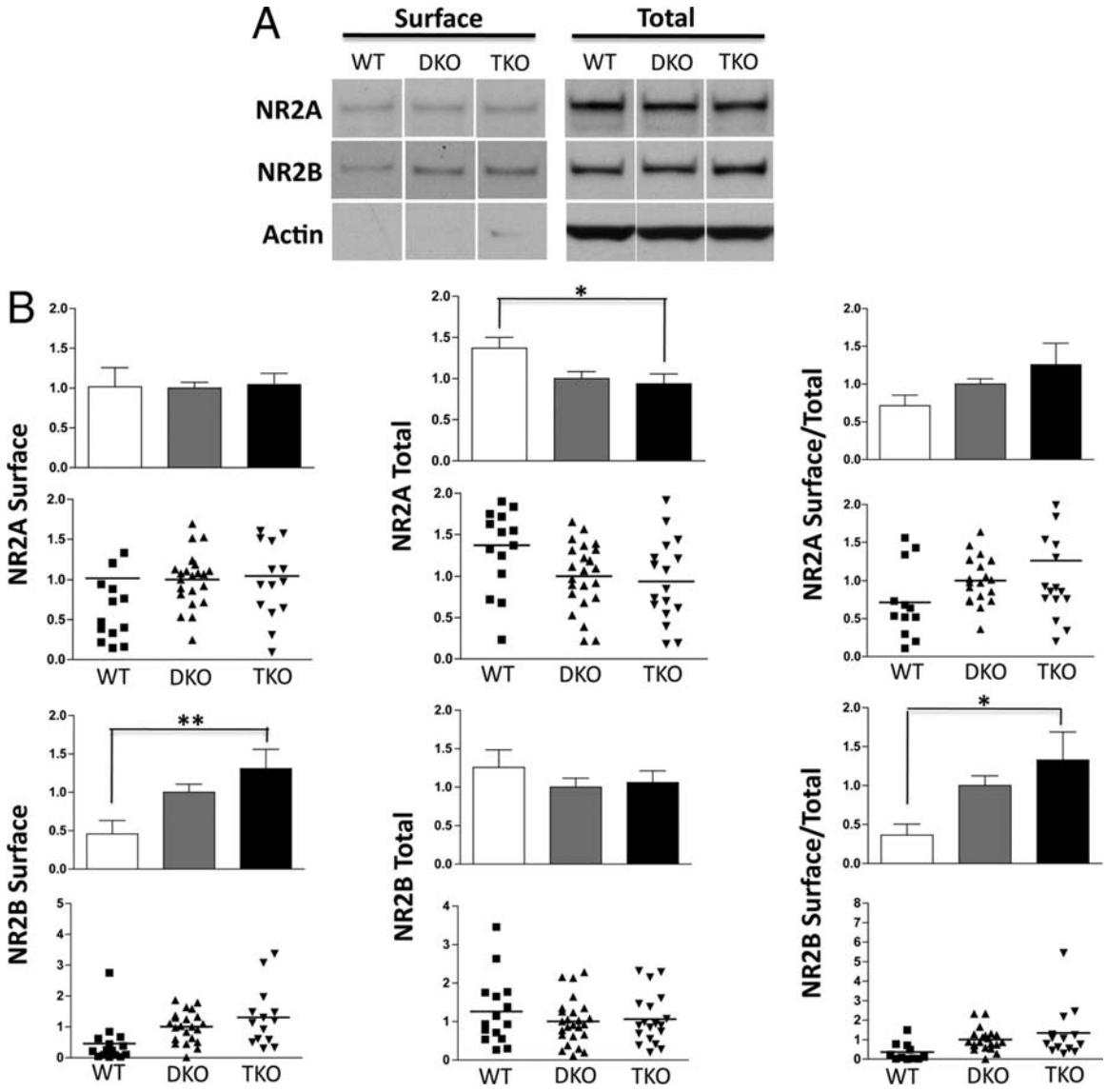
A
Surface
Total
WT
DKO
TKO
WT
DKO
TKO
NR2A
NR2B
Actin
B
NR2A Surface
NR2A Total
NR2A Surface/Total
NR2B Surface
NR2B Total
NR2B Surface/Total
*
**
*
WT
DKO
TKO

# Figure 5.8

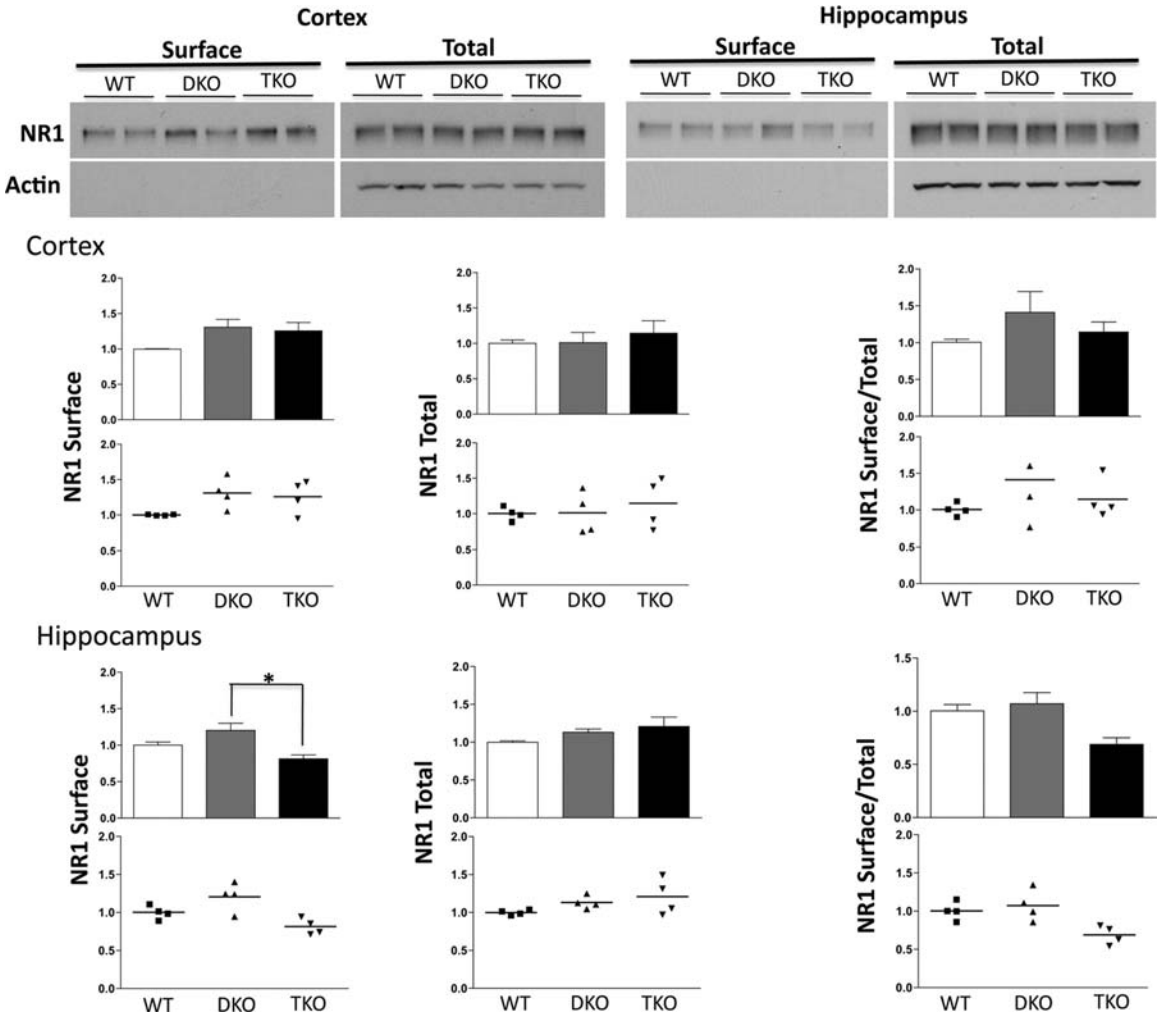
Cortex
Surface
Total
Hippocampus
Surface
Total
WT
DKO
TKO
NR1
Actin
Cortex
NR1 Surface
NR1 Total
NR1 Surface/Total
Hippocampus
*

**Figure 5.9**

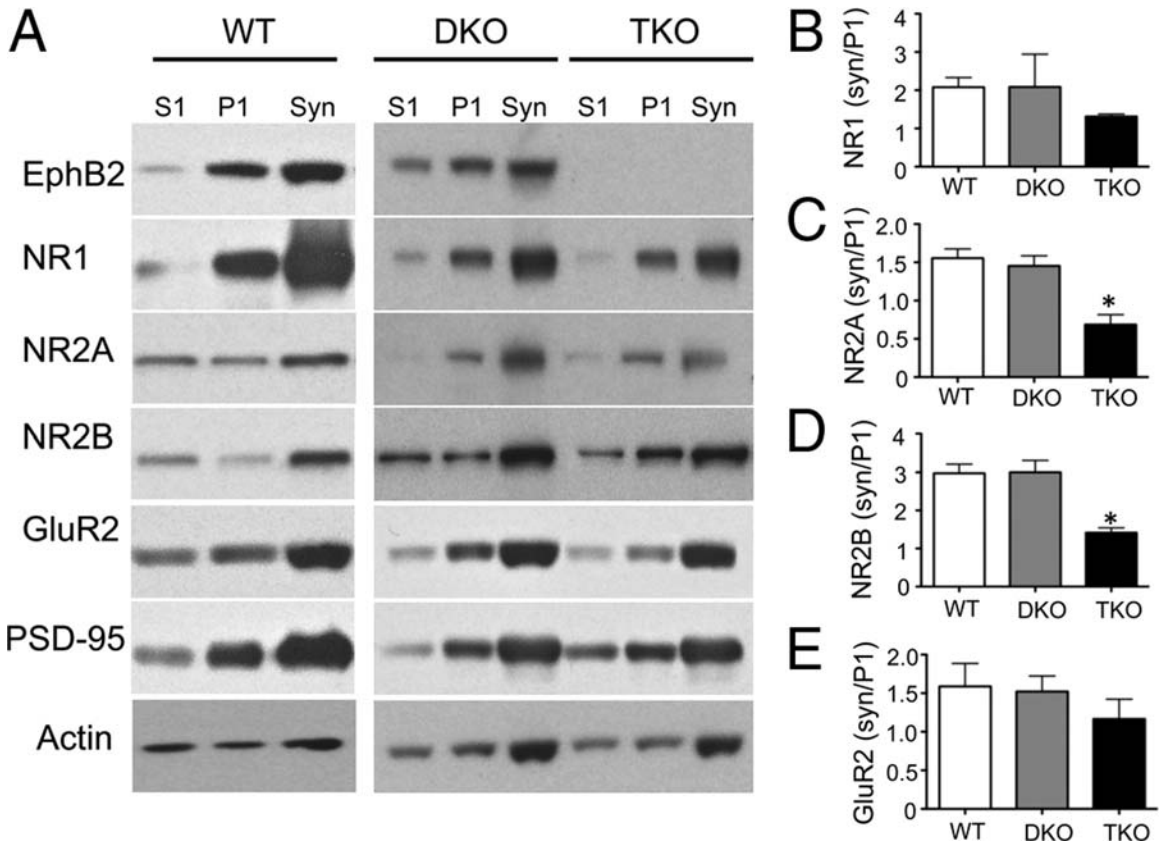
A
WT
DKO
TKO
S1
P1
Syn
EphB2
NR1
NR2A
NR2B
GluR2
PSD-95
Actin
B
NR1 (syn/P1)
C
NR2A (syn/P1)
D
NR2B (syn/P1)
E
GluR2 (syn/P1)
WT
DKO
TKO
*

## References


Andersson, E.R. (2011). The role of endocytosis in activating and regulating signal transduction. Cell Mol Life Sci.

Antion, M.D., Christie, L.A., Bond, A.M., Dalva, M.B., and Contractor, A. (2010). Ephrin-B3 regulates glutamate receptor signaling at hippocampal synapses. Mol Cell Neurosci *45*, 378-388.

Aoto, J., and Chen, L. (2007). Bidirectional ephrin/Eph signaling in synaptic functions. Brain Res *1184*, 72-80.

Attwood, B.K., Bourgognon, J.M., Patel, S., Mucha, M., Schiavon, E., Skrzypiec, A.E., Young, K.W., Shiosaka, S., Korostynski, M., Piechota, M.*, et al.* (2011). Neuropsin cleaves EphB2 in the amygdala to control anxiety. Nature *473*, 372-375.

Barkus, C., McHugh, S.B., Sprengel, R., Seeburg, P.H., Rawlins, J.N., and Bannerman, D.M. (2010). Hippocampal NMDA receptors and anxiety: at the interface between cognition and emotion. Eur J Pharmacol *626*, 49-56.

Barria, A., and Malinow, R. (2005). NMDA receptor subunit composition controls synaptic plasticity by regulating binding to CaMKII. Neuron *48*, 289-301.

Battaglia, A.A., Sehayek, K., Grist, J., McMahon, S.B., and Gavazzi, I. (2003). EphB receptors and ephrin-B ligands regulate spinal sensory connectivity and modulate pain processing. Nat Neurosci *6*, 339-340.

Beekman, J.M., and Coffer, P.J. (2008). The ins and outs of syntenin, a multifunctional intracellular adaptor protein. J Cell Sci *121*, 1349-1355.

Biederer, T., Sara, Y., Mozhayeva, M., Atasoy, D., Liu, X., Kavalali, E.T., and Sudhof, T.C. (2002). SynCAM, a synaptic adhesion molecule that drives synapse assembly. Science *297*, 1525-1531.

Biederer, T., and Scheiffele, P. (2007). Mixed-culture assays for analyzing neuronal synapse formation. Nat Protoc *2*, 670-676.

Blackstone, C.D., Moss, S.J., Martin, L.J., Levey, A.I., Price, D.L., and Huganir, R.L. (1992). Biochemical characterization and localization of a non-N-methyl-D-aspartate glutamate receptor in rat brain. J Neurochem *58*, 1118-1126.

Bohana-Kashtan, O., Pinna, L.A., and Fishelson, Z. (2005). Extracellular phosphorylation of C9 by protein kinase CK2 regulates complement-mediated lysis. Eur J Immunol *35*, 1939-1948.

Boone, C., Bussey, H., and Andrews, B.J. (2007). Exploring genetic interactions and networks with yeast. Nat Rev Genet *8*, 437-449.

Bouvier, D., Corera, A.T., Tremblay, M.E., Riad, M., Chagnon, M., Murai, K.K., Pasquale, E.B., Fon, E.A., and Doucet, G. (2008). Pre-synaptic and post-synaptic localization of EphA4 and EphB2 in adult mouse forebrain. J Neurochem *106*, 682-695.

Bredt, D.S., and Nicoll, R.A. (2003). AMPA receptor trafficking at excitatory synapses. Neuron *40*, 361-379.

Bresler, T., Shapira, M., Boeckers, T., Dresbach, T., Futter, M., Garner, C.C., Rosenblum, K., Gundelfinger, E.D., and Ziv, N.E. (2004). Postsynaptic

density assembly is fundamentally different from presynaptic active zone assembly. J Neurosci *24*, 1507-1520.
Bruckner, K., Pablo Labrador, J., Scheiffele, P., Herb, A., Seeburg, P.H., and Klein, R. (1999). EphrinB ligands recruit GRIP family PDZ adaptor proteins into raft membrane microdomains. Neuron *22*, 511-524.
Brummelkamp, T.R., Bernards, R., and Agami, R. (2002). A system for stable expression of short interfering RNAs in mammalian cells. Science *296*, 550-553.
Buchert, M., Schneider, S., Meskenaite, V., Adams, M.T., Canaani, E., Baechi, T., Moelling, K., and Hovens, C.M. (1999). The junction-associated protein AF-6 interacts and clusters with specific Eph receptor tyrosine kinases at specialized sites of cell-cell contact in the brain. J Cell Biol *144*, 361-371.
Bundesen, L.Q., Scheel, T.A., Bregman, B.S., and Kromer, L.F. (2003). Ephrin-B2 and EphB2 regulation of astrocyte-meningeal fibroblast interactions in response to spinal cord lesions in adult rats. J Neurosci *23*, 7789-7800.
Calo, L., Cinque, C., Patane, M., Schillaci, D., Battaglia, G., Melchiorri, D., Nicoletti, F., and Bruno, V. (2006). Interaction between ephrins/Eph receptors and excitatory amino acid receptors: possible relevance in the regulation of synaptic plasticity and in the pathophysiology of neuronal degeneration. J Neurochem *98*, 1-10.
Cao, J.L., Ruan, J.P., Ling, D.Y., Guan, X.H., Bao, Q., Yuan, Y., Zhang, L.C., Song, X.J., and Zeng, Y.M. (2008). Activation of peripheral ephrinBs/EphBs signaling induces hyperalgesia through a MAPKs-mediated mechanism in mice. Pain *139*, 617-631.
Cesa, R., Premoselli, F., Renna, A., Ethell, I.M., Pasquale, E.B., and Strata, P. (2011). Eph receptors are involved in the activity-dependent synaptic wiring in the mouse cerebellar cortex. PLoS One *6*, e19160.
Chen, B.S., and Roche, K.W. (2007). Regulation of NMDA receptors by phosphorylation. Neuropharmacology *53*, 362-368.
Chen, W., Wieraszko, A., Hogan, M.V., Yang, H.A., Kornecki, E., and Ehrlich, Y.H. (1996). Surface protein phosphorylation by ecto-protein kinase is required for the maintenance of hippocampal long-term potentiation. Proc Natl Acad Sci U S A *93*, 8688-8693.
Chen, Y., Fu, A.K., and Ip, N.Y. (2011). Eph receptors at synapses: Implications in neurodegenerative diseases. Cell Signal.
Chen, Z.L., Yoshida, S., Kato, K., Momota, Y., Suzuki, J., Tanaka, T., Ito, J., Nishino, H., Aimoto, S., Kiyama, H., and et al. (1995). Expression and activity-dependent changes of a novel limbic-serine protease gene in the hippocampus. J Neurosci *15*, 5088-5097.
Chih, B., Engelman, H., and Scheiffele, P. (2005). Control of excitatory and inhibitory synapse formation by neuroligins. Science *307*, 1324-1328.
Chubykin, A.A., Atasoy, D., Etherton, M.R., Brose, N., Kavalali, E.T., Gibson, J.R., and Sudhof, T.C. (2007). Activity-dependent validation of excitatory versus inhibitory synapses by neuroligin-1 versus neuroligin-2. Neuron *54*, 919-931.

Cisse, M., Halabisky, B., Harris, J., Devidze, N., Dubal, D.B., Sun, B., Orr, A., Lotz, G., Kim, D.H., Hamto, P.*, et al.* (2011). Reversing EphB2 depletion rescues cognitive functions in Alzheimer model. Nature *469*, 47-52.

Conner, S.D., and Schmid, S.L. (2003). Regulated portals of entry into the cell. Nature *422*, 37-44.

Conover, J.C., Doetsch, F., Garcia-Verdugo, J.M., Gale, N.W., Yancopoulos, G.D., and Alvarez-Buylla, A. (2000). Disruption of Eph/ephrin signaling affects migration and proliferation in the adult subventricular zone. Nat Neurosci *3*, 1091-1097.

Contractor, A., Rogers, C., Maron, C., Henkemeyer, M., Swanson, G.T., and Heinemann, S.F. (2002). Trans-synaptic Eph receptor-ephrin signaling in hippocampal mossy fiber LTP. Science *296*, 1864-1869.

Cowan, C.W., Shao, Y.R., Sahin, M., Shamah, S.M., Lin, M.Z., Greer, P.L., Gao, S., Griffith, E.C., Brugge, J.S., and Greenberg, M.E. (2005). Vav family GEFs link activated Ephs to endocytosis and axon guidance. Neuron *46*, 205-217.

Cull-Candy, S.G., and Leszkiewicz, D.N. (2004). Role of distinct NMDA receptor subtypes at central synapses. Sci STKE *2004*, re16.

Dalva, M.B., McClelland, A.C., and Kayser, M.S. (2007). Cell adhesion molecules: signalling functions at the synapse. Nat Rev Neurosci *8*, 206-220.

Dalva, M.B., Takasu, M.A., Lin, M.Z., Shamah, S.M., Hu, L., Gale, N.W., and Greenberg, M.E. (2000). EphB receptors interact with NMDA receptors and regulate excitatory synapse formation. Cell *103*, 945-956.

Dong, Y., Mao-Ying, Q.L., Chen, J.W., Yang, C.J., Wang, Y.Q., and Tan, Z.M. (2011). Involvement of EphB1 receptor/ephrinB1 ligand in bone cancer pain. Neurosci Lett *496*, 163-167.

Egea, J., and Klein, R. (2007). Bidirectional Eph-ephrin signaling during axon guidance. Trends Cell Biol *17*, 230-238.

Essmann, C.L., Martinez, E., Geiger, J.C., Zimmer, M., Traut, M.H., Stein, V., Klein, R., and Acker-Palmer, A. (2008). Serine phosphorylation of ephrinB2 regulates trafficking of synaptic AMPA receptors. Nat Neurosci *11*, 1035-1043.

Ethell, I.M., Irie, F., Kalo, M.S., Couchman, J.R., Pasquale, E.B., and Yamaguchi, Y. (2001). EphB/syndecan-2 signaling in dendritic spine morphogenesis. Neuron *31*, 1001-1013.

Fasen, K., Cerretti, D.P., and Huynh-Do, U. (2008). Ligand binding induces Cbl-dependent EphB1 receptor degradation through the lysosomal pathway. Traffic *9*, 251-266.

Ficarro, S.B., McCleland, M.L., Stukenberg, P.T., Burke, D.J., Ross, M.M., Shabanowitz, J., Hunt, D.F., and White, F.M. (2002). Phosphoproteome analysis by mass spectrometry and its application to Saccharomyces cerevisiae. Nat Biotechnol *20*, 301-305.

Filosa, A., Paixao, S., Honsek, S.D., Carmona, M.A., Becker, L., Feddersen, B., Gaitanos, L., Rudhard, Y., Schoepfer, R., Klopstock, T.*, et al.* (2009). Neuron-glia communication via EphA4/ephrin-A3 modulates LTP through glial glutamate transport. Nat Neurosci *12*, 1285-1292.

Flanagan, J.G., and Vanderhaeghen, P. (1998). The ephrins and Eph receptors in neural development. Annu Rev Neurosci *21*, 309-345.
Fu, A.K., Hung, K.W., Fu, W.Y., Shen, C., Chen, Y., Xia, J., Lai, K.O., and Ip, N.Y. (2011). APC(Cdh1) mediates EphA4-dependent downregulation of AMPA receptors in homeostatic plasticity. Nat Neurosci *14*, 181-189.
Fujii, S., Kuroda, Y., Ito, K., and Kato, H. (2000). Long-term potentiation induction--a synaptic catch mechanism released by extracellular phosphorylation. Neuroscience *96*, 259-266.
Gardner, S.M., Takamiya, K., Xia, J., Suh, J.G., Johnson, R., Yu, S., and Huganir, R.L. (2005). Calcium-permeable AMPA receptor plasticity is mediated by subunit-specific interactions with PICK1 and NSF. Neuron *45*, 903-915.
Genander, M., and Frisen, J. (2010). Ephrins and Eph receptors in stem cells and cancer. Curr Opin Cell Biol *22*, 611-616.
Graf, E.R., Zhang, X., Jin, S.X., Linhoff, M.W., and Craig, A.M. (2004). Neurexins induce differentiation of GABA and glutamate postsynaptic specializations via neuroligins. Cell *119*, 1013-1026.
Greer, P.L., Hanayama, R., Bloodgood, B.L., Mardinly, A.R., Lipton, D.M., Flavell, S.W., Kim, T.K., Griffith, E.C., Waldon, Z., Maehr, R.*, et al.* (2010). The Angelman Syndrome protein Ube3A regulates synapse development by ubiquitinating arc. Cell *140*, 704-716.
Greger, I.H., and Esteban, J.A. (2007). AMPA receptor biogenesis and trafficking. Curr Opin Neurobiol *17*, 289-297.
Grembecka, J., Cierpicki, T., Devedjiev, Y., Derewenda, U., Kang, B.S., Bushweller, J.H., and Derewenda, Z.S. (2006). The binding of the PDZ tandem of syntenin to target proteins. Biochemistry *45*, 3674-3683.
Groc, L., Bard, L., and Choquet, D. (2009). Surface trafficking of N-methyl-D-aspartate receptors: physiological and pathological perspectives. Neuroscience *158*, 4-18.
Grootjans, J.J., Reekmans, G., Ceulemans, H., and David, G. (2000). Syntenin-syndecan binding requires syndecan-synteny and the co-operation of both PDZ domains of syntenin. J Biol Chem *275*, 19933-19941.
Grootjans, J.J., Zimmermann, P., Reekmans, G., Smets, A., Degeest, G., Durr, J., and David, G. (1997). Syntenin, a PDZ protein that binds syndecan cytoplasmic domains. Proc Natl Acad Sci U S A *94*, 13683-13688.
Grunwald, I.C., Korte, M., Adelmann, G., Plueck, A., Kullander, K., Adams, R.H., Frotscher, M., Bonhoeffer, T., and Klein, R. (2004). Hippocampal plasticity requires postsynaptic ephrinBs. Nat Neurosci *7*, 33-40.
Grunwald, I.C., Korte, M., Wolfer, D., Wilkinson, G.A., Unsicker, K., Lipp, H.P., Bonhoeffer, T., and Klein, R. (2001). Kinase-independent requirement of EphB2 receptors in hippocampal synaptic plasticity. Neuron *32*, 1027-1040.
Guan, X.H., Lu, X.F., Zhang, H.X., Wu, J.R., Yuan, Y., Bao, Q., Ling, D.Y., and Cao, J.L. (2010). Phosphatidylinositol 3-kinase mediates pain behaviors induced by activation of peripheral ephrinBs/EphBs signaling in mice. Pharmacol Biochem Behav *95*, 315-324.

Guo, W., Zou, S., Guan, Y., Ikeda, T., Tal, M., Dubner, R., and Ren, K. (2002). Tyrosine phosphorylation of the NR2B subunit of the NMDA receptor in the spinal cord during the development and maintenance of inflammatory hyperalgesia. J Neurosci *22*, 6208-6217.

Han, Y., Song, X.S., Liu, W.T., Henkemeyer, M., and Song, X.J. (2008). Targeted mutation of EphB1 receptor prevents development of neuropathic hyperalgesia and physical dependence on morphine in mice. Mol Pain *4*, 60.

Hendelman, W.J., and Aggerwal, A.S. (1980). The Purkinje neuron: I. A Golgi study of its development in the mouse and in culture. J Comp Neurol *193*, 1063-1079.

Henderson, J.T., Georgiou, J., Jia, Z., Robertson, J., Elowe, S., Roder, J.C., and Pawson, T. (2001). The receptor tyrosine kinase EphB2 regulates NMDA-dependent synaptic function. Neuron *32*, 1041-1056.

Henkemeyer, M., Itkis, O.S., Ngo, M., Hickmott, P.W., and Ethell, I.M. (2003). Multiple EphB receptor tyrosine kinases shape dendritic spines in the hippocampus. J Cell Biol *163*, 1313-1326.

Henley, J.M., Barker, E.A., and Glebov, O.O. (2011). Routes, destinations and delays: recent advances in AMPA receptor trafficking. Trends Neurosci *34*, 258-268.

Heuser, J.E., and Anderson, R.G. (1989). Hypertonic media inhibit receptor-mediated endocytosis by blocking clathrin-coated pit formation. J Cell Biol *108*, 389-400.

Himanen, J.P., Chumley, M.J., Lackmann, M., Li, C., Barton, W.A., Jeffrey, P.D., Vearing, C., Geleick, D., Feldheim, D.A., Boyd, A.W.*, et al.* (2004). Repelling class discrimination: ephrin-A5 binds to and activates EphB2 receptor signaling. Nat Neurosci *7*, 501-509.

Hirbec, H., Perestenko, O., Nishimune, A., Meyer, G., Nakanishi, S., Henley, J.M., and Dev, K.K. (2002). The PDZ proteins PICK1, GRIP, and syntenin bind multiple glutamate receptor subtypes. Analysis of PDZ binding motifs. J Biol Chem *277*, 15221-15224.

Holland, S.J., Gale, N.W., Gish, G.D., Roth, R.A., Songyang, Z., Cantley, L.C., Henkemeyer, M., Yancopoulos, G.D., and Pawson, T. (1997). Juxtamembrane tyrosine residues couple the Eph family receptor EphB2/Nuk to specific SH2 domain proteins in neuronal cells. EMBO J *16*, 3877-3888.

Holtmaat, A., and Svoboda, K. (2009). Experience-dependent structural synaptic plasticity in the mammalian brain. Nat Rev Neurosci *10*, 647-658.

Hoogenraad, C.C., Milstein, A.D., Ethell, I.M., Henkemeyer, M., and Sheng, M. (2005). GRIP1 controls dendrite morphogenesis by regulating EphB receptor trafficking. Nat Neurosci *8*, 906-915.

Huang, Y.H., Lin, Y., Mu, P., Lee, B.R., Brown, T.E., Wayman, G., Marie, H., Liu, W., Yan, Z., Sorg, B.A.*, et al.* (2009). In vivo cocaine experience generates silent synapses. Neuron *63*, 40-47.

Ikonomovic, M.D., Mizukami, K., Warde, D., Sheffield, R., Hamilton, R., Wenthold, R.J., and Armstrong, D.M. (1999). Distribution of glutamate receptor subunit NMDAR1 in the hippocampus of normal elderly and patients with Alzheimer's disease. Exp Neurol *160*, 194-204.

Irie, F., Okuno, M., Pasquale, E.B., and Yamaguchi, Y. (2005). EphrinB-EphB signalling regulates clathrin-mediated endocytosis through tyrosine phosphorylation of synaptojanin 1. Nat Cell Biol *7*, 501-509.
Irie, F., and Yamaguchi, Y. (2002). EphB receptors regulate dendritic spine development via intersectin, Cdc42 and N-WASP. Nat Neurosci *5*, 1117-1118.
Isaac, J.T., Ashby, M.C., and McBain, C.J. (2007). The role of the GluR2 subunit in AMPA receptor function and synaptic plasticity. Neuron *54*, 859-871.
Ishikawa, H.O., Takeuchi, H., Haltiwanger, R.S., and Irvine, K.D. (2008a). Four-jointed is a Golgi kinase that phosphorylates a subset of cadherin domains. Science *321*, 401-404.
Ishikawa, Y., Horii, Y., Tamura, H., and Shiosaka, S. (2008b). Neuropsin (KLK8)-dependent and -independent synaptic tagging in the Schaffer-collateral pathway of mouse hippocampus. J Neurosci *28*, 843-849.
Izumi, A., Iijima, Y., Noguchi, H., Numakawa, T., Okada, T., Hori, H., Kato, T., Tatsumi, M., Kosuga, A., Kamijima, K.*, et al.* (2008). Genetic variations of human neuropsin gene and psychiatric disorders: polymorphism screening and possible association with bipolar disorder and cognitive functions. Neuropsychopharmacology *33*, 3237-3245.
Jin, Y., and Garner, C.C. (2008). Molecular mechanisms of presynaptic differentiation. Annu Rev Cell Dev Biol *24*, 237-262.
Johnston, C.L., Cox, H.C., Gomm, J.J., and Coombes, R.C. (1995). Fibroblast growth factor receptors (FGFRs) localize in different cellular compartments. A splice variant of FGFR-3 localizes to the nucleus. J Biol Chem *270*, 30643-30650.
Katoh, M., Hattori, Y., Sasaki, H., Tanaka, M., Sugano, K., Yazaki, Y., Sugimura, T., and Terada, M. (1992). K-sam gene encodes secreted as well as transmembrane receptor tyrosine kinase. Proc Natl Acad Sci U S A *89*, 2960-2964.
Kawashima, T., Okuno, H., Nonaka, M., Adachi-Morishima, A., Kyo, N., Okamura, M., Takemoto-Kimura, S., Worley, P.F., and Bito, H. (2009). Synaptic activity-responsive element in the Arc/Arg3.1 promoter essential for synapse-to-nucleus signaling in activated neurons. Proc Natl Acad Sci U S A *106*, 316-321.
Kayser, M.S., Lee, A.C., Hruska, M., and Dalva, M.B. (2011). Preferential control of basal dendritic protrusions by EphB2. PLoS One *6*, e17417.
Kayser, M.S., McClelland, A.C., Hughes, E.G., and Dalva, M.B. (2006). Intracellular and trans-synaptic regulation of glutamatergic synaptogenesis by EphB receptors. J Neurosci *26*, 12152-12164.
Kayser, M.S., Nolt, M.J., and Dalva, M.B. (2008). EphB receptors couple dendritic filopodia motility to synapse formation. Neuron *59*, 56-69.
Kerchner, G.A., and Nicoll, R.A. (2008). Silent synapses and the emergence of a postsynaptic mechanism for LTP. Nat Rev Neurosci *9*, 813-825.
Kessels, H.W., and Malinow, R. (2009). Synaptic AMPA receptor plasticity and behavior. Neuron *61*, 340-350.

Kim, E., and Sheng, M. (2004). PDZ domain proteins of synapses. Nat Rev Neurosci *5*, 771-781.
Klein, R. (2009). Bidirectional modulation of synaptic functions by Eph/ephrin signaling. Nat Neurosci *12*, 15-20.
Ko, J., Yoon, C., Piccoli, G., Chung, H.S., Kim, K., Lee, J.R., Lee, H.W., Kim, H., Sala, C., and Kim, E. (2006). Organization of the presynaptic active zone by ERC2/CAST1-dependent clustering of the tandem PDZ protein syntenin-1. J Neurosci *26*, 963-970.
Kobayashi, H., Kitamura, T., Sekiguchi, M., Homma, M.K., Kabuyama, Y., Konno, S., Kikuchi, S., and Homma, Y. (2007). Involvement of EphB1 receptor/EphrinB2 ligand in neuropathic pain. Spine (Phila Pa 1976) *32*, 1592-1598.
Koroll, M., Rathjen, F.G., and Volkmer, H. (2001). The neural cell recognition molecule neurofascin interacts with syntenin-1 but not with syntenin-2, both of which reveal self-associating activity. J Biol Chem *276*, 10646-10654.
Kumar, S., Rezaei-Ghaleh, N., Terwel, D., Thal, D.R., Richard, M., Hoch, M., Mc Donald, J.M., Wullner, U., Glebov, K., Heneka, M.T.*, et al.* (2011). Extracellular phosphorylation of the amyloid beta-peptide promotes formation of toxic aggregates during the pathogenesis of Alzheimer's disease. EMBO J *30*, 2255-2265.
Kuner, R. (2010). Central mechanisms of pathological pain. Nat Med *16*, 1258-1266.
Lai, K.O., and Ip, N.Y. (2009). Synapse development and plasticity: roles of ephrin/Eph receptor signaling. Curr Opin Neurobiol *19*, 275-283.
Lau, C.G., and Zukin, R.S. (2007). NMDA receptor trafficking in synaptic plasticity and neuropsychiatric disorders. Nat Rev Neurosci *8*, 413-426.
Lau, L.F., Mammen, A., Ehlers, M.D., Kindler, S., Chung, W.J., Garner, C.C., and Huganir, R.L. (1996). Interaction of the N-methyl-D-aspartate receptor complex with a novel synapse-associated protein, SAP102. J Biol Chem *271*, 21622-21628.
Lavezzari, G., McCallum, J., Lee, R., and Roche, K.W. (2003). Differential binding of the AP-2 adaptor complex and PSD-95 to the C-terminus of the NMDA receptor subunit NR2B regulates surface expression. Neuropharmacology *45*, 729-737.
Legendre, P., Rosenmund, C., and Westbrook, G.L. (1993). Inactivation of NMDA channels in cultured hippocampal neurons by intracellular calcium. J Neurosci *13*, 674-684.
Lein, E.S., Hawrylycz, M.J., Ao, N., Ayres, M., Bensinger, A., Bernard, A., Boe, A.F., Boguski, M.S., Brockway, K.S., Byrnes, E.J.*, et al.* (2007). Genome-wide atlas of gene expression in the adult mouse brain. Nature *445*, 168-176.
Liebl, D.J., Morris, C.J., Henkemeyer, M., and Parada, L.F. (2003). mRNA expression of ephrins and Eph receptor tyrosine kinases in the neonatal and adult mouse central nervous system. J Neurosci Res *71*, 7-22.
Lim, B.K., Matsuda, N., and Poo, M.M. (2008). Ephrin-B reverse signaling promotes structural and functional synaptic maturation in vivo. Nat Neurosci *11*, 160-169.

Lin, D., Gish, G.D., Songyang, Z., and Pawson, T. (1999). The carboxyl terminus of B class ephrins constitutes a PDZ domain binding motif. J Biol Chem *274*, 3726-3733.
Lin, K.T., Sloniowski, S., Ethell, D.W., and Ethell, I.M. (2008). Ephrin-B2-induced cleavage of EphB2 receptor is mediated by matrix metalloproteinases to trigger cell repulsion. J Biol Chem *283*, 28969-28979.
Lin, Y., Skeberdis, V.A., Francesconi, A., Bennett, M.V., and Zukin, R.S. (2004). Postsynaptic density protein-95 regulates NMDA channel gating and surface expression. J Neurosci *24*, 10138-10148.
Litterst, C., Georgakopoulos, A., Shioi, J., Ghersi, E., Wisniewski, T., Wang, R., Ludwig, A., and Robakis, N.K. (2007). Ligand binding and calcium influx induce distinct ectodomain/gamma-secretase-processing pathways of EphB2 receptor. J Biol Chem *282*, 16155-16163.
Liu, S., Liu, W.T., Liu, Y.P., Dong, H.L., Henkemeyer, M., Xiong, L.Z., and Song, X.J. (2011). Blocking EphB1 Receptor Forward Signaling in Spinal Cord Relieves Bone Cancer Pain and Rescues Analgesic Effect of Morphine Treatment in Rodents. Cancer Res *71*, 4392-4402.
Liu, S.J., and Cull-Candy, S.G. (2005). Subunit interaction with PICK and GRIP controls Ca2+ permeability of AMPARs at cerebellar synapses. Nat Neurosci *8*, 768-775.
Liu, W.T., Han, Y., Li, H.C., Adams, B., Zheng, J.H., Wu, Y.P., Henkemeyer, M., and Song, X.J. (2009). An in vivo mouse model of long-term potentiation at synapses between primary afferent C-fibers and spinal dorsal horn neurons: essential role of EphB1 receptor. Mol Pain *5*, 29.
Liu, Z., Conroy, W.G., Stawicki, T.M., Nai, Q., Neff, R.A., and Berg, D.K. (2008). EphB receptors co-distribute with a nicotinic receptor subtype and regulate nicotinic downstream signaling in neurons. Mol Cell Neurosci *38*, 236-244.
Lohman, R.J., Jones, N.C., O'Brien, T.J., and Cocks, T.M. (2009). A regulatory role for protease-activated receptor-2 in motivational learning in rats. Neurobiol Learn Mem *92*, 301-309.
Lu, W., and Roche, K.W. (2011). Posttranslational regulation of AMPA receptor trafficking and function. Curr Opin Neurobiol.
Lupien, S.J., McEwen, B.S., Gunnar, M.R., and Heim, C. (2009). Effects of stress throughout the lifespan on the brain, behaviour and cognition. Nat Rev Neurosci *10*, 434-445.
Mabb, A.M., Judson, M.C., Zylka, M.J., and Philpot, B.D. (2011). Angelman syndrome: insights into genomic imprinting and neurodevelopmental phenotypes. Trends Neurosci *34*, 293-303.
Maik-Rachline, G., Shaltiel, S., and Seger, R. (2005). Extracellular phosphorylation converts pigment epithelium-derived factor from a neurotrophic to an antiangiogenic factor. Blood *105*, 670-678.
Mani, R., St Onge, R.P., Hartman, J.L.t., Giaever, G., and Roth, F.P. (2008). Defining genetic interaction. Proc Natl Acad Sci U S A *105*, 3461-3466.
Margolis, S.S., Salogiannis, J., Lipton, D.M., Mandel-Brehm, C., Wills, Z.P., Mardinly, A.R., Hu, L., Greer, P.L., Bikoff, J.B., Ho, H.Y.*, et al.* (2010). EphB-

mediated degradation of the RhoA GEF Ephexin5 relieves a developmental brake on excitatory synapse formation. Cell *143*, 442-455.
Marston, D.J., Dickinson, S., and Nobes, C.D. (2003). Rac-dependent trans-endocytosis of ephrinBs regulates Eph-ephrin contact repulsion. Nat Cell Biol *5*, 879-888.
Matsumoto-Miyai, K., Ninomiya, A., Yamasaki, H., Tamura, H., Nakamura, Y., and Shiosaka, S. (2003). NMDA-dependent proteolysis of presynaptic adhesion molecule L1 in the hippocampus by neuropsin. J Neurosci *23*, 7727-7736.
Matys, T., Pawlak, R., Matys, E., Pavlides, C., McEwen, B.S., and Strickland, S. (2004). Tissue plasminogen activator promotes the effects of corticotropin-releasing factor on the amygdala and anxiety-like behavior. Proc Natl Acad Sci U S A *101*, 16345-16350.
McClelland, A.C., Hruska, M., Coenen, A.J., Henkemeyer, M., and Dalva, M.B. (2010). Trans-synaptic EphB2-ephrin-B3 interaction regulates excitatory synapse density by inhibition of postsynaptic MAPK signaling. Proc Natl Acad Sci U S A *107*, 8830-8835.
McClelland, A.C., Sheffler-Collins, S.I., Kayser, M.S., and Dalva, M.B. (2009). Ephrin-B1 and ephrin-B2 mediate EphB-dependent presynaptic development via syntenin-1. Proc Natl Acad Sci U S A *106*, 20487-20492.
McMahon, S.A., and Diaz, E. (2011). Mechanisms of excitatory synapse maturation by trans-synaptic organizing complexes. Curr Opin Neurobiol *21*, 221-227.
Migani, P., Bartlett, C., Dunlop, S., Beazley, L., and Rodger, J. (2007). Ephrin-B2 immunoreactivity distribution in adult mouse brain. Brain Res *1182*, 60-72.
Migani, P., Bartlett, C., Dunlop, S., Beazley, L., and Rodger, J. (2009). Regional and cellular distribution of ephrin-B1 in adult mouse brain. Brain Res *1247*, 50-61.
Moeller, M.L., Shi, Y., Reichardt, L.F., and Ethell, I.M. (2006). EphB receptors regulate dendritic spine morphogenesis through the recruitment/phosphorylation of focal adhesion kinase and RhoA activation. J Biol Chem *281*, 1587-1598.
Monyer, H., Burnashev, N., Laurie, D.J., Sakmann, B., and Seeburg, P.H. (1994). Developmental and regional expression in the rat brain and functional properties of four NMDA receptors. Neuron *12*, 529-540.
Murai, K.K., and Pasquale, E.B. (2011). Eph receptors and ephrins in neuron-astrocyte communication at synapses. Glia *59*, 1567-1578.
Myme, C.I., Sugino, K., Turrigiano, G.G., and Nelson, S.B. (2003). The NMDA-to-AMPA ratio at synapses onto layer 2/3 pyramidal neurons is conserved across prefrontal and visual cortices. J Neurophysiol *90*, 771-779.
Nguyen, H.T., Dalmasso, G., Yan, Y., Obertone, T.S., Sitaraman, S.V., and Merlin, D. (2008). Ecto-phosphorylation of CD98 regulates cell-cell interactions. PLoS One *3*, e3895.
Nishimura, T., Yamaguchi, T., Tokunaga, A., Hara, A., Hamaguchi, T., Kato, K., Iwamatsu, A., Okano, H., and Kaibuchi, K. (2006). Role of numb in dendritic

spine development with a Cdc42 GEF intersectin and EphB2. Mol Biol Cell *17*, 1273-1285.
Nolt, M.J., Lin, Y., Hruska, M., Murphy, J., Sheffler-Colins, S.I., Kayser, M.S., Passer, J., Bennett, M.V., Zukin, R.S., and Dalva, M.B. (2011). EphB controls NMDA receptor function and synaptic targeting in a subunit-specific manner. J Neurosci *31*, 5353-5364.
Olsen, J.V., Blagoev, B., Gnad, F., Macek, B., Kumar, C., Mortensen, P., and Mann, M. (2006). Global, in vivo, and site-specific phosphorylation dynamics in signaling networks. Cell *127*, 635-648.
Opazo, P., and Choquet, D. (2010). A three-step model for the synaptic recruitment of AMPA receptors. Mol Cell Neurosci *46*, 1-8.
Orikawa, Y., Kato, H., Seto, K., Kobayashi, N., Yoshinaga, K., Hamano, H., Hori, Y., Meyer, T., and Takei, M. (2010). Z-360, a novel therapeutic agent for pancreatic cancer, prevents up-regulation of ephrin B1 gene expression and phosphorylation of NR2B via suppression of interleukin-1 beta production in a cancer-induced pain model in mice. Mol Pain *6*, 72.
Papa, M., Bundman, M.C., Greenberger, V., and Segal, M. (1995). Morphological analysis of dendritic spine development in primary cultures of hippocampal neurons. J Neurosci *15*, 1-11.
Pasquale, E.B. (2008). Eph-ephrin bidirectional signaling in physiology and disease. Cell *133*, 38-52.
Pasquale, E.B. (2010). Eph receptors and ephrins in cancer: bidirectional signalling and beyond. Nat Rev Cancer *10*, 165-180.
Pawlak, D., Tankiewicz, A., Matys, T., and Buczko, W. (2003). Peripheral distribution of kynurenine metabolites and activity of kynurenine pathway enzymes in renal failure. J Physiol Pharmacol *54*, 175-189.
Pawlak, R., Rao, B.S., Melchor, J.P., Chattarji, S., McEwen, B., and Strickland, S. (2005). Tissue plasminogen activator and plasminogen mediate stress-induced decline of neuronal and cognitive functions in the mouse hippocampus. Proc Natl Acad Sci U S A *102*, 18201-18206.
Penzes, P., Beeser, A., Chernoff, J., Schiller, M.R., Eipper, B.A., Mains, R.E., and Huganir, R.L. (2003). Rapid induction of dendritic spine morphogenesis by trans-synaptic ephrinB-EphB receptor activation of the Rho-GEF kalirin. Neuron *37*, 263-274.
Penzes, P., Cahill, M.E., Jones, K.A., VanLeeuwen, J.E., and Woolfrey, K.M. (2011). Dendritic spine pathology in neuropsychiatric disorders. Nat Neurosci *14*, 285-293.
Perez-Otano, I., and Ehlers, M.D. (2005). Homeostatic plasticity and NMDA receptor trafficking. Trends Neurosci *28*, 229-238.
Petros, T.J., Bryson, J.B., and Mason, C. (2010). Ephrin-B2 elicits differential growth cone collapse and axon retraction in retinal ganglion cells from distinct retinal regions. Dev Neurobiol *70*, 781-794.
Philpot, B.D., Cho, K.K., and Bear, M.F. (2007). Obligatory role of NR2A for metaplasticity in visual cortex. Neuron *53*, 495-502.
Philpot, B.D., and Zukin, R.S. (2010). Synapse-specific metaplasticity: to be silenced is not to silence 2B. Neuron *66*, 814-816.

Pitulescu, M.E., and Adams, R.H. (2010). Eph/ephrin molecules--a hub for signaling and endocytosis. Genes Dev *24*, 2480-2492.
Prybylowski, K., Chang, K., Sans, N., Kan, L., Vicini, S., and Wenthold, R.J. (2005). The synaptic localization of NR2B-containing NMDA receptors is controlled by interactions with PDZ proteins and AP-2. Neuron *47*, 845-857.
Prybylowski, K., and Wenthold, R.J. (2004). N-Methyl-D-aspartate receptors: subunit assembly and trafficking to the synapse. J Biol Chem *279*, 9673-9676.
Rao, A., Kim, E., Sheng, M., and Craig, A.M. (1998). Heterogeneity in the molecular composition of excitatory postsynaptic sites during development of hippocampal neurons in culture. J Neurosci *18*, 1217-1229.
Redegeld, F.A., Caldwell, C.C., and Sitkovsky, M.V. (1999). Ecto-protein kinases: ecto-domain phosphorylation as a novel target for pharmacological manipulation? Trends Pharmacol Sci *20*, 453-459.
Robbins, E.M., Krupp, A.J., Perez de Arce, K., Ghosh, A.K., Fogel, A.I., Boucard, A., Sudhof, T.C., Stein, V., and Biederer, T. (2010). SynCAM 1 adhesion dynamically regulates synapse number and impacts plasticity and learning. Neuron *68*, 894-906.
Rodenas-Ruano, A., Perez-Pinzon, M.A., Green, E.J., Henkemeyer, M., and Liebl, D.J. (2006). Distinct roles for ephrinB3 in the formation and function of hippocampal synapses. Dev Biol *292*, 34-45.
Ruan, J.P., Zhang, H.X., Lu, X.F., Liu, Y.P., and Cao, J.L. (2010). EphrinBs/EphBs signaling is involved in modulation of spinal nociceptive processing through a mitogen-activated protein kinases-dependent mechanism. Anesthesiology *112*, 1234-1249.
Sahin, M., Greer, P.L., Lin, M.Z., Poucher, H., Eberhart, J., Schmidt, S., Wright, T.M., Shamah, S.M., O'Connell, S., Cowan, C.W.*, et al.* (2005). Eph-dependent tyrosine phosphorylation of ephexin1 modulates growth cone collapse. Neuron *46*, 191-204.
Salter, M.W., and Kalia, L.V. (2004). Src kinases: a hub for NMDA receptor regulation. Nat Rev Neurosci *5*, 317-328.
Sanz-Clemente, A., Matta, J.A., Isaac, J.T., and Roche, K.W. (2010). Casein kinase 2 regulates the NR2 subunit composition of synaptic NMDA receptors. Neuron *67*, 984-996.
Sara, Y., Biederer, T., Atasoy, D., Chubykin, A., Mozhayeva, M.G., Sudhof, T.C., and Kavalali, E.T. (2005). Selective capability of SynCAM and neuroligin for functional synapse assembly. J Neurosci *25*, 260-270.
Segura, I., Essmann, C.L., Weinges, S., and Acker-Palmer, A. (2007). Grb4 and GIT1 transduce ephrinB reverse signals modulating spine morphogenesis and synapse formation. Nat Neurosci *10*, 301-310.
Selkoe, D.J. (2002). Alzheimer's disease is a synaptic failure. Science *298*, 789-791.
Shen, K., and Cowan, C.W. (2010). Guidance molecules in synapse formation and plasticity. Cold Spring Harb Perspect Biol *2*, a001842.
Shen, K., and Scheiffele, P. (2010). Genetics and cell biology of building specific synaptic connectivity. Annu Rev Neurosci *33*, 473-507.

Sheng, M., Cummings, J., Roldan, L.A., Jan, Y.N., and Jan, L.Y. (1994). Changing subunit composition of heteromeric NMDA receptors during development of rat cortex. Nature *368*, 144-147.
Shevchenko, A., Wilm, M., Vorm, O., and Mann, M. (1996). Mass spectrometric sequencing of proteins silver-stained polyacrylamide gels. Anal Chem *68*, 850-858.
Shi, Y., Pontrello, C.G., DeFea, K.A., Reichardt, L.F., and Ethell, I.M. (2009). Focal adhesion kinase acts downstream of EphB receptors to maintain mature dendritic spines by regulating cofilin activity. J Neurosci *29*, 8129-8142.
Siddiqui, T.J., and Craig, A.M. (2010). Synaptic organizing complexes. Curr Opin Neurobiol *21*, 132-143.
Simon, A.M., de Maturana, R.L., Ricobaraza, A., Escribano, L., Schiapparelli, L., Cuadrado-Tejedor, M., Perez-Mediavilla, A., Avila, J., Del Rio, J., and Frechilla, D. (2009). Early changes in hippocampal Eph receptors precede the onset of memory decline in mouse models of Alzheimer's disease. J Alzheimers Dis *17*, 773-786.
Sinz, A. (2006). Chemical cross-linking and mass spectrometry to map three-dimensional protein structures and protein-protein interactions. Mass Spectrom Rev *25*, 663-682.
Skeberdis, V.A., Chevaleyre, V., Lau, C.G., Goldberg, J.H., Pettit, D.L., Suadicani, S.O., Lin, Y., Bennett, M.V., Yuste, R., Castillo, P.E., and Zukin, R.S. (2006). Protein kinase A regulates calcium permeability of NMDA receptors. Nat Neurosci *9*, 501-510.
Slack, S., Battaglia, A., Cibert-Goton, V., and Gavazzi, I. (2008). EphrinB2 induces tyrosine phosphorylation of NR2B via Src-family kinases during inflammatory hyperalgesia. Neuroscience *156*, 175-183.
Sloniowski, S., and Ethell, I.M. (2011). Looking forward to EphB signaling in synapses. Semin Cell Dev Biol.
Snyder, E.M., Nong, Y., Almeida, C.G., Paul, S., Moran, T., Choi, E.Y., Nairn, A.C., Salter, M.W., Lombroso, P.J., Gouras, G.K., and Greengard, P. (2005). Regulation of NMDA receptor trafficking by amyloid-beta. Nat Neurosci *8*, 1051-1058.
Sobczyk, A., Scheuss, V., and Svoboda, K. (2005). NMDA receptor subunit-dependent [Ca2+] signaling in individual hippocampal dendritic spines. J Neurosci *25*, 6037-6046.
Song, X.J., Cao, J.L., Li, H.C., Zheng, J.H., Song, X.S., and Xiong, L.Z. (2008a). Upregulation and redistribution of ephrinB and EphB receptor in dorsal root ganglion and spinal dorsal horn neurons after peripheral nerve injury and dorsal rhizotomy. Eur J Pain *12*, 1031-1039.
Song, X.J., Zheng, J.H., Cao, J.L., Liu, W.T., Song, X.S., and Huang, Z.J. (2008b). EphrinB-EphB receptor signaling contributes to neuropathic pain by regulating neural excitability and spinal synaptic plasticity in rats. Pain *139*, 168-180.

St-Denis, N.A., and Litchfield, D.W. (2009). Protein kinase CK2 in health and disease: From birth to death: the role of protein kinase CK2 in the regulation of cell proliferation and survival. Cell Mol Life Sci *66*, 1817-1829.
Stagi, M., Fogel, A.I., and Biederer, T. (2010). SynCAM 1 participates in axo-dendritic contact assembly and shapes neuronal growth cones. Proc Natl Acad Sci U S A *107*, 7568-7573.
Sturla, L.M., Merrick, A.E., and Burchill, S.A. (2003). FGFR3IIIS: a novel soluble FGFR3 spliced variant that modulates growth is frequently expressed in tumour cells. Br J Cancer *89*, 1276-1284.
Sudhof, T.C. (2008). Neuroligins and neurexins link synaptic function to cognitive disease. Nature *455*, 903-911.
Suetterlin, P., Marler, K.M., and Drescher, U. (2011). Axonal ephrinA/EphA interactions, and the emergence of order in topographic projections. Semin Cell Dev Biol.
Sutherland, B.W., Toews, J., and Kast, J. (2008). Utility of formaldehyde cross-linking and mass spectrometry in the study of protein-protein interactions. J Mass Spectrom *43*, 699-715.
Sze, C., Bi, H., Kleinschmidt-DeMasters, B.K., Filley, C.M., and Martin, L.J. (2001). N-Methyl-D-aspartate receptor subunit proteins and their phosphorylation status are altered selectively in Alzheimer's disease. J Neurol Sci *182*, 151-159.
Takasu, M.A., Dalva, M.B., Zigmond, R.E., and Greenberg, M.E. (2002). Modulation of NMDA receptor-dependent calcium influx and gene expression through EphB receptors. Science *295*, 491-495.
Tallafuss, A., Constable, J.R., and Washbourne, P. (2010). Organization of central synapses by adhesion molecules. Eur J Neurosci *32*, 198-206.
Tamura, H., Ishikawa, Y., Hino, N., Maeda, M., Yoshida, S., Kaku, S., and Shiosaka, S. (2006). Neuropsin is essential for early processes of memory acquisition and Schaffer collateral long-term potentiation in adult mouse hippocampus in vivo. J Physiol *570*, 541-551.
Tang, X.X., Pleasure, D.E., and Ikegaki, N. (1997). cDNA cloning, chromosomal localization, and expression pattern of EPLG8, a new member of the EPLG gene family encoding ligands of EPH-related protein-tyrosine kinase receptors. Genomics *41*, 17-24.
Tang, Y.P., Shimizu, E., Dube, G.R., Rampon, C., Kerchner, G.A., Zhuo, M., Liu, G., and Tsien, J.Z. (1999). Genetic enhancement of learning and memory in mice. Nature *401*, 63-69.
Terashima, A., Cotton, L., Dev, K.K., Meyer, G., Zaman, S., Duprat, F., Henley, J.M., Collingridge, G.L., and Isaac, J.T. (2004). Regulation of synaptic strength and AMPA receptor subunit composition by PICK1. J Neurosci *24*, 5381-5390.
Tolias, K.F., Bikoff, J.B., Burette, A., Paradis, S., Harrar, D., Tavazoie, S., Weinberg, R.J., and Greenberg, M.E. (2005). The Rac1-GEF Tiam1 couples the NMDA receptor to the activity-dependent development of dendritic arbors and spines. Neuron *45*, 525-538.

Tolias, K.F., Bikoff, J.B., Kane, C.G., Tolias, C.S., Hu, L., and Greenberg, M.E. (2007). The Rac1 guanine nucleotide exchange factor Tiam1 mediates EphB receptor-dependent dendritic spine development. Proc Natl Acad Sci U S A *104*, 7265-7270.

Tomita, T., Tanaka, S., Morohashi, Y., and Iwatsubo, T. (2006). Presenilin-dependent intramembrane cleavage of ephrin-B1. Mol Neurodegener *1*, 2.

Tong, G., Shepherd, D., and Jahr, C.E. (1995). Synaptic desensitization of NMDA receptors by calcineurin. Science *267*, 1510-1512.

Torres, R., Firestein, B.L., Dong, H., Staudinger, J., Olson, E.N., Huganir, R.L., Bredt, D.S., Gale, N.W., and Yancopoulos, G.D. (1998). PDZ proteins bind, cluster, and synaptically colocalize with Eph receptors and their ephrin ligands. Neuron *21*, 1453-1463.

Tovar, K.R., and Westbrook, G.L. (1999). The incorporation of NMDA receptors with a distinct subunit composition at nascent hippocampal synapses in vitro. J Neurosci *19*, 4180-4188.

Tzingounis, A.V., and Wadiche, J.I. (2007). Glutamate transporters: confining runaway excitation by shaping synaptic transmission. Nat Rev Neurosci *8*, 935-947.

van Spronsen, M., and Hoogenraad, C.C. (2010). Synapse pathology in psychiatric and neurologic disease. Curr Neurol Neurosci Rep *10*, 207-214.

Varoqueaux, F., Aramuni, G., Rawson, R.L., Mohrmann, R., Missler, M., Gottmann, K., Zhang, W., Sudhof, T.C., and Brose, N. (2006). Neuroligins determine synapse maturation and function. Neuron *51*, 741-754.

Vihanto, M.M., Vindis, C., Djonov, V., Cerretti, D.P., and Huynh-Do, U. (2006). Caveolin-1 is required for signaling and membrane targeting of EphB1 receptor tyrosine kinase. J Cell Sci *119*, 2299-2309.

Walsh, D.M., and Selkoe, D.J. (2004). Deciphering the molecular basis of memory failure in Alzheimer's disease. Neuron *44*, 181-193.

Wang, C.Y., Chang, K., Petralia, R.S., Wang, Y.X., Seabold, G.K., and Wenthold, R.J. (2006). A novel family of adhesion-like molecules that interacts with the NMDA receptor. J Neurosci *26*, 2174-2183.

Wang, P.Y., Petralia, R.S., Wang, Y.X., Wenthold, R.J., and Brenowitz, S.D. (2011). Functional NMDA receptors at axonal growth cones of young hippocampal neurons. J Neurosci *31*, 9289-9297.

Washbourne, P., Bennett, J.E., and McAllister, A.K. (2002). Rapid recruitment of NMDA receptor transport packets to nascent synapses. Nat Neurosci *5*, 751-759.

Wilcox, K.C., Lacor, P.N., Pitt, J., and Klein, W.L. (2011). Abeta oligomer-induced synapse degeneration in Alzheimer's disease. Cell Mol Neurobiol *31*, 939-948.

Wiseman, R.L., Chin, K.T., Haynes, C.M., Stanhill, A., Xu, C.F., Roguev, A., Krogan, N.J., Neubert, T.A., and Ron, D. (2009). Thioredoxin-related Protein 32 is an arsenite-regulated Thiol Reductase of the proteasome 19 S particle. J Biol Chem *284*, 15233-15245.

Wyszynski, M., Valtschanoff, J.G., Naisbitt, S., Dunah, A.W., Kim, E., Standaert, D.G., Weinberg, R., and Sheng, M. (1999). Association of AMPA receptors

with a subset of glutamate receptor-interacting protein in vivo. J Neurosci *19*, 6528-6537.
Xia, Z., Dudek, H., Miranti, C.K., and Greenberg, M.E. (1996). Calcium influx via the NMDA receptor induces immediate early gene transcription by a MAP kinase/ERK-dependent mechanism. J Neurosci *16*, 5425-5436.
Xu, J., Litterst, C., Georgakopoulos, A., Zaganas, I., and Robakis, N.K. (2009). Peptide EphB2/CTF2 generated by the gamma-secretase processing of EphB2 receptor promotes tyrosine phosphorylation and cell surface localization of N-methyl-D-aspartate receptors. J Biol Chem *284*, 27220-27228.
Yashiro, K., and Philpot, B.D. (2008). Regulation of NMDA receptor subunit expression and its implications for LTD, LTP, and metaplasticity. Neuropharmacology *55*, 1081-1094.
Yashiro, K., Riday, T.T., Condon, K.H., Roberts, A.C., Bernardo, D.R., Prakash, R., Weinberg, R.J., Ehlers, M.D., and Philpot, B.D. (2009). Ube3a is required for experience-dependent maturation of the neocortex. Nat Neurosci *12*, 777-783.
Zheng, X., Zhang, L., Wang, A.P., Bennett, M.V., and Zukin, R.S. (1997). Ca2+ influx amplifies protein kinase C potentiation of recombinant NMDA receptors. J Neurosci *17*, 8676-8686.
Zhuang, Z., Yang, B., Theus, M.H., Sick, J.T., Bethea, J.R., Sick, T.J., and Liebl, D.J. (2011). EphrinBs regulate D-serine synthesis and release in astrocytes. J Neurosci *30*, 16015-16024.
Zimina, E.P., Fritsch, A., Schermer, B., Bakulina, A.Y., Bashkurov, M., Benzing, T., and Bruckner-Tuderman, L. (2007). Extracellular phosphorylation of collagen XVII by ecto-casein kinase 2 inhibits ectodomain shedding. J Biol Chem *282*, 22737-22746.
Zimmer, M., Palmer, A., Kohler, J., and Klein, R. (2003). EphB-ephrinB bi-directional endocytosis terminates adhesion allowing contact mediated repulsion. Nat Cell Biol *5*, 869-878.
Ziv, N.E., and Smith, S.J. (1996). Evidence for a role of dendritic filopodia in synaptogenesis and spine formation. Neuron *17*, 91-102.
Zorumski, C.F., Yang, J., and Fischbach, G.D. (1989). Calcium-dependent, slow desensitization distinguishes different types of glutamate receptors. Cell Mol Neurobiol *9*, 95-104.
Zukin, R.S., and Bennett, M.V. (1995). Alternatively spliced isoforms of the NMDARI receptor subunit. Trends Neurosci *18*, 306-313.